

11-15-2017

Development of Remote Hydroxylation via Redox Catalysis and Mild Activation of Thioglycosides for O-Glycosylation

Kristina Deveaux

Louisiana State University and Agricultural and Mechanical College, kristinalacey91@gmail.com

Follow this and additional works at: https://digitalcommons.lsu.edu/gradschool_dissertations

 Part of the [Organic Chemistry Commons](#)

Recommended Citation

Deveaux, Kristina, "Development of Remote Hydroxylation via Redox Catalysis and Mild Activation of Thioglycosides for O-Glycosylation" (2017). *LSU Doctoral Dissertations*. 4167.

https://digitalcommons.lsu.edu/gradschool_dissertations/4167

This Dissertation is brought to you for free and open access by the Graduate School at LSU Digital Commons. It has been accepted for inclusion in LSU Doctoral Dissertations by an authorized graduate school editor of LSU Digital Commons. For more information, please contact gradetd@lsu.edu.

DEVELOPMENT OF REMOTE HYDROXYLATION VIA REDOX
CATALYSIS AND MILD ACTIVATION OF THIOLYGLYCOSIDES FOR
O-GLYCOSYLATION

A Dissertation

Submitted to the Graduate Faculty of the
Louisiana State University and
Agricultural and Mechanical College
in partial fulfillment of the
requirements for the degree of
Doctor of Philosophy

in

The Department of Chemistry

by
Kristina Deveaux
B.S., Georgia Southern University, 2012
December 2017

*“She is clothed with strength
and dignity, and she laughs
without fear of the future.”
Proverbs 31:25*

ACKNOWLEDGMENTS

First, to my advisor, Dr. Justin R. Ragains, sincere thanks for your guidance and helpful critiques, which have molded me into the scientist I am today. Thank you to my committee members, Professors Evgueni Nesterov, George Stanley, and Wayne Newhauser for their words of encouragement and availability during my time here. To my group members, past and present, I greatly appreciate the consistent encouragement and advice that made my transition and tenure here a pleasant experience.

I am extremely grateful for the immense love and overwhelming support my family and friends have shown me. A special thank you to the friends that became my sisters. Our friendships are invaluable to me and I sincerely hope they last a lifetime. I would like to acknowledge my wonderful husband, Brandon. Thank you for being my inspiration. Your love and reassurance has been a priceless source of motivation for me and I am truly blessed to have you in my life.

I would also like to express my appreciation for my amazing parents, Wentworth and Angela Deveaux. I would not be here today without the sacrifices that you both made for our family and I cannot begin to explain how eternally grateful I am. Thank you for your consistent prayers and constant communication that always brightened my day and for instilling principles and values in me that have kept me grounded.

Finally, I give all the glory and honor to God for without Him, I would not have had the strength to make it this far. I am exceedingly thankful.

TABLE OF CONTENTS

ACKNOWLEDGEMENTS.....	iii
LIST OF SCHEMES.....	vi
LIST OF FIGURES	ix
ABSTRACT.....	xi
CHAPTER 1: REVIEW OF C-H FUNCTIONALIZATION AND VISIBLE-LIGHT PHOTOREDOX CATALYSIS.....	1
1.1 Introduction	1
1.2 Guided vs. Innate Functionalization	2
1.3 Guided and Innate Functionalization Examples	3
1.4 Visible-Light Photoredox Catalysis.....	12
1.5 Literature Examples Supporting Proposed Transformation	15
1.6 Conclusion	19
1.7 References	19
CHAPTER 2: REMOTE C-H FUNCTIONALIZATION VIA REDOX CATALYSIS	22
2.1 Introduction	22
2.2 Synthesis of Sulfonamides and Sulfonate Esters	23
2.3 Sulfonamide Substrate Screen	29
2.4 Control Experiments.....	30
2.5 Attempted Hydroxylation of Tetrahydropyrrole and Tetrahydrofuran Derivatives.....	32
2.6 Screening of Sulfonamides with Light Excluded	35
2.7 Attempted Arylation Using Nucleophilic Arenes as Cosolvents	38
2.8 Conclusion	40
2.9 Experimental	41
2.10 References	59
CHAPTER 3: REVIEW OF CHEMICAL O-GLYCOSYLATION.....	62
3.1 Introduction	62
3.2 Possible Mechanistic Pathways and Contributors to Stereochemical Outcome.....	62
3.3 Glycosyl Acceptors.....	69
3.4 Glycosyl Donors	71
3.5 Conclusion	80
3.6 References	81
CHAPTER 4: TOWARDS THE DEVELOPMENT OF METAL-FREE O-GLYCOSYLATION METHODS USING THIOLYGLYCOSIDES	85
4.1 Introduction	85
4.2 Synthesis of Thioglycoside Donors	87

4.3 Importance of the <i>p</i> -Methoxy Side Chain for Glycosylation	88
4.4 Exploring Thioglycoside Activation Under Ultraviolet Irradiation	92
4.5 Conclusion	96
4.6 Experimental	96
4.7 References	108
CHAPTER 5: DEVELOPMENT OF ACID-PROMOTED GLYCOSYLATION OF ALCOHOLS WITH THIOGLYCOSIDES	111
5.1 Introduction	111
5.2 Mechanistic Proposal for Acid-Promoted Remote Glycosylation	112
5.3 Pilot Experiment and Optimization of Glycosylation Method.....	113
5.4 Establishment of Substrate Scope	
5.5 Future Work.....	120
5.6 Conclusion	121
5.7 Experimental	121
5.8 References	133
APPENDIX A: COPYRIGHT RELEASES	135
APPENDIX B: NMR SPECTRA OF COMPOUNDS FOUND IN CHAPTER 2.....	137
APPENDIX C: NMR SPECTRA OF COMPOUNDS FOUND IN CHAPTER 4.....	165
APPENDIX D: NMR SPECTRA OF COMPOUNDS FOUND IN CHAPTER 5.....	189
VITA.....	209

LIST OF SCHEMES

Scheme 1.1	Oxidation of casbene by cytochrome P450 monooxygenases	1
Scheme 1.2	Example of innate functionalization using pyridine derivatives	3
Scheme 1.3	Direct arylation of quinine with aryl boronic acid.....	4
Scheme 1.4	Directed functionalization of isonicotinamide derivative.....	5
Scheme 1.5	Iron catalyzed hydroxylation of acetoxy menthane.....	6
Scheme 1.6	Regioselective hydroxylation of menthol derivative.....	7
Scheme 1.7	Remote desaturation of 3-cholestanyl acetate.....	8
Scheme 1.8	Remote desaturation via benzophenone directing group.....	9
Scheme 1.9	Simultaneous desaturation of three molecules of cholesterol.....	10
Scheme 1.10	Regioselective hydroxylation of menthol derivative.....	10
Scheme 1.11	Proposed transformation for photoredox catalytic C-H functionalization.....	12
Scheme 1.12	Oxidative quenching cycle of Ir(ppy) ₃	14
Scheme 1.13	Reductive quenching cycle of Ir(ppy) ₃	15
Scheme 1.14	Arylation-addition via photo-Meerwein reaction.....	17
Scheme 1.15	Radical-polar crossover using tetrathiafulvalene	18
Scheme 1.16	Radical-polar crossover catalyzed by copper(II) chloride.....	19
Scheme 2.1	Initial mechanistic proposal for remote functionalization.....	23
Scheme 2.2	Synthesis of sulfonate ester for optimization.....	23
Scheme 2.3	Synthesis of tetrahydrofuran sulfonate ester derivative.....	26
Scheme 2.4	Attempted synthesis of carbamate-protected pyrrolidine derivative.....	27
Scheme 2.5	Successful synthesis of <i>N</i> -tosyl sulfonate ester.....	28

Scheme 2.6	Synthesis of <i>N</i> -tosyl prolinol sulfonate ester derivative.....	28
Scheme 2.7	Standard conditions for remote hydroxylation.....	30
Scheme 2.8	Single electron transfer from ground state <i>fac</i> -Ir(ppy) ₃	32
Scheme 2.9	Experiment to probe for possible intramolecular processes.....	32
Scheme 2.10	Proposed mechanism for Flourolead-mediated ring expansion.....	34
Scheme 2.11	Proposed mechanism for ring expansion.....	35
Scheme 2.12	Mechanistic hypothesis for light excluded experiments.....	37
Scheme 2.13	Conditions for the attempted arylation of isoamyl sulfonate ester.....	38
Scheme 2.14	Mechanistic hypothesis for TTF-promoted hydroxylation.....	39
Scheme 2.15	Conditions for attempted TTF-promoted arylation.....	40
Scheme 3.1	Possible mechanistic pathways of glycosylation.....	63
Scheme 3.2	Neighboring group participation.....	66
Scheme 3.3	Solvent effect on glycosylation by (A) diethyl ether and (B) acetonitrile.....	67
Scheme 3.4	Preferred conformation of oxacarbenium ion in acetonitrile and dioxane based on QM calculations.....	69
Scheme 3.6	AgClO ₄ promoted glycosylation with glycosyl iodide.....	72
Scheme 3.7	NIS-I ₂ -TMSOTf promoted glycosylation of disarmed glycosyl iodide.....	73
Scheme 3.8	Glycosylation of thioglycoside acceptor with glycosyl fluoride donor.....	74
Scheme 3.9	Synthesis of trisaccharide via thioglycoside donor.....	75
Scheme 3.10	Activation of phenylselenoglycosides with catalytic diphenyldiselenide.....	76
Scheme 3.11	Activation of trichloroacetimidate donor with mild acid.....	77

Scheme 3.12 Remote activation of STAz leaving group via alkylation.....	78
Scheme 3.13 Remote activation of <i>n</i> -pentenyl glycosides.....	79
Scheme 3.14 <i>gem</i> -2,2-dimethyl 4-pentenyl glycoside.....	80
Scheme 4.1 Proposed mechanism for metal-free glycosylation.....	86
Scheme 4.2 Synthesis of alkyl iodides from 3-bromopropanol.....	87
Scheme 4.3 Synthesis of alkyl iodides from 3-buten-1-ol.....	88
Scheme 4.4 Synthesis of tetrabenzyl thioglycoside donors.....	89
Scheme 4.5 Glycosylation experiment with UV light.....	92
Scheme 4.6 Fragmentation of Umemoto's reagent by UV light.....	93
Scheme 5.1 Hypervalent iodine(III) reagent (PIFA)-promoted glycosylation.....	111
Scheme 5.2 Glycoylation with a Piv-protected sulfinyl glycoside.....	112
Scheme 5.3 Mechanistic proposal for acid-promoted glycosylation.....	113
Scheme 5.4 Acid-promoted glycosylation using 4-aryl-3-butenylthioglycoside.....	114
Scheme 5.5 4-aryl-3-butenylthioglycoside as an acceptor.....	116
Scheme 5.6 By-products from glycosylation with tetrabenzoyl donor 5.10.....	120
Scheme 5.7 Proposed synthesis of trisaccharide 5.30.....	120

LIST OF FIGURES

Figure 1.1 [Fe(CF ₃ SO ₃) ₂ ((S,S,R)-mcpp)].....	6
Figure 1.2 Structures of three common transition metal photoredox catalysts.....	13
Figure 1.3 Isatoic anhydride.....	18
Figure 2.1 <i>o</i> -triazenesulfonyl chloride (Tz ^o Cl).....	22
Figure 2.2 Isolated yields of sulfonamides.....	24
Figure 2.3 Methylation of sulfonamides.....	25
Figure 2.4 Results from substrate screen using sulfonamides.....	29
Figure 2.5 Deviations from standard conditions in Scheme 2.10.....	30
Figure 2.6 Results from attempted hydroxylation of heterocycle derivatives.....	33
Figure 2.7 Results from light excluded experiments using sulfonamides.....	36
Figure 3.1 General representations of <i>alpha</i> and <i>beta</i> anomers (PG = protecting group).....	64
Figure 3.2 Molecular orbital theory (MOB) and dipole moment theory (DMT) of the anomeric effect.....	65
Figure 3.3 Generic representation of glycosyl acceptors.....	70
Figure 3.4 Examples of protected glycosyl donors.....	71
Figure 3.5 Glycosyl donor leaving groups.....	81
Figure 4.1 Selected reagents used to activate thioglycosides.....	85
Figure 4.2 Glycosylation experiments with metal-free glycosylation conditions.....	89
Figure 4.3 Putative EDA complex.....	90
Figure 4.4 Glycosyl donor (4.27) and Umemoto's reagent UV-vis experiment.....	91
Figure 4.5 Glycosyl donor (4.29) and Umemoto's reagent UV-vis	

experiment.....	91
Figure 4.6 Glycosylation experiments with DTBMP.....	95
Figure 4.7 Glycosylation experiments with selected acceptors.....	95
Figure 5.1 Trichloroacetimidate glycosyl donor.....	112
Figure 5.2 Glycosylation optimization.....	115
Figure 5.3 Glycosylation substrate scope.....	118

ABSTRACT

The focus of this dissertation is the development of a C-H functionalization method using predox catalysis and the synthesis of saccharides using thioglycosides. Chapter 1 is a review of C-H functionalization and visible-light photoredox catalysis. Over the years there have been many significant contributions to the field of C-H functionalization. Select examples have been discussed and a foundation for the method developed in chapter 2 has been outlined. Chapter 2 discusses the development and optimization of a C-H functionalization method. This approach uses the Tz^o directing group and Ir(ppy)₃ to activate a remote C-H bond via 1,6- and 1,7-radical translocation. It was confirmed that this method required acid and Ir(ppy)₃ to afford decent yields of the hydroxylated products. An array of sulfonamides and sulfonate esters were screened in efforts to expand the substrate scope.

Chapter 3 provides an overview of chemical O-glycosylation. Stereoselective synthesis of oligosaccharides has been a challenge that many researchers have made attempts to address over the years. Select examples of glycosylation methods have been discussed along with the benefits and shortcomings. In chapter 4, a mild, metal-free method for glycosylation with thioglycosides is established and optimized. Thioglycosides are frequently employed in glycosylations due to their chemical stability, however, the harsh/toxic conditions necessary to activate them is a major downfall. To address this concern, 4-aryl-3-butenylthioglycosides were activated using visible-light in the presence of Umemoto's reagent. A putative EDA complex forms and initiates departure of the leaving group. Changing the light source from blue LEDs to violet LEDs, improved the reaction time (24 hours to 2 hours) without compromising yield.

Observations made during these experiments paved the way for the method developed in Chapter 5.

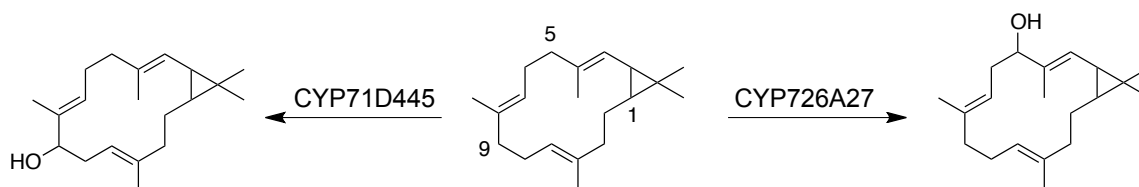
Chapter 5 outlines an acid-promoted glycosylation of 4-aryl-3-butenylthioglycosides. In an effort to combine the stability of thioglycosides with the reactivity of trichloroacetimidates, activation of 4-aryl-3-butenylthioglycosides was demonstrated with 10 mol% of triflic acid (or TMSOTf). Glycosidic linkages were formed within in good to excellent yields and stereoselectivity can be achieved by neighboring group participation. 4-Aryl-3-butenylthioglycosides exhibit low reactivity at -20°C and this latency will ultimately be exploited in the synthesis of a trisaccharide.

CHAPTER 1: REVIEW OF C-H FUNCTIONALIZATION AND VISIBLE-LIGHT PHOTOREDOX CATALYSIS

1.1 Introduction

Nature has served as an inspiration to scientists for centuries. Numerous synthetic transformations have been inspired by nature and chemists have aimed to develop “biomimetic” transformations in an effort to improve the step- and atom-economy of multistep synthesis. A particularly useful transformation is the selective activation of C-H bonds. When this occurs in nature, it is frequently via an enzymatic pathway. For example, classes of enzymes known to oxidize molecules during biosynthesis are called oxygenases.^{1a}

Hamberger and coworkers recently reported the discovery of two such enzymes of the cytochrome P450 monooxygenase class, CYP71D445 and CYP726A27^{1b} (Scheme 1.1). This finding came as they were researching the biosynthesis of medically relevant macrocyclic diterpenoids in plants of the genus *Euphorbia*. Hamberger concluded that these monooxygenases regioselectively oxidize casbene, a simple bicyclic diterpenoid that is considered as the first intermediate toward the biosynthesis of several complex diterpenoids. CYP71D445 selectively adds a hydroxyl group to C9 of casbene while CYP726A27 hydroxylates C5. A series of subsequent oxidations and a cyclization result in a compound known as jolkinol C, a diterpine that is a potential



Scheme 1.1 Oxidation of casbene by cytochrome P450 monooxygenases

intermediate in the biosynthesis of ingenol mebutate, a natural product known for its anticancer activity¹.

This example serves as one of many ways that nature reveals elegant and useful processes through scientific exploration. Aliphatic C-H bonds are widely regarded as unreactive or inert, however, they are ubiquitous in organic compounds. Functionalizing C-H bonds is beneficial to the synthetic chemist, as it obviates the incorporation of multiple synthetic steps in a sequence in order to form one bond. Once a bond is functionalized, you now have a reactive group that can participate in additional reactions to increase the complexity of a molecule. In addition to this benefit, recent advances in C-H functionalization²⁶ have provided mild conditions that tolerate other functional groups present. The early years of investigation into activation of inert C-H bonds was plagued with conditions that were either harsh or low yielding. In addition to this, the processes were relatively unselective. When these otherwise inert C-H bonds are treated as synthetically useful functional groups, synthetic methods are more efficient and step-economical. This improvement has far reaching implications and could lead to the affordable synthesis of expensive and synthetically challenging natural products and drugs.

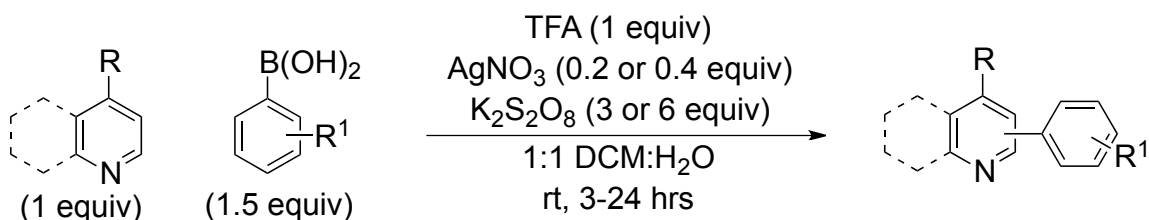
1.2 Guided vs. Innate Functionalization

Methods to functionalize C-H bonds has increased exponentially over the past century^{22-23,26}. Since this area of investigation was discovered, a general trend has developed, and methods of functionalizing C-H bonds can be grouped into two main categories²⁷. The first category is innate C-H functionalization. As implied, such activation is based on the innate reactivity of the molecule. Whether it is promoted by

steric or electronic factors, functionalization depends on the natural reactivity of a C-H bond. The second category is guided C-H functionalization. This method of activation involves directing groups that are either covalently bonded or coordinated to the compounds C-H-bearing. These groups can be activated chemically, photochemically or thermally³⁰ and guide activation to a specific C-H bond allowing for highly selective functionalization, a characteristic that is invaluable to synthetic chemists.

1.3 Guided and Innate Functionalization Examples

While coupling reactions such as the Suzuki and Heck reaction are popular methods for functionalizing aromatic rings, they require the use of aryl halides to determine the regioselectivity. By contrast, C-H arylation based on intrinsic reactivity obviates aryl halides. An example of direct arylation of heterocycles has been reported² and, in this example, the regioselectivity depends on the innate reactivity of the nitrogen containing aromatic rings. Under catalysis by silver nitrate (AgNO_3) with persulfate as a co-oxidant, aryl boronic acids were coupled to heterocycles with the regioselectivity being dependent on the heterocycle used (Scheme 1.2). For example, pyridine favored functionalization at C2 twofold over functionalization at C4. Regioselectivity varied when

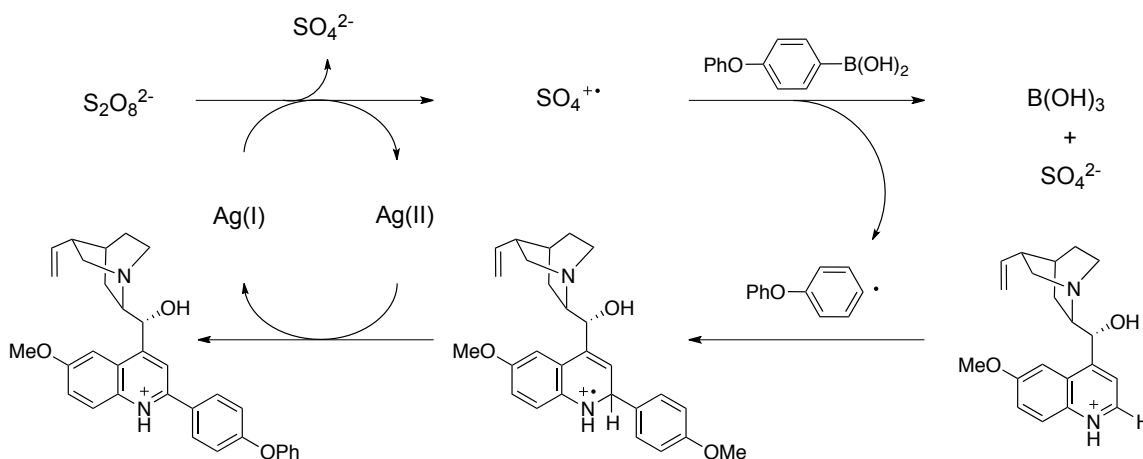


Scheme 1.2 Example of innate functionalization using pyridine derivatives

pyrimidines, pyridazines or pyrazines were employed and also when additional functional groups such as ketones, halides, and nitriles were added to the pyridine

rings. In each case, functionalization occurred at the most electron deficient site on the molecule. It is important to note that aryl halides are unreactive under the reaction conditions. More electron rich rings such as indole, imidazole and 1,3,5-triazine were low yielding or did not produce the desired product. On the other hand, this method employed a variety of aryl boronic acids. Electron rich boronic acids decreased reaction times while electron poor boronic acids required twice the amount of catalyst and persulfate.

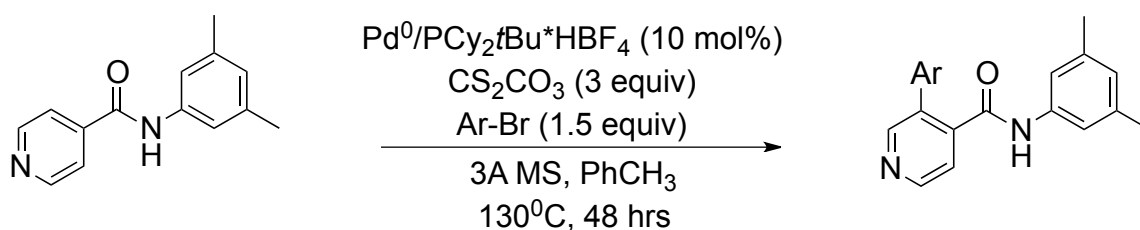
Mechanistically speaking, the silver salt reduces the persulfate ion to two species, the sulfate dianion and a sulfate radical anion (Scheme 1.3). This radical anion



Scheme 1.3 Direct arylation of quinine with aryl boronic acid

then reacts with the aryl boronic acid and induces homolytic cleavage of the carbon-boron bond to furnish the corresponding aryl radical. The aryl radical then adds to the TFA salt of the heterocycle to produce an intermediary nitrogen centered radical cation. Subsequent oxidation by the silver II salt then regenerates the catalyst and furnishes the product².

Alternatively, a reported example of a guided approach to functionalizing pyridines³ resulted in products that favored the C3 and C4 position of the heterocycle (Scheme 1.4). The substrates used nicotinic and isonicotinic amide derivatives, compounds that are commonly used in the pharmaceutical industry for their biological activity. In this method, an amide group at the *para* or *meta* position relative to the nitrogen directs aryl groups to the C3 position when the amide is *para* and the C4

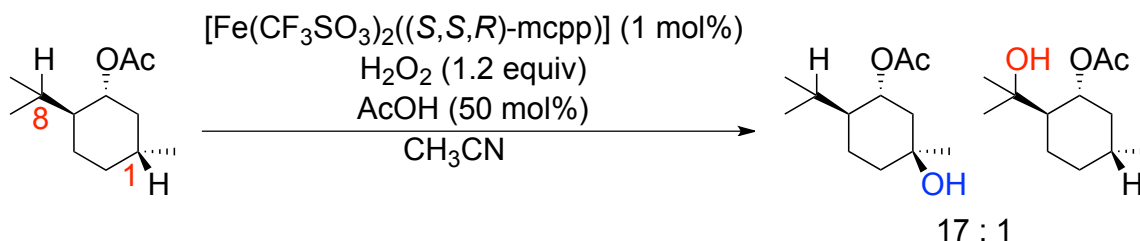


Scheme 1.4 Directed functionalization of isonicotinamide derivative

position when the amide is *meta*. During method development of this method, it was discovered that 3,5-dimethylphenyl was the optimal amide *N*-substituent for directing as it showed high selectivity for monoarylation with excellent yields. The more electron withdrawing amides (perfluorophenyl, 2,6-difluoro or 4-trifluoromethylphenyl) showed low selectivity and low yields. This observation shows that these groups make the pyridine rings more electron poor and less reactive. The method tolerates functional groups such as ethers, halides, and esters and yields for the monoarylated products ranged from 27% to 94%. The amide can then be converted to the acid via hydrolysis with 4M HCl.

While innate characteristics such as electronic properties can enable site predictability with regard to functionalization, sterics can play a part as well. Non-heme catalysts have proven to be excellent oxidation catalysts that function under relatively

mild conditions^{3,4}. Such an iron catalyst designed by Costas *et al.*, effectively functionalized various cyclohexane derivatives in a regioselective manner in the presence of hydrogen peroxide as an oxidant⁶ (Scheme 1.5). A menthol derivative,



Scheme 1.5 Iron catalyzed hydroxylation of acetoxy menthane

acetoxy menthane, has two sites groups, both of which are susceptible to hydroxylation under the reaction conditions. However, the system exhibits a 17:1 preference for the C1 position over C8 in 62% yield. The reasoning for this can be attributed to the bulky isopropyl group undergoing steric interactions with the methyl groups of pinene-bearing ligands found on the iron catalyst (Figure 1.1). This steric hindrance makes the hydrogen at C1 more accessible to hydrogen abstraction.

An oxygen bound to the metal center is thought to be the source of the hydroxyl group. If this is the case, then it is reasonable to predict that the functionalization will

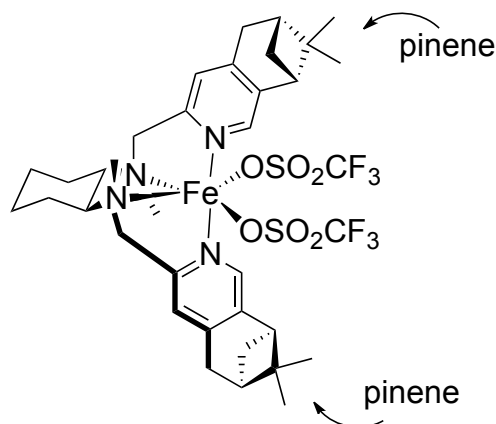
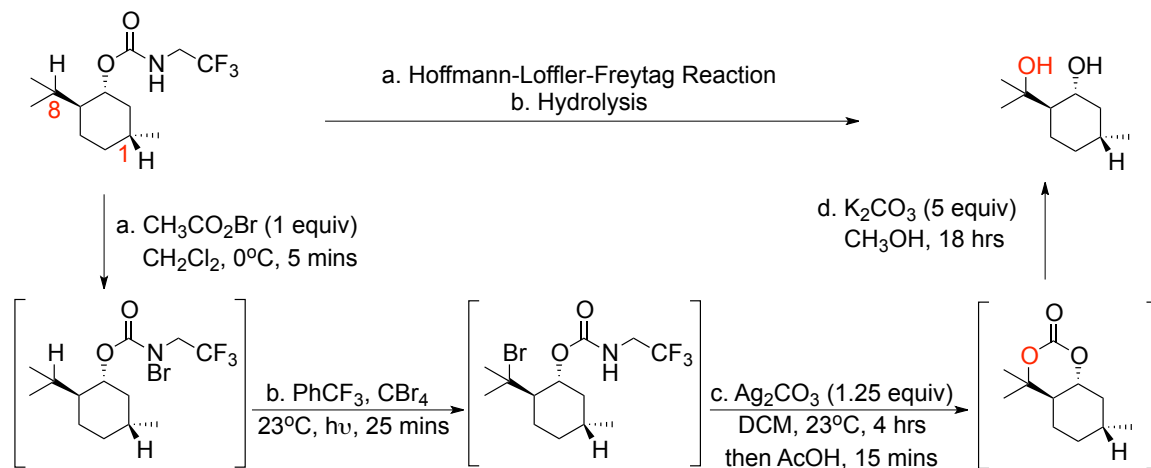


Figure 1.1 $[\text{Fe}(\text{CF}_3\text{SO}_3)_2((S,S,R)\text{-mcpp})]$

occur at the least sterically hindered site. Also, the hydrogen at C1 that is a part of the cyclohexyl ring is in a fixed orientation as opposed to the freely rotating isopropyl group and this may contribute to the selectivity of the transformation.

Menthol has also been used to showcase a site-specific functionalization via a *N*-trifluoroethyl carbamate directing group⁹. In this example, selectivity is the opposite to that of the iron-catalyzed oxidation. Several 1,3-diols were successfully synthesized by this procedure that was inspired by the Hoffmann-Löffler-Freytag³² reaction (Scheme 1.6). Treatment of the carbamate with acetyl hypobromite (AcOBr) oxidizes it to the *N*-

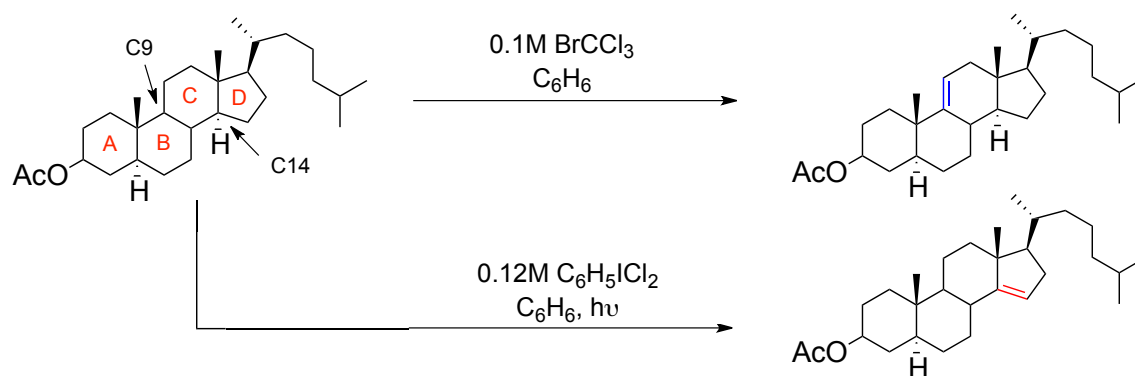


Scheme 1.6 Regioselective hydroxylation of menthol derivative

bromocarbamate, which is then irradiated and subsequently forms a nitrogen-centered radical as a result of homolytic bond cleavage. A 1-6 hydrogen transfer occurs followed by halogen transfer resulting in an alkyl bromide at that site. Cyclization occurs to form a carbonate in the presence of silver carbonate (AgCO_3) that is then hydrolyzed to afford the diol. In this case, only one isomer is produced and functionalization occurs only on the tertiary carbon of the isopropyl group. This method was employed in the total

synthesis of eudesmane terpenes starting from commercially available reagents (butyraldehyde and methyl vinyl ketone)⁸.

Remote desaturation is a useful C-H functionalization transformation as well, and several intriguing methods have been reported¹⁰⁻¹⁵. Cholesterol has a myriad of C-H bonds that are relatively inert, making it an excellent model system for C-H functionalization. Breslow and co-workers found that irradiation of cholesterol in halogenated solvents such as carbon tetrachloride (CCl₄) and bromotrichloromethane (BrCCl₃) resulted in desaturation of the C ring with high selectivity for C9¹¹ with cholestanyl acetate (Scheme 1.7). In bromotrichloromethane, the reaction proceeds via



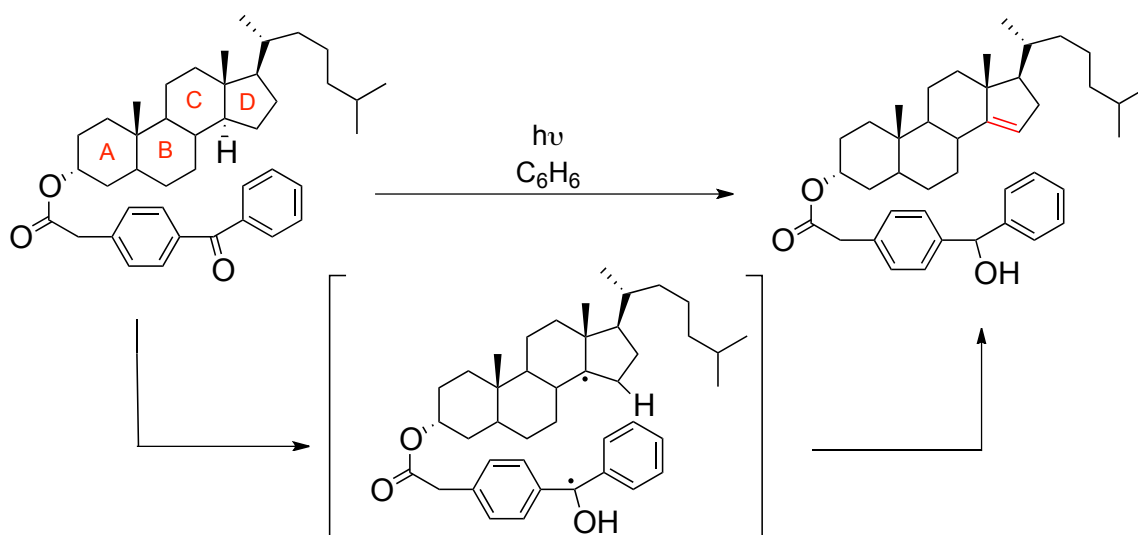
Scheme 1.7 Remote desaturation of 3-cholestanyl acetate

radical formation at C9 and subsequent bromination. Over the course of the workup, dehydrohalogenation occurs to afford the alkene product. This transformation was, however, plagued with difficult workup and purification as a result of tar-like by products.

To combat this issue, irradiation in phenyliodine dichloride (C₆H₅ICl₂), a source of chlorine, produced a much cleaner reaction upon workup with silver perchlorate (AgClO₄) in aqueous acetone. Selectivity, however, suffered as mixtures of products were produced; 1:1 desaturation at C9 in ring C and C14 in ring D occurred. Several years later in 1976, Breslow tethered phenyliodine dichloride to a molecule of

cholesterol via an ester bond to the A ring¹². This appendage acted as a directing group and allowed for selective desaturation of cholesterol.

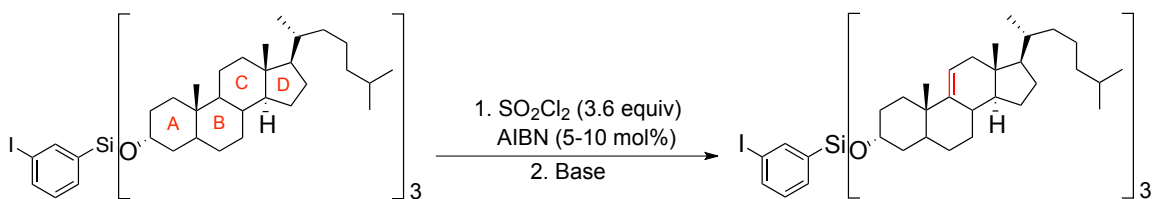
A more regioselective approach to desaturation of cholestanols from Breslow involved a covalently bonded benzophenone ester that directs olefin formation¹³ (Scheme 1.8). In this example, the rigid and bulky benzophenone group folded onto the



Scheme 1.8 Remote desaturation via benzophenone directing group

bottom face of the molecule as the methyl groups on the top face induced negative steric interactions. The carbonyl is aptly aligned with the axial hydrogen at C14, and excitation of the benzophenone ester by irradiation in benzene results in an oxygen radical that abstracts the hydrogen at that carbon. The benzhydryl radical then removes the hydrogen at C15 to form the olefin product. This desaturation of the D ring is the only alkene product observed in 55% yield.

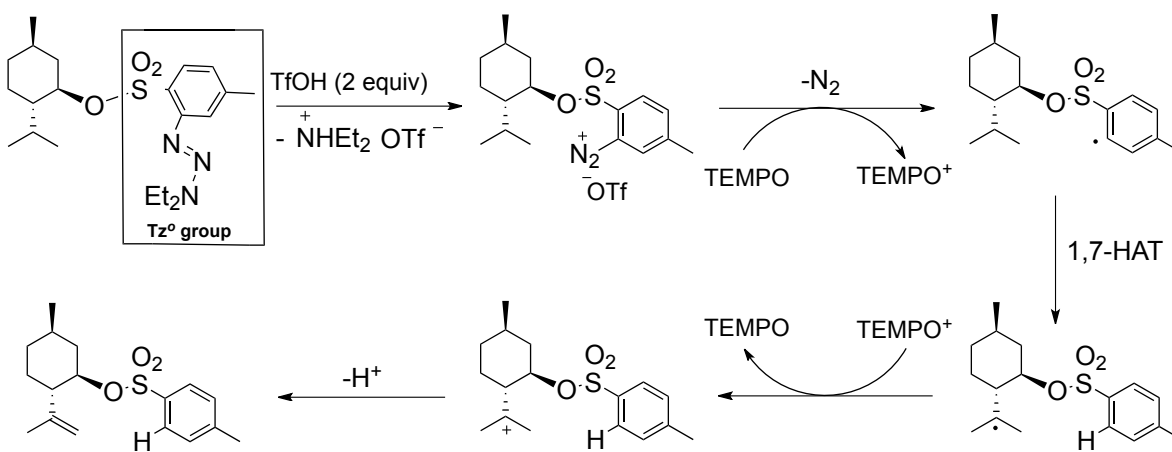
Alternatively, reversal of selectivity is achieved by using a silyl ether directing group (Scheme 1.9). In this example of guided desaturation, desaturation occurs at C9 of the C ring¹⁴. This appendage impressively regenerates the active intermediate and,



Scheme 1.9 Simultaneous desaturation of three molecules of cholesterol

as shown, enables selective olefin formation at C9 of three molecules of cholesterol that are all bonded to the silicon. Irradiation of the silyl ether with 1.2 equivalents of sulfuryl chloride per molecules of cholesterol (3.6 equivalents total) and 5-10 mol % of azobisisobutyronitrile (AIBN) results in the tri (9-chloro) intermediate. Subsequent base-promoted dehydrohalogenation results in desaturation of the C ring, the only identifiable indication of desaturation, in over 66% yield. The silyl-oxygen bond is easily formed compared to esters and therefore can be used in cases where esterification is an arduous task.

Recently, Baran and coworker reported a method for remote desaturation, which incorporated a directing group specifically designed to guide a 1-7 intramolecular hydrogen abstraction (Scheme 1.10). The *o*-tosyl triazene sulfonyl chloride (Tz^oCl)



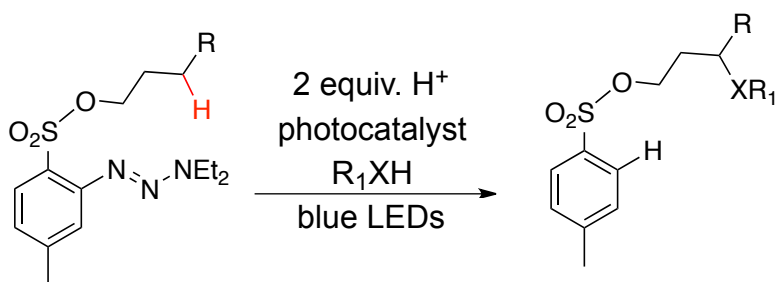
Scheme 1.10 Regioselective hydroxylation of menthol derivative

covalently bonds to functional groups already present on substrate molecules such as alcohols or amines, and the corresponding compound reacts under the conditions to yield desaturation products¹⁶. A masked aryl diazonium ion is generated from a triazene after treatment with 2 equivalents of triflic acid at room temperature (or 3 equivalents of trifluoroacetic acid at 60°C) and subsequently accepts an electron from TEMPO (1 equivalent) to produce a high-energy aryl radical and TEMPO⁺. This radical then undergoes a 1,7 hydrogen atom transfer to furnish an alkyl radical. The radical translocation process has now remotely activated an otherwise inert C-H bond. The alkyl radical is then oxidized by TEMPO⁺ to form a carbocation and, finally, elimination produces the olefin product. Pertinent to the design of this directing group is the fact that, over the course of the reaction, the Tz^o group is converted to a synthetically useful tosylate, which can enable further functionalization.

This method afforded a wide range of desaturated compounds in moderate to good yields and facilitated predictable hydrogen abstraction with good functional group tolerance and a mild oxidation reagent under metal-free conditions. However, substituting TEMPO for a metal salt capable of oxidizing and reducing the respective intermediates would allow for development of a catalytic method for functionalization. Baran and coworkers initially attempted to this with copper(II) bromide (5 mol%) that underperformed and only produced up to 40% yield of the desaturation product. In addition to this low yield, they also saw evidence of trivial reduction (resulting from hydrogen abstraction from the solvent) and incorporation of bromide from the catalyst at the alkyl radical carbon. The trivial reduction product was suppressed by switching the

solvent to nitromethane, a solvent less susceptible to hydrogen abstraction, and the brominated product was no longer produced when they used TEMPO as an alternative.

Although developing a catalytic method with copper salts proved to be unsuccessful, we envisioned activation of the Tz^o group via photoredox catalysis (Scheme 1.11). Such a method would allow use of catalytic amounts of transition metal salts to reduce the diazonium salt and oxidize the alkyl radical to the carbocation. In addition to this, catalyst activation could be performed mildly by simply irradiating with visible light, and the low catalyst loading would be an improvement over the use of



Scheme 1.11 Proposed transformation for photoredox catalytic C-H functionalization

stoichiometric reagents demonstrated in many of the above examples. We also sought to capitalize on the radical-polar crossover and, instead, add nucleophiles to the reaction to generate new C-X bonds instead of elimination. A wide variety of nucleophiles could be employed such as water, alcohols, amines, and even nucleophilic arenes such as furan or pyrrole. We sought to approach this project by employing visible-light photoredox catalysis (VLPRC), a method that would obviate stoichiometric oxidants/reductants and allow for milder activation.

1.4 Visible-Light Photoredox Catalysis

Several of the transformations mentioned previously in this chapter depend upon the formation of a carbon-centered radical. In the past decade, there has been a significant increase in the use of transition metal polypyridyl complexes to catalyze various synthetic organic transformations using visible-light promotion^{17,24,25}. Exposure of these polypyridyl complexes to visible light results in an excited state species that engage in single electron transfer (SET) and they have been demonstrated to be effective species for activating C-H bonds. Common photocatalysts (Figure 1.2) include

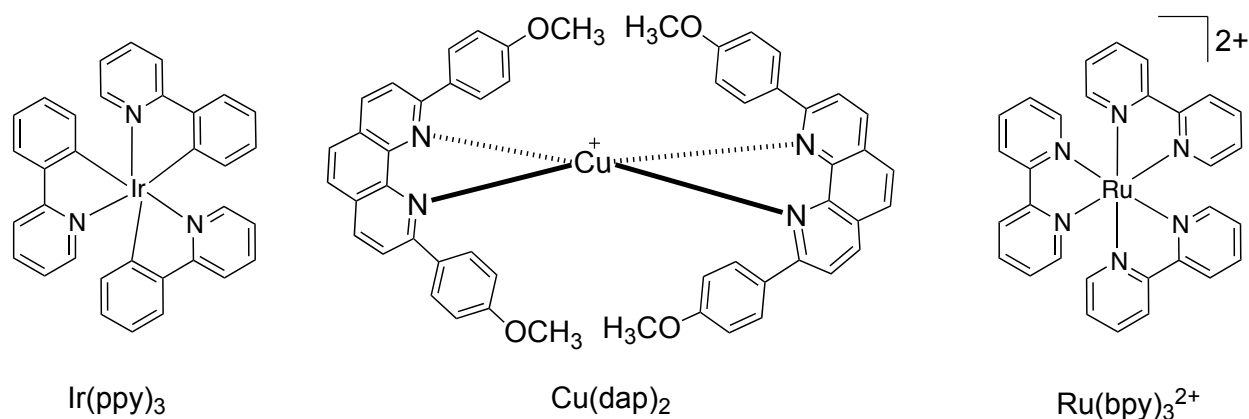


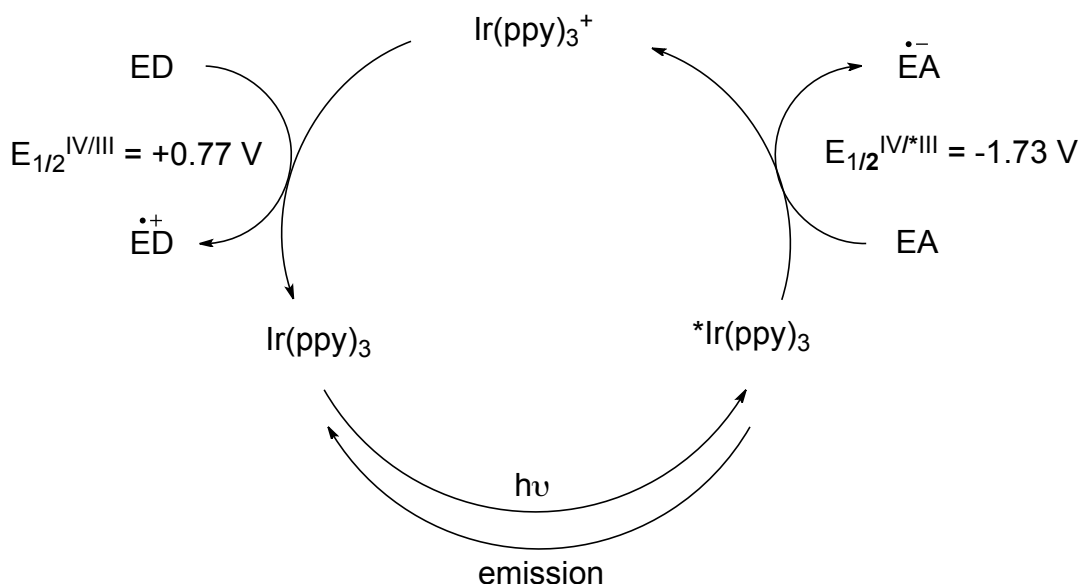
Figure 1.2 Structures of three common transition metal photoredox catalysts

metal-based complexes of iridium and ruthenium, however, eosin Y and 9,10-dicyanoanthracene, both organic dyes, are also capable of behaving as SET catalysts following visible light irradiation.¹⁷ To give further detail on the photocatalytic processes involving SET, the properties of *fac*-Ir(ppy)₃ will be used to discuss photoredox catalytic cycles (scheme 1.12/1.13).

1.4.1 Visible-Light Photoredox Catalysis Cycle

Upon irradiation with a visible light source such as blue LEDs or a simple household light bulb, *fac*-Ir(ppy)₃ absorbs visible light and subsequently undergoes a

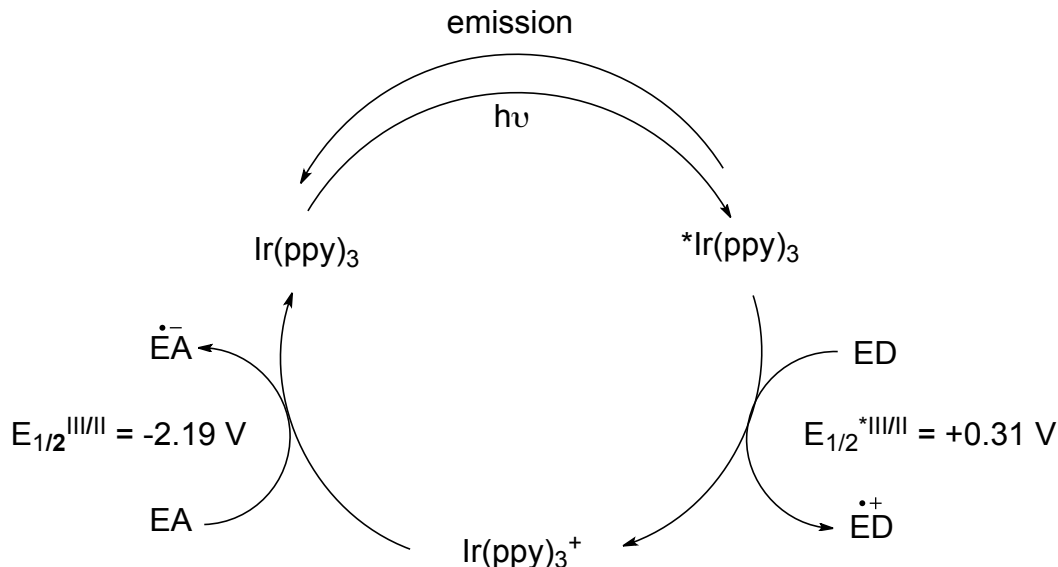
metal to ligand charge transfer (MLCT) resulting in an excited state species.¹⁷ In the presence of an electron acceptor (EA) such as an aryldiazonium salt, the catalyst enters the oxidative quenching cycle (Scheme 1.12) and reduces the salt by donating an



Scheme 1.12 Oxidative quenching cycle of Ir(ppy)₃

electron. The oxidized photocatalyst is then capable of accepting an electron from a donor in solution to regenerate *fac*-Ir(ppy)₃.

In the event that an electron donor is present upon irradiation of *fac*-Ir(ppy)₃, the photocatalyst goes through the reductive quenching cycle (Scheme 1.13)¹⁷. Analogous to the oxidative quenching cycle, the excited state species forms upon irradiation, however, *fac*-Ir(ppy)₃ accepts an electron from an appropriate donor such as BNAH (1-benzyl-1,4-dihyronicotinamide) and is reduced. The catalyst can then donate an electron to an acceptor *in situ* and consequently return to the resting state. This characteristic allows for milder transformations utilizing catalytic amounts of reagents to



Scheme 1.13 Reductive quenching cycle of Ir(ppy)_3

initiate the reaction. In addition to this, reactions can be performed at room temperature, in some cases, with an inexpensive visible light source such as a fluorescent light bulb.

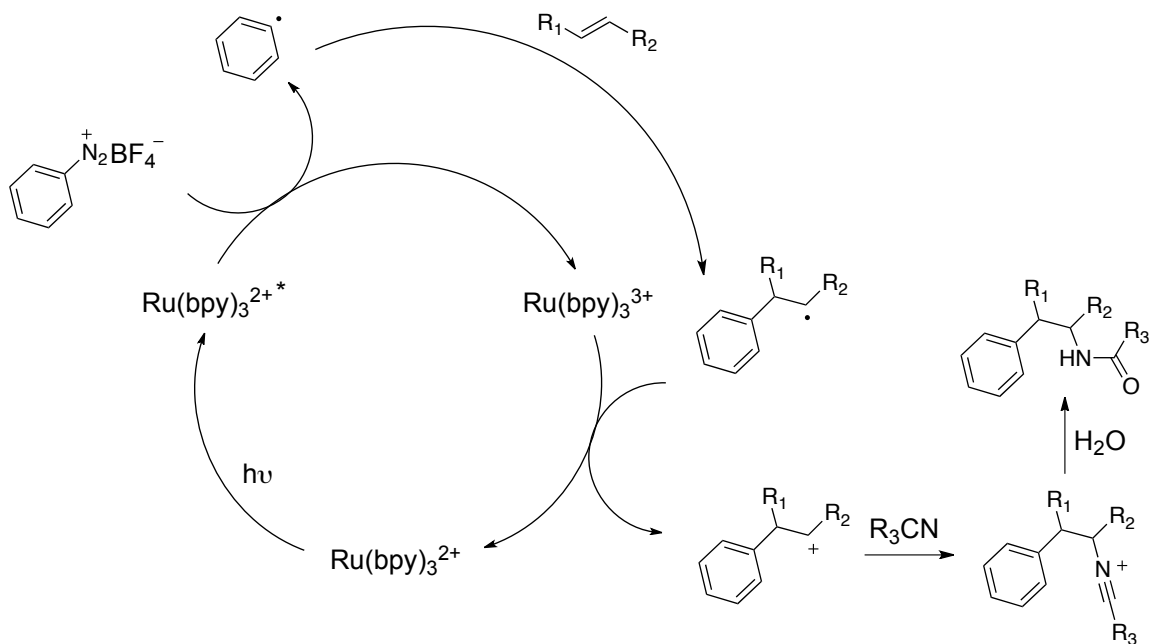
When developing a reaction, it is important to know the reduction potential of the photocatalysts. With respect to iridium, in the oxidative quenching cycle the excited species $^*\text{Ir(ppy)}_3$ is a very effective reductant based on its reduction potential, $E_{1/2}^{\text{IV}^*/\text{III}} = -1.73 \text{ V vs SCE}^{29}$ (saturated calomel electrode), when compared to ground state Ir(ppy)_3 ($E_{1/2}^{\text{IV/III}} = +0.78 \text{ V vs SCE}^{29}$). The reduction potential of the ground state, however, shows that it is a good oxidant of alkyl radicals. The catalyst can therefore play the roles of both an oxidizing and reducing agent. A similar trend is seen in the reductive quenching cycle as the excited state species is a better oxidant ($E_{1/2}^{*\text{III/II}} = +0.31 \text{ V vs SCE}^{29}$) than the ground state ($E_{1/2}^{\text{III/II}} = -2.20 \text{ V vs SCE}^{29}$), however, *fac*- Ir(ppy)_3 is a strong reductant and can easily donate an electron to return to the resting state.

1.5 Literature Examples Supporting Proposed Transformation

We envisioned employing *fac*-Ir(ppy)₃ and visible light to promote the desired transformation. Baran's Tz^o group was identified as a viable directing group. As demonstrated by Baran and coworkers and many other researchers, arene diazonium groups are capable of accepting an electron and subsequently releasing N₂ to furnish an aryl radical¹⁶. Baran further demonstrated that radical translocation followed by a radical-polar crossover could be achieved using appropriate reagents; all of these are mechanistically required for this proposed transformation.

Common aryl radical precursors include aryl halides, diaryliodonium salts, aryl sulfonyl chlorides, and triarylsulfonium salts²⁵. Arene diazonium salts also fall into this category and are the easiest to reduce while being relatively simple to synthesize. A report demonstrating electrochemical reduction of arene diazonium salts by mercury electrodes was published in 1958 by Elofson and coworkers³³. This functional group has been used frequently for various synthetic transformations and reduced by several different means such as electron transfer from metal cations²⁸. Additionally, photocatalysts have been shown to reduce aryl diazonium salts in the presence of visible light²⁵.

A photo-Meerwein reaction that involved photochemical reduction of substituted arene diazonium salts ($E_{\text{red}} = -0.1$ to $+0.5$ V vs. SCE)²⁸ using only 0.5 mol% of a Ru(bpy)₃²⁺ ($E_{1/2}^{\text{III/II}} = -0.81$ V vs SCE)¹⁷ catalyst was reported by König and coworkers³¹ (Scheme 1.14). Following the oxidative quenching cycle, the formed aryl radical adds to an olefin and produces a secondary benzylic radical. The alkyl radical is now primed to donate an electron (ED in Scheme 1.12) to the oxidized catalyst furnishing a carbocation, which is then trapped by a nitrile and then H₂O *in situ* to

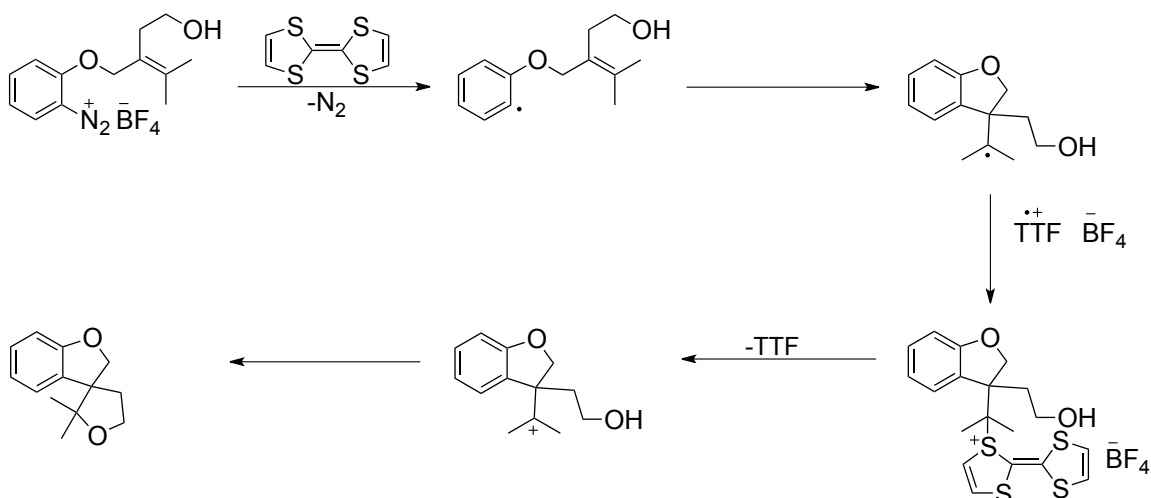


Scheme 1.14 Arylation-addition via photo-Meerwein reaction

ultimately form the amide product. The radical-polar crossover exhibited in this case is an advantageous process that would make functionalization using different nucleophiles a controlled and feasible transformation.

There have been many examples of radical-polar crossover processes in the literature¹⁸⁻²¹. Notably, Murphy and coworkers showcased the use of tetrathiafulvalene as an efficient electron donor that reduced an arene diazonium salt in situ¹⁸ (Scheme 1.15). The aryl radical then cyclizes intramolecularly onto an alkene and subsequently forms a secondary alkyl radical. The radical-cation of TTF then combines with the alkyl radical and the intermediate sulfonium salt undergoes an S_N2 reaction to furnish a carbocation that is then attacked by a nucleophile to produce the functionalized product.

Another example published by Weinreb tethers isatoic anhydride (Figure 1.3) to pyrrolidine and the aniline is converted to a diazonium group upon treatment with nitrous acid (Scheme 1.16)²¹. Once formed, the diazonium cation accepts an electron



Scheme 1.15 Radical-polar crossover using tetrathiafulvalene

from copper(I) and generates an aryl radical that then undergoes a 1,5-hydrogen atom transfer. Copper (II) subsequently oxidizes the intermediary secondary radical forming an N-acyl iminium ion, which is then hydrolyzed by an alcohol in situ.

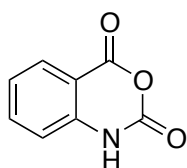
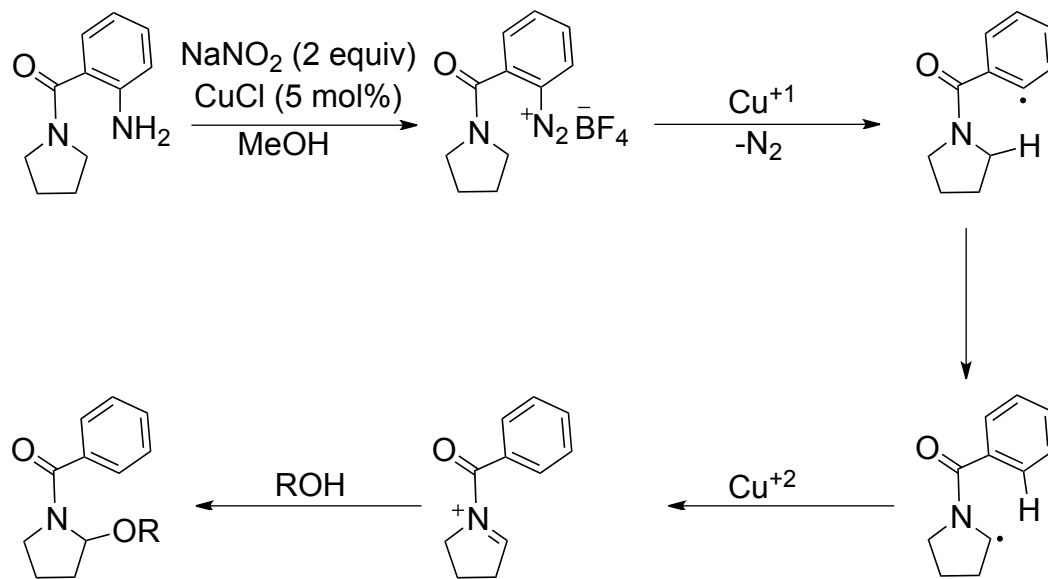


Figure 1.3 Isatoic anhydride

Each reaction discussed in this section involved hydrogen atom transfer. The concept of this process, however, is not a recent development. Though the mechanism was not understood until the 1950s³⁴, the Hoffmann-Löffler-Freytag reaction was discovered by the trio between the 1800s and 1900s³². In their example and the reports subsequently published by researchers confirming the mechanism, a 1,5 or 1,6 hydrogen abstraction is involved in the hydrogen atom transfer step and results in an alkyl radical³⁵. This same reaction was the inspiration for Baran's diol synthesis⁹ that was previously mentioned in this chapter.



Scheme 1.16 Radical-polar crossover catalyzed by copper(II) chloride

1.6 Conclusion

In summary, there have been many advances in the realm of C-H functionalization in the past several decades. Mild methods for activating these ubiquitous bonds would enable researchers to perform late stage functionalizations of complex molecules without affecting existing functional groups. Developing a catalytic method would also make overall synthesis cheaper and easier to scale up. In this chapter, selected methods were discussed to demonstrate guided and innate functionalization of aromatic rings as well as aliphatic carbons, showcased using menthol and cholesterol derivatives. In addition, a brief discussion of visible-light photoredox catalysis, arene diazonium salts as electron acceptors, and radical-polar crossover laid the foundation for the following chapter and the initial direction of this project.

1.7 References

1. (a) Groves, J. T., *Nat. Chem.* **2014**, 6, 89-91.; (b) Luo, D.; Callari, R.; Hamberger, B.; Wubshet, S. G.; Nielsen, M. T.; Andersen-Ranberg, J.; Hallström, B. M.; Cozzi, F.; Heider, H.; Møller, B. L.; Staerk, D.; Hamberger, B., *Proc. Natl. Acad. Sci. U. S. A.* **2016**, 113, E5082-E5089.
2. Seiple, I. B.; Su, S.; Rodriguez, R. A.; Gianatassio, R.; Fujiwara, Y.; Sobel, A. L.; Baran, P. S., *J. Am. Chem. Soc.* **2010**, 132, 13194-13196.
3. Wasa, M.; Worrell, B. T.; Yu, J., *Angew. Chem. Int. Ed.* **2010**, 49, 1275-1277.
4. Chen, M. S.; White, M. C., *Science.* **2007**, 318, 783-787.
5. Vermeulen, N. A.; Chen, M. S.; White, M. C., *Tetrahedron.* **2008**, 65, 3078-3084.
6. Gomez, L.; Garcia-Bosch, I.; Company, A.; Benet-Buchholz, J.; Polo, A.; Sala, X.; Ribas, X.; Costas, M., *Angew. Chem. Int. Ed.* **2009**, 48, 5720-5723.
7. Que Jr., L., *Acc. Chem. Res.* **2007**, 40, 493-500.
8. Chen, K.; Baran, P. S., *Nature.* **2009**, 459, 824-828.
9. Chen, K.; Richter, J. M.; Baran, P. S., *J. Am. Chem. Soc.* **2008**, 130, 7247-7249.
10. Pierce, C. J.; Hilinski, M. K., *Org. Lett.* **2014**, 16, 6504-6507.
11. Breslow, R.; Dale, J. A.; Kalicky, P.; Liu, S. Y.; Washburn, W. N., *J. Am. Chem. Soc.* **1972**, 94, 3276-3278.
12. Breslow, R.; Corcoran, R. J.; Snider, B. B.; Doll, R. J.; Khanna, P. L.; Kaleya, R., *J. Am. Chem. Soc.* **1976**, 99, 905-915.
13. Breslow, R.; Baldwin, S.; Flechtner, T.; Kalicky, P.; Liu, S.; Washburn, W., *J. Am. Chem. Soc.* **1973**, 95, 3251-3262.
14. Breslow, R.; Heyer, D., *J. Am. Chem. Soc.* **1982**, 104, 2045-2046.
15. Garcia-Granados, A.; Lopez, P. E.; Melguizo, E.; Parra, A.; Simeo, Y. *J. Org. Chem.*, **2007**, 72, 3500-3509.
16. Vioca, A.; Mendoza, A.; Gutekunst, W. R.; Fraga, J. O.; Baran, P. S., *Nature.* **2012**, 4, 629-635.
17. Prier, C. K.; Rankic, D. A.; MacMillan, D. W. C., *Chem. Rev.* **2013**, 113, 5322-5363.

18. Koizumi, T.; Bashir, N.; Kennedy, A. R.; Murphy, J. A., *J. Chem. Soc., Perkin Trans. 1.* **1999**, 3637-3643.
19. Murphy, J. A.; Rasheed, F.; Roome, S. J.; Lewis, N., *Chem. Commun.* **1996**, 737-738.
20. Martin, A.; Perez-Martin, I.; Suarez, E., *Org. Lett.* **2005**, 7, 2027-2030.
21. Han, G.; McIntosh, M. C; Weinreb, S. M., *Tet. Lett.* **1994**, 35, 5813-5816.
22. Newhouse, T.; Baran, P. S., *Angew. Chem. Int. Ed.* **2011**, 50, 3362-3374.
23. Hartwig, J. F., *J. Am. Chem. Soc.* **2016**, 138, 2-24.
24. Goddard, J.; Ollivier, C.; Fensterbank, L., *Acc. Chem. Res.* **2016**, 49, 1924-1936.
25. Ghosh, I.; Marzo, L.; Das, A.; Skaikh, R.; König, B., *Acc. Chem. Res.* **2016**, 49, 1566-1577.
26. Davies, H. M. L.; Morton, D., *J. Org. Chem.* **2016**, 81, 343-350.
27. Bruckl, T.; Baxter, R. D.; Ishihara, Y.; Baran, P. S., *Acc. Chem. Res.* **2012**, 45, 826-839.
28. Galli, C., *Chem. Rev.* **1988**, 88, 765-792.
29. Teegardin, K.; Day, J. I.; Chan, J.; Weaver, J., *Org. Process Res. Dev.* **2016**, 20, 1156-1163.
30. Robertson, J.; Pillai, J.; Lush, R. K., *Chem. Soc. Rev.* **2001**, 30, 94-103.
31. Hari, D. P.; Hering, T.; König, B., *Angew. Chem. Int. Ed.* **2014**, 53, 725-728.
32. (a) Hofmann, A. W., *Ber.* **1883**, 16, 558-560.; (b) Hofmann, A. W., *Ber.* **1885**, 18, 5-23.; (c) Hofmann, A. W., *Ber.* **1885**, 18, 109-131.
33. Eloffson, R. M.; *Can. J. Chem.*, **1958**, 36, 1207.
34. Wawzonek, S.; Thelen, P. J., *J. Am. Chem. Soc.* **1950**, 72, 2118-2120.
35. Corey, E. J.; Hertler, W. R., *J. Am. Chem. Soc.* **1960**, 82, 1657-1668.

CHAPTER 2: REMOTE C-H FUNCTIONALIZATION VIA REDOX CATALYSIS

2.1 Introduction

We envisioned using a guided method of C-H functionalization catalyzed by a visible-light photoredox catalyst. The ability of the catalyst to play a dual role in the transformation by reducing and oxidizing intermediates would eliminate the need for external oxidants or reducing agents. By reacting Baran's *o*-triazenesulfonyl chloride¹ (**2.1**, Figure 2.1) with an alcohol or amine, generation of several sulfonate esters and

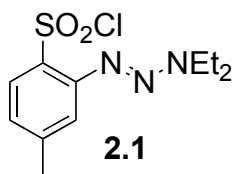


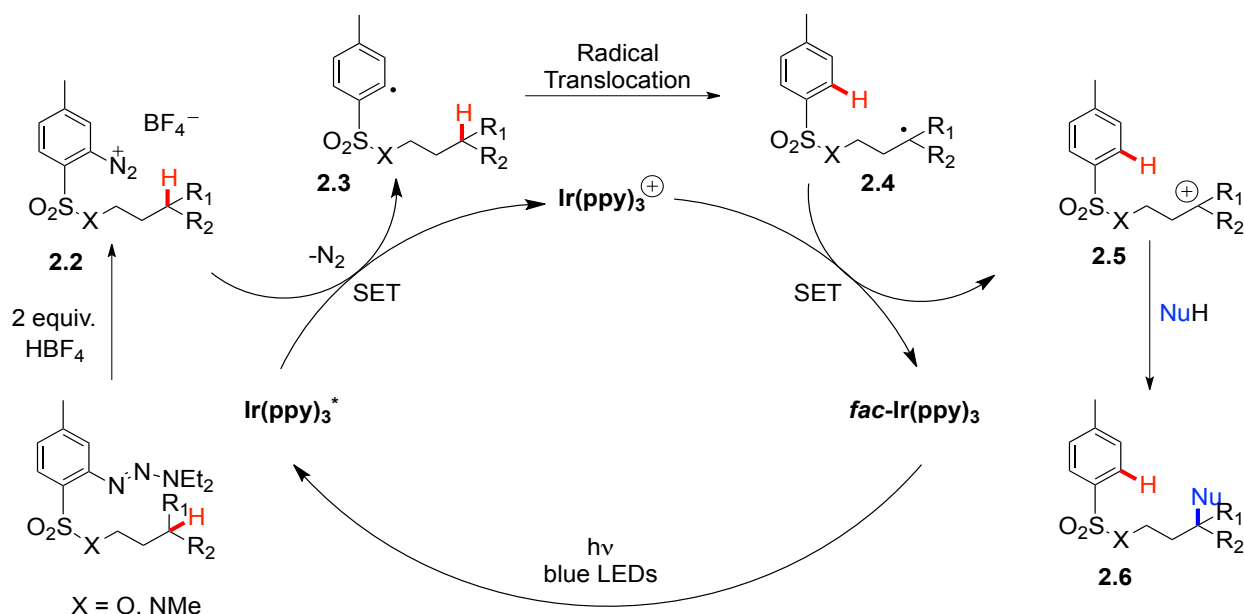
Figure 2.1 *o*-triazenesulfonyl chloride (Tz^oCl)

sulfonamides would be possible, enabling development of a site selective method as this directing group demonstrated a preference for 1-7 hydrogen abstraction¹.

The initial mechanistic proposal (Scheme 2.1) involved release of aryl diazonium ion **2.2** by treatment of the Tz^o substrate with two equivalents of a strong acid such as tetrafluoroboric acid. Irradiation of the photocatalyst *fac*-Ir(ppy)₃ with visible light ($\lambda=455$ nm, 4W blue LEDs) will enable the excited-state transitional metal complex ($E_{1/2}^{IV/*III} = -1.73$ V vs. SCE)² to reduce the formed diazonium ion ($E_{red} = 0.1$ to $+0.5$ V vs. SCE)³ which spontaneously releases nitrogen via homolytic cleavage to furnish aryl radical **2.3**. This high energy, electron-poor radical then translocates as the substrate

*Portions of this chapter previously appeared in [Kyle A. Hollister, Elizabeth S. Conner, Mark, L. Spell, Kristina Deveaux, Léa Maneval, Micheal W. Beal, Justin R. Ragains, Remote Hydroxylation through Radical Translocation and Polar Crossover, 5/26/2015]. They are reprinted by permission of [John Wiley and Sons.]

undergoes a 1,7-hydrogen atom abstraction. The more energetically favorable, stable alkyl radical **2.4** ($E_{\text{ox}} = 0$ to $+0.75$ V vs. SCE)⁴ can then be oxidized to carbocation **2.5** by $\text{Ir}(\text{ppy})_3^+$ ($E_{1/2}^{\text{IV/III}} = +0.77$ V vs. SCE)². Subsequent nucleophilic attack would furnish the desired functionalized product **2.6**. It is important to note that, in the course of this

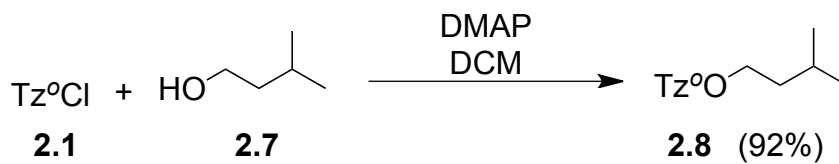


Scheme 2.1 Initial mechanistic proposal for remote functionalization

transformation, the Tz^{o} group is converted to a tosylate, which is a common leaving group in organic synthesis. This provides the opportunity for further functionalization of the substrate.

2.2 Synthesis of Sulfonamides and Sulfonate Esters

To explore our proposed method for remote functionalization, a series of substrates was synthesized using $\text{Tz}^{\text{o}}\text{Cl}$ (Figure 2.1, Scheme 2.2) and commercially available



Scheme 2.2 Synthesis of sulfonate ester for optimization

alcohols and amines. Two general methods were employed¹. For generation of sulfonate esters, the corresponding alcohol reacted with Tz^oCl (**2.1**) in the presence of 4-dimethylaminopyridine in DCM (Scheme 2.2) In this manner, isoamyl alcohol was coupled to the sulfonyl chloride. The corresponding sulfonate ester **2.8** was isolated in 92% yield and used for optimization of this remote functionalization method.

Sulfonamides were synthesized (Figure 2.2) similarly by treatment of several commercially available amines with Tz^oCl (**2.1**) and sodium bicarbonate (instead of

Entry	Substrate	Yield
1	$\text{Tz}^{\text{o}}\text{NH}-\text{CH}_2\text{CH}_2\text{CH}_2\text{CH}_2\text{CH}_3$ 2.9	74%
2	$\text{Tz}^{\text{o}}\text{NH}-\text{CH}_2\text{CH}_2\text{CH}_2\text{CH}_2\text{Ph}$ 2.10	82%
3	$\text{Tz}^{\text{o}}\text{NH}-\text{CH}_2\text{CH}_2\text{CH}(\text{Ph})\text{CH}_2\text{Ph}$ 2.11	84%
4	$\text{Tz}^{\text{o}}\text{NH}-\text{CH}_2\text{CH}_2-\text{C}_6\text{H}_4\text{-OH}$ 2.12	77%
5	$\text{Tz}^{\text{o}}\text{NH}-\text{CH}(\text{CO}_2\text{Me})\text{CH}_2\text{CH}_2\text{CH}_3$ 2.13	64%

Figure 2.2 Isolated yields of sulfonamides

DMAP) in dichloromethane in good yields¹. The results are summarized in Figure 2.2 and range between 64 and 84% yield. Three of the sulfonamides were further subjected to methylation (Figure 2.3). After reacting each substrate with sodium hydride followed

by iodomethane, the corresponding methylated sulfonamides **2.14** to **2.16** were generated in good to excellent yields (91-93%).

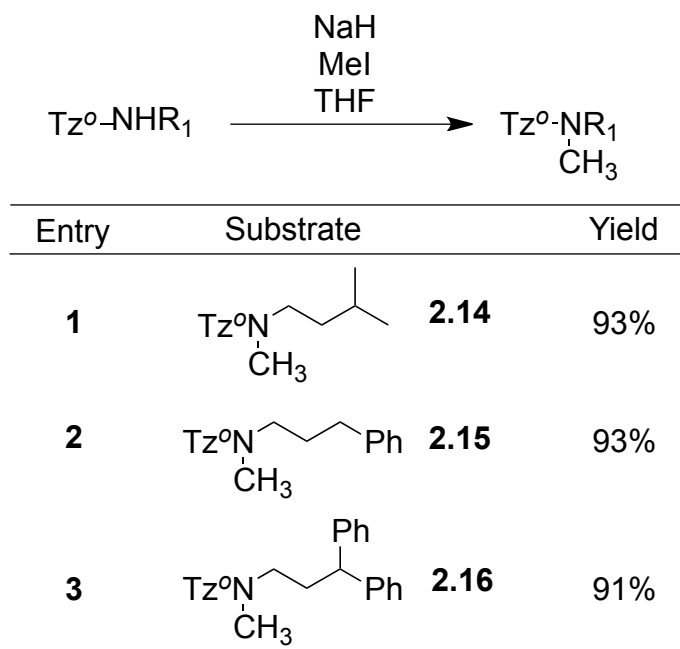
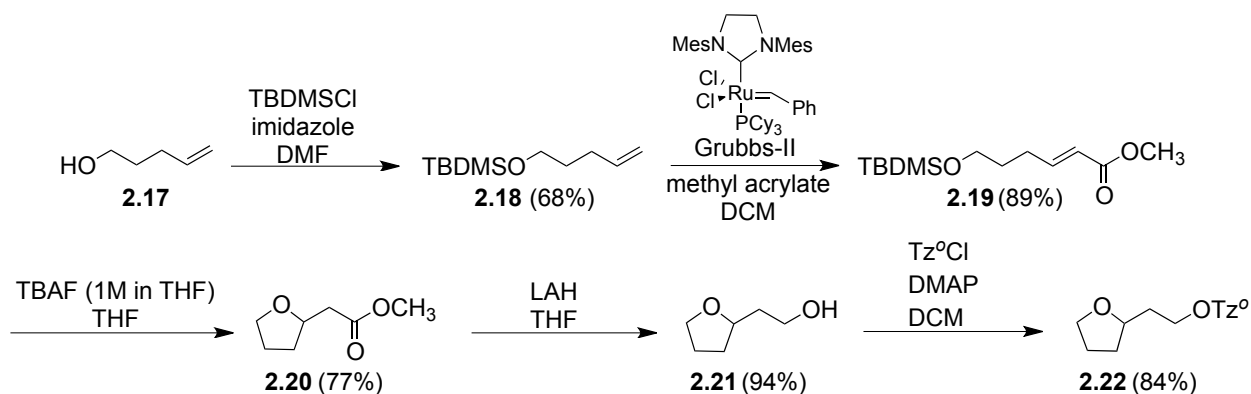


Figure 2.3 Methylation of sulfonamides

Four additional sulfonate esters were synthesized for a study on the substrate scope. With the goal of showing examples of hydroxylation adjacent to a heteroatom, pyrrolidine and tetrahydrofuran derivatives were synthesized. However, since the corresponding alcohol in each case was not commercially available, multi-step synthesis was employed. Sulfonyl ester **2.22** was generated in five steps beginning with silyl protection of pentene-1-ol using TBDMSCl⁷ (Scheme 2.3).

The alcohol was initially protected as Mol and Dinger reported that primary alcohols assist in the degradation of 1st and 2nd generation Grubbs catalysts (Scheme 2.3)⁸. TBDMS protected compound **2.18** was then converted to alpha-beta unsaturated ester **2.19** via cross metathesis with methyl acrylate in the presence of Grubbs 2nd generation catalyst while refluxing in dichloromethane⁹. Formation of intermediate **2.20** was initially

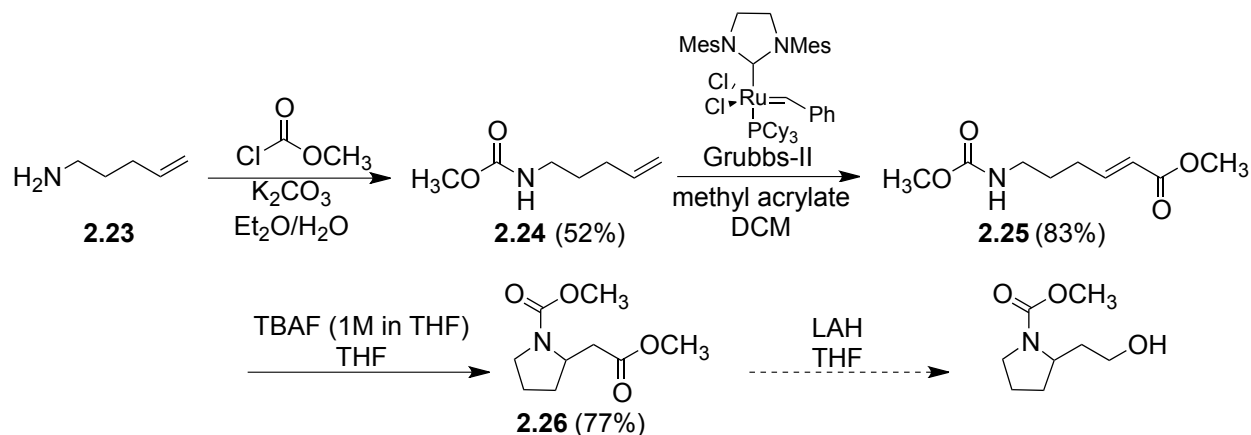


Scheme 2.3 Synthesis of tetrahydrofuran sulfonate ester derivative

a separate deprotection and cyclization procedure however, a paper by Rouche and co workers demonstrated an intramolecular Michael addition using TBAF¹⁰. Their proposed mechanism suggests that TBAF ($\text{Bu}_4\text{N}^+ \text{F}^-$) acts as a mild base¹¹ to deprotonate the alcohol substrate, which then attacks the alkene to furnish the cyclized product. Since TBAF is a common reagent used to liberate alcohols from the corresponding silyl ether, I proposed a one-pot deprotection/Michael addition reaction. By adding an extra equivalent of TBAF, the alcohol was deprotected in situ and the excess TBAF initiated the cyclization. The resulting methyl ester **2.20** was isolated in 77% yield then reduced to the primary alcohol using lithium aluminum hydride¹². To complete the synthesis, **2.21** was converted to the Tz° ester in 84% yield.

Synthesis of the pyrrolidine derivative (**2.26**) followed a similar synthetic pathway (Scheme 2.4). In this case, the amine was protected as the corresponding carbamate. As previously mentioned, amines reductively quench photocatalysts and, for this reason, the final substrate needed to have a protecting group to prevent this undesired process. This sequence of steps, however, came with much trial and error. The initial attempt involved converting the 4-penten-1-amine (**2.23**) to the corresponding methyl *N*-(5-pentenyl)carbamate **2.24** using methyl chloroformate¹³. This product was isolated in

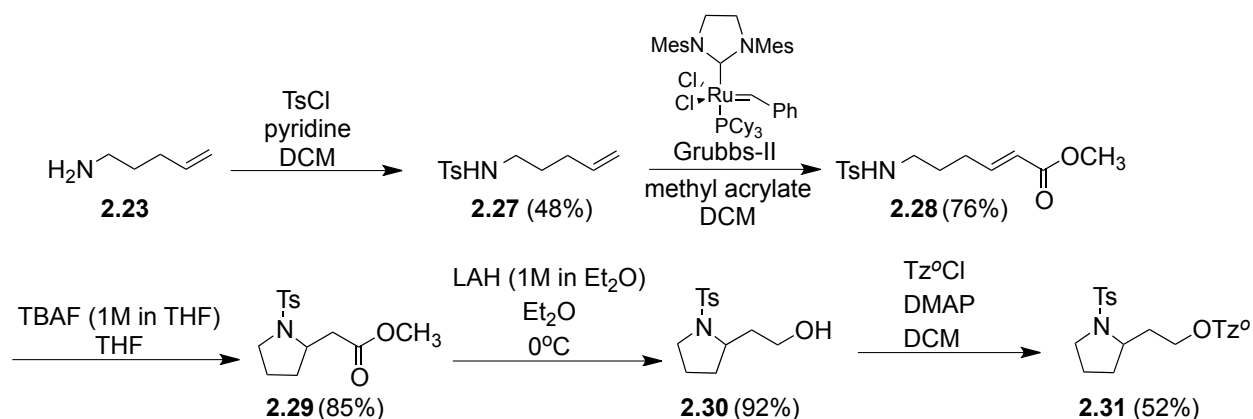
52% yield and was then subjected to cross metathesis with methyl acrylate⁹. The alpha-beta unsaturated ester **2.25** was then cyclized to give heterocycle **2.26** in 77% yield¹⁰. Initial attempts to reduce the ester to the primary alcohol with LAH were futile as reduction of the methyl carbamate protecting group also occurred. This was evident as the crude ¹H NMR spectrum showed loss of both methyl ester and methyl carbamate.



Scheme 2.4 Attempted synthesis of carbamate-protected pyrrolidine derivative

The alternate protecting group proposed was tosylate as it was expected to be less susceptible to reduction but also stable to the acidic conditions of the hydroxylation method¹⁴. Proceeding with synthesis of the sulfonate ester, 4-penten-1-amine was protected as sulfonamide **2.27** using *p*-toluenesulfonyl chloride (TsCl) and pyridine (Scheme 2.5)¹⁵. The resulting compound was then converted to the alpha-beta unsaturated ester via cross metathesis with methyl acrylate in the presence of Grubbs' second-generation catalyst⁹. Intermediate **2.28** was then treated with potassium *tert*-butoxide in an attempt to furnish the tetrahydropyrrole **2.29**, a procedure specifically optimized for aza-Michael additions using tosyl-protected amines¹⁶. This reaction, however, was unsuccessful as trace amounts of the anticipated product were

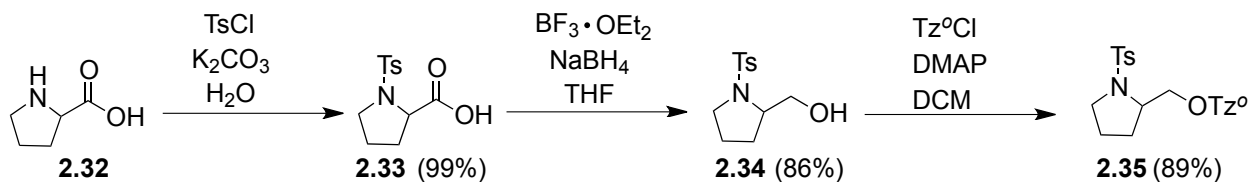
recovered. Alternatively, in the presence of TBAF, compound **2.28** was converted to the tosylated pyrrolidine in 85% yield¹⁰. The methyl ester was successfully reduced to



Scheme 2.5 Successful synthesis of *N*-tosyl sulfonate ester

primary alcohol¹² **2.30** and subsequent coupling with $\text{Tz}^{\text{O}}\text{Cl}$ furnished the sulfonate ester **2.31** in 52% yield.

The third heterocyclic analog synthesized was compound **2.35** (Scheme 2.6). Proline was tosylated using TsCl under basic conditions¹⁷. Subsequent reduction of



Scheme 2.6 Synthesis of *N*-tosyl prolinol sulfonate ester derivative

carboxylic acid **2.33** to the primary alcohol is completed by sodium borohydride in the presence of boron trifluoride diethyletherate¹⁷. The desired substrate was isolated in 89% yield after treatment of prolinol derivative **2.35** with $\text{Tz}^{\text{O}}\text{Cl}$, DMAP and DCM. These compounds were ultimately subjected to the optimized reaction conditions.

2.3 Sulfonamide Substrate Screen

Irradiation of sulfonamide **2.11** under the optimized reaction conditions for 18 hours yielded 28% of the desired hydroxylated product **2.38**. The isoamyl sulfonamide analog **2.9** yielded 29% of the corresponding hydroxyl substituted product, however, the diazenylation product **2.37** shown in Figure 2.4 was also isolated in 11% yield. It is noteworthy that this side reaction was not observed in the reaction with the diphenyl derivative **2.11**. This by-product would arise from another molecule of the diazonium

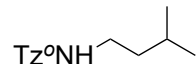
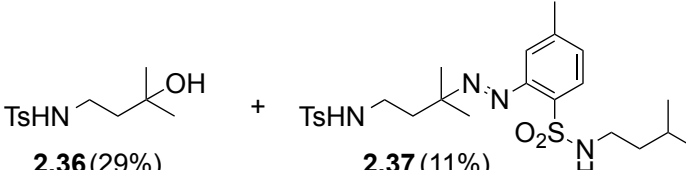
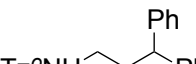
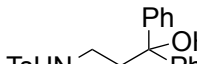
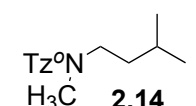
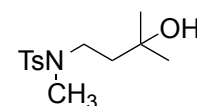
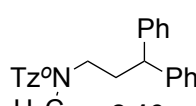
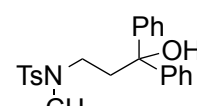
Entry	Substrate	Product(s) (% yield)
1	 2.9	 2.36 (29%) + 2.37 (11%)
2	 2.11	 2.38 (28%)
3	 2.14	 2.39 (33%)
4	 2.16	 2.40 (41%)

Figure 2.4 Results from substrate screen using sulfonamides

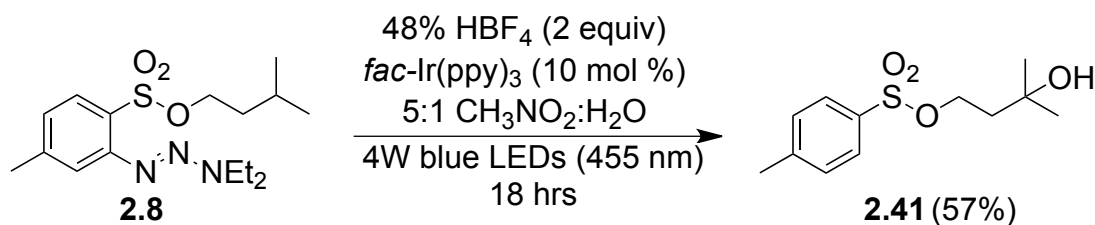
species coupling with the tertiary radical or the carbocation that forms upon radical translocation (Scheme 2.1).

As the experimental results of sulfonamide derivatives show in entries 1 and 2 of Figure 2.4, these substrates produce significantly less of the hydroxylated product than

the corresponding sulfonate ester derivatives. The methylated sulfonamides **2.14** and **2.16** were subjected to the standard conditions (entries 3 and 4, Figure 2.4). Slightly better yields were afforded, 34% and 41% respectively. It is important to note that the diazenylation product was not observed with the methylated analog of **2.9** (Figure 2.4).

2.4 Control Experiments

Treatment of isoamyl sulfonate ester **2.8** with 10 mol% *fac*-Ir(ppy)₃ and 48% aqueous HBF₄ in a 5:1 mixture of MeNO₂/H₂O with vigorous stirring and irradiation for 18 hours with 4W blue LEDs (455 nm) yielded 57% of the hydroxylated product **2.41** (Scheme 2.7)²¹. This result was used as the standard when analyzing the results of the control experiments that are summarized in figure 2.5.



Scheme 2.7 Standard conditions for remote hydroxylation

To gauge the necessity of acid in this method, 48% HBF₄ was omitted. Upon treatment with 2 equivalents of acid, the triazene is expected to generate the diazonium ion, which is then reduced by excited state *fac*-Ir(ppy)₃. For this reason, we predicted that the reaction would not proceed without acid and entry 1 of Figure 2.4 confirmed

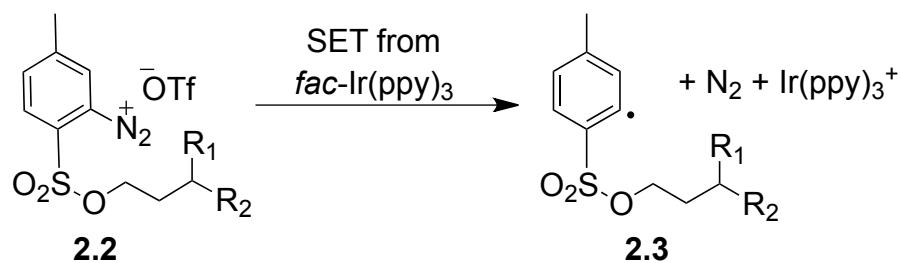
Entry	Deviation from Std. Cond.	Irradiation time (h)	% yield
1	no acid	18	0
2	<i>fac</i> -Ir(ppy) ₃ excluded	18	11
3	light excluded	4	40
4	light excluded	18	50

Figure 2.5 Deviations from standard conditions in Scheme 2.10

this. No desired product was isolated since the reactive species, the diazonium ion, remained masked as the triazene and this confirms that its release is necessary to initiate the reaction.

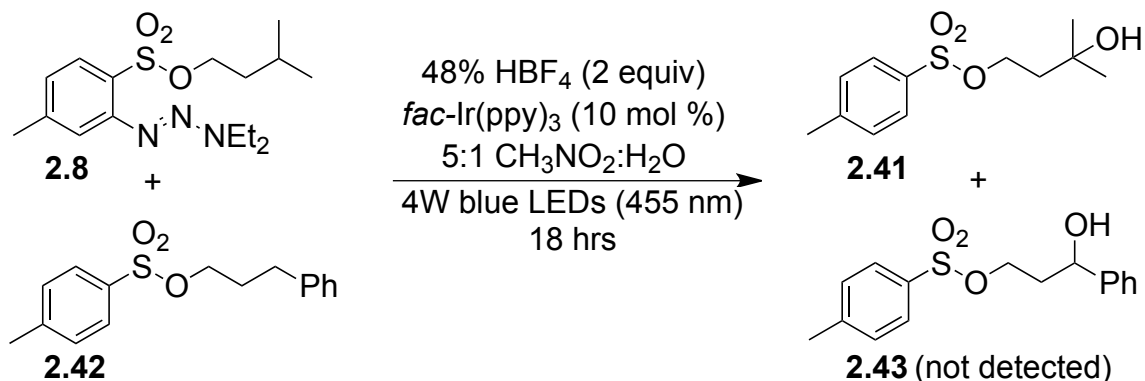
The second control experiment was performed without addition of the iridium catalyst. After 18 hours of irradiation, the hydroxylated product **2.41** was isolated in 11% yield (entry 2, Figure 2.5). This result suggests that the aryl radical is still being generated albeit in lower concentrations than in the presence of *fac*-Ir(ppy)₃. Diazonium salts are known to spontaneously release nitrogen gas while in solution³ and this could account for the small amount of product being generated. Although product was isolated, this reaction shows that the catalyst is necessary as it greatly increases the efficiency of the method with regards to yield and reaction time.

The most enlightening control experiment was performed in the absence of light (entries 3 and 4, Figure 2.5). This reaction was conducted twice for different lengths of time (4 hours and 18 hours). Since we confirmed that the reaction is not initiated until acid has been added, all of the reagents except 48% HBF₄ were added to the reaction before the flask was double wrapped in aluminum foil to omit all light sources. After this was done, HBF₄ was added to the reaction, which was monitored in the dark for the specified amount of time. Surprisingly, the hydroxylated product **2.41** was isolated in 40% after 4 hours while a longer reaction time led to a slightly higher yield of 50%. Formation of the product without irradiation in a percent yield range close to that of the optimized conditions suggests that this reaction is not a true photochemical process. This also implies that ground state *fac*-Ir(ppy)₃² could possibly undergo SET to generate the aryl radical (Scheme 2.8) and ultimately form **2.41**.



Scheme 2.8 Single electron transfer from ground state *fac*-Ir(ppy)₃

Finally, to determine whether or not this transformation was an intramolecular process, one equivalent of 3-phenylpropyl 4-methylbenzenesulfonate (**2.42**) was added to a typical reaction employing the standard conditions (Scheme 2.9). After 18 hours of irradiation, ¹H NMR revealed no hydroxylation of the benzene sulfonate as resonances corresponding to the benzyl alcohol **2.43** were absent. However, evidence of the hydroxylated isoamyl product **2.41** was detected. This result suggests that the radical translocation is an intramolecular event.



Scheme 2.9 Experiment to probe for possible intramolecular processes

2.5 Attempted Hydroxylation of Tetrahydropyrrole and Tetrahydrofuran Derivatives

Experiments using the pyrrolidine and tetrahydrofuran derivatives (**2.22**, **2.31**, and **2.35**) were performed using the standard reaction conditions (2 equiv. 48% HBF₄,

10 mol % *fac*-Ir(ppy)₃, 5:1 CH₃NO₂:H₂O). 1,7 radical translocation from the aryl ring to the tertiary carbon adjacent to the heteroatom in both substrates was expected (Figure 2.6). The neighboring electronegative oxygen or nitrogen would decrease the oxidation

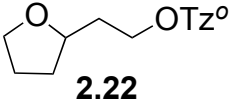
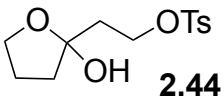
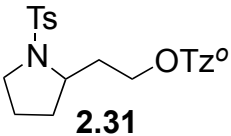
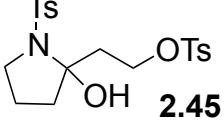
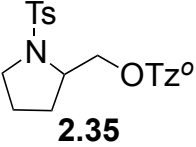
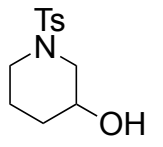
Entry	Substrate	Product
1	 2.22	 2.44 not observed
2	 2.31	 2.45 not observed
3	 2.35	 2.46 (73%)

Figure 2.6 Results from attempted hydroxylation of heterocycle derivatives

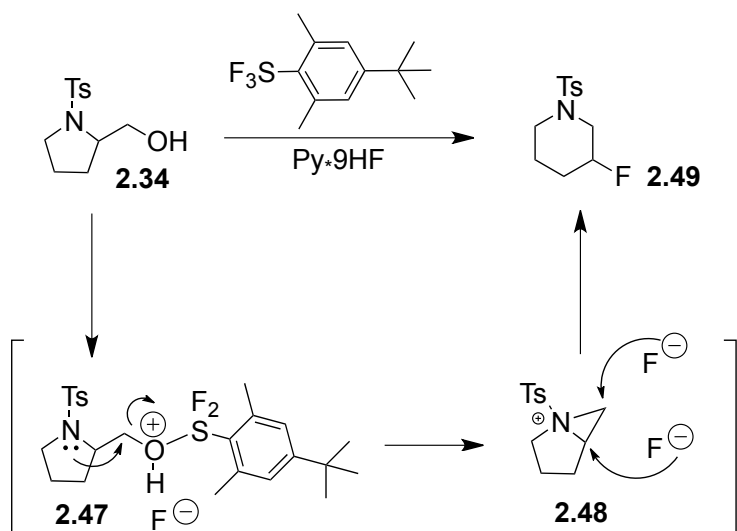
potential²² of the alkyl radical allowing it to be converted easily to the carbocation. This tertiary carbocation would also be resonance stabilized by the presence of the heteroatom.

Initial screening of sulfonyl ester **2.22** under the hydroxylation conditions did not yield the expected product (**2.44**, Figure 2.6). In an effort to troubleshoot the reaction, alternative acids were substituted in place of 48% HBF₄ as there was a concern about degradation of the heterocycle under the strongly acidic conditions. Considering that the pK_a of HBF₄ is -0.44^{23a}, acids that were slightly less acidic but strong enough to liberate the diazonium salt were proposed as alternatives. Attempts to hydroxylate with two equivalents of acetic acid (pK_a: 4.76)^{23b} were unsuccessful. After stirring under

irradiation overnight, there was still no consumption of the sulfonyl ester via TLC. This observation led to the use of the more acidic trifluoroacetic acid (pKa: 0.23)^{23c}. In this case, the diazonium salt was liberated, however, the reaction did not show a clean conversion to hydroxylation product as seen with previous substrates. The ¹H NMR spectrum was complex and suggested degradation of the substrate or product. Similar results were seen with sulfonate ester **2.31** as no product (**2.45**) was observed upon screening with the standard conditions.

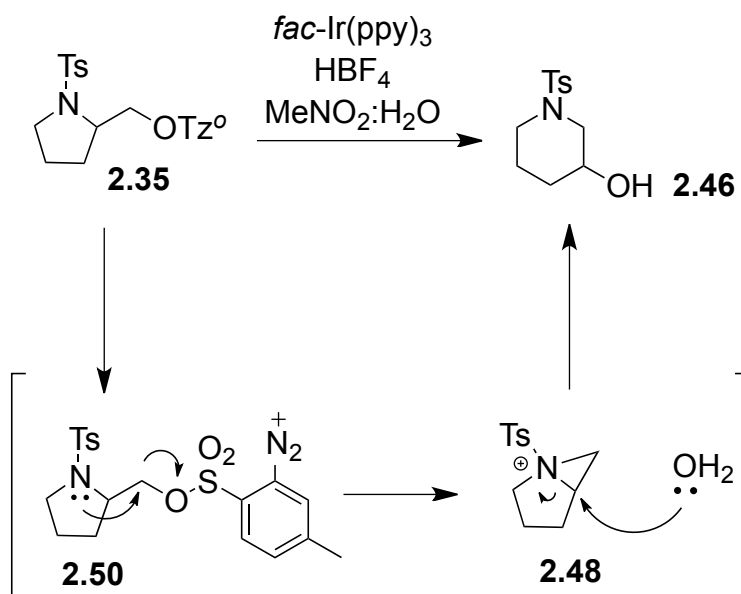
Subjecting the tetrahydropyrrole derivative **2.35** to the hydroxylation conditions did not produce the desired product although when monitoring the reaction by TLC, new spots were observed. The ¹H NMR spectrum looked promising as evidence of a hydroxyl-bearing carbon was present. The crude mixture was purified via flash chromatography in an attempt to identify any products that may have formed. Purification led to compound in **2.46**, and its structure was confirmed based on NMR analysis and comparison to literature reports²⁴.

A paper published by Haufe and coworkers²⁵ provided insight as to how compounds **2.46** formed under the reaction conditions (Scheme 2.10). The authors



Scheme 2.10 Proposed mechanism for Fluorolead-mediated ring expansion

demonstrated that *N*-tosyl prolinol **2.34** could displace a leaving group generated by Fluolead in situ in the presence of Olah's reagent (Py*9HF) (Scheme 2.10). This substitution forms an intermediate aziridinium ion (**2.48**). Subsequent attack by fluorine results in ring expansion and alkyl fluoride **2.49**. Likewise, I proposed that sulfonamide **2.35** could follow a similar pathway in the acidic environment of the standard conditions (Scheme 2.11). Sulfonamide **2.35** would have released the diazonium ion to form the tosylated prolinol **2.50**. Nucleophilic attack by water on **2.48** would explain the hydroxylated product observed (**2.46**).



Scheme 2.11 Proposed mechanism for ring expansion

2.6 Screening of Sulfonamides with Light Excluded

After screening the initial sulfonamides and sulfonate esters with the optimized reaction conditions, efforts were turned to screening several of the substrates in the dark. Such experiments were necessary after the results from the light excluded controls. A comparison of isolated yields of the functionalized products is summarized in

Figure 2.7. In addition to the sulfonamides screened in section 2.5, the 3-phenyl propyl amine (2.15), tyramine (2.12), and methyl leucine (2.13) sulfonamides were subjected to the standard conditions with light excluded.

Similar to the control experiment, when the reactions were performed without irradiation, the hydroxylated products were isolated in nearly the same yields. Of the examples shown, each result was slightly lower than with irradiation with the exception of the tyramine and methyl leucine derivatives (entries 4 and 5, Figure 2.7). The

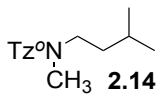
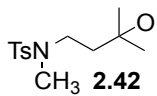
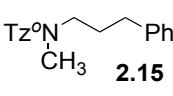
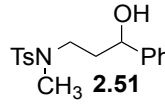
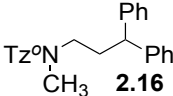
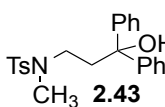
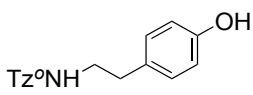
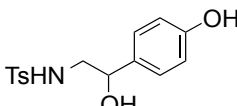
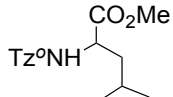
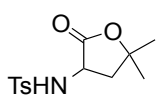
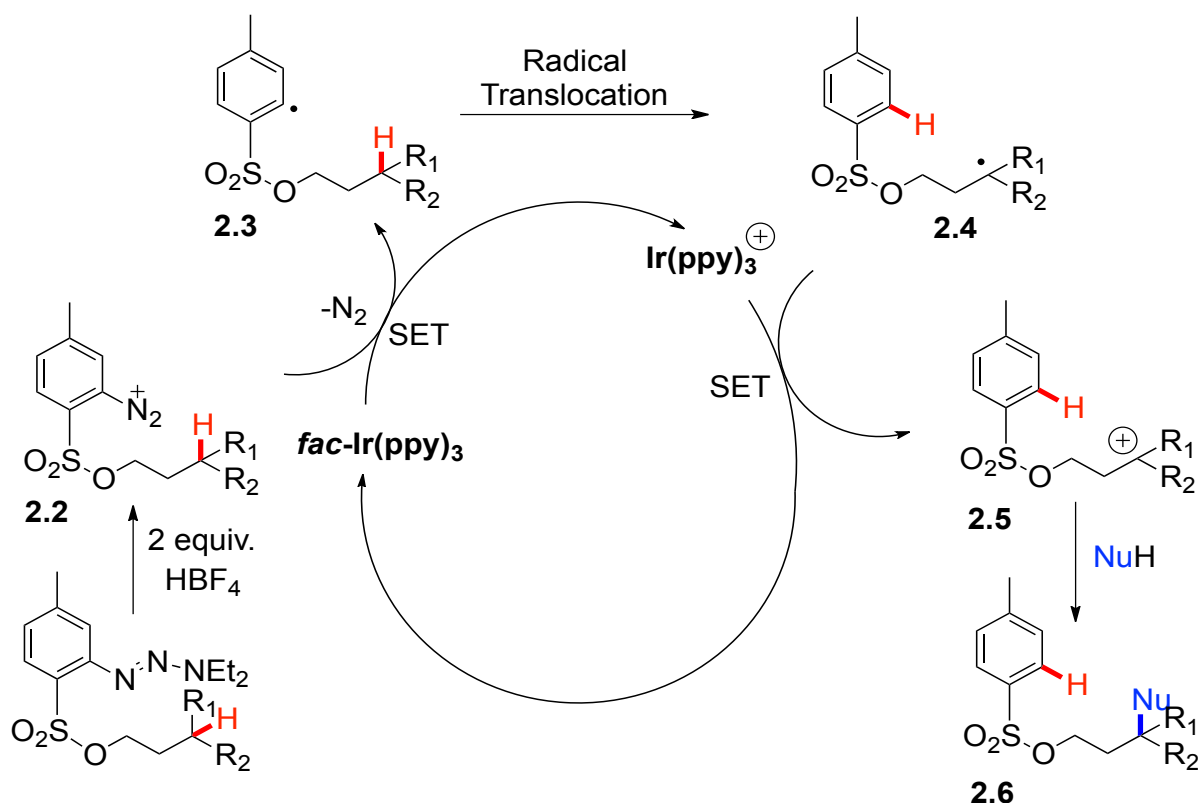
Entry	Substrate	Product	% yield with irradiation	% yield w/o irradiation
1	 2.14	 2.42	34	33
2	 2.15	 2.51	56	51
3	 2.16	 2.43	41	35
4	 2.12	 2.52	56	61
5	 2.13	 2.53	47	48

Figure 2.7 Results from light excluded experiments using sulfonamides

difference, however, is still negligible. These two sulfonamides both produced interesting results. Isolation of 2.52 demonstrated that, when 1,7 hydrogen abstraction is not an option, 1,6 abstraction occurs just as efficiently provided the abstracted hydrogen is

benzylic. From the methyl leucine sulfonamide, compound **2.53** is generated when the carbonyl of the methyl ester attacks the carbocation. Loss of the methoxy group to affords the lactone compound.

Due to the results of the light exclusion experiments we proposed a mechanistic hypothesis (Scheme 2.12) similar to the initial mechanism proposed in Scheme 2.1. Instead of SET from the excited species, electron transfer would occur from ground state *fac*-Ir(ppy)₃ ($E_{1/2}^{IV/III} = +0.77$ V vs. SCE)² to the diazonium ion **2.2** ion ($E_{red} = 0.1$ to



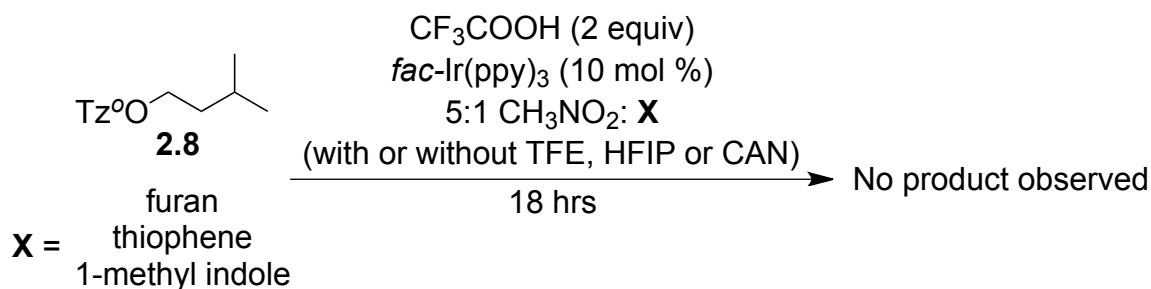
Scheme 2.12 Mechanistic hypothesis for light excluded experiments

+0.5 V vs. SCE)³. This process seems quite unfavorable however, when paired with the subsequent irreversible release of N₂, SET could happen. Radical translocation affords the tertiary radical **2.4** that can return the catalyst to ground state by SET to furnish the

carbocation **2.5**. The functionalized product **2.6** is then generated after nucleophilic attack of the carbocation.

2.7 Attempted Arylation Using Nucleophilic Arenes as Cosolvents

After observing the hydroxylation of the isoamyl sulfonate ester (**2.8** Scheme 2.7), the next goal was to exploit the intermediate carbocation by employing other nucleophiles. Nucleophilic arenes such as furan, thiophene and 1-methyl indole were used as cosolvents **X** in place of water (Scheme 2.13). Since the acid in the standard conditions was an aqueous tetrafluoroboric acid solution, it was substituted with trifluoroacetic acid to completely eliminate water from the experiment. The use of 10 mol % *fac*-Ir(ppy)₃ and nitromethane remained the same and the reactions were observed for 18 hours.



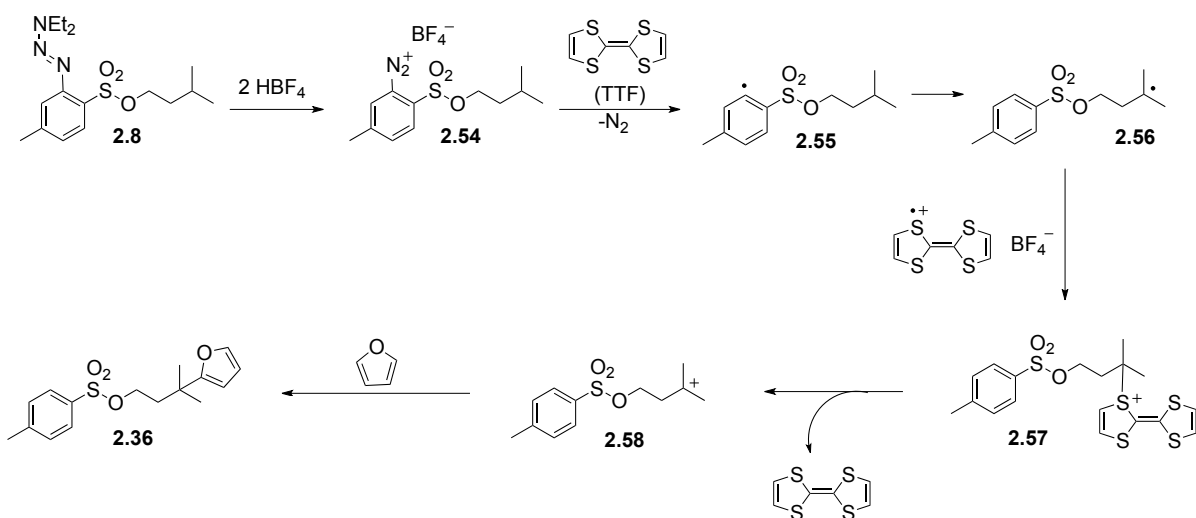
Scheme 2.13 Conditions for the attempted arylation of isoamyl sulfonate ester

Initial experiments performed with the nucleophilic arenes were unsuccessful. After analysis of the crude ¹H NMR showed none of the desired product, several additives were used to attempt to promote intermediate formation. The first additive used was hexafluoroisopropanol (HFIP) in a 5:1:1 ratio of CH_3NO_2 :**X**:HFIP. We hypothesized that the polar environment resulting from water in the standard reaction conditions was necessary for carbocation formation. Therefore, a polar additive was

employed. Unfortunately, HFIP and subsequent attempts using trifluoroethanol (5:1:1 ratio of CH_3NO_2 :**X**:TFE) were ineffective.

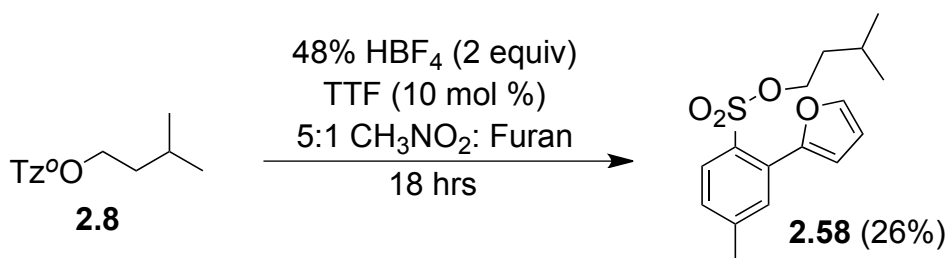
Next, to further encourage formation of the carbocation, an external oxidant was added in an effort to generate a higher concentration of $\text{Ir}(\text{ppy})_3^+$. To accomplish this, tris(4-bromophenyl)ammoniumyl hexachloroantimonate (TBAH) and ceric ammonium nitrate (CAN) were used as additives (5 mol %). In each of these six experiments (each oxidizing agent and the three nucleophilic arenes) none of the arylated product was observed.

The final attempt to arylate the tertiary carbon involved the use of an alternative reagent for single electron transfer and radical-polar crossover. Murphy and coworkers demonstrated that tetrathiofulvalene (TTF) was capable of SET and the intermediate radical cation facilitates radical-polar crossover²⁶. For this reason, we hypothesized that release of diazonium ion **2.54** in the presence of TTF would generate aryl radical **2.55** (Scheme 2.14). Subsequent translocation and radical-polar crossover would afford carbocation **2.58** followed by nucleophilic attack by furan.



Scheme 2.14 Mechanistic hypothesis for TTF-promoted hydroxylation

We substituted *fac*-Ir(ppy)₃ with 10 mol % TTF and used 48% HBF₄ to release the diazonium ion (Scheme 2.15). The isoamyl substrate **2.8** was stirred with these reagents in a 5:1 mixture of CH₃NO₂ and furan. After 18 hours, there was no desired product present in the crude ¹H NMR spectrum, however, column chromatography resulted in the isolation of compound **2.58**. This result suggests that reaction of the aryl radical with furan competes with radical translocation and efforts to discourage this process will be considered in the future.



Scheme 2.15 Conditions for attempted TTF-promoted arylation

2.8 Conclusion

In summary, we have demonstrated that catalyst and acid are vital to good isolated yields of the functionalized product of a variety of sp³ C-H bonds. However, we have also shown that this is not a photoredox process since the transformation proceeds in an efficient manner in the absence of light. Attempts to hydroxylate the pyrrolidine and tetrahydrofuran derivatives were ineffective though the ring expansion results were intriguing and warrant further research. Finally, efforts made to employ nucleophilic arenes were unsuccessful and resulted in addition of the nucleophile to the aryl radical.

Overall, however, this method represents a mild and efficient procedure for site-selective installation of hydroxyl groups at remote C-H sites. The tosylate generated in

the product is also useful as the leaving group can be further functionalized by other nucleophiles. Future work on this project will address the issues encountered with employment of alternative nucleophiles and hydroxylation of heterocycles.

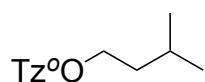
2.9 Experimental

2.9.1 General Methods

^1H NMR and ^{13}C NMR spectroscopy was conducted using a Bruker AV-400 or AV-500 spectrometer. Mass spectra were attained using an Agilent 6210 electrospray time-of-flight mass spectrometer. Optical rotation was measured using a JASCO P-2000 polarimeter. All materials were received from commercial suppliers and used without further purification. Flash column chromatography was accomplished using high purity grade 60 Å silica gel (Fluka[®] Analytical). Qualitative TLC was performed on aluminum sheets (Merck, silica gel, F254) and observed via UV absorption (254 nm) and staining with anisaldehyde or KMnO_4 . Deuterated solvents were acquired from Cambridge Isotope Labs. Tz°Cl and all Tz° -containing compounds were synthesized according to literature procedure.¹ All reactions were carried out under an atmosphere of dry nitrogen. Remote hydroxylation reactions were conducted in round bottom flasks and irradiated with 4W blue LEDs (Creative Lighting Solutions, $\lambda_{\text{max}} = 455 \text{ nm}$), which were wrapped around a crystallizing dish or kept in the dark by wrapping the flask in aluminum foil.

2.9.2 Procedures and Characterization

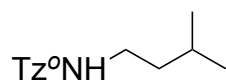
Synthesis of **2.8**:



Started with 1.0 g (3.5 mmol) Tz°Cl , 0.243 g (2.76 mmol) isoamyl alcohol, 0.675

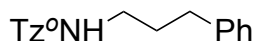
g (5.53 mmol) DMAP and 5.6 mL CH₂Cl₂. Silica gel chromatography (gradient run from 10% EtOAc in hexanes to 20% EtOAc in hexanes) afforded 0.895 g (95%) of a yellow oil. Spectral data matched that previously reported in literature.²¹

Synthesis of **2.9**:



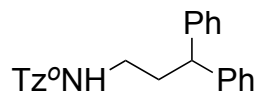
Started with 0.300 g (1.04 mmol) Tz^oCl, 0.17 mL (1.5 mmol) isoamyl amine, 4.5 mL sat. NaHCO₃, and 4.5 mL CH₂Cl₂. Silica gel chromatography (20% EtOAc in hexanes) afforded 0.261 g (74%) of a yellow oil. Spectral data matched that previously reported in literature.²¹

Synthesis of **2.10**:



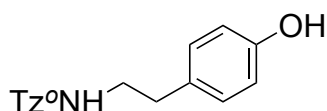
Started with 0.300 g (1.04 mmol) Tz^oCl, 0.21 mL (1.5 mmol) 3-phenylpropylamine, 4.5 mL sat. NaHCO₃, and 4.5 mL CH₂Cl₂. Silica gel chromatography (gradient run from 5% EtOAc in hexanes to 20% EtOAc in hexanes) afforded 0.330 g (82%) of an orange oil. ¹H NMR (400 MHz, CDCl₃) δ 7.82 (d, *J* = 8.0 Hz, 1H), 7.38 (t, *J* = 1.3 Hz, 1H), 7.27 – 7.20 (m, 2H), 7.19 – 7.14 (m, 1H), 7.10 – 7.05 (m, 2H), 7.02 (ddd, *J* = 8.1, 1.7, 0.8 Hz, 1H), 5.56 (t, *J* = 6.4 Hz, 1H), 3.85 (app. d, *J* = 6.9 Hz, 2H), 3.75 (app. d, *J* = 6.7 Hz, 2H), 2.92 (q, *J* = 6.8 Hz, 2H), 2.65 – 2.55 (m, 2H), 2.39 (s, 3H), 1.82 – 1.72 (m, 2H), 1.43 – 1.22 (m, 6H). ¹³C NMR (126 MHz, CDCl₃) δ 147.5, 144.0, 141.3, 129.3, 129.2, 128.6, 128.5, 126.1, 125.7, 118.3, 50.0, 43.4, 42.5, 33.1, 31.6, 21.8, 14.6, 11.4; HRMS *m/z* calcd for C₂₀H₂₉N₄O₂S [M+H]⁺ 389.2006, found 389.2000.

Synthesis of **2.11**:



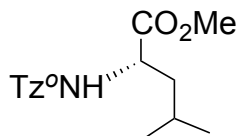
Started with 0.150 g (0.520 mmol) Tz^oCl, 0.153 g (0.720 mmol) 3,3-diphenylpropylamine, 2 ml sat. NaHCO₃ and 2 mL CH₂Cl₂. Silica gel chromatography (15% EtOAc in hexanes) afforded 0.202 g (84%) of an off-white residue. Spectral data matched that previously reported in literature.²¹

Synthesis of **2.12**:



Started with 0.200 g (0.690 mmol) Tz^oCl, 0.133 g (0.970 mmol) tyramine, 3 ml sat. NaHCO₃ and 3 mL CH₂Cl₂. Silica gel chromatography (gradient run from 20% EtOAc in hexanes to 40% EtOAc in hexanes) afforded 0.207 g (77%) of a yellow oil. Spectral data matched that previously reported in literature.²¹

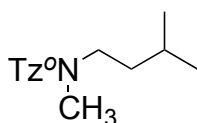
Synthesis of **2.13**:



To a round bottom flask containing 0.263 mg (1.45 mmol) L-leucine methyl ester HCl salt², 9.0 mL sat. NaHCO₃ and 4.5 mL CH₂Cl₂ was added a solution of 0.300 g (1.04 mmol) Tz^oCl in 1 mL CH₂Cl₂ dropwise. The resulting mixture was allowed to stir under N₂ at room temperature for 15 h until complete consumption of starting material was observed via TLC. The aqueous layer was then separated from the organic layer

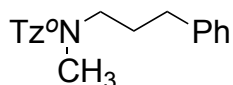
and extracted with 3 x 10 mL CH₂Cl₂. The combined organic layers were dried over Na₂SO₄, filtered and concentrated *in vacuo*. Silica gel chromatography (gradient run from 10% EtOAc in hexanes to 20% EtOAc in hexanes) afforded 0.266 g (64%) of a pale yellow solid. Spectral data matched that previously reported in literature¹.

Synthesis of **2.14**:



To a stirred 0°C solution of 0.261 g (0.770 mmol) **2.11** in 12 mL dry THF was added 0.037 g (0.92 mmol) 60% oil-dispersed sodium hydride. After 1 hour, the reaction mixture was removed from the ice bath and placed in an 80°C oil bath. 0.11 mL (2.4 mmol) iodomethane was then added. After 2 hours, the reaction mixture was removed from the oil bath and allowed to cool. 15 mL H₂O was then added at once followed by 15 mL CH₂Cl₂ and the layers were separated. The aqueous layer was extracted with an additional 2 x 15 mL CH₂Cl₂. The combined organic layers were dried over Na₂SO₄, filtered and concentrated. Silica gel chromatography (12 g silica gel, gradient run from 5% EtOAc in hexanes to 10% EtOAc in hexanes) afforded 0.255 g (93%) of a pale yellow oil. Spectral data matched that previously reported in literature.²¹

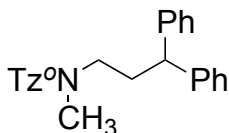
Synthesis of **2.15**:



For procedure, see synthesis of **2.14**. Started with 0.330 g (0.850 mmol) **2.10**, 0.041 g (1.02 mmol) 60 % oil-dispersed sodium hydride, 0.13 mL (2.0 mmol) iodomethane and 13.5 mL dry THF. Obtained 0.320 g (93%) of an orange oil. ¹H NMR

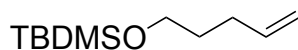
(500 MHz, CDCl₃) δ 7.79 (d, *J* = 8.1 Hz, 1H), 7.36 – 7.22 (m, 3H), 7.20 – 7.11 (m, 3H), 6.99 (d, *J* = 8.1 Hz, 1H), 3.80 (s, 4H), 3.24 (t, *J* = 7.2 Hz, 2H), 2.85 (s, 3H), 2.63 (t, *J* = 8.0 Hz, 2H), 2.38 (s, 3H), 1.86 (t, *J* = 7.7 Hz, 2H), 1.34 (s, 3H), 1.23 (s, 3H); ¹³C NMR (126 MHz, CDCl₃) δ 149.3, 143.8, 141.7, 130.8, 128.5, 128.4, 125.9, 125.3, 119.6, 49.8, 49.1, 41.8, 34.7, 32.9, 29.7, 21.6, 14.6, 11.5; HRMS (*m/z*) calcd for C₂₁H₃₁N₄O₂S [M+H]⁺ 403.2162, found 403.2162.

Synthesis of **2.16**:



For procedure, see synthesis of **2.14**. Started with 0.282 g (0.610 mmol) **2.11**, 0.029 g (0.73 mmol) 60 % oil-dispersed sodium hydride, 0.09 mL (2 mmol) iodomethane and 9.5 mL dry THF. Obtained 0.265 g (91%) of a viscous yellow oil. Spectral data matched that previously reported in literature.²¹

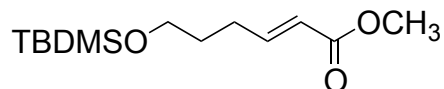
Synthesis of **2.18**:



1.50 g (17.4 mmol) 4-pentene-1-ol was dissolved in 58.0 mL DMF under N₂ and cooled to 0°C. 3.41 g (22.6 mmol) *tert*-butyldimethylsilyl chloride and 3.56 g (52.3 mmol) imidazole was then added to the solution and the reaction slowly warmed to room temperature and stirred overnight. The solution was diluted with 110 mL 1M HCl (aq) and extracted with Et₂O (2 x 120 mL). The organic layers were concentrated and the resulting residue was partitioned between 110 mL 10% LiBr (aq) and Et₂O (2 x 120 mL) then dried over MgSO₄. Purification of the crude material via flash chromatography on

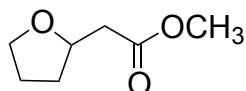
silica gel (10% DCM in hexanes) afforded 2.36 g (68%) of a colorless oil, known compound **2.18**. Spectral data matched that previously reported in literature.⁴

Synthesis of **2.19**:



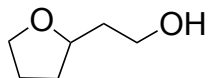
7.14 g (74.9 mmol) methyl acrylate was added to a solution of 1.50 g (7.49 mmol) **2.19** and 0.064 g (0.075 mmol) Grubbs 2nd generation catalyst in CH₂Cl₂ under N₂. The solution was refluxed overnight in an oil bath. Upon cooling to room temperature, the solvent was evaporated and the crude mixture was purified via flash chromatography on silica gel (3% EtOAc in hexanes) to afford 1.72 g (89%) of colorless oil, known compound **2.19**. Spectral data matched that reported in literature.⁹

Synthesis of **2.20**:



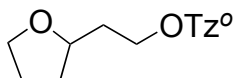
0.300 g (1.16 mmol) **2.19** was dissolved in 5.4 mL THF under N₂ followed by the addition of 5.1 mL (5.1 mmol) 1M TBAF in THF and the reaction stirred overnight at room temperature. To the reaction mixture was added 10 mL H₂O and 10 mL sat. NaHCO₃ (aq). The aqueous layer was extracted with CH₂Cl₂ (2 x 10 mL) and washed with 10 mL sat. NaCl (aq) then dried over MgSO₄. Purification of the crude material via flash chromatography on silica gel (15% EtOAc in hexanes) afforded 0.128 g (77%) of a pale yellow oil, known compound **2.20**. Spectral data matched that previously reported in literature.⁶

Synthesis of **2.21**:



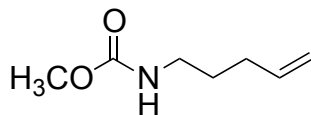
0.100 g (0.694 mmol) **2.20** was dissolved in 10 mL Et₂O under N₂ and cooled to 0°C followed by the slow addition of a solution of 0.053 g (1.4 mmol) LAH in 14 mL Et₂O. The mixture stirred at 0°C for 30 mins then continued stirring at room temperature for 3 hrs. The solution was once again cooled to 0°C then treated with 2.2 mL 5M NaOH, filtered, washed with THF (3 x 5 mL) and concentrated to yield 0.076 g (94%) of a colorless oil which required no further purification. Spectral data matched that previously reported in literature.³³

Synthesis of **2.22**:



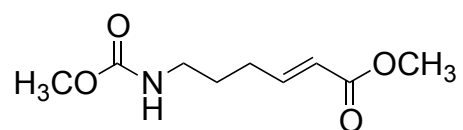
Started with 0.237 g (0.817 mmol) Tz^oCl, 0.076 g (0.65 mmol) **2.21**, 0.160 g (1.31 mmol) DMAP and 1.3 mL CH₂Cl₂. Silica gel chromatography (gradient run from 10% EtOAc in hexanes to 25% EtOAc in hexanes) afforded 0.201 g (84%) of an orange oil. ¹H NMR (400 MHz, CDCl₃) δ 7.83 (d, *J* = 8.1 Hz, 1H), 7.36 (s, 1H), 6.98 (d, *J* = 8.1 Hz, 1H), 4.13 (t, *J* = 6.6 Hz, 2H), 3.87 – 3.74 (m, 6H), 3.63 (q, *J* = 7.4 Hz, 1H), 2.38 (s, 3H), 1.95 – 1.86 (m, 1H), 1.85 – 1.77 (m, 4H), 1.45 – 1.38 (m, 1H), 1.34 (t, *J* = 7.0 Hz, 3H), 1.26 (t, *J* = 6.9 Hz, 3H). ¹³C NMR (100 MHz, CDCl₃) δ 149.3, 145.2, 130.6, 126.0, 125.2, 118.4, 75.6, 68.0, 67.7, 49.4, 42.4, 35.0, 31.3, 25.6, 21.8, 14.6, 11.4; HRMS *m/z* calcd for C₁₇H₂₇N₃O₄S (M+Na)⁺ 370.1780, found 370.1805.

Synthesis of **2.24**:



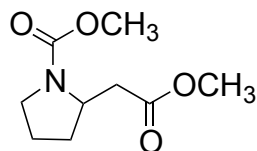
To a solution of 1.0 g (12 mmol) 4-penten-1-amine in 11 mL Et₂O was added a solution of 5.2 g (37 mmol) K₂CO₃ in 15 mL H₂O. 1.4 mL (17 mmol) methyl chloroformate was added dropwise over 30 minutes and the reaction was stirred at room temperature for 1 hour. The aqueous layer was separated and organic layer was washed with 20 mL 1N HCl, 20 mL sat. NaCl (aq), and dried over MgSO₄. Upon filtration, solvent was evaporated to give x g crude material. Silica gel chromatography (gradient run from 5% EtOAc in hexanes to 15% EtOAc in hexanes) afforded 0.898 g (52%) of a colorless liquid. Spectral data matched that previously reported in literature.²⁹

Synthesis of **2.25**:



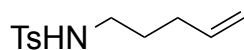
5.0 mL (55 mmol) methyl acrylate was added to a solution of 0.790 g (5.52 mmol) **2.24** and 0.047 g (0.055 mmol) Grubbs 2nd generation catalyst in 20 mL CH₂Cl₂ under N₂. The solution was refluxed overnight in an oil bath. Upon cooling to room temperature, the solvent was evaporated and the crude mixture was purified via flash chromatography on silica gel (35% EtOAc in hexanes) to afford 0.917 g (83%) of colorless oil, known compound **2.25**. Spectral data matched that previously reported in literature.²⁷

Synthesis of **2.26**:



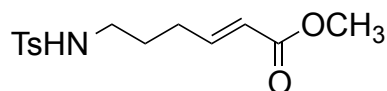
0.100 g (0.500 mmol) **2.25** was dissolved in 5.0 mL THF under N₂ and cooled to 0°C followed by the addition of 0.55 mL (0.55 mmol) 1M TBAF in THF. The reaction was allowed to warm slowly to room temperature and stirred overnight. The mixture was quenched with 7 mL sat. NH₄Cl (aq) and extracted with EtOAc (2 x 7 mL) then dried over MgSO₄. Purification of the crude material via flash chromatography on silica gel (25% EtOAc in hexanes) afforded 0.076 g (76%) of a colorless oil. Spectral data matched that previously reported in literature.²⁸

Synthesis of **2.27**:



To a solution of 1.1 g (12 mmol) 4-penten-1-amine in 24 mL CH₂Cl₂ was added in succession 2.6 g (13 mmol) TsCl and 3.0 mL (36 mmol) pyridine under N₂. The reaction stirred overnight at room temperature, then 24 mL H₂O and 24 mL Et₂O was added. The aqueous layer was extracted with Et₂O (2 x 24 mL) then washed with 24 mL sat. NaCl (aq) and dried over MgSO₄. Purification of the crude material via flash chromatography on silica gel (40% EtOAc in hexanes) afforded 1.4 g (48%) of a pale yellow oil. Spectral data matched that reported in literature.²⁹

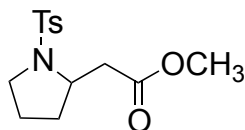
Synthesis of **2.28**:



4.5 mL (58 mmol) methyl acrylate was added to a solution of 1.2 g (5.0 mmol) **2.27** and 0.43 g (0.059 mmol) Grubbs 2nd generation catalyst in 20 mL CH₂Cl₂ under N₂. The solution was refluxed overnight in an oil bath. Upon cooling to room temperature, the solvent was evaporated and the crude mixture was purified via flash

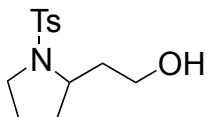
chromatography on silica gel (35% EtOAc in hexanes) to afford 1.13 g (76%) of a colorless oil. Spectral data matched that reported in literature.³⁰

Synthesis of **2.29**:



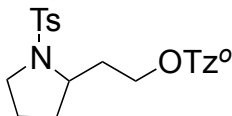
0.500 g (1.680 mmol) ester **2.28** was dissolved in 17.0 mL THF under N₂ and cooled to 0°C followed by the addition of 1.85 mL (1.85 mmol) 1M TBAF in THF. The reaction was allowed to warm slowly to room temperature and stirred overnight. The mixture was quenched with 25 mL sat. NH₄Cl (aq) and extracted with EtOAc (2 x 25 mL) and then dried over MgSO₄. Purification of the crude material via flash chromatography on silica gel (25% EtOAc in hexanes) afforded 0.425 g (85%) of a white solid. Spectral data matched that reported in literature.³¹

Synthesis **2.30**:



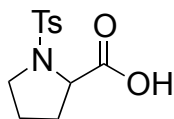
0.311 g (1.05 mmol) **2.29** was dissolved in 3.4 mL Et₂O under N₂ followed by the slow addition of 0.34 mL (0.340 mmol) 1M LAH in Et₂O at room temperature. The mixture stirred for 3 hours, then the solution was cooled to 0°C and then treated sequentially with 2.5 mL Et₂O, 0.06 mL H₂O, 0.06 mL 1N NaOH, and 0.19 mL H₂O. The precipitate was filtered and the filtrate was dried over Na₂SO₄, filtered and concentrated to yield 0.261 g (92%) of a pale yellow oil which required no further purification. Spectral data matched that reported in literature.³²

Synthesis of **2.31**:



Started with 0.067 g (0.23 mmol) Tz^oCl, 0.050 g (0.19 mmol) **2.30**, 0.046 g (0.37 mmol) DMAP, and 0.40 mL CH₂Cl₂. Silica gel chromatography (gradient run from 10% EtOAc in hexanes to 40% EtOAc in hexanes) afforded 0.051 g (52%) of a yellow oil. ¹H NMR (400 MHz, CDCl₃) δ 7.84 (d, *J* = 8.1 Hz, 1H), 7.66 (d, *J* = 8.0 Hz, 2H), 7.39 (s, 1 H), 7.29 (d, *J* = 7.9 Hz, 2H), 7.00 (d, *J* = 8.0 Hz, 1H) 4.17 (t, *J* = 6.2 Hz, 2H), 3.83 (q, *J* = 7.12 Hz, 4H), 3.66 (quin, *J* = 6.4 Hz, 1H), 3.34 (quin, *J* = 5.7 Hz, 1H), 3.17 – 3.11 (m, 1H) 2.42 (s, 3H), 2.40 (s, 3H), 2.31 - 2.23 (m, 1H), 1.88 – 1.79 (m, 1H), 1.62 – 1.57 (m, 3H), 1.46 – 1.40 (m, 1 H), 1.36 (t, *J* = 7.0 Hz, 3H), 1.29 (t, *J* = 7.1 Hz, 3H); ¹³C NMR (100 MHz, CDCl₃) δ 149.2, 145.2, 143.4, 134.2, 130.4, 129.7, 127.5, 125.8, 125.0, 118.3, 67.7, 57.7, 49.3, 49.0, 42.4, 35.6, 31.1, 24.0, 21.7, 21.5, 14.5, 11.3; HRMS *m/z* calcd for C₂₄H₃₄N₄O₅S₂ (M+Na)⁺ 523.2080, found 523.2051.

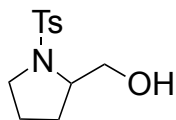
Synthesis of **2.33**:



To a solution of 5.0 g (43 mmol) proline in 43.4 mL H₂O at 0°C was added 12.6 g (91.2 mmol) K₂CO₃ added followed by 9.9 g (52 mmol) TsCl in three portions over 1 hour. The reaction mixture warmed slowly to room temperature over night and was subsequently acidified to pH 2 using conc. HCl and then extracted with 250 mL CH₂Cl₂. The organic layer was dried over Na₂SO₄, filtered, and solvent was removed *in vacuo*. Crude material was redissolved in CH₂Cl₂ and the product was precipitated with

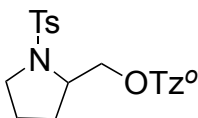
pentane to give 11.6 g (quantitative yield) of a white solid. Spectral data matched that previously reported in literature.¹⁷

Synthesis of **2.34**:



To a mixture of 3.3 g (86 mmol) NaBH₄ in 75 mL dry THF at 0°C was added 13.9 mL (113 mmol) BF₃·OEt₂ dropwise over 1 hour. A solution of 11.6 g (43.1 mmol) **2.33** in 55 mL dry THF was added dropwise to the reaction, which was then allowed to warm slowly to room temperature overnight. Slow addition of 75 mL MeOH quenched the reaction followed by addition of 50 mL 10% HCl (aq). The resulting solution was stirred at 60°C in an oil bath. After two hours, the reaction was cooled to room temperature and neutralized to pH 7 with 29 mL 3N NaOH. Volatiles were removed *in vacuo* and product was extracted into 30 mL CH₂Cl₂. Concentration afforded 9.4 g (86%) of a white solid that required no further purification. Spectral data matched that previously reported in literature.¹⁷

Synthesis of **2.35**:

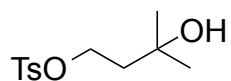


Started with 0.500 g (1.73 mmol) Tz^oCl, 0.353 g (1.38 mmol) **2.34**, 0.337 g (2.76 mmol) DMAP and 2.8 mL CH₂Cl₂. Silica gel chromatography (gradient run from 10% EtOAc in hexanes to 30% EtOAc in hexanes) afforded 0.627 g (89%) of a white solid. ¹H NMR (400 MHz, CDCl₃) δ 7.86 (d, *J* = 8.1 Hz, 1H), 7.64 (d, *J* = 8.3 Hz, 2H), 7.39 (s, 1H), 7.29 (d, *J* = 8.1 Hz, 2H), 7.02 (d, *J* = 8.1 Hz, 1H), 4.31 (dd, *J* = 9.9, 3.7 Hz, 1H),

3.97 (t, $J = 10.0, 8.9$ Hz, 1H), 3.84 (q, $J = 6.6$ Hz, 4H), 3.78 – 3.71 (m, 1H), 3.42 – 3.34 (m, 1H), 3.05 (ddd, $J = 10.0, 8.5, 6.5$ Hz, 1H), 2.42 (s, 3H), 2.41 (s, 3H), 1.97 – 1.89 (m, 1H), 1.86 – 1.74 (m, 1H), 1.64 – 1.49 (m, 2H), 1.36 (t, $J = 7.2$ Hz, 3H), 1.29 (t, $J = 7.1$ Hz, 3H). ^{13}C NMR (100 MHz, CDCl_3) δ 149.5, 145.6, 143.9, 134.0, 130.8, 129.9, 127.7, 125.9, 125.4, 118.6, 71.3, 58.0, 49.5, 42.5, 28.7, 23.9, 21.9, 21.7, 14.6, 11.5; HRMS m/z calcd for $\text{C}_{23}\text{H}_{32}\text{N}_4\text{NaO}_5\text{S}_2$ $[\text{M}+\text{Na}]^+$ 531.1706, found 531.1701. $[\alpha]_D^{25} = -68.5$ ($c = 1$, DCM).

Typical procedure for remote hydroxylation and control experiments:

Synthesis of **2.41**:



To a vigorously stirred 20°C solution of 0.100 g (0.293 mmol) triazene **2.8** and 0.0192 g (0.0293 mmol) *fac*- $\text{Ir}(\text{ppy})_3$ in 10 mL CH_3NO_2 and 2 mL deionized H_2O was added 76.5 μL (0.586 mmol) 48% HBF_4 via gas-tight syringe. After 4 minutes, irradiation of the solution with blue LEDs ($\lambda_{\text{max}}=455$ nm) commenced and the reaction mixture was stirred vigorously for 18.5 h. 10 mL of 5% $\text{NaHCO}_3(\text{aq.})$ was then added at once followed by 10 mL CH_2Cl_2 and the resulting layers were separated. The aqueous layer was extracted with an additional 2 x 10 mL CH_2Cl_2 . The combined organic layers were dried over Na_2SO_4 , filtered and concentrated to yield 117.3 mg crude material. Silica gel chromatography (gradient run from 20% EtOAc in hexanes to 30% EtOAc in hexanes) afforded 43.4 mg (57%) of a yellow oil. Spectral data matched that previously reported in literature.²¹

Entry 2, Figure 2.4: No catalyst

Started with 0.100 g (0.293 mmol) triazene **2.8**, 76.5 μL (0.586 mmol) 48% HBF_4 , 2 mL deionized H_2O (2 mL) and 10 mL MeNO_2 . Purification via flash chromatography on silica gel (30% EtOAc in hexanes) afforded 0.009 g (10%) of **2.41** after concentration.

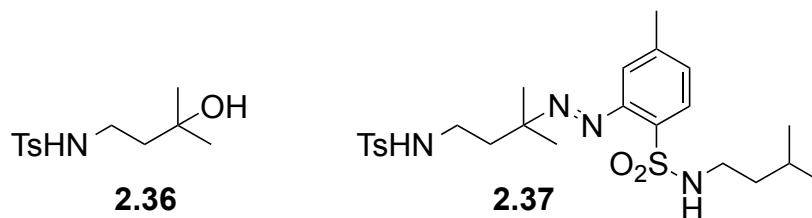
Entry 4, Figure 2.4: No light (18.5 h)

Started with 0.100 g (0.293 mmol) triazene **2.8**, 0.0192 g (0.0293 mmol) *fac*- $\text{Ir}(\text{ppy})_3$, 76.5 μL (0.586 mmol) 48% HBF_4 , 2 mL deionized H_2O (2 mL) and 10 mL MeNO_2 . The reaction flask was wrapped in foil before addition of the acid. Purification via flash chromatography on silica gel (30% EtOAc in hexanes) afforded 0.038 g (51%) of **2.41** after concentration.

Entry 3, Figure 2.4: No light (4 h)

Started with 0.100 g (0.293 mmol) triazene **2.8**, 0.0192 g (0.0293 mmol) *fac*- $\text{Ir}(\text{ppy})_3$, 76.5 μL (0.586 mmol) 48% HBF_4 , 2 mL deionized H_2O (2 mL) and 10 mL MeNO_2 . The reaction flask was wrapped in foil before addition of the acid. Purification via flash chromatography on silica gel (30% EtOAc in hexanes) afforded 0.030 g (41%) of **2.41** after concentration.

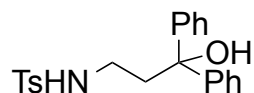
Synthesis of **2.36** and **2.37**:



Started with 0.100 g (0.293 mmol) **2.9**, 0.0192 g (0.0293 mmol) *fac*- $\text{Ir}(\text{ppy})_3$, 76.5 μL (0.586 mmol) 48% HBF_4 , 2 mL deionized H_2O and 10 mL CH_3NO_2 . Irradiated for 18 h. Silica gel chromatography (gradient run from 20% EtOAc in hexanes to 30% EtOAc

in hexanes) afforded 0.022 g (29%) of **2.36** (yellow-brown solid) and 0.017 g (11%) of **2.47** (yellow oil). **2.36**: ^1H NMR (400 MHz, CDCl_3) δ 7.76 (d, J = 7.9 Hz, 2H), 7.31 (d, J = 7.9 Hz, 2H), 5.65 (t, J = 5.7 Hz, 1H), 3.09 (q, J = 6.2 Hz, 2H), 2.42 (s, 3H), 1.91 (s, 1H), 1.63 (t, J = 6.4 Hz, 2H), 1.16 (s, 6H); ^{13}C NMR (100 MHz, CDCl_3) δ 143.4, 136.8, 129.8, 127.2, 71.5, 40.8, 39.8, 29.6, 21.6; HRMS m/z calcd for $\text{C}_{12}\text{H}_{19}\text{NO}_3\text{S}$ ($\text{M}+\text{Na}$) $^+$ 280.0984, found 280.0984. **2.37**: ^1H NMR (400 MHz, CDCl_3) δ 7.95 (d, J = 7.9 Hz, 1H), 7.70 (d, J = 8.1 Hz, 2H), 7.38 (d, J = 7.8 Hz, 1H), 7.27 (d, J = 7.8 Hz, 2H), 7.16 (s, 1H), 5.06 (t, J = 6.0 Hz, 1H), 4.96 (t, J = 5.8 Hz, 1H), 3.02 (quin, J = 6.9 Hz, 4H), 2.48 (s, 3H), 2.41 (s, 3H), 2.11 (t, J = 7.06 Hz, 2H), 1.62 – 1.55 (m, 1H), 1.39 – 1.35 (m, 2H), 1.33 (s, 6H), 0.84 (s, 3H), 0.82 (s, 3H); ^{13}C NMR (100 MHz, CDCl_3) δ 148.0, 144.9, 143.3, 136.9, 133.0, 130.8, 129.7, 129.4, 127.0, 117.5, 71.3, 41.9, 40.4, 39.2, 38.3, 25.4, 25.0, 22.2, 21.5, 21.5; HRMS m/z calcd for $\text{C}_{24}\text{H}_{36}\text{N}_4\text{O}_4\text{S}_2$ ($\text{M}+\text{Na}$) $^+$ 509.2280, found 509.2254.

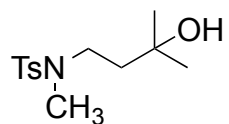
Synthesis of **2.38**:



Started with 0.136 g (0.293 mmol) **2.11**, 0.0192 g (0.0293 mmol) *fac*- $\text{Ir}(\text{ppy})_3$, 76.5 μL (0.586 mmol) 48% HBF_4 , 2 mL deionized H_2O and 10 mL CH_3NO_2 . Irradiated for 18 h. Silica gel chromatography (gradient run from 20% EtOAc in hexanes to 30% EtOAc in hexanes) afforded 0.031 g (28%) of a pale yellow solid. ^1H NMR (400 MHz, CDCl_3) δ 7.63 (d, J = 8.2 Hz, 2H), 7.33-7.15 (m, 12H), 5.26 (t, J = 5.9 Hz, 1H), 2.92 (q, J = 6.1 Hz, 2H), 2.48 (t, J = 6.2 Hz, 2H), 2.41 (d, J = 3.6 Hz, 3H); ^{13}C NMR (100 MHz,

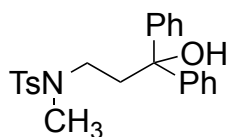
CDCl_3) δ 145.9, 143.3, 136.8, 129.7, 128.5, 127.4, 127.2, 126.0, 79.1, 40.2, 39.8, 21.6;
HRMS m/z calcd for $\text{C}_{22}\text{H}_{23}\text{NO}_3\text{S}$ ($\text{M}+\text{Na}$)⁺ 404.1297, found 404.1288.

Synthesis of **2.39**:



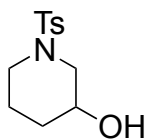
Started with 0.103 g (0.289 mmol) **2.14**, 0.0192 g (0.0293 mmol) *fac*-Ir(ppy)₃, 76.5 μL (0.586 mmol) 48% HBF_4 , 2 mL deionized H_2O and 10 mL CH_3NO_2 . Irradiated for 18 h. Silica gel chromatography (gradient run from 30% EtOAc in hexanes to 40% EtOAc in hexanes) afforded 0.026 g (33%) of a yellow oil. Spectral data matched that previously reported in literature.²¹

Synthesis of **2.40**:



Started with 0.140 g (0.293 mmol) **2.16**, 0.0192 mg (0.0293 mmol) *fac*-Ir(ppy)₃, 76.5 μL (0.586 mmol) 48% HBF_4 , 2 mL deionized H_2O and 10 mL CH_3NO_2 . Irradiated for 18 h. Silica gel chromatography (gradient run from 10% EtOAc in hexanes to 30% EtOAc in hexanes) afforded 0.048 g (41%) of a yellow solid. Spectral data matched that previously reported in literature.²¹

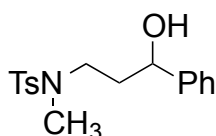
Synthesis of **2.46**:



Started with 0.075 g (0.15 mmol) **2.35**, 0.010 mg (0.015 mmol) *fac*-Ir(ppy)₃, 38.3 μL (0.293 mmol) 48% HBF₄, 1 mL deionized H₂O and 5 mL CH₃NO₂. Irradiated for 18 h. Silica gel chromatography (gradient run from 10% EtOAc in hexanes to 30% EtOAc in hexanes) afforded 0.028 g (73%) of a yellow oil. Spectral data matched that reported in literature.³⁰

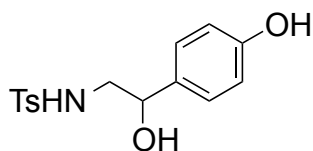
Representative procedure for dark reactions:

Synthesis of **2.51**:



Started with 0.118 g (0.293 mmol) triazene **2.15**, 0.0192 g (0.0293 mmol) *fac*-Ir(ppy)₃, 76.5 μL (0.586 mmol) 48% HBF₄, 2 mL deionized H₂O and 10 mL MeNO₂. The reaction flask was wrapped in foil before addition of the acid. Quenched with 5 mL 5% NaHCO₃ then extracted three times with 10 mL CH₂Cl₂. The organic layers were dried over Na₂SO₄ then filtered and concentrated. Purification via flash chromatography on silica gel (30% EtOAc in hexanes) afforded 0.048 g (51%) of a yellow oil. Spectral data matched that previously reported in literature.²¹

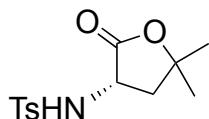
Synthesis of **2.52**:



Started with 0.114 g (0.293 mmol) triazene **2.12**, 0.0192 g (0.0293 mmol) *fac*-Ir(ppy)₃, 76.5 μL (0.5858 mmol) 48% HBF₄, 2 mL deionized H₂O and 10 mL MeNO₂. The reaction flask was wrapped in foil before addition of the acid. Quenched with 5 mL 5%

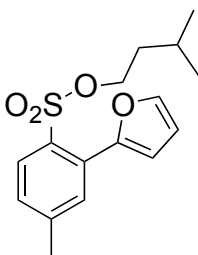
NaHCO₃ then extracted three times with 10 mL CH₂Cl₂. The organic layers were dried over Na₂SO₄ then filtered and concentrated. Purification via flash chromatography on silica gel (30% EtOAc in hexanes) afforded 0.055 g (61%) of a yellow oil. Spectral data matched that previously reported in literature.²¹

Synthesis of **2.53**:



Started with 0.117 g (0.293 mmol) triazene **2.13**, 0.0192 g (0.0293 mmol) *fac*-Ir(ppy)₃, 76.5 μL (0.586 mmol) 48% HBF₄, 2 mL deionized H₂O and 10 mL MeNO₂. The reaction flask was wrapped in foil before addition of the acid. Quenched with 5 mL 5% NaHCO₃ then extracted three times with 10 mL CH₂Cl₂. The organic layers were dried over Na₂SO₄ then filtered and concentrated. Purification via flash chromatography on silica gel (gradient run from 10% EtOAc in hexanes to 30% EtOAc in hexanes) afforded 0.040 g (48%) of a pale yellow oil. Spectral data matched that previously reported in literature.²¹

Synthesis of **2.58**:



Started with 0.100 g (0.293 mmol) triazene **2.8**, 0.006 g (0.03 mmol) TTF, 76.5 μL (0.586 mmol) 48% HBF₄, 2 mL deionized H₂O and 10 mL MeNO₂. Reaction stirred without irradiation under ambient light for 18 hours. Quenched with 5 mL 5% NaHCO₃

then extracted three times with 10 mL CH₂Cl₂. The organic layers were dried over Na₂SO₄ then filtered and concentrated. Silica gel chromatography (gradient run from 100% hexanes to 5% EtOAc in hexanes) afforded 0.023 g (26%) of an orange oil. ¹H NMR (500 MHz, CDCl₃) δ 8.04 (d, *J* = 8.2 Hz, 1H), 7.67 (s, 1H), 7.56 (d, *J* = 1.7 Hz, 1H), 7.28 (d, *J* = 8.0 Hz, 1H), 7.16 (d, *J* = 3.5 Hz, 1H), 6.54 (dd, *J* = 3.5, 1.8 Hz, 1H), 4.01 (t, *J* = 6.6 Hz, 2H), 2.48 (s, 3H), 1.56 (dt, *J* = 13.5, 6.7 Hz, 1H), 1.44 (q, *J* = 6.7 Hz, 2H), 0.81 (s, 3H), 0.80 (s, 3H). ¹³C NMR (126 MHz, CDCl₃) δ 149.3, 144.5, 143.2, 131.2, 128.5, 112.8, 112.1, 69.6, 38.8 37.5, 24.5, 23.1, 22.3, 21.7; HRMS *m/z* calcd for C₁₆H₂₁O₄S [M+H]⁺ 309.1155, found 309.1152.

2.10 References

1. Vioca, A.; Mendoza, A.; Gutekunst, W. R.; Fraga, J. O.; Baran, P. S., *Nature*. **2012**, 4, 629-635.
2. Teegardin, K.; Day, J. I.; Chan, J.; Weaver, J., *Org. Process Res. Dev.* **2016**, 20, 1156-1163.
3. Galli, C., *Chem. Rev.* **1988**, 88, 765-792.
4. Wayner, D.D.; McPhee, D. J.; Griller, D. J., *J. Am. Chem. Soc.* **1988**, 110, 132-137
5. Kimball, D. B.; Haley, M. M., *Angew. Chem. Intl. Ed.* **2002**, 41, 3338-3351.
6. Prier, C. K.; Rankic, D. A.; MacMillan, D. W. C., *Chem. Rev.* **2013**, 113, 5322-5363.
7. Stang, E. M.; White, C. M., *J. Am. Chem. Soc.* **2001**, 133, 14892-14895.
8. (a) Dinger, M. B.; Mol, J. C., *Organometallics* **2003**, 22, 1089-1095. (b) Dinger, M. B.; Mol, J. C., *Eur. J. Inorg. Chem.* **2003**, 2827-2833.
9. Bahde, R. J.; Rychnovsky, S. D., *Org. Lett.* **2008**, 10, 4017-4020.
10. Bates, R. H.; Shotwell, J. B.; Roush, W. R., *Org. Lett.* **2008**, 10, 4343-4346.
11. Cox, P. D.; Terpinski, J.; Lawrynowicz, W., *J. Org. Chem.* **1984**, 49, 3216-3129.
12. Laxmi, Y. R. S.; Iyenger, D. S., *Synthesis*, **1996**, 5, 594-596.

13. Nicolai, S.; Sedigh-Zadeh, R.; Waser, J., *J. Org. Chem.* **2013**, 78, 3783-3801.
14. (a) Righi, P.; Scardovi, N.; Marotta, E.; Peter, T.; Zwanenburg, B., *Org. Lett.* **2002**, 4, 497-500. (b) Fuller, P. H.; Kim, J-W.; Chemler, S. R., *J. Am. Chem. Soc.* **2008**, 130, 17630-17639
15. Hegedus, S.; McKearin, J. M., *J. Am. Chem. Soc.* **1982**, 104, 2444-2451.
16. Enkisch, C.; Schneider, C., *Eur. J. Org. Chem.* **2009**, 5549-5564.
17. Zhang, W.; Qin Y.; Zhang, W.; Luo, M., *Arkivoc* **2005**, xiv, 39-48.
18. E Silva, M. J.; Srivastava, R. M.; Doboszewski, B.; Cottier, L.; Sinou, D., *Het. Comm.* **2010**, 16, 105-111
19. Sanders, S. D.; Ruiz-Olalla, A.; Johnson, J. S., *Chem. Comm.* **2009**, 34, 5135-5137.
20. Krapcho, A. P.; *Synthesis* **1982**, 10, 805-822.
21. Hollister, K. A.; Conner, E. S.; Spell, M. L.; Deveaux, K.; Maneval, L.; Beal, M. W.; Ragains, J. R., *Angew. Chem. Intl. Ed.* **2015**, 54, 7837.
22. Roth, H. G., Romero, N. A.; Nicewicz, D. A., *Synlett*, **2016**, 27, A-J.
23. (a) Friestad, G. K.; Branchaud, B. P., Tetrafluoroboric Acid, *e-EROS*. **2001**. (b) Reisinger, H.; King, C. J., *Ing. Eng. Chem. Res.* **1995**, 34, 845-852. (c) Muckerman, J. T.; Skone, J. H.; Ning, M.; Wasada-Tsutsui, Y., *Biochem. Biophys. Acta.* **2013**, 1827, 882-891.
24. Zhu, S.; Ye, L.; Wu, W.; Jiang, H., *Tetrahedron*, **2013**, 69, 1232-1235.
25. Hugenberg, V.; Fröhlich, R.; Haufe, G., *Org. Biomol. Chem.* **2010**, 8, 5682-5691.
26. Murphy, J. A.; Rasheed, F.; Roome, S. J.; Lewis, N., *Chem. Commun.* **1996**, 737-738.
27. Shono, T.; Matsumura, Y.; Kanazawa, T.; Habuka, M.; Uchida, K.; Toyoda, K., *J. Chem. Res. Mini.* **1984**, 10, 2876-2889.
28. Harayama, H.; Abe, A.; Sakada, T.; Kimura, M.; Fugami, K; Tanaka, S.; Tamaru, Y., *J. Org. Chem.* **1997**, 62, 2113-2122.
29. Hegedus, L. S.; McKearin, J. M., *J. Am. Chem. Soc.* **1982**, 104, 2444-2451.
30. Jin, J. Y.; Wu, X.; Tian, G. R., *Synth. Commun.* **2005**, 35, 2535-2541.
31. Kim, H.; Lee, C., *Org. Lett.* **2011**, 13, 2050-2053.

32. Littler, B. J.; Gallagher, T.; Boddy, I. K.; Riordan, P. D., *Synlett.* **1997**, 1, 22-24.
33. Lazarides, L.; Smith, S. A.; Stocker, R.; Theobald, C. J., WO2008101867 (A1), 2008

CHAPTER 3: REVIEW OF CHEMICAL O-GLYCOSYLATION

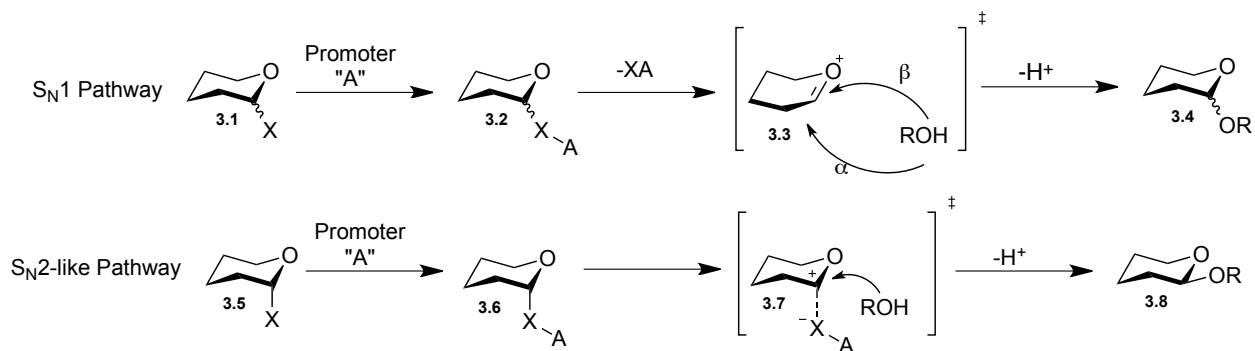
3.1 Introduction

Over the past few decades, research efforts to understand the role of carbohydrates in the body and its implications in medical and biological research has increased.¹ When oligosaccharides are covalently linked to molecules such as proteins or lipids they are called glycoconjugates (glycoproteins and glycolipids, respectively).² Glycoconjugates were found to have specialized roles in biological processes such as cell-cell recognition.³ One can envision exploiting this function of membrane-bound oligosaccharides to improve drug-targeting accuracy or develop carbohydrate-based therapeutic agents.

While great progress has been made towards elucidating the function of glycosylation and oligosaccharides in the body, scientists would greatly benefit from the amount of material that can be provided through improved methods of chemical glycosylation. Methods to isolate oligosaccharides from biological sources often produce small amounts of a complex mixture of carbohydrates.⁴ In an effort to generate serviceable quantities of homogeneous oligosaccharides, methods for developing stereoselective glycosidic linkages via chemical glycosylations have been heavily investigated. These methods have to be robust and versatile to overcome the many challenges of generating oligosaccharides synthetically. The reactivity of both the glycosyl donor and acceptor, choice of solvent, and conformation induced by the protecting groups are important considerations.

3.2 Possible Mechanistic Pathways and Contributors to Stereochemical Outcomes

Formation of glycosidic linkages involves substitution at the anomeric carbon of a sugar. The electrophile, or glycosyl donor, “donates” the anomeric carbon while the glycosyl acceptor serves as the nucleophile. A leaving group bonded to the anomeric carbon is displaced after being activated by a promoter and subsequent attack on that carbon results in the formation of a glycosidic linkage. O-glycosylation is the term used to describe the transformation when the nucleophile is a hydroxyl (-OH) group. Chemical glycosylations generally undergo S_N1 and S_N2-like mechanistic pathways similar to those depicted in Scheme 3.1^{5,6}.



Scheme 3.1 Possible mechanistic pathways of glycosylation

3.2.1 S_N1 & S_N2-like Mechanistic Pathways

Following an S_N1 pathway, departure of the leaving group is facilitated by activation of the glycosyl donor by promoter “A” (Scheme 3.1). Attack from the top or bottom face of oxocarbenium ion **3.3** by the glycosyl acceptor (ROH) forms the desired glycosylation product (**3.4**). This pathway generally leads to a mixture of anomers as the stereochemistry of the newly formed anomeric bond is not controlled.

Alternatively, via the S_N2 pathway (Scheme 3.1), activation of the leaving group by promoter “A” results in a contact ion pair (**3.7**) that has a positive charge at the anomeric carbon. The anomeric carbon is then attacked on the opposite face resulting

in inversion at the anomeric carbon. While Scheme 3.1 illustrates this pathway with C-X in the axial position, one can envision the same process with the leaving group in the equatorial position as well^{5,6}.

Alpha and *beta* are the terms used to describe the configuration of glycosides at the anomeric carbon. A *trans* relationship between the C₅-C₆ bond and the C-X bond of the anomeric carbon, for the purposes of this dissertation, is referred to as the *alpha* anomer (Figure 3.1). On the other hand, a *cis* relationship depicts the *beta* anomer. The ability to selectively form *alpha* or *beta* anomers is key in the synthesis of oligosaccharides, especially for glycobiology applications where enzyme catalyzed glycosylations are stereoselective.

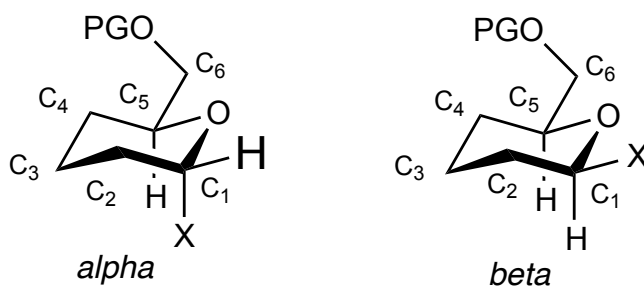


Figure 3.1 General representations of *alpha* and *beta* anomers (PG = protecting group)

3.2.2 Anomeric Effect

Also known as the Edward-Lemieux effect⁷, the anomeric effect refers to the propensity of electronegative atoms at the anomeric carbon to lie in the axial position as opposed to the equatorial position. This axial preference, according to molecular orbital theory (MOB), suggests that the lone pair on the ring oxygen stabilizes the aptly aligned σ^* of the C-X bond through hyperconjugation⁸ (**3.9**) (Figure 3.2). To further support this predilection, the dipole moment theory (DMT) suggests that the dipoles of the heteroatoms repel when the C-X bond is in the equatorial position^{7b} (**3.12**). However,

when in the axial position (**3.11**), the dipoles are situated opposite of each other, thus making it the more favorable orientation. Based on these proposed theories, the anomeric effect is worth keeping in consideration when interpreting the stereochemical outcome of an equilibrated reaction. The anomeric effect, however, plays a minor role as far as kinetic control is concerned and poor selectivity is often observed with glycosylations.

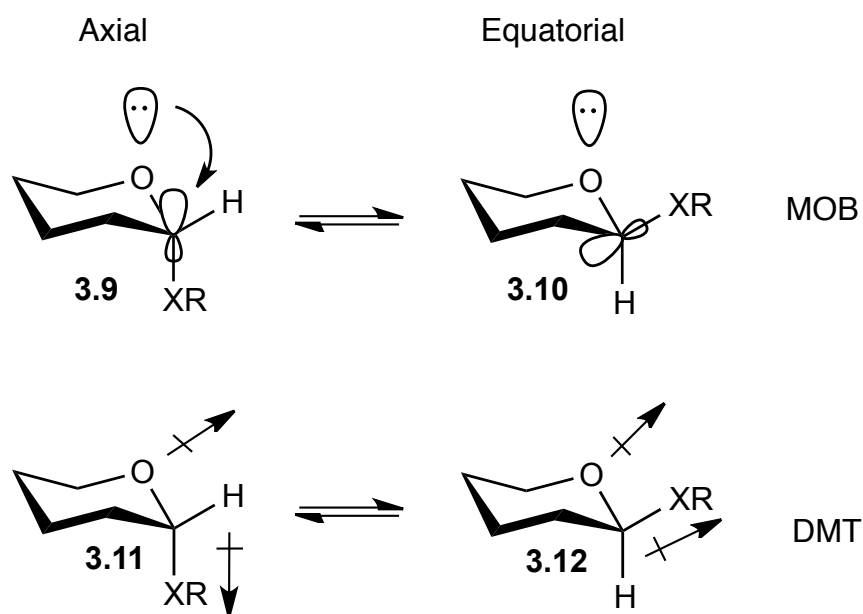
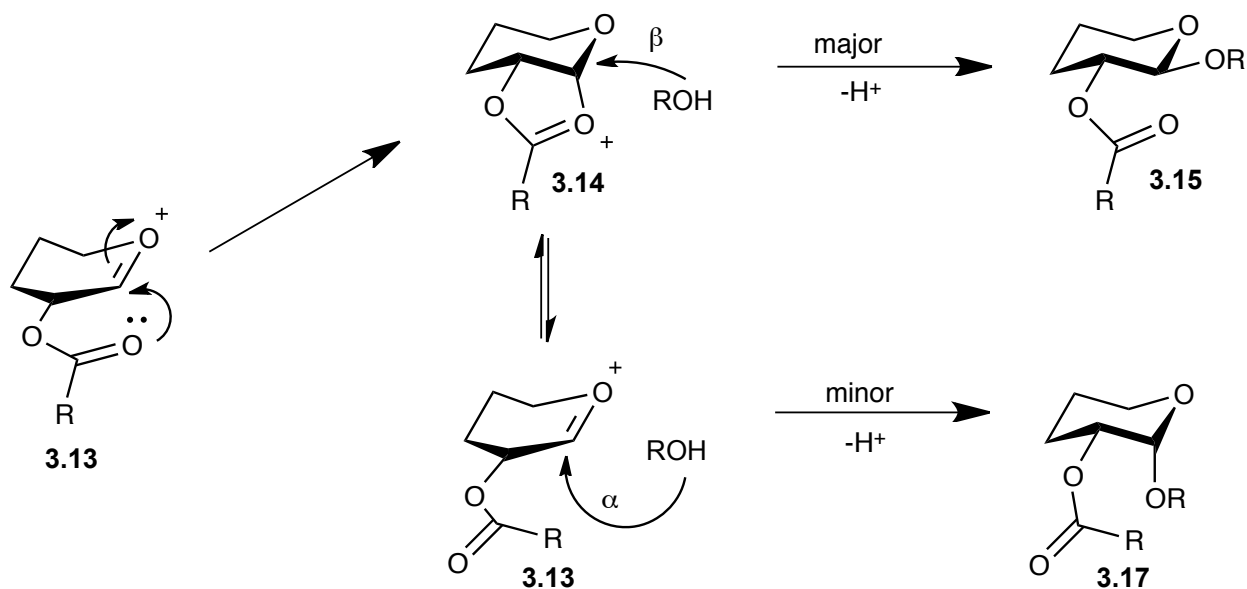


Figure 3.2 Molecular orbital theory (MOB) and dipole moment theory (DMT) of the anomeric effect

3.2.3 Neighboring Group Participation

Additional factors contribute to the selectivity of chemical glycosylations. One of the most powerful techniques employed to encourage complete selectivity is the installment of a carbonyl containing protecting group at the C₂ position. Acetyl-, benzoyl-, and pivaloyl-protecting groups are common examples. Following the formation of oxocarbenium ion **3.13**, attack of the carbonyl on the anomeric carbon results in onium ion **3.14** (Scheme 3.2) where one face of the intermediate is blocked. Nucleophilic

attack on the top face results in generation of a single isomer. While this is generally the observation, in some cases the minor isomer also forms. This anomer is a result of the reversible nature of the orthoester intermediate^{9,10}. Oxonium ion **3.14** reverts back to **3.13** and attack on the bottom face results in the *alpha* anomer (**3.17**).

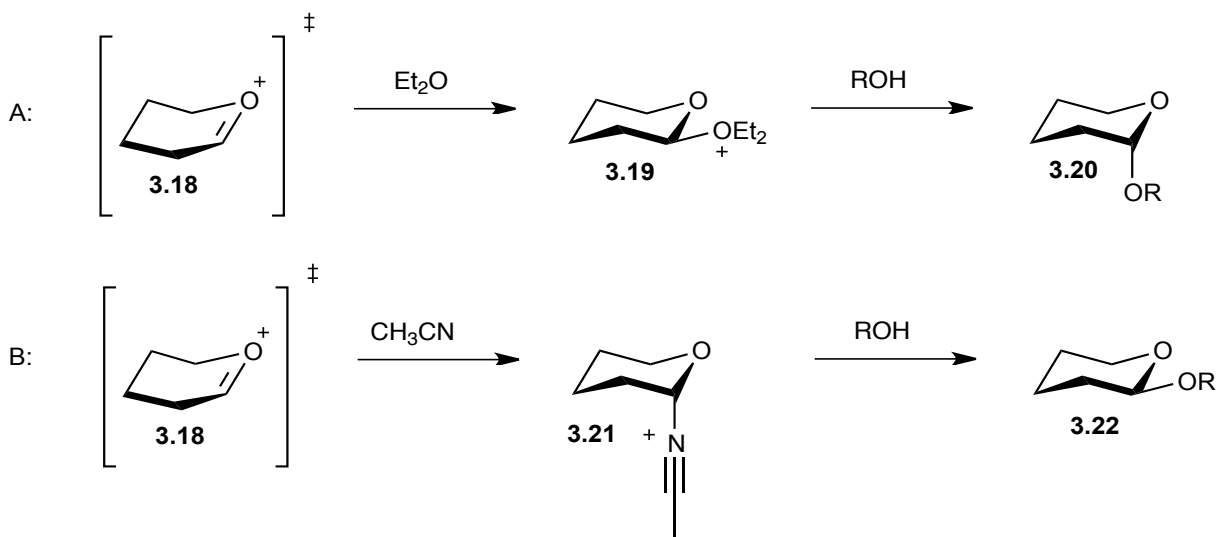


Scheme 3.2 Neighboring group participation

3.2.4 Effect of Solvents on Stereochemical Outcome

It has been observed that the solvent used for glycosylation affects the stereochemical outcome of the transformation. Common solvents employed for glycosylations range from dichloromethane, diethyl ether, and dioxane to less nonpolar solvents such as acetonitrile and nitromethane. It was postulated that nucleophilic solvents such as nitriles and ethers have a more direct impact on stereochemical outcome as they coordinate to the oxocarbenium ion^{7a,11}. The selective formation of either the *alpha* or *beta* anomer, however, depended on more than the solvent. It was determined that, in some cases, the reactivity of the glycosyl donor and the reaction temperature^{11d} were the biggest determinants of how selective the reaction was.

Ethers favored formation of the *alpha* anomer regardless of the type of donor and glycosylations at low temperatures (below 0°C) showed excellent stereoselectivity¹². It is suggested that solvolysis (Scheme 3.3 A) of the oxocarbenium ion (**3.18**) by ethers such



Scheme 3.3 Solvent effect on glycosylation by (A) diethyl ether and (B) acetonitrile as tetrahydrofuran (THF) or diethyl ether (Et₂O) results in oxonium ion with a preference for the *beta* anomer (**3.19**). S_N2-like nucleophilic attack of the glycosyl acceptor leads to formation of the *alpha* anomer (**3.20**) as the major product¹³.

Solvents such as nitriles depend on both temperature and reactivity of the glycosyl donor to guide selectivity. Acetonitrile and propionitrile have been used in a series of investigations into the effect of nitriles on stereochemistry. In one example, Schmidt^{11d} demonstrated that treatment of trichloroacetimidates (a highly reactive class of glycosyl donors) with trifluoromethyl trifluoromethanesulfonate (TMSOTf) at -80°C in propionitrile afforded *beta*-glycosides as the major products. Schmidt attributes this result to the formation of the α-nitrilium ion (similar to **3.21** in Scheme 3.3 B) that is quickly generated due to the facile release of the leaving group under the reaction

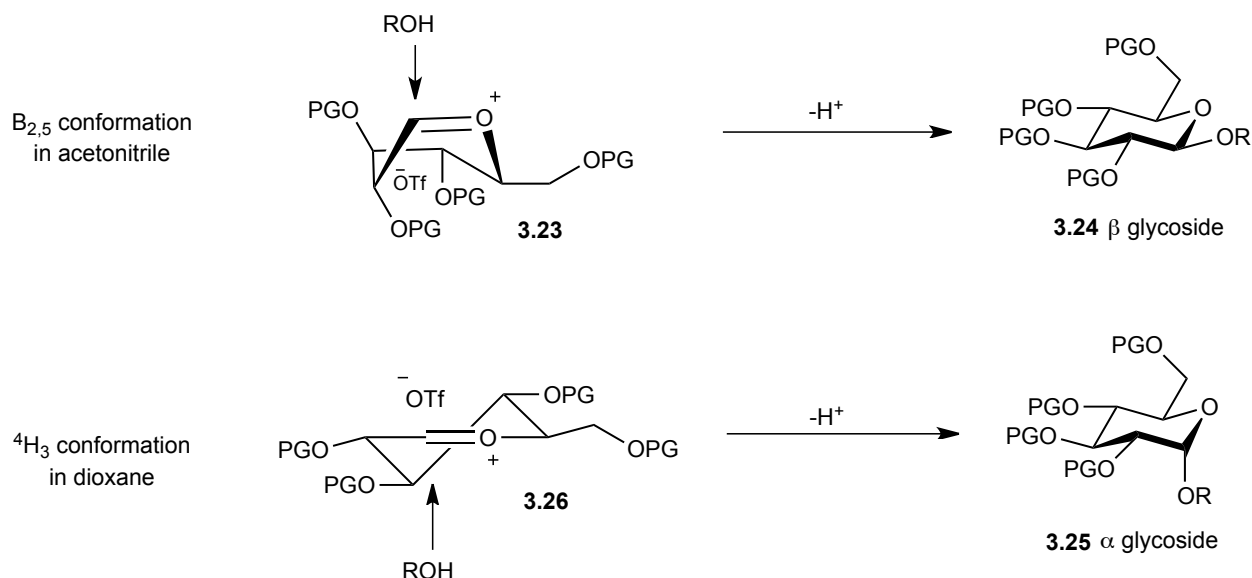
conditions. Since the observed $\alpha:\beta$ ratio is not reliant on the anomeric configuration of the glycosyl donor, the nitrilium ion is presumed to be the common intermediate and formation of the products follow an S_N2 -like pathway.

Alternatively, another report by Schmidt and coworkers demonstrated that step-wise addition of the substrates was necessary to observe the desired selectivity. Stereoselective glycosylation relied on pre-activation of the halogen leaving group of glycosyl bromides and chlorides in acetonitrile at -15°C before addition of the acceptor^{11b}. Subsequent generation of the *alpha* anomer as the major product led to the assumption that attack of the acceptor on the anomeric carbon occurred via an S_N2 -like pathway with the β -nitrilium ion as the leaving group.

In recent years another theory about solvent effects has been proposed. Hünenberger and coworkers postulate that the solvents are not actively participating in the reaction mechanism¹⁴. Instead, the polarity of the solvent determines the preferred conformation of the oxocarbenium ion. In addition, the proximity and location of the counterion relative to the oxocarbenium cation ultimately dictates which face the acceptor attacks to afford the corresponding anomer. This concept is termed by the authors as the “conformer and counterion distribution” hypothesis¹⁴.

Based on quantum-mechanical (QM) calculations, when in acetonitrile the oxocarbenium-triflate ion complex prefers to adopt mainly the $B_{2,5}$ ring conformation (**3.23**) (Scheme 3.4). In this configuration, the *alpha* side of the ring is inaccessible by nucleophiles due to the steric interactions of the exocyclic substituents in addition to the propensity for the counterion to coordinate on the *alpha* face¹⁴. Thus, attack occurs from the more accessible face of the intermediate resulting in predominantly the β anomer

(**3.24**), the selectivity seen experimentally with glycosylations in nitrile solvents¹¹. In dioxane, the ⁴H₃ conformer (**3.25**) is preferred (Scheme 3.4). Though sterics seems to



Scheme 3.4 Preferred conformation of oxocarbenium ion in acetonitrile and dioxane based on QM calculations

have less control on nucleophilic attack, the counterion (when in dioxane) tightly coordinates to the oxocarbenium ion on the *beta* side of the intermediate¹⁴. Attack therefore occurs on the *alpha* side and results in the corresponding *alpha* anomer, the selectivity experimentally observed with glycosylations in ethereal solvents¹². It was observed that the polarity of the solvent determines how strongly coordinated the counterion is with the oxocarbenium ion. In solvents with lower polarity such as dioxane, the counterion lies very close to the carbocation (on the *beta* side) while in more polar solvents like acetonitrile, the counterion exhibits a weaker coordination (on the *alpha* side)¹⁴.

3.3 Glycosyl Acceptors

As previously mentioned, glycosyl acceptors are the nucleophiles involved in the formation of glycosidic linkages. O-Glycosylation is a result of unprotected hydroxyl groups of, e.g., carbohydrate alcohols attacking the anomeric carbon of the glycosyl donor (Figure 3.3). Nucleophilicity of the acceptor plays a major role in reactivity and mechanistic pathways of glycosylation with less reactive acceptors favor S_N1 pathways

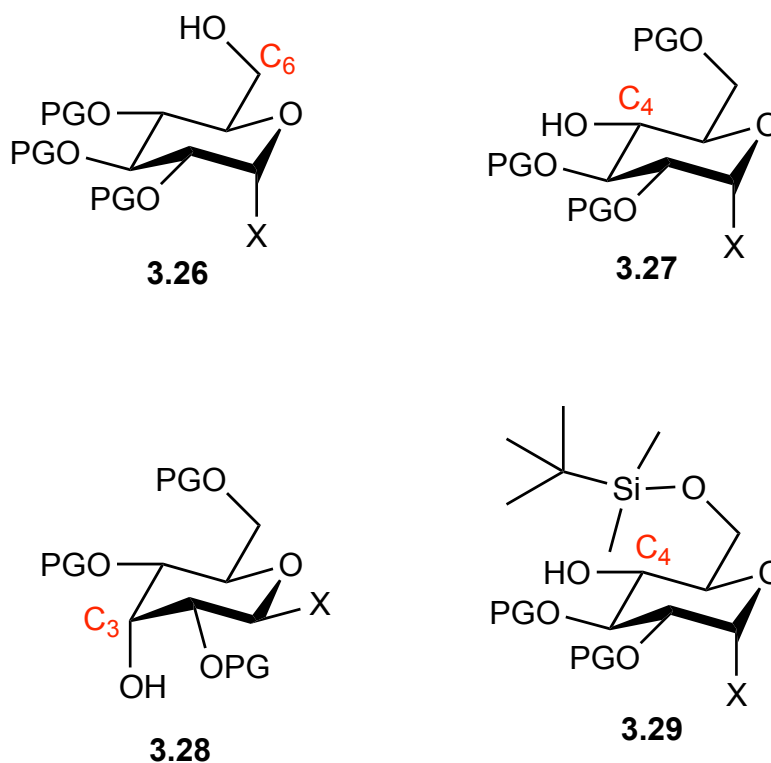


Figure 3.3 Generic representations of glycosyl acceptors and more reactive acceptors favor the S_N2 pathway¹⁵. Primary alcohols like the unprotected hydroxyl group at C₆ (**3.26**) are generally more reactive than secondary alcohols (C₁₋₄). Of the secondary alcohols, C₄ (**3.27**, **3.29**) hydroxyl groups are among the least nucleophilic and thus the least reactive. Another observation is that equatorial hydroxyl groups are generally more nucleophilic than axial hydroxyl groups (**3.28**).

Protecting groups also have an influence on the nucleophilicity of the acceptor. While the structure of the protecting groups can affect the conformation, the bulkiness of

the group can affect the reactivity of the alcohol. For example, a bulky group such as a *tert*-butyldimethylsilyl at C₆ would greatly reduce the nucleophilicity of C₄ hydroxyl groups (**3.29**) and thus makes formation of a glycosidic linkage exceedingly difficult. Also, as can be expected, the presence of electron donating groups (i.e. PG = Bn, Me) on the glycosyl acceptor contributes to an increase in reactivity of the nucleophile while the opposite affect is observed with electron withdrawing groups (i.e. PG = Bz, Ac).

3.4 Glycosyl Donors

3.4.1 Protecting Groups

Similar to glycosyl acceptors, glycosyl donors are generally protected with groups that mask the hydroxyl substituents on the sugar. While the protecting groups, in some cases, affect the nucleophilicity of the heteroatom at the anomeric carbon, glycosyl donors are categorized according to the propensity of the protecting groups to stabilize the intermediate oxocarbenium ion. Superarmed donors are those that are protected with bulky groups (i.e. *tert*-butyldimethylsilyl ethers) that prompt formation of a twist boat conformation of the donor with the C-O bonds adopting a pseudoaxial orientation (Figure 3.4)¹⁶. Electrostatic interactions between the C-O bonds and the forming oxocarbenium ion result in a highly stable intermediate. Armed donors are less reactive than the superarmed donors but are still capable of stabilizing the oxocarbenium ion

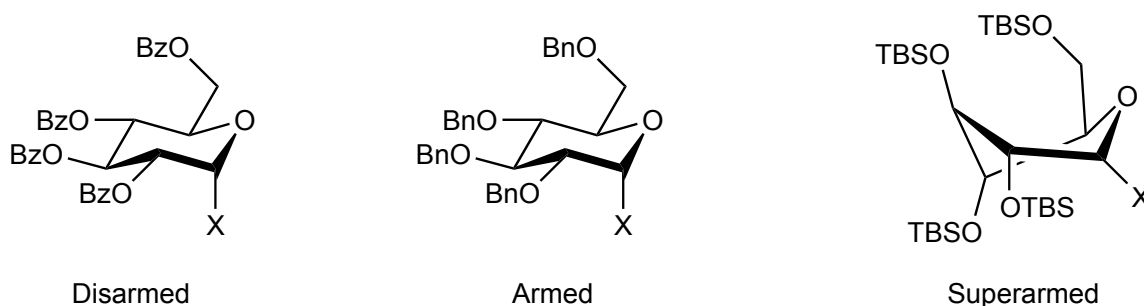


Figure 3.4 Examples of protected glycosyl donors

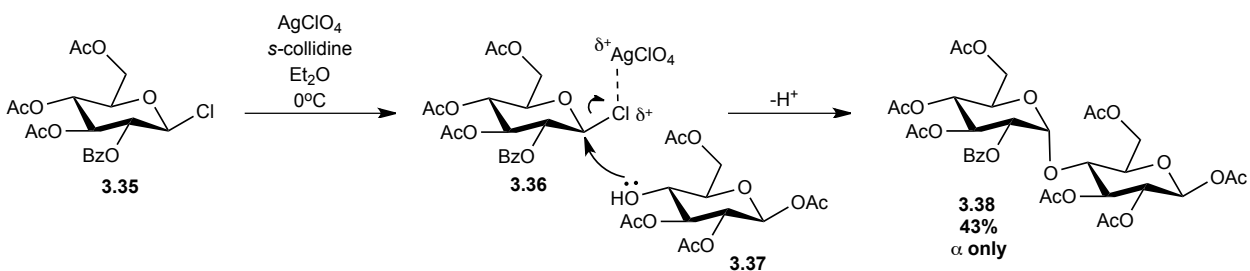
due to the electron donating nature of the protecting groups¹⁷. Groups in this category are generally ethers such as benzyl or methyl ethers. Lastly, disarmed donors typically bear electron-withdrawing groups like benzoyl, pivaloyl or acetyl esters and are the least reactive donors¹⁸. Due to the electron-withdrawing characteristics of the esters, the oxocarbenium ion is destabilized.

3.4.2 Types of Glycosyl Donors

A. Glycosyl Halides

Glycosyl halides have been exploited as glycosyl donors for more than a century.¹⁹ Reported independently by Koenigs and Knorr²⁰ and also Fischer and Armstrong²¹, glycosyl bromides and chlorides successfully formed glycosidic linkages with alcohols in the presence of halophiles. Examples of halophiles used are salts of silver or mercury (introduced as an activator decades after reports with silver salts) such as AgOTf, AgClO₄, HgBr₂, or Hg(CN)₂.²²

Synthesis of disaccharide **3.38** was achieved by activating disarmed donor **3.35** in the presence of silver perchlorate^{22a} (Scheme 3.6). Coordination of chloride **3.35** to the

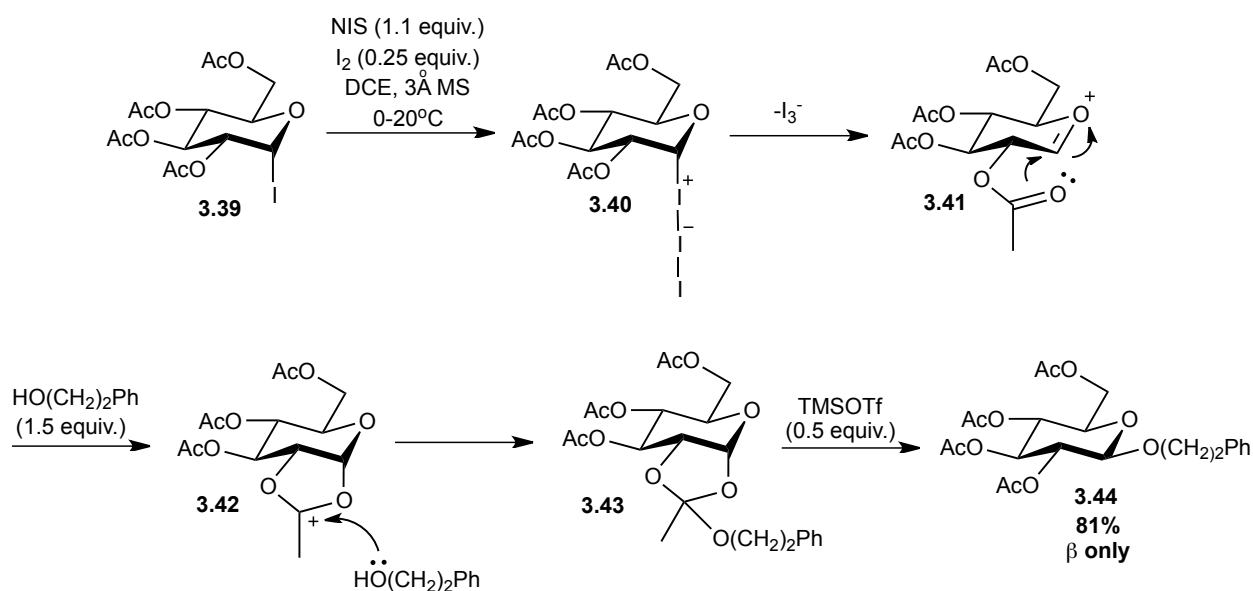


Scheme 3.6 AgClO₄ promoted glycosylation with glycosyl chloride

silver salt results in a more electrophilic anomeric carbon. Attack of C₄ acceptor **3.37** resulted in formation of **3.38**. This selective transformation affords only the α anomer, even in the presence of the benzoyl ester at C₂.

Later, glycosyl iodides were presented as more reactive donors that may obviate toxic heavy metals. Similar to bromides, iodides were quite unstable, however, it was demonstrated that glycosyl iodides were highly tunable and varying the temperature along with the protecting groups on the donors could afford highly stereoselective reactions^{22b}. Non-heavy metal salts were also found to be efficient for activation of the reactive halides.

In one example reported by Stachulski and coworkers²³, disarmed glycosyl iodides were activated in the presence of *N*-iodosuccinimide (NIS) and iodine (I₂) along with trifluoromethyl trifluoromethanesulfonate (TMSOTf) (0°C to -15°C) (Scheme 3.7). It was



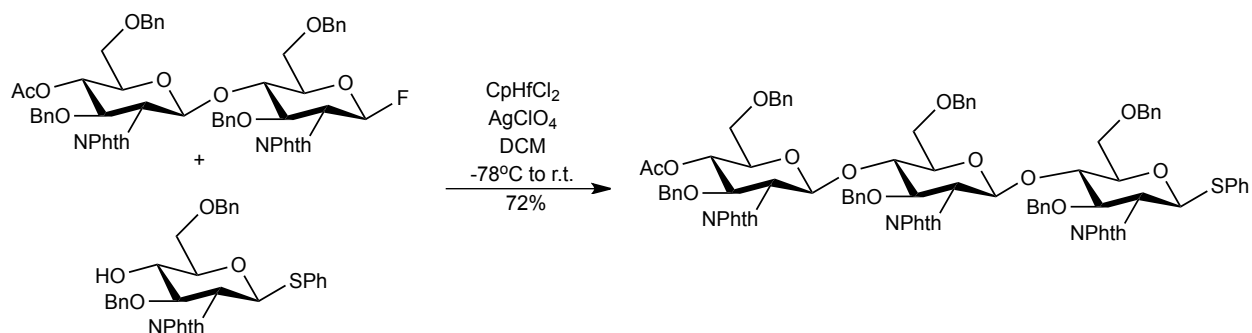
Scheme 3.7 NIS-I₂-TMSOTf promoted glycosylation of disarmed glycosyl iodide observed that this system would produce *beta* anomers as the major glycosides even when metal salts such as FeCl₃ and CuCl were used (with I₂ at 20°C). Activation of glycosyl iodide **3.39** with iodine results in intermediate **3.40**. Loss of the triiodide leaving group and neighboring group participation by the acetate group is followed by attack of the alcohol acceptor onto the oxonium species. The observed orthoester **3.43** reported

by the authors is then converted to glycoside **3.44** upon addition of TMSOTf, added after complete consumption of **3.39**. This selective reaction afforded 81% of *beta* glycoside **3.44**.²³

The instability of glycosyl halides was addressed when Mukaiyama demonstrated activation of glycosyl fluorides with SnCl₂-AgClO₄²⁴. More stable than other glycosyl halides, chemically and thermally, glycosyl fluorides were viable alternatives. In recent years, methods using TMSOTf²⁵ and triflic acid²⁶ (TfOH) have also materialized adding to the portfolio of mild activation of glycosyl fluorides. Since the introduction of glycosyl halides as glycosyl donors, many advancements have been made that continue to tackle the downfalls of these reactive but unstable glycosides²⁷.

B. Chalcogenoglycosides (Alkyl/Aryl)

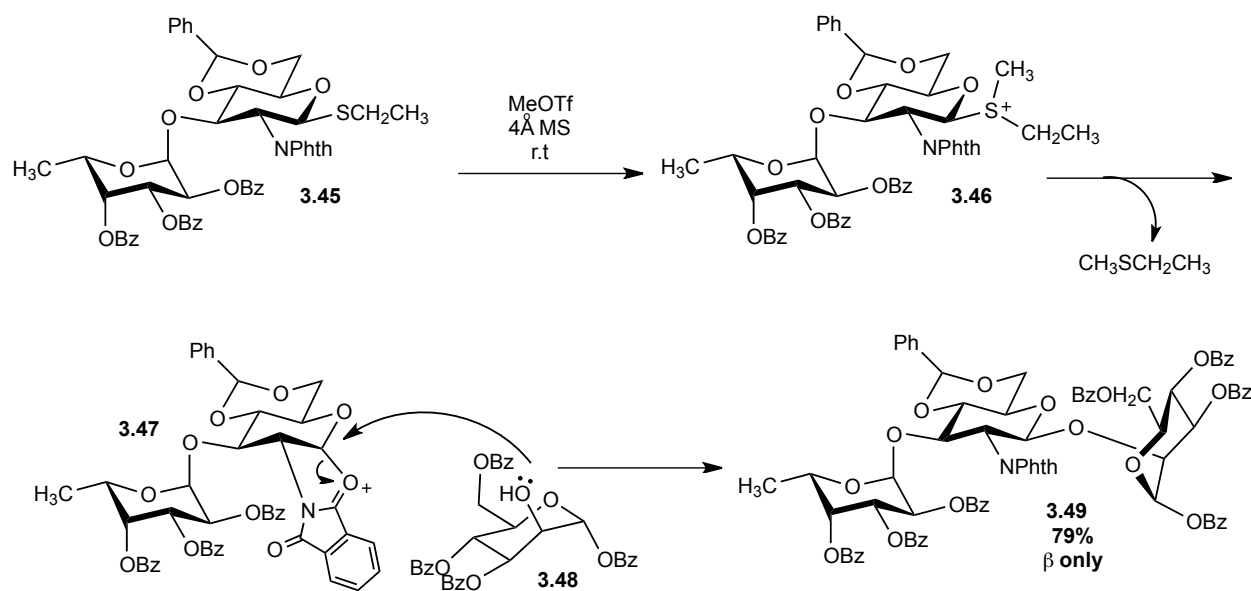
Chalcogenoglycosides generally bear alkyl or aryl selenides or sulfides at the anomeric carbon (selenoglycosides and thioglycosides). The stability of chalcogenoglycosides is useful for the orthogonal synthesis of oligosaccharides as activation of other glycosyl donors in their presence can be carried out without disturbing the C-S or C-Se bond²⁸ (Scheme 3.8). At the inception of their use as glycosyl donors, these highly stable glycosides often required mercury and silver salts



Scheme 3.8 Glycosylation of thioglycoside acceptor with glycosyl fluoride donor

(similar to glycosyl halides) for their activation (e.g., PhHgOTf²⁹ and AgOTf³⁰).

However, in later years, methods for activation without the use of silver or mercury were realized and reports of activation with systems such as NIS/TfOH³⁰ and iodonium dicollidine perchlorate³¹ (IDCP). The common denominator here is the use of electrophilic species that have an affinity for sulfur and selenium. Generation of sulfonium and selenonium ions converts the sulfides and selenides into more efficient leaving groups resulting in formation of the oxocarbenium intermediate. Lönn demonstrated this process when ethyl thioglycoside **3.45** was activated by methyl triflate (MeOTf) to form an intermediate sulfonium ion³² (Scheme 3.9). Ethyl methyl sulfide was



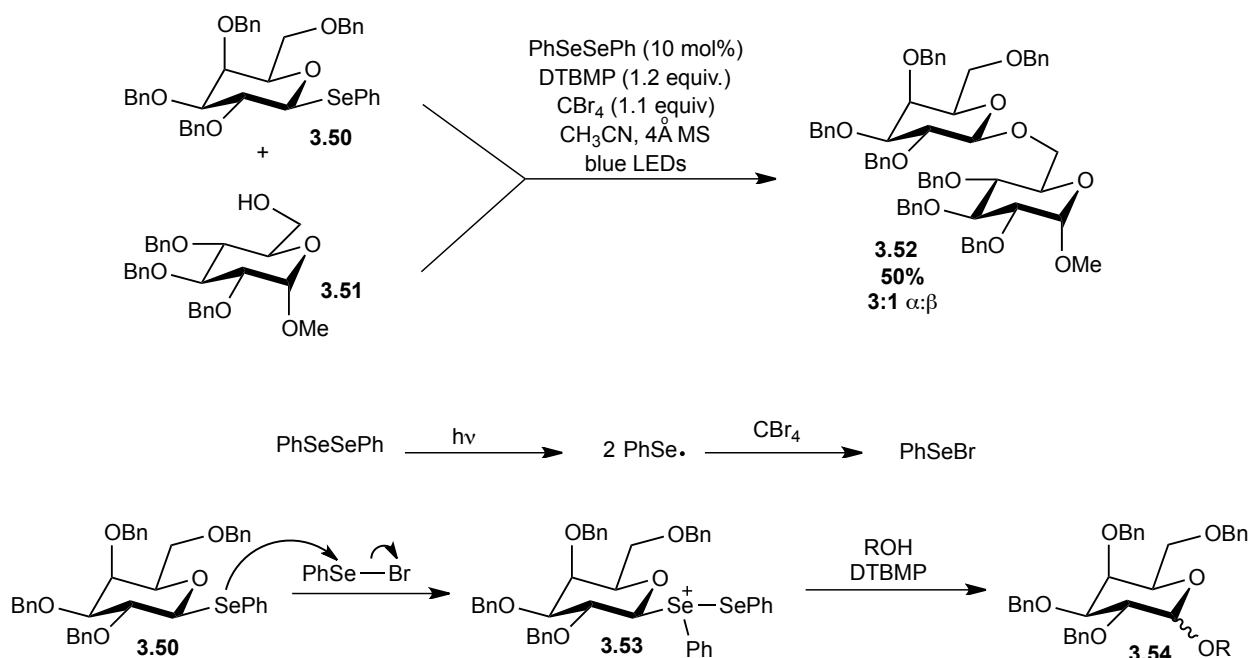
Scheme 3.9 Synthesis of trisaccharide via thioglycoside donor

the resulting by-product and attack of **3.48** afforded the corresponding trisaccharide **3.49**.

A mild procedure for activation was established when Sinay and coworkers exposed seleno and thioglycosides to an electric current³³. This process resulted in selenium and sulfur radical cations via single electron transfer (SET) following anodic oxidation. The

oxocarbenium ion is generated after the radical cations fragment rapidly and irreversibly. The desired saccharides are isolated accompanied by disulfides and diselenides as by-products. This SET process was also observed when chalcogenoglycosides were activated under visible-light promotion³⁴. Photochemical oxidation provided access to the mild activation of chalcogenoglycosides without the use of the specialized equipment employed with electrochemical oxidation.

Spell and coworkers demonstrated glycosylation of phenylselenoglycosides utilizing visible-light (blue LEDs) and diphenyldiselenide to promote activation (Scheme 3.10)³⁵. Visible-light induced homolysis of the Se-Se bond results in a phenylselenenyl radical that reacts with carbon tetrabromide (CBr₄) to generate PhSeBr *in situ*. PhSeBr then reacts with selenium at the anomeric carbon of the glycosyl donor **3.50** resulting in intermediate **3.53**. The promoter, diphenyldiselenide (PhSeSePh), is then regenerated as the alcohol acceptor reacts to form the corresponding disaccharide **3.54**.

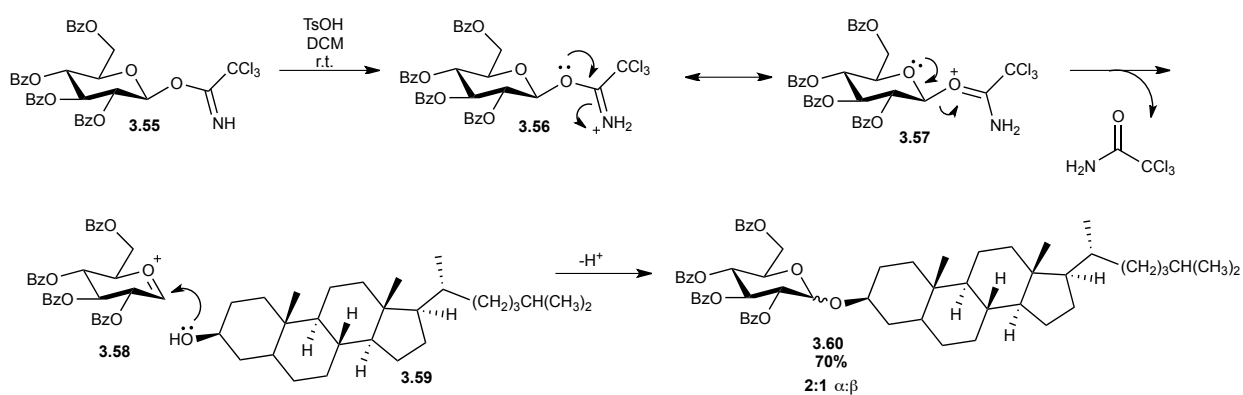


Scheme 3.10 Activation of phenylselenoglycosides with catalytic diphenyldiselenide (DTBMP = 2,6-di-*tert*-butyl-4-methylpyridine)

Overall, chalcogenoglycosides represent a very versatile group of glycosyl donors. The stability of seleno and thioglycosides enables selective activation of other donors in their presence. Exploiting their stability and continued development of mild reaction conditions would make chalcogenoglycosides a viable tool for the synthesis of oligosaccharides.

C. Glycosyl Imidates

Glycosyl imidates are a highly reactive class of glycosyl donors with *O*-glycosyl trichloroacetimidates, first reported by Schmidt and coworkers³⁶, being among the most widely used glycosides. It has been demonstrated on numerous occasions that a variety of promoters efficiently activate trichloroacetimidates. Popular conditions include TMSOTf^{37a} and BF₃·OEt₂^{37b}, however, methods using lanthanide salts such as Yb(OTf)₃^{37c}, and HClO₄-SiO₂^{37d} have also been developed. Coordination (or protonation) of the nitrogen of the leaving group to (or by) the promoter activates the glycosyl donor (see **3.55** and **3.56**, Scheme 3.11). This interaction triggers departure of

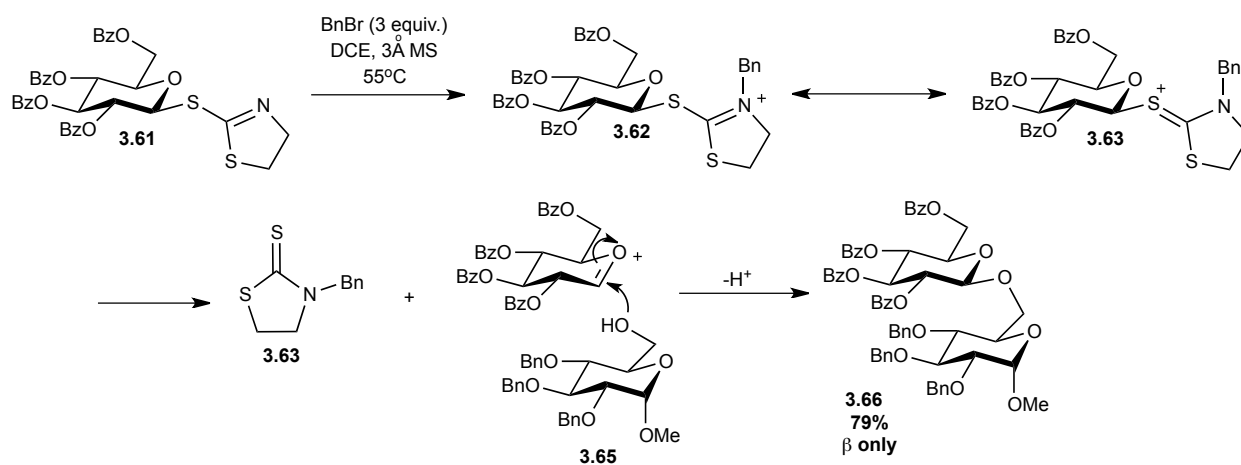


Scheme 3.11 Activation of trichloroacetimidate donor with mild acid

the imidoyl leaving group resulting in generation of trichloroacetamide as the by-product accompanied by the glycoside product.

Schmidt and coworkers demonstrated that weak acids such as *p*-toluenesulfonic acid (TsOH) protonated trichloroacetimidate donors **3.55** to generate **3.56** (Scheme 3.11).³⁸ Expulsion of the leaving group affords trichloroacetamide and subsequent attack of cholesterol affords glycoside **3.60**. In this manner, the glycosylation of cholesterol was formed in 70% yield (2:1 α : β). Schmidt also demonstrated that the activation was more selective with boron trifluoride diethyl etherate ($\text{BF}_3 \cdot \text{OEt}_2$) at lower temperatures. At -18°C with $\text{BF}_3 \cdot \text{OEt}_2$, **3.60** was isolated in 78% and 1:13 α : β ratio.³⁸

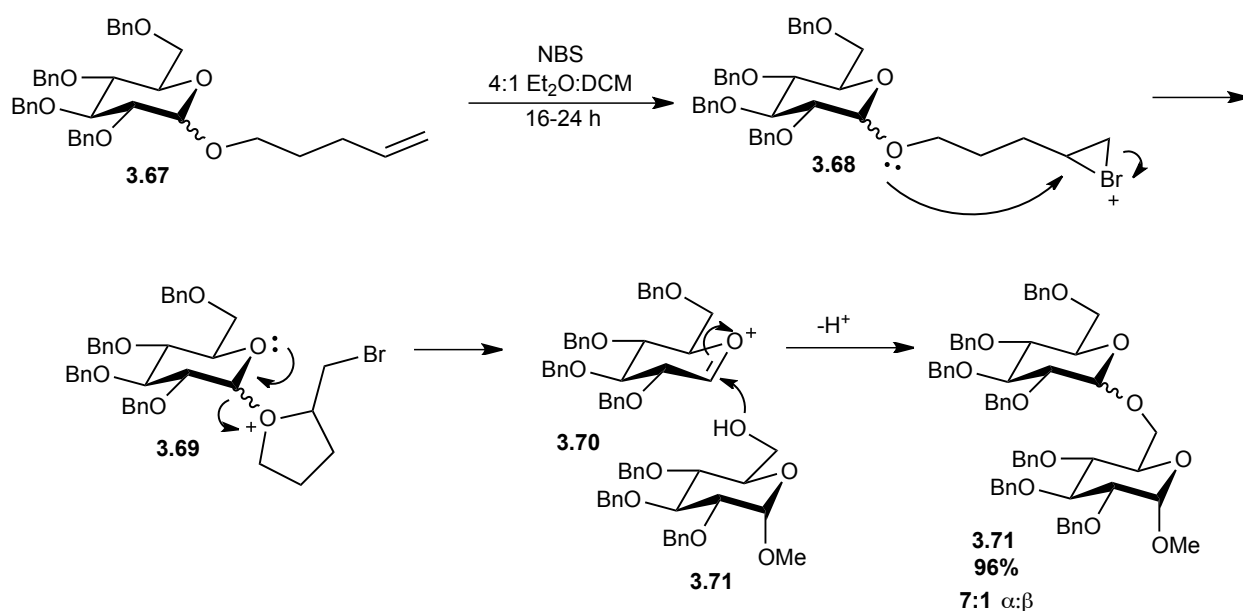
S-imidates (thioimidates) are also used in chemical glycosylations, activated by a range of conditions from mercury salts ($\text{Hg}(\text{NO}_3)_2$)³⁹ to alkylating agents such as methyl triflate (MeOTf) and benzyl bromide (BnBr)⁴⁰. S-Thiazolinylnyl (STaz) glycosides, reported by Demchenko and coworkers, were activated by BnBr , which resulted in alkylation of the nitrogen to afford **3.62** (Scheme 3.12). This positively charged species facilitates



Scheme 3.12 Remote activation of STaz leaving group via alkylation
 departure of the leaving group and generation of the alkylated thiazolinylnyl by-product
 observed (**3.64**).⁴⁰

D. Alkenyl Glycosides

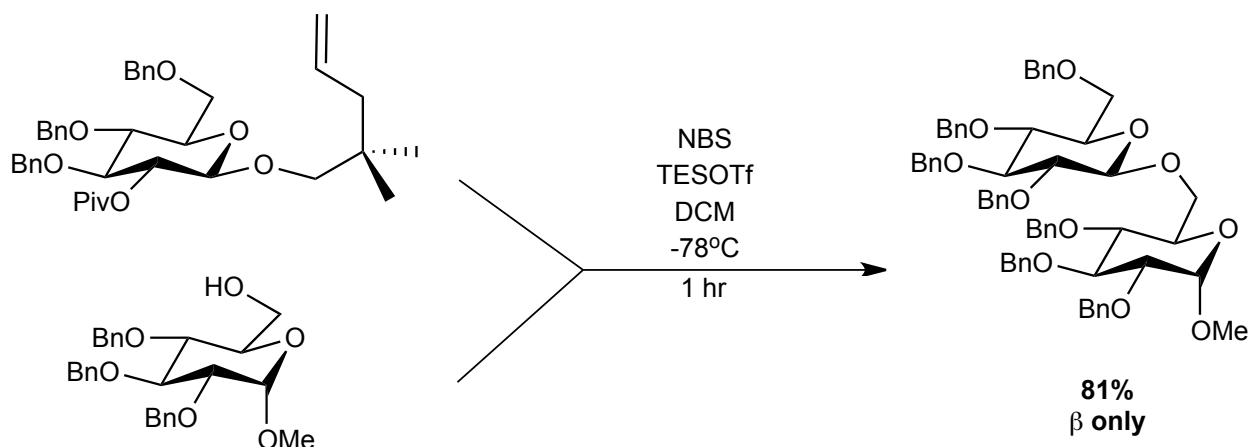
A well-known glycosyl donor in this category is the *n*-pentenyl glycoside. First introduced by Frasier-Reid⁴¹, this class of glycosides bears a pendant alkene that is activated by reaction of the alkene to form a bromonium (**3.68**) or iodonium ion generated from NBS or NIS, respectively (Scheme 3.13). The resulting halonium ion is then attacked by the anomeric oxygen, which affords a cationic tetrahydrofuran intermediate (**3.69**). The oxocarbenium ion is then generated as the active leaving group departs and glycosidic linkages are formed following attack of a glycosyl acceptor.



Scheme 3.13 Remote activation of *n*-pentenyl glycosides

The rate of reaction of *n*-pentenyl glycosides was drastically increased with the introduction of *geminal* methyl groups. For example, *gem*-2,2-dimethyl 4-pentenyl glycosides exhibited an eleven fold increase (16-24h to 1h) in the reaction rate⁴² (Scheme 3.14). This observation is a result of the conformation induced by the methyl groups (Thorpe-Ingold effect). By bringing the alkene in closer proximity with the exocyclic oxygen, cyclization and ultimately the formation of the glycosidic linkage

occurs more efficiently. This analog of the *n*-pentenyl glycoside is also activated with NBS and follows the same mechanistic pathway in scheme 3.13. These glycosyl donors exhibit great stability, similar to thioglycosides, and the mechanism of activation of them makes them attractive options for glycosylation.



Scheme 3.14 *gem*-2,2-dimethyl 4-pentenyl glycoside

3.5 Conclusion

Since oligosaccharides were identified as vital to bodily functions, research efforts have been continuously made to develop mild and selective chemical glycosylation methods to provide serviceable quantities of pure oligosaccharides for study. A reliable procedure to generate oligosaccharides depends greatly upon the ability to tune the leaving groups' reactivity to encourage orthogonality under the reaction conditions. The above discussion of select leaving groups, however, is not all-inclusive. Many other leaving groups for glycosylations have been developed over the years including, but not limited to, sulfoxides, diazirines, silyl ethers, carbonates, and phosphates (Figure 3.5). We would eventually seek to design a glycosyl donor that combines the incredible stability of thioglycosides with the easy activation using catalytic acid of the trichloroacetimidates. Inspired by the mechanistic pathway of *n*-pentenyl

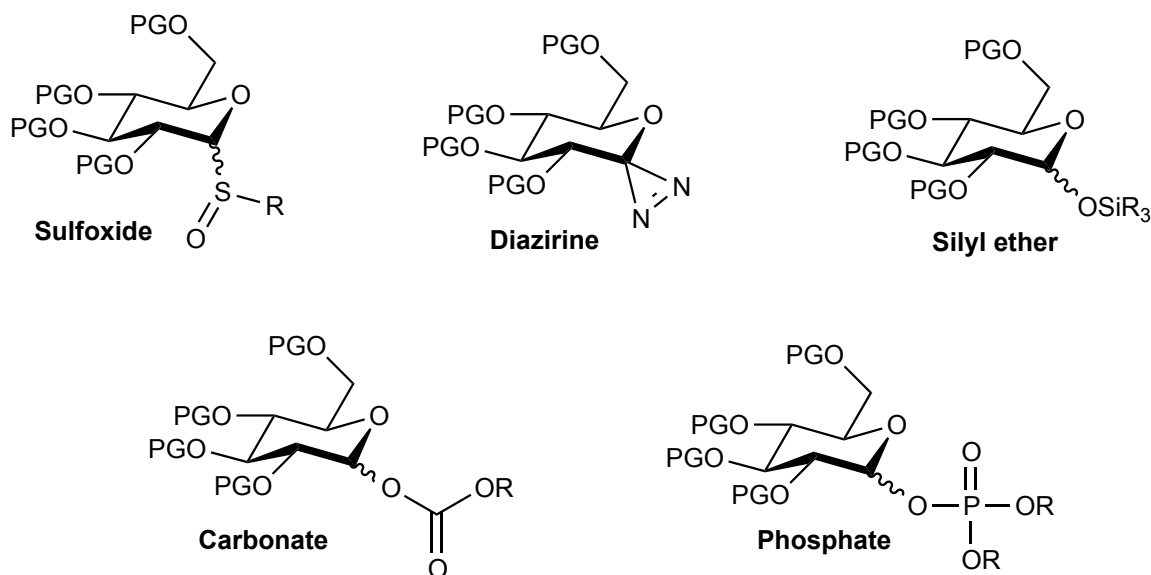


Figure 3.5 Glycosyl donor leaving groups

glycosides, efforts toward the development of such an O-glycosylation is discussed in the following chapters.

3.6 References

1. Merry, A. H.; Merry, C. L. R., *EMBO Rep.* **2005**, 6, 900-903.
2. (a) Huang, K. T.; Winssinger, N., *Eur. J. Org. Chem.* **2007**, 1887-1890. (b) Montreuil, J., *Adv. Carbohydr. Chem. Biochem.* **1980**, 37, 157. (c) Sharon, N., *Sci. Am.* **1974**, 230, 78.
3. (a) Hakamori, S.; *Annu. Rev. Biochem.* **1981**, 50, 733. (b) Li, Y-T.; Li, S-C., *Adv. Carbohydr. Chem. Biochem.* **1982**, 40, 235.
4. Schmidt, R. R., *Angew. Chem. Int. Ed. Engl.* **1986**, 25, 212-235.
5. Barres, F.; Hindsgaul, O., *Modern Synthetic Methods* **1995**, 7, 281-330.
6. Hosoya, T.; Takano, T.; Kosma, P.; Rosenau, T., *J. Org. Chem.* **2014**, 79, 7889-7894.
7. (a) Lemieux, R. *Pure. Appl. Chem.* **1971**, 25, 527. (b) Edward, J. T., *Chem. Ind.* **1955**, 1102-1104.
8. (a) Romers, C.; Altona, C.; Buys, H. R., Havinga, E., *Top. Stereochem.* **1969**, 4, 39-97; (b) Ardan, Z.; Lucken, E. A. C., *Helv. Chim. Acta.* **1973**, 56, 1715-1719.

9. Miljkovic, M.; Jokic, A.; Davidson, E. A., *Carbohydr. Res.* **1971**, 17, 155-164.
10. Miljkovic, M.; Glisin, D.; Gligorijevic, M. *J. Org. Chem.* **1975**, 40, 1054-1057.
11. (a) Vankar, D.; Vankar, P. S.; Behrendt, M.; Schmidt, R. R., *Tetrahedron.* **1992**, 47, 9985.; (b) Schmidt, R. R.; Rücker, E.; *Tetrahedron Lett.* **1980**, 6, 357.; (c) Schmidt, R. R.; J. Michel, J., *J. Carbohydr. Chem.* **1985**, 4, 141.; (d) Schmidt, R. R.; Behrendt, M.; Toepfer, A., *Synlett.* **1990**, 694.
12. (a) Wulff, G.; Röhle, G., *Angew. Chem. Int. Ed.* **1974**, 13, 157-170.; (b) Wulff, G.; Schmidt, W. *Carbohydr. Res.* **1977**, 53, 33.; (c) Wegmann, B; Schmidt, R. R., *Carbohydr. Chem.* **1987**, 6, 357.
13. Demchenko, A. V.; *Handbook of Chemical Glycosylation: Advances in Stereoselectivity and Therapeutic Relevance.* Wiley-VCH. ISBN 978-3-527-31780-6. **2008**, 1-27.
14. Satoh, H.; Halvor, H. S.; Manabe, S.; van Gunsteren, W. F; Hünenberger, P. H., *J. Chem. Theory Comput.* **2010**, 6, 1783-1797.
15. van der Vorm, Hansen, T.; Overkleeft, H. S.; van der Marel, G. A.; Codée, J. D. *C. Chem. Sci.* **2017**, 8, 1867-1875.
16. Pederson, C. M.; Nordstrøm, L. U.; Bols, M., *J. Am. Chem. Soc.* **2007**, 129, 9222-9235.
17. (a) Moitessier, N.; Chapleur, Y., *Tetrahedron Lett.* **2003**, 44, 1731-1735. (b) Haines, A. H., *Adv. Carbohydr. Chem. Biochem.* **1976**, 33, 11-109.
18. Zhang, Z. Y.; Ollman, I. R.; Ye, X-S.; Wischant, R.; Baasov, T.; Wong, C-H., *J. Am. Chem. Soc.* **1999**, 121, 734-753.
19. Ranade, S. C.; Demchenko, A. V., *J. Carbohydr. Chem.* **2013**, 32, 1-43.
20. Koenigs, W.; Knorr, E., *Ber. Deutsch. Chem. Ges.* **1901**, 34, 957-981.
21. Fischer, E.; Armstrong, E. F., *Ber. Deutsch. Chem. Ges.* **1901**, 34, 2885-2900.
22. (a) Paulsen, H., *Chem. Soc. Rev.* **1984**, 13, 15-45. (b) Gervay-Hague, J., *Acc. Chem. Res.* **2016**, 49, 35-47.
23. Perrie, J. A.; Harding, J. R.; King, C.; Sinnott, D.; Stachulski, A. V., *Org. Lett.* **2003**, 5, 4545-4548.
24. Mukaiyama, T.; Murai, Y.; Shoda, S., *Chem. Lett.* **1981**, 431-432.

25. Hashimoto, S.; Hayashi, M.; Noyori, R., *Tetrahedron Lett.* **1984**, 25, 1379-1382.
26. Huang, K. T.; Winssinger, N., *Eur. J. Org. Chem.* **2007**, 1887-1890.
27. Yang, Y.; Yu, B., *Chem. Rev.* **2017**, 117, 12281-12356.
28. Yang, Y.; Yu, B., *Tetrahedron*, **2014**, 70, 1023-1046.
29. Garegg, P. J.; Henrichson, C.; Norberg, T., *Carbohydr. Res.* **1983**, 116, 162-165.
30. (a) Konradsson, P.; Mootoo, D. R.; McDevitt, R. E.; Fraser-Reid, B., *J. Chem. Soc. Chem. Commun.* **1990**, 270-272.; (b) Konradsson, P.; Udodong, U. E.; Fraser-Reid, B., *Tetrahedron Lett.* **1990**, 31, 4313-4316.; (c) Veeneman, G. H.; van Leeuwen, S. H.; van Boom, J. H., *Tetrahedron Lett.* **1990**, 31, 1331-1334.
31. Veeneman, G. H.; van Boom, J. H., *Tetrahedron Lett.* **1990**, 31, 275-278.
32. Lönn, H., *Carbohydr. Res.* **1985**, 139, 105-113.
33. (a) Amatore, C.; Jutand, A.; Mallet, J. M.; Meyer, G.; Sinay, P., *J. Chem. Soc., Chem. Commun.* **1990**, 718-719. (b) Sinay, P., *Pure Appl. Chem.* **1991**, 63, 519-528.
34. (a) Mao, R-Z.; Xiong, D-C.; Guo, F.; Li, Q.; Duan, J.; Ye, X-S., *Org. Chem. Front.* **2016**, 3, 737. (b) Wever, W. J.; Cinelli, M. A.; Bowers, A. A., *Org. Lett.* **2013**, 15 30-33.
35. Spell, M. L.; Wang, X.; Wahba, A. E.; Conner, E.; Ragains, J. R., *Carbohydr. Res.* **2013**, 369, 42-47.
36. Schmidt, R. R.; Michel, J., *Angew. Chem. Int. Ed. Engl.* **1980**, 19, 731-732.
37. (a) Schaubach, R.; Hemberger, J.; Kinzy, W., *Liebigs Ann. Chem.* **1991**, 607-614.; (b) Zimmermann, P.; Bommer, B.; Bär, T.; Schmidt, R. R. **1988**, 7, 435., (c) Adinolfi, M.; Iadonisi, A.; Ravidà, A., *Synlett.* **4**, 583-586.; (d) Du, Y.; Wei, G.; Cheng, S.; Huaa, Y.; Linhardt, R. J., *Tetrahedron Lett.* **2006**, 47, 307-310.
38. Schmidt, R. R.; Michel, J., *J. Carbohydr. Res.* **1985**, 4, 141.
39. Hanessian, S.; Bacquet, C.; Lehong, N., *Carbohydr. Res.* **1980**, 80, c17-c22.
40. Kaeothip, S.; Pornsuriyasak, P.; Rath, N. P.; Demchenko, A. V., *Org. Lett.* **2009**, 11, 799-802.
41. Fraser-Reid, B.; Konradsson, P.; Mootoo, D. R.; Udodong, U., *J. Chem. Soc., Chem. Commun*, **1988**, 823-825.

42. Fortin, M.; Kaplan, J.; Pham, K.; Kirk, S.; Andrade, R. B., *Org. Lett.* **2009**, 11, 3594-3597.

CHAPTER 4: TOWARDS THE DEVELOPMENT OF METAL-FREE O-GLYCOSYLATION METHODS USING THIOLYGLYCOSIDES

4.1 Introduction

Activation of thioglycosides has proven to be challenging over the years due to their stability. Methods for their activation generally fall into four categories¹: halonium reagents (NIS/AgOTf, Selectfluor/BF₃·OEt₂)^{2,3}, organosulfur/selenium promoters (PhSeOTf, MPBT/Tf₂O)^{4,5}, thiophilic metal salts (AgBF₄, Hg(OAc)₂)^{6,7} and chemical/electrochemical/photochemical induced single electron transfer (-e⁻/Bu₄NBF₄, DDQ/hν)^{8,9} (Figure 4.1). Visible-light photochemical methods for thioglycoside activation

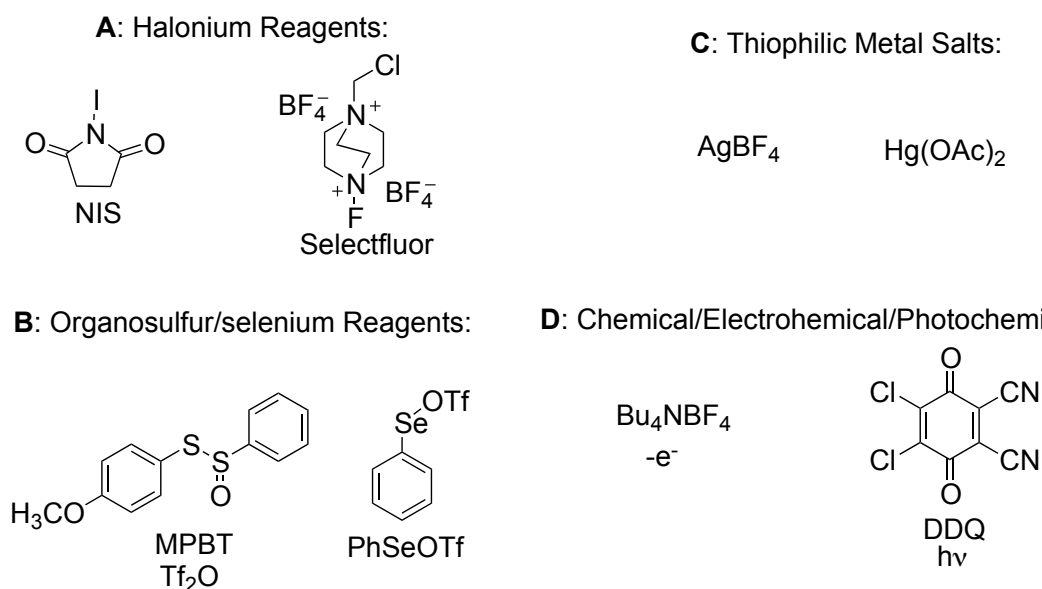


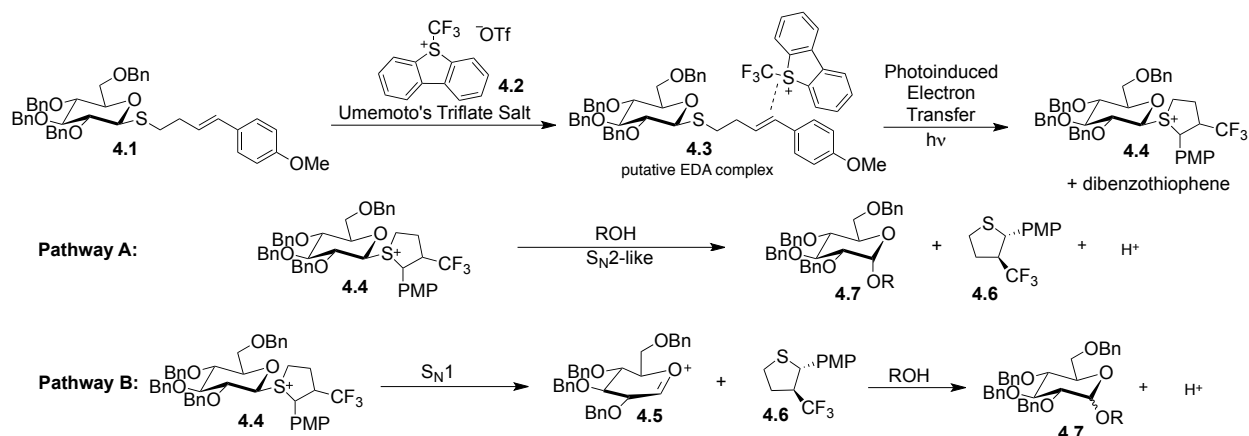
Figure 4.1 Selected reagents used to activate thioglycosides

are especially appealing as the use of visible light to promote the transformation would be a gateway into development of a mild method for glycosylation.

Portions of this chapter previously appeared in [Mark L. Spell, Kristina Deveaux, Caitlin G. Bresnahan, Bradley L. Bernard, William Sheffield, Revati Kumar, Justin R. Ragains, A Visible-Light-Promoted O-Glycosylation with a Thioglycoside Donor, 4/18/2016]. They are reprinted by permission of [John Wiley and Sons.]

Similar to the mechanistic pathway of *n*-pentenyl glycosides where the anomeric oxygen attacks the tethered bromonium species to form a cyclized intermediate¹⁰, we envisioned a system that promoted nucleophilic attack by sulfur. Along with literature precedent demonstrating interception of trifluoromethyl radicals by styrene in the presence of visible-light photocatalysts¹¹, we anticipated using a visible-light photocatalyst with a thioglycoside that incorporated a styrenic moiety to avoid direct generation of a sulfur centered radical cation. However, we would soon discover that photocatalysts were not necessary for our method.

Thioglycoside **4.1** containing the electron rich styrenic moiety was found to form an electron donor-acceptor (EDA) complex with Umemoto's reagent **4.2** (Scheme 4.1). This complex may facilitate the generation and transfer of trifluoromethyl radical to



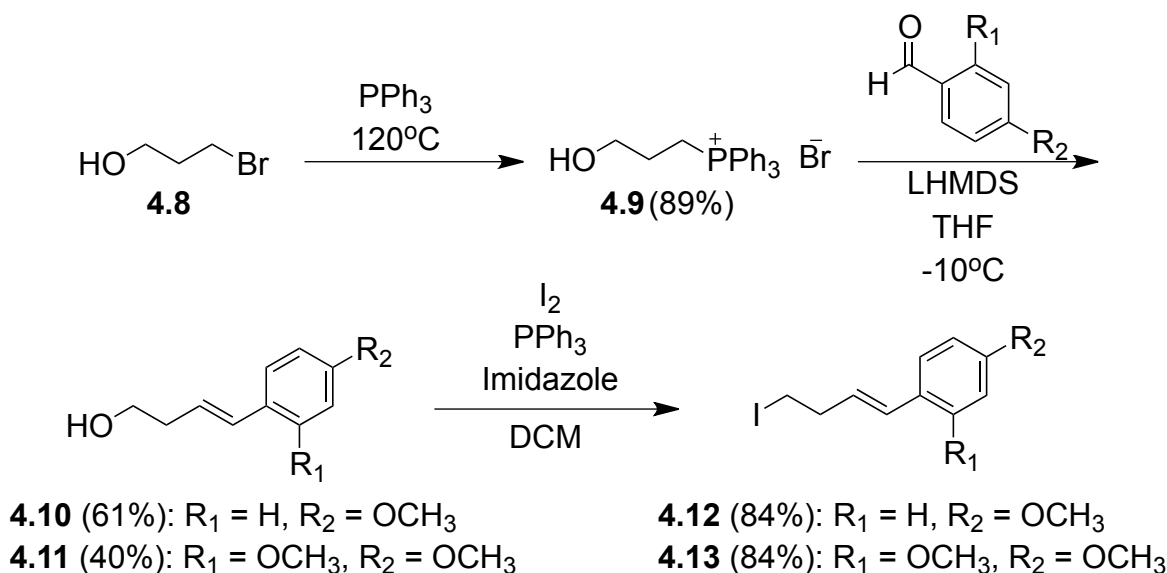
Scheme 4.1 Proposed mechanism for metal-free glycosylation

styrene as **4.3** absorbs a photon of visible-light *in the absence of a metal catalyst*. Once this intermediate forms, sulfur is primed to attack the electrophilic benzyl carbon eventually generating the tetrahydrothiophenium intermediate **4.4** via an S_N1 (B, Scheme 4.1) or S_N2-like (A, Scheme 4.1) pathway. Loss of the tetrahydrothiophene and attack of an alcohol would result in generation of the glycosylated product **4.7**. Efforts

toward supporting the proposed mechanism and attendant experimental observations that changed the course of this project are described herein.

4.2 Synthesis of Thioglycoside Donors

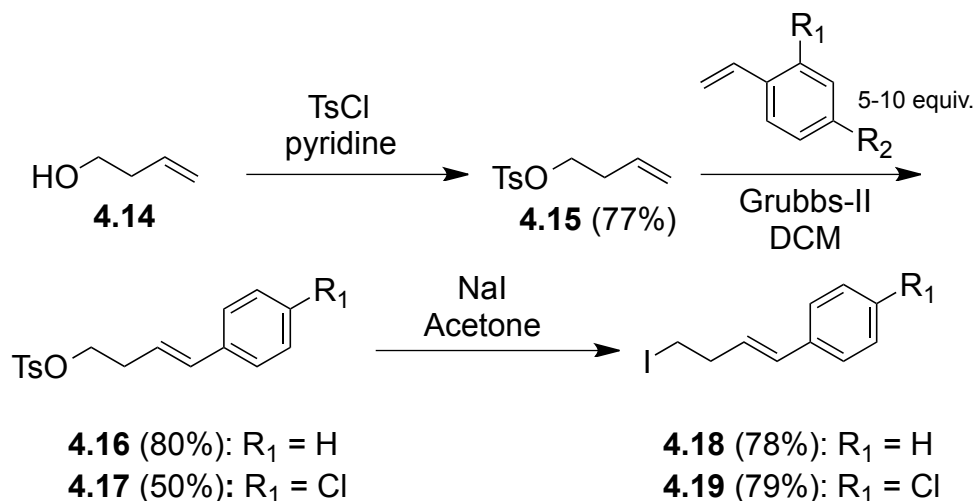
Styrene bearing alkyl iodides **4.12** and **4.13** used for the synthesis of the thioglycosides were synthesized starting with 3-bromopropanol (Scheme 4.2). Phosphonium **4.9** was generated in 89% yield after heating 3-bromopropanol with triphenylphosphine at 120°C¹². Wittig reaction between **4.9** and the benzaldehyde derivatives in the presence of LHMDS at -20°C gave alcohols **4.10** and **4.11** in



Scheme 4.2 Synthesis of alkyl iodides from 3-bromopropanol

moderate yields¹³. Then, **4.10** and **4.11** were converted to the alkyl iodides **4.12** and **4.13** following treatment with triphenylphosphine, I₂ and imidazole in DCM^{14a}. Two additional alcohols were generated from tosylate **4.15** that was a result of reacting 3-buten-1-ol with tosyl chloride in pyridine (Scheme 4.3)^{15a}. Cross-metathesis of **4.15** with styrene or *p*-chlorostyrene in the presence of Grubbs second generation catalyst gave

4.16 (80%) and **4.17** (50%)^{16a}. Substitution with sodium iodide in acetone produced alkyl iodides **4.18** and **4.19** in good yields^{14b}.

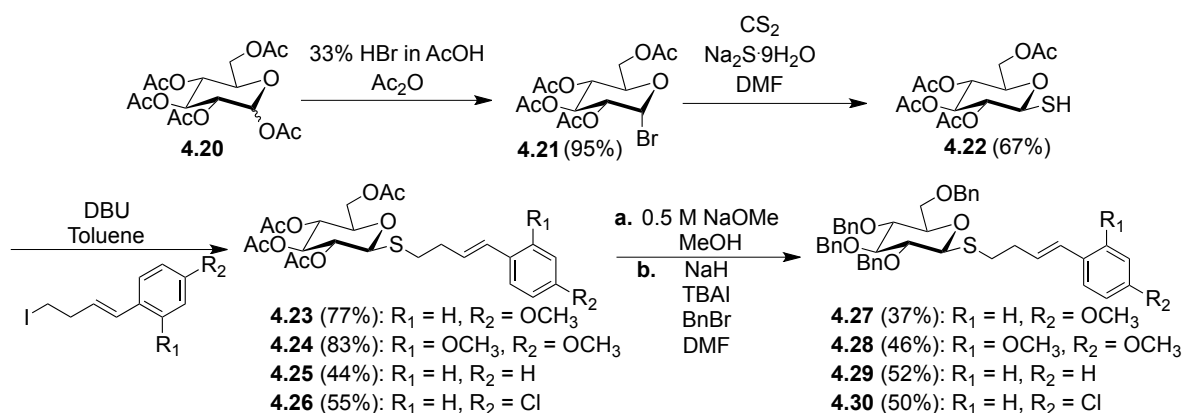


Scheme 4.3 Synthesis of alkyl iodides from 3-buten-1-ol

The synthesis of the thioglycoside donors followed a general procedure with substitution of the various styrenes to generate the corresponding product (Scheme 4.4). Beginning with glucose pentaacetate, conversion to glycosyl bromide **4.21** was achieved by treatment with 33% HBr/AcOH and Ac₂O¹⁷. **4.21** then reacted with CS₂ and Na₂S·9H₂O in DMF to form mercapto glucose **4.22**¹⁸.

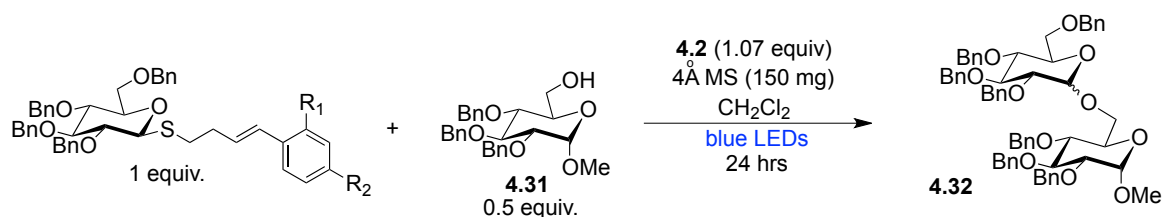
Alkylation of **4.22** with alkyl iodides **4.12**, **4.13**, **4.18**, and **4.19** results in a series of *tetra*-acetyl donors bearing the corresponding side chain^{14b}. Thioglycosides **4.23** - **4.26** were then deacetylated using 0.5M NaOMe in MeOH and subsequently converted to the benzylated donors **4.27** - **4.30** after reacting with benzyl bromide, NaH, and TBAI in DMF^{14b}. These substrates were used for initial experiments exploring the proposed transformation in Scheme 4.1.

4.3 Importance of the *p*-Methoxy Side Chain for Glycosylation



Scheme 4.4 Synthesis of tetrabenzyl thioglycoside donors

The pilot experiment (Figure 4.2) using 0.15 mmol of *p*-methoxy donor **4.27** resulted in 75% of the glycosylated product (**4.32**) when irradiated (blue LEDs, 455 nm)



Entry	Thioglycoside	Yield (%)	$\alpha:\beta$ Ratio
1	4.27	75	1.6:1
2	4.28	61	1.4:1
3	4.29	0	n.a.
4	4.30	0	n.a.

Figure 4.2 Glycosylation experiments with metal-free glycosylation conditions

in the presence of C6-OH acceptor **4.31** (0.5 equiv), Umemoto's reagent **4.2** (1.07 equiv.) and 4Å MS (150 mg) for 24 hours (entry 1, Figure 4.2)^{14b}. Upon addition of Umemoto's reagent, a color change from colorless to yellow was observed signaling the formation of the putative EDA complex (Figure 4.3).²⁴ Glycosyl donor **4.28**, irradiated under the same conditions afforded 61% of the desired product. The yellow color of **4.28** however, made it questionable to assume that an EDA complex with Umemoto's reagent was formed. Thioglycosides with the more electron poor styrenic moieties (**4.29** and **4.30**) showed no consumption of the donors resulting in no disaccharide formation. There was also no color change observed in the presence of **4.2**, leading to the assumption that generation of the EDA complex requires electron rich styrenes.

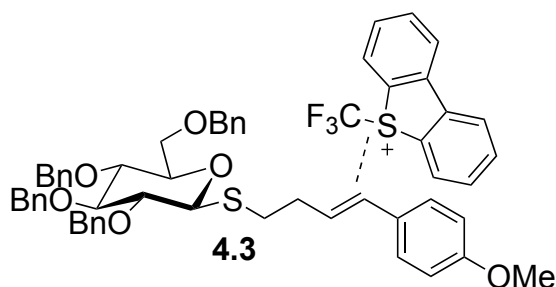


Figure 4.3 Putative EDA complex

Alkyl and most aryl thioglycosides do not absorb visible light, and the thioglycoside donor does not react without irradiation and Umemoto's reagent. If an EDA complex forms with the styrene of the glycosyl donor and Umemoto's reagent, we predicted that the mixture of both would show absorbance in the visible light region. UV-vis spectra of donor **4.27** in MeCN (Figure 4.4) showed no absorbance in the visible-light region while a solution of Umemoto's reagent alone showed weak absorbance between 385 and 410 nm. However, upon mixing the two compounds, absorbance increased and trailed well into the visible light region^{14b}. The absorbance of

thioglycoside **4.29** was also measured (Figure 4.5). After no product was formed using this donor, it was expected that the UV-vis spectrum of a solution of **4.29** would show no

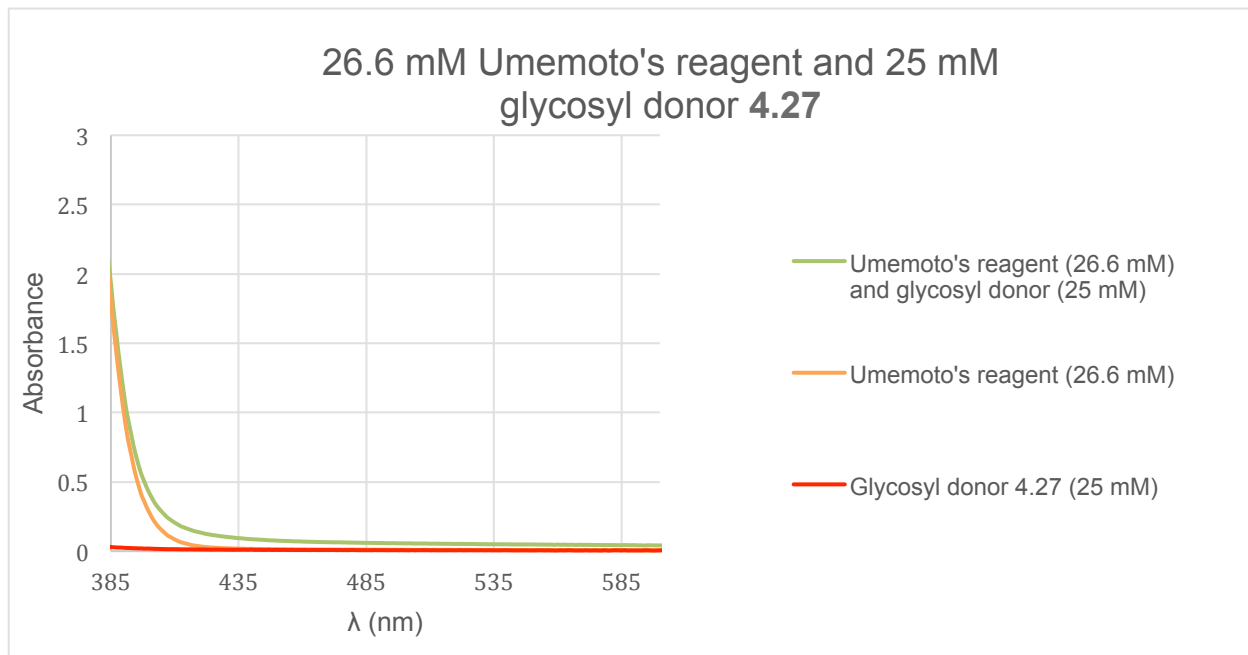


Figure 4.4 Glycosyl donor (4.27) and Umemoto's reagent UV-vis experiment

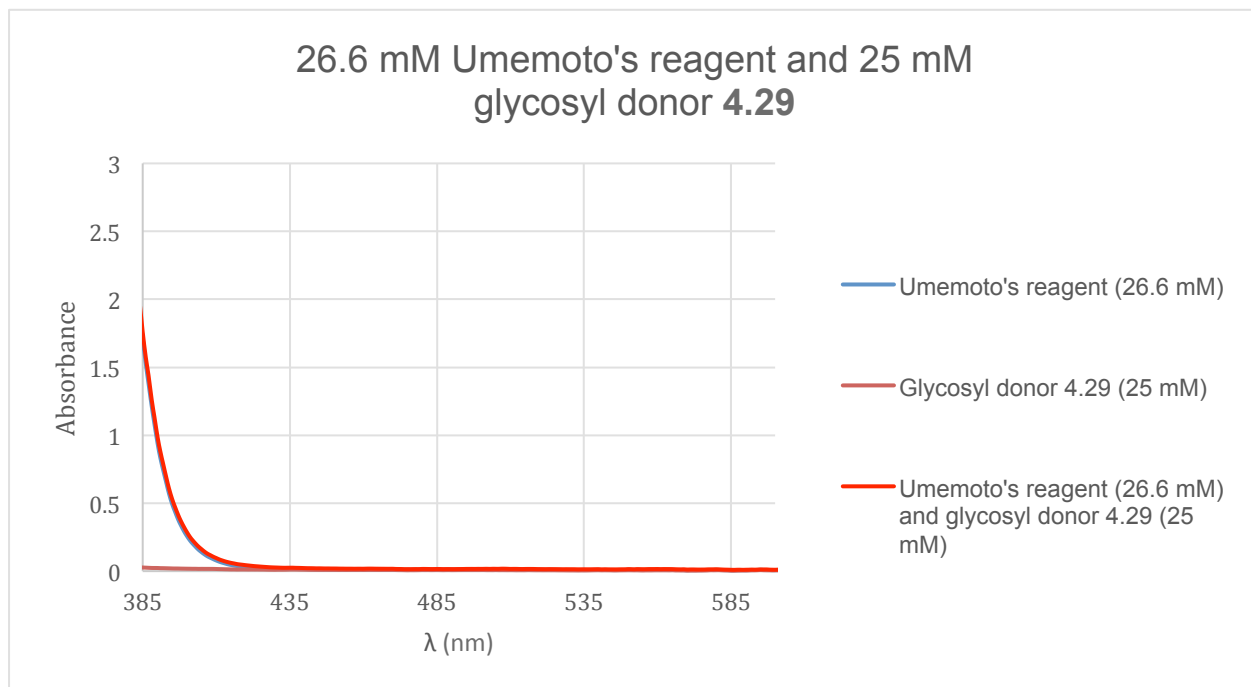


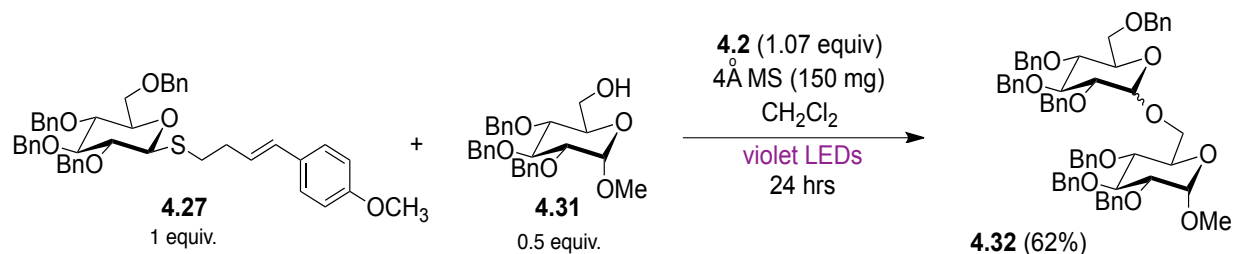
Figure 4.5 Glycosyl donor (4.29) and Umemoto's reagent UV-vis experiment

new absorbance in the visible-light region and this was subsequently confirmed. Similarly, as predicted, a mixture of glycosyl donor **4.29** with Umemoto's reagent did not show any change in absorbance.

Along with the results from the irradiation of **4.29** and **4.30** under the glycosylation conditions, the lack of color change, and the UV-vis analysis of **4.29**, the necessity of the electron rich styrene was confirmed. The lack of reactivity of the electron-poor thioglycosides can be attributed to the lack of EDA complex formation with electron-poor styrenes indicated by a lack of new absorption at 455 nm in the visible light region in the presence of Umemoto's reagent.

4.4 Exploring Thioglycoside Activation Under Ultraviolet Irradiation

While Umemoto's reagent alone did not show much absorbance in the visible light window, analysis of the compound's UV-vis spectra indicated that it was capable of absorbing ultraviolet light. As such, we predicted that UV irradiation would lead to higher reactivity. Not only this, but the putative EDA complex appeared to have a higher extinction coefficient at lower wavelengths. A trial experiment was performed with donor **4.27**, acceptor **4.31**, Umemoto's reagent, and 4Å MS, however the reaction was irradiated with violet LEDs (405 nm) (Scheme 4.5). After 24 hours, the reaction was complete with a 62% isolated yield (1.7:1 α : β) of disaccharide **4.32**. While this result was slightly lower in yield compared to the blue LEDs-irradiated experiment (75%), it

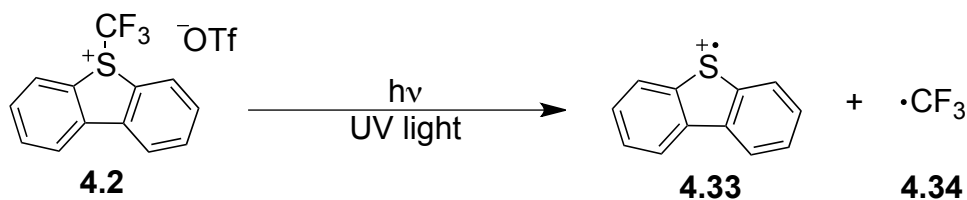


Scheme 4.5 O-Glycosylation experiment with UV light

was promising and warranted further optimization.

For a direct comparison of the reaction efficiency between blue and violet LEDs, an NMR experiment was performed. Two solutions of thioglycoside **4.27**, acceptor **4.31**, Umemoto's reagent and 2,6-di-*tert*-butyl-4-methylpyridine (DTBMP) in CD₃CN were irradiated. DTBMP was used in place of molecular sieves to ensure a homogenous solution and neutralize any triflic acid that may be generated. One of the prepared solutions was irradiated with blue LEDs while the other was exposed to violet LEDs. After 3 hours, 52% of **4.27** had been converted at 455nm while 86% of **4.27** was converted with violet LEDs. As a follow-up experiment, I dissolved Umemoto's reagent in CD₃CN and subjected the solution to irradiation for 1 hour with blue LEDs and violet LEDs separately. While the reagent remained in tact after exposure to blue LEDs, 32% of the reagent was consumed under ultraviolet light irradiation and peaks corresponding to dibenzothiophene were present in the aromatic region.

These results suggested that further optimization could be beneficial and that higher reactivity may be achieved with violet LED irradiation. Ye and coworkers reported that simply irradiating a solution of S-trifluoromethyldibenzothiophenium **4.2** with UV light caused homolytic fragmentation resulting in the formation of dibenzothiophene radical cation and CF₃ radical (Scheme 4.6)^{19a}. Generation of a high concentration of CF₃ radical with UV light irradiation could possibly reduce the reaction time (24 hours



Scheme 4.6 Fragmentation of Umemoto's reagent by UV light

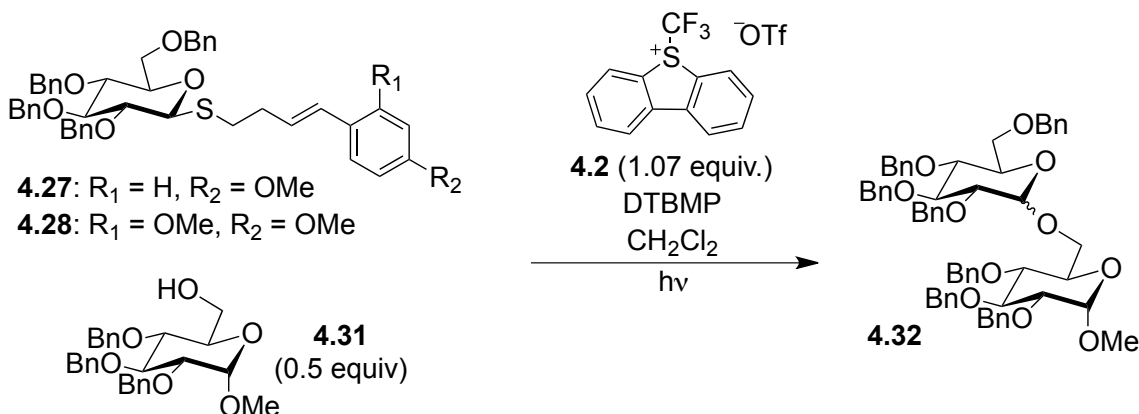
with blue LEDs) potentially resulting in an increase in yield. Bearing in mind that the EDA complex appears to have a higher extinction coefficient at 405nm than Umemoto's reagent, it is possible that both the EDA complex and UV light induced fragmentation of Umemoto's reagent are contributing to the yield.

While molecular sieves are generally used to maintain anhydrous conditions, they also act as a base to prevent generation of triflic acid and proved to be necessary for the efficient glycosylation with blue LEDs^{14b}. Concerns that the shorter wavelength of the violet LEDs were unable to efficiently irradiate the reaction (thus resulting in lower yields) led to the use of a bulky, nonnucleophilic base in place of molecular sieves because of the light scattering that they cause^{19b}.

Substituting DTMBP for molecular sieves resulted in 61% of disaccharide **4.32** (1.6:1 α : β) (entry 1, Figure 4.6). This result was similar to the glycosylation with molecular sieves (62%; α : β). Decreasing the amount of base to 0.6 equivalents, however, resulted in a clean transformation that was complete *in only 2 hours* and yielded 83% of the disaccharide (1.2:1 α : β) (entry 2). To probe whether or not a more electron rich donor would result in higher yields, dimethoxy glycosyl donor **4.28** was reacted under the glycosylation conditions from entry 2 and resulted in a slightly lower yield (72%, 1.1:1 α : β) after 2 hours of irradiation (entry 3).

Interestingly, when irradiated with blue LEDs in the presence of DTBMP (0.6 equiv.) *p*-methoxy donor **4.27** afforded only 51% yield (1.1:1 α : β) of the disaccharide while 2,4-dimethoxy donor **4.28** yielded 86% (1.2:1 α : β) (entries 4 and 5). These reactions, however, still took 24 hours to complete. Since violet light resulted in high

yields coupled with shorter reactions times using *p*-methoxy thioglycoside **4.27**, violet LEDs were used in the experiments that followed.



Entry	Donor	DTBMP equiv.	hν Source	Rxn Time ^a	Yield (%)	α:β
1	4.27	1.2	violet LEDs	24	61	1.6:1
2	4.27	0.6	violet LEDs	2	83	1.2:1
3	4.28	0.6	violet LEDs	2	72	1.1:1
4	4.27	0.6	blue LEDs	24	51	1.1:1
5	4.28	0.6	blue LEDs	24	86	1.2:1

[a] Reactions stirred for 24 hours unless the acceptor was consumed in a shorter amount of time via TLC.

Figure 4.6 Glycosylation experiments with DTBMP

Initial attempts to expand the substrate scope began with structurally simple alcohol, 5-hexen-1-ol (Figure 4.7) After 1 hour of stirring, TLC showed evidence of consumption of the alcohol leading to the assumption that the reaction was complete. Analysis of the crude ¹H NMR revealed peaks corresponding to the tetrahydrothiophene

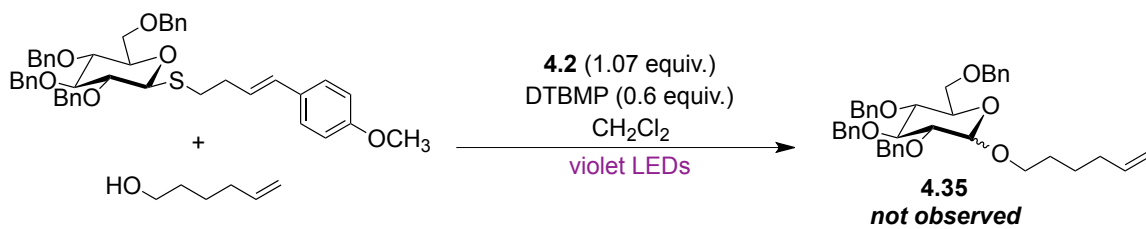


Figure 4.7 Glycosylation experiments with selected acceptors

by-product **4.6**, however, none of the desired glycosylated product was detected. It appeared that the alkene of the acceptor was being degraded under the reaction conditions. To suppress this unwanted reaction, sacrificial alkenes were used as additives (hexane and styrene). In both cases, there was still consumption of the acceptor without any significant amount of the desired product. Though these initial results were exciting, incompatibility with electroneutral alkenes was discouraging. We opted to develop an alternative alkene-compatible method.

4.5 Conclusion

In summary, synthesis of four thioglycosides bearing a 4-aryl-3-butenyl side chain and subsequent screening with the initial visible light irradiation conditions led to the conclusion that electron rich rings assist with the generation of the putative EDA complex. Observation of the absorption spectra of Umemoto's reagent resulted in glycosylation experiments that utilized UV-light as an alternative irradiation source. This change, along with the use of DTBMP as an alternative base, produced very exciting results as the reaction time of the previous method exhibited a twelvefold decrease while maintaining good yields. Although initial attempts to synthesize other glycosidic linkages were unsuccessful, efforts were continued to expand the scope of this reaction. Further details on scope and additional optimization of this method are described in Chapter V.

4.6 Experimental

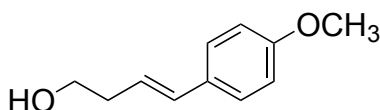
4.6.1 General Methods

Reagents were purchased from Sigma Aldrich and used as received. Flash column chromatography was performed using 60Å silica gel purchased from Sigma

Aldrich. ^1H NMR and ^{13}C NMR spectroscopy were performed on a Bruker AV-400 and AV- 500 spectrometer. Mass spectra were obtained using an Agilent 6210 electrospray time-of-flight mass spectrometer. UV-vis spectrophotometry was performed on a Varian Cary50 UV/vis spectrophotometer. Analytical and preparative TLC were conducted on aluminum sheets (Merck, silica gel 60, F254). Compounds were visualized by UV absorption (254 nm) and staining with anisaldehyde. 5 mL Pyrex micro reaction vessels (Supelco) were used in the glycosylation reactions. The triflate salt of Umemoto's reagent was used in all glycosylations. All glassware was flame-dried under vacuum and backfilled with dry nitrogen prior to use. Deuterated solvents were obtained from Cambridge Isotope Labs. All solvents were purified according to the method of Grubbs.²³

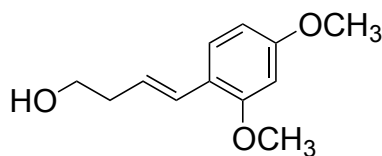
4.6.2 Procedures and Characterization

Synthesis of **4.10**



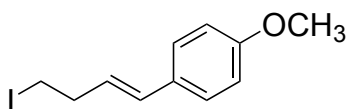
To a mixture of 4.0 g (9.97 mmol) 3-hydroxypropyltriphenylphosphonium bromide¹² in 23 mL dry THF at -20°C was added 22.9 mL (22.9 mmol) LHMDS (1M in THF) dropwise. The mixture stirred for one hour at -20°C then 1.0 mL (8.2 mmol) of anisaldehyde was added dropwise. This resulting mixture stirred for another hour at -20°C before slowly warming to room temperature and was then stirred overnight. The reaction was quenched using 50 mL sat. NH_4Cl (aq), extracted with 50 mL EtOAc, then dried over Na_2SO_4 . Silica gel chromatography (20% EtOAc in hexanes) afforded 0.890 g (61%) of a white solid Spectral data matched that reported in literature.^{13b}

Synthesis of **4.11**



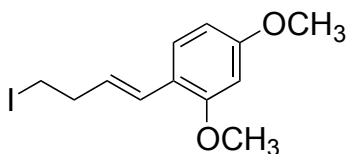
See synthesis of **4.10** for procedure. Started with 4.0 g (9.97 mmol) **4.9**, 20 mL dry THF, 22.9 mL (22.9 mmol) LHMDS, and 1.4 g (8.4 mmol) 2,4-dimethoxy benzaldehyde in 2.9 mL dry THF. Silica gel chromatography (gradient run from 20% EtOAc in hexanes to 30% EtOAc in hexanes) afforded 0.700 g (40%) of a colorless oil. Spectral data matched that reported in literature.^{13b}

Synthesis of **4.12**



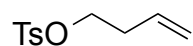
1.8 g (6.9 mmol) triphenylphosphine and 1.7 g (6.7 mmol) I₂ was dissolved in 26 mL CH₂Cl₂ and stirred for 10 minutes at room temperature. 0.77 g (11 mmol) imidazole was added in one portion and reaction stirred for another 10 minutes at room temperature. A solution of 0.80 g (4.5 mmol) **4.10** in 5 mL CH₂Cl₂ was added to the reaction. 30 mL sat. Na₂S₂O₅ was added and the layers were separated. The aqueous layer was extracted with CH₂Cl₂ (2 x 30 mL) and the organic layers were dried over MgSO₄. Silica gel chromatography (5% EtOAc in hexanes) afforded 1.1 g (84%) of a yellow solid. Spectral data matched that reported in literature.^{14b}

Synthesis of **4.13**



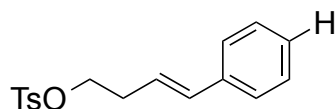
See synthesis of **4.12** for procedure. Started with 1.2 g (4.6 mmol) triphenylphosphine, 1.2 g (4.7 mmol) I₂, 0.52 g (7.6 mmol) imidazole, 0.64 g (3.1 mmol) **4.11** in 21 mL CH₂Cl₂. Silica gel chromatography (5 % EtOAc in hexanes) afforded 0.82 g (84%) of a colorless oil. ¹H NMR (500 MHz, CDCl₃) δ 7.33 (d, *J* = 8.4 Hz, 1H), 6.69 (d, *J* = 15.9 Hz, 1H), 6.46 (d, *J* = 8.4 Hz, 1H), 6.42 (s, 1H), 6.02 (dt, *J* = 15.9, 7.0 Hz, 1H), 3.81 (s, 3H), 3.80 (s, 3H), 3.22 (t, *J* = 7.4 Hz, 2H), 2.76 (q, *J* = 7.3, 2H). ¹³C NMR (126 MHz, CDCl₃) δ 160.3, 157.6, 127.4, 127.1, 126.7, 119.2, 104.9, 98.5, 55.5, 55.4, 37.66, 5.7. HRMS *m/z* Calcd for C₁₂H₁₆IO₂ [M+H]⁺ 319.0189, found 319.0196.

Synthesis of **4.15**



3.6 mL (42 mmol) of 3-buten-1-ol was added to 6.0 mL pyridine and cooled to 0°C. 7.9 g (42 mmol) TsCl was added in one portion to the solution and the reaction was stirred at that temperature until completed via TLC. The mixture was diluted with 100 mL Et₂O then poured into 50 mL of a cold 25% aqueous HCl solution. The resulting layers were separated and extracted with 50 mL Et₂O then dried over MgSO₄. Concentration of the filtrate afforded 7.3 g (77%) of a colorless liquid. Spectral data matched that reported in literature.^{15b}

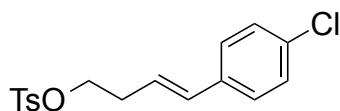
Synthesis of **4.16**



7.6 mL (66 mmol) styrene was added to a solution of 1.50 g (6.63 mmol) **4.15** and 0.056 g (0.066 mmol) Grubbs 2nd generation catalyst in 20 mL CH₂Cl₂ under N₂. The solution was refluxed overnight in an oil bath. Upon cooling to room temperature, the

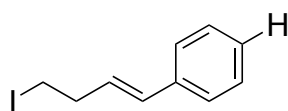
solvent was evaporated to give the crude mixture. Silica gel chromatography (gradient run from 100% hexanes to 20% EtOAc in hexanes) afforded 1.6 g (80%) of a white solid. Spectral data matched that reported in literature.^{14b}

Synthesis of **4.17**



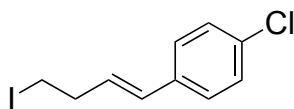
See synthesis of **4.16** for procedure. Started with 4.0 mL (33.15 mmol) *p*-chlorostyrene, 0.056 g (0.066 mmol) Grubbs 2nd generation catalyst, and 1.5 g (6.6 mmol) **4.15** in 20 mL CH₂Cl₂. Silica gel chromatography (gradient run from 100% hexanes to 20% EtOAc in hexanes) afforded 1.1 g (50%) of a white solid. ¹H NMR (500 MHz, CDCl₃) δ 7.78 (d, *J* = 8.3 Hz, 2H), 7.30 (d, *J* = 8.2 Hz, 2H), 7.25 (d, *J* = 8.6 Hz, 2H), 7.18 (d, *J* = 8.5 Hz, 2H), 6.34 (d, *J* = 15.9 Hz, 1H), 5.98 (dt, *J* = 15.8, 7.0 Hz, 1H), 4.13 (t, *J* = 6.5 Hz, 2H), 2.54 (q, *J* = 7.8, 7.2 Hz, 2H), 2.42 (s, 3H). ¹³C NMR (126 MHz, CDCl₃) δ 144.8, 135.4, 133.1, 132.1, 129.9, 128.7, 127.9, 127.4, 124.7, 69.5, 32.5, 21.6.

Synthesis of **4.18**



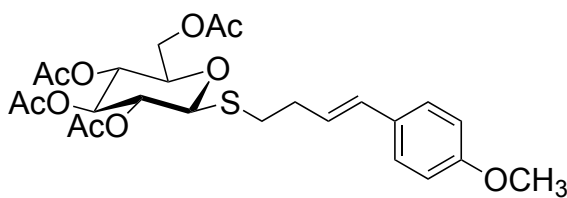
2.2 g (15 mmol) NaI was added to 1.5 g (5.0 mmol) **4.16** in 14 mL acetone at room temperature. The reaction was stirred until completed via TLC followed by filtration through a pad of celite. The filter cake was washed with pentane (2 x 15 mL). The filtrate was then washed with 20 mL H₂O then 20 mL sat. NaCl (aq), dried over Na₂SO₄ and concentrated to afford 1.0 g (78%) of a colorless oil that required no further purification. Spectral data matched that reported in literature.^{14b}

Synthesis of **4.19**



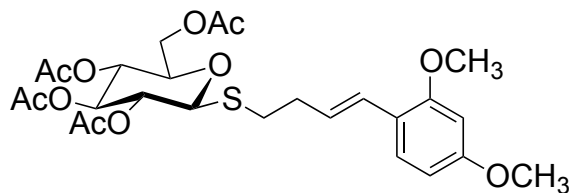
See synthesis of **4.18** for procedure. Started with 1.5 g (10.2 mmol) NaI and 1.1 g (3.3 mmol) **4.17** in 10 mL acetone. Following workup, 0.76 g (79%) of a yellow oil was isolated. ^1H NMR (500 MHz, CDCl_3) δ 7.28 (s, 4H), 6.41 (d, $J = 15.8$ Hz, 1H), 6.11 (dt, $J = 15.8, 6.9$ Hz, 1H), 3.23 (t, $J = 7.2$ Hz, 2H), 2.77 (q, $J = 7.1, 6.5$ Hz, 2H). ^{13}C NMR (126 MHz, CDCl_3) δ 135.7, 133.2, 131.3, 129.4, 128.9, 127.6, 37.3, 4.9.

Synthesis of **4.23**



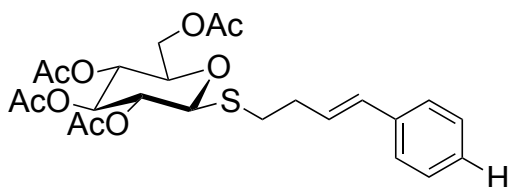
0.70 mL (4.7 mmol) of DBU was added to 1.7 g (4.7 mmol) of 2,3,4,6-tetra-O-acetyl-1-mercapto- β -D-glucopyranoside¹⁸ in 10 mL toluene at -10°C . After 10 minutes, 1.3 g (4.7 mmol) of alkyl iodide **4.12** in 3.7 mL toluene was added dropwise. The reaction was stirred at -10°C for 2 hours until completed via TLC. 20 mL of H_2O was added to quench the reaction. The resulting solution was then extracted with CH_2Cl_2 (2 x 58 mL). The organic layer was further diluted with 58 mL CH_2Cl_2 , washed with 43 mL 1M H_2SO_4 , 43 mL sat. NaHCO_3 (aq), and 43 mL sat. NaCl (aq) then dried over Na_2SO_4 . Silica gel chromatography (gradient run from 15% EtOAc in hexanes to 25% EtOAc in hexanes) afforded 1.9 g (77%) of a white solid. Spectral data matched that previously reported in literature.^{14b}

Synthesis of **4.24**



See synthesis of **4.23** for procedure. Started with 0.36 mL (2.4 mmol) DBU, 0.87 g (2.4 mmol) **4.22** in 5 mL toluene, 0.76 g (2.4 mmol) alkyl iodide **4.13** in 2 mL toluene. Silica gel chromatography (gradient run from 20% EtOAc in hexanes to 50% EtOAc in hexanes) afforded 1.1 g (83%) of a pale yellow solid. ^1H NMR (500 MHz, CDCl_3) δ 7.29 (d, $J = 8.4$ Hz, 1H), 6.64 (d, $J = 15.9$ Hz, 1H), 6.50 – 6.36 (m, 2H), 6.05 (dt, $J = 15.9$, 6.9 Hz, 1H), 5.20 (t, $J = 9.4$ Hz, 1H), 5.06, (t, $J = 9.8$ Hz, 1H), 5.02 (t, $J = 9.8$ Hz, 1H), 4.52 (d, $J = 10.2$ Hz, 1H), 4.22 (dd, $J = 12.3$, 5.0 Hz, 1H), 4.11 (dd, $J = 12.3$, 2.3 Hz, 1H), 3.79 (s, 3H), 3.78 (s, 3H), 3.69 (ddd, $J = 10.1$, 5.0, 2.4 Hz, 1H), 2.88 – 2.67 (m, 2H), 2.49 (dddd, $J = 10.6$, 8.8, 4.5, 2.6 Hz, 2H), 2.05 (s, 3H), 2.02 (s, 3H), 2.00 (s, 3H), 1.99 (s, 3H). ^{13}C NMR (126 MHz, CDCl_3) δ 170.6, 170.1, 169.4, 169.4, 160.2, 157.4, 127.2, 126.3, 125.9, 119.3, 104.8, 98.4, 83.7, 75.8, 73.9, 69.9, 68.3, 62.2, 55.4, 55.3, 33.9, 30.1, 20.7, 20.7, 20.6, 20.6. HRMS m/z Calcd for $\text{C}_{26}\text{H}_{35}\text{O}_{11}\text{S}$ $[\text{M}+\text{H}]^+$ 555.1895, found 555.1896. $[\alpha]_D^{25} = -28.7$ ($c = 1$, DCM).

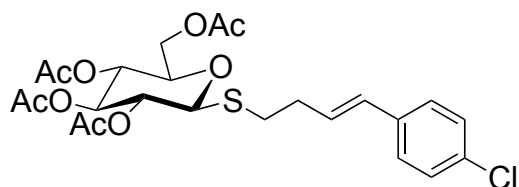
Synthesis of **4.25**



See synthesis of **4.23** for procedure. Started with 0.58 mL (3.9 mmol) DBU, 1.4 g (3.8 mmol) **4.22** in 11.4 mL toluene, and 1.0 g (3.9 mmol) alkyl iodide **4.14** in 2.6 mL toluene. Silica gel chromatography (gradient run from 20% EtOAc in hexanes to 30%

EtOAc in hexanes) afforded 0.820 g (44%) of a white solid. ^1H NMR (500 MHz, CDCl_3) δ 7.34 (d, $J = 7.2\text{Hz}$, 2H), 7.29 (t, $J = 7.6\text{Hz}$, 2H), 7.21 (t, $J = 7.2\text{Hz}$, 1H), 6.44 (d, $J = 15.8\text{Hz}$, 1H), 6.20 (dt, $J = 15.8, 6.9\text{ Hz}$, 1H), 5.26 - 5.18 (m, 1H), 5.14 - 5.00 (m, 2H), 4.52 (d, $J = 10.1\text{ Hz}$, 1H), 4.25 (dd, $J = 12.4, 5.0\text{ Hz}$, 1H), 4.15 (dd, $J = 12.4, 2.3\text{ Hz}$, 1H), 3.72 (ddd, $J = 10.1, 5.0, 2.4\text{ Hz}$, 1H), 2.91 - 2.74 (m, 2H), 2.59 - 2.45 (m, 2H), 2.07 (s, 3H), 2.04 (s, 3H), 2.03 (s, 3H), 2.01 (s, 3H). ^{13}C NMR (126 MHz, CDCl_3) δ 170.8, 170.3, 169.5, 137.4, 131.8, 128.7, 128.0, 127.4, 126.2, 83.8, 76.1, 74.1, 70.0, 68.5, 62.3, 33.4, 29.4, 20.9, 20.9, 20.8, 20.2. HRMS m/z Calcd for $\text{C}_{24}\text{H}_{30}\text{NaO}_9\text{S}$ $[\text{M}+\text{Na}]^+$ 517.1503, found 517.1499. $[\alpha]_D^{25} = -40.3$ ($c = 1$, DCM).^{14b}

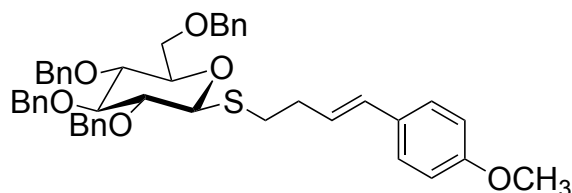
Synthesis of **4.26**



See synthesis of **4.23** for procedure. Started with 0.33 mL (2.2 mmol) DBU, 0.80g (2.2 mmol) **4.22** in 4 mL toluene, and 0.64 g (2.2 mmol) alkyl iodide **4.15** in 2.5 mL toluene. Silica gel chromatography (gradient run from 20% EtOAc in hexanes to 30% EtOAc in hexanes) afforded 0.61 g (55%) of a white solid. ^1H NMR (500 MHz, CDCl_3) δ 7.28 (app. s, 4H), 6.41 (d, $J = 15.8\text{ Hz}$, 1H), 6.19 (dt, $J = 15.8, 6.9\text{ Hz}$, 1H), 5.24 (d, $J = 9.4\text{ Hz}$, 1H), 5.16 - 5.04 (m, 2H), 4.53 (d, $J = 10.0\text{ Hz}$, 1H), 4.27 (dd, $J = 12.4, 4.9\text{ Hz}$, 1H), 4.17 (d, $J = 14.6\text{ Hz}$, 1H), 3.74 (ddd, $J = 10.0, 4.9, 2.3\text{ Hz}$, 1H), 2.93 - 2.77 (m, 2H), 2.53 (m, 2H), 2.09 (s, 3H), 2.06 (s, 3H), 2.05 (s, 3H), 2.03 (s, 3H). ^{13}C NMR (126 MHz, CDCl_3) δ 170.8, 170.4, 169.6, 135.9, 133.0, 130.7, 128.9, 128.8, 127.58, 83.7, 76.9, 76.2, 74.0, 69.9, 68.5, 62.3, 33.4, 29.7, 20.9, 20.9, 20.8, 20.8.

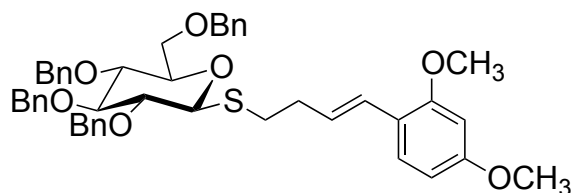
HRMS m/z Calcd for C₂₄H₃₀ClO₉S [M+H]⁺ 529.1294, found 529.1286. [α]_D²⁵ = -10.2 (c = 0.94, DCM).

Synthesis of **4.27**



To a solution of 1.9 g (3.6 mmol) **4.23** in 44.4 mL MeOH was added 1.9 mL (1.9 mmol) of 1M NaOMe. The reaction was stirred overnight at room temperature. Solvent was removed *in vacuo* and the resulting solid was redissolved in 36.0 mL DMF. To this solution was added 0.261 g (0.706 mmol) of TBAI followed by 1.1 g (26 mmol) of 60% oil dispersed NaH at 0°C. After 30 minutes at this temperature, 2.8 mL (24 mmol) of benzyl bromide was added dropwise. The reaction warmed slowly to room temperature and stirred overnight until complete via TLC. At 0°C the reaction was quenched with 45 mL sat. NH₄Cl (aq.) then extracted with Et₂O (2 x 45 mL), washed with 45 mL sat. NaCl (aq.), and dried over Na₂SO₄. Silica gel chromatography (gradient run from 5% EtOAc in hexanes to 10% EtOAc in hexanes) afforded 0.960 g (37%) of a white solid. Spectral data matched that previously reported in literature.^{14b}

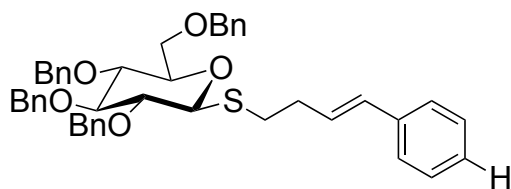
Synthesis of **4.28**



See synthesis of **4.27** for procedure. Started with 0.801 g (1.44 mmol) **4.24**, 18.1 mL MeOH, and 0.79 mL (0.79 mmol) of 1M NaOMe. Resulting solid was dissolved in

14.7 mL DMF followed by 0.106 g (0.290 mmol) TBAI, 0.432 g (10.8 mmol) of 60% oil dispersed NaH, and 1.2 mL (9.9 mmol) of benzyl bromide. Silica gel chromatography (gradient run from 20% EtOAc in hexanes to 30% EtOAc in hexanes) afforded 0.495 g (46%) of a pale yellow solid. ^1H NMR (500 MHz, CDCl_3) δ 7.43 – 7.20 (m, 20H), 7.16 (d, J = 5.0 Hz, 3H), 6.67 (d, J = 15.9 Hz, 1H), 6.43 (d, J = 9.9 Hz, 2H), 6.12 (ddd, J = 16.1, 8.0, 5.9 Hz, 1H), 4.92 (dd, J = 10.6, 5.9 Hz, 2H), 4.82 (dd, J = 14.6, 11.0 Hz, 2H), 4.73 (d, J = 10.1 Hz, 1H), 4.66 – 4.51 (m, 2H), 4.48 (dd, J = 9.9, 2.4 Hz, 1H), 3.80 (s, 3H), 3.78 (s, 3H), 3.72 – 3.64 (m, 2H), 3.61 (t, J = 9.3 Hz, 1H), 3.51 – 3.39 (m, 2H), 2.86 (qt, J = 12.7, 7.5 Hz, 2H), 2.57 (q, J = 7.4 Hz, 2H). ^{13}C NMR (126 MHz, CDCl_3) δ 160.3, 157.7, 138.7, 138.4, 138.3, 138.2, 128.6, 128.6, 128.6, 128.6, 128.2, 128.0, 127.9, 127.9, 127.9, 127.8, 127.5, 127.2, 125.8, 119.8, 104.9, 98.6, 86.9, 85.5, 82.0, 79.3, 78.2, 75.9, 75.7, 75.3, 73.7, 69.3, 55.6, 55.6, 34.3, 31.2. HRMS m/z Calcd for $\text{C}_{46}\text{H}_{51}\text{O}_7\text{S}$ $[\text{M}+\text{H}]^+$ 747.3350, found 747.3333. $[\alpha]_D^{25} = +2.8$ (c = 0.17, DCM).

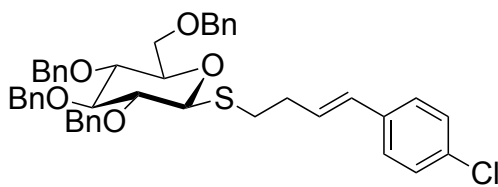
Synthesis of **4.29**



See synthesis of **4.27** for procedure. Started with 0.210 g (0.425 mmol) **4.25**, 5.4 mL MeOH, and 0.23 mL (0.23 mmol) of 1M NaOMe. Resulting solid was dissolved in 4.3 mL DMF followed by 0.03 g (0.09 mmol) TBAI, 0.13 g (3.2 mmol) of 60% oil dispersed NaH, and 0.35 mL (2.9 mmol) of benzyl bromide. Silica gel chromatography (gradient run from 5% EtOAc in hexanes to 10% EtOAc in hexanes) afforded 0.153 g (52%) of a white solid. ^1H NMR (500 MHz, CDCl_3) δ 7.39 - 7.14 (m, 25H), 6.43 (d, J =

15.8 Hz, 1H), 6.24 (dt, $J = 15.8, 6.9$ Hz, 1H), 4.92 (d, $J = 10.7$ Hz, 2H), 4.86 - 4.79 (m, 2H), 4.74 (d, $J = 10.2$ Hz, 1H), 4.62 - 4.53 (m, 3H), 4.49 (d, $J = 9.7$ Hz, 1H), 3.75 (dd, $J = 10.9, 1.9$ Hz, 1H), 3.71 - 3.65 (m, 2H), 3.61 (m, $J = 9.4$ Hz, 1H), 3.50 - 3.43 (m, 2H), 2.94 - 2.80 (m, 2H), 2.59 (q, $J = 6.7$ Hz, 2H). ^{13}C NMR (126 MHz, CDCl_3) δ 138.7, 138.4, 138.2, 138.1, 137.6, 131.5, 128.6, 128.6, 128.6, 128.5, 128.5, 128.5, 128.12, 127.9, 127.9, 127.9, 127.9, 127.8, 127.7, 127.3, 126.3, 86.8, 85.5, 82.0, 79.3, 78.1, 75.9, 75.7, 75.2, 73.6, 69.3, 33.8, 30.9. HRMS m/z Calcd for $\text{C}_{44}\text{H}_{46}\text{NaO}_5\text{S}$ $[\text{M}+\text{Na}]^+$ 709.2958, found 709.2977. $[\alpha]_D^{25} = -7.5$ ($c = 1$, DCM).^{14b}

Synthesis of **4.30**



See synthesis of **4.27** for procedure. Started with 0.57 g (1.1 mmol) **4.26**, 13.6 mL MeOH, and 0.59 mL (0.59 mmol) of 1M NaOMe. Resulting solid was dissolved in 11 mL DMF followed by 0.08 g (0.2 mmol) TBAI, 0.32 g (8.1 mmol) of 60% oil dispersed NaH, and 0.88 mL (7.420 mmol) of benzyl bromide. Silica gel chromatography (gradient run from 10% EtOAc in hexanes to 15% EtOAc in hexanes) afforded 0.395 g (50%) of a white solid. ^1H NMR (500 MHz, CDCl_3) δ 7.39 – 7.12 (m, 24H), 6.37 (d, $J = 15.9$ Hz, 1H), 6.21 (dt, $J = 15.8, 6.8$ Hz, 1H), 4.91 (dd, $J = 10.6, 5.3$ Hz, 2H), 4.87 – 4.79 (m, 2H), 4.75 (d, $J = 10.2$ Hz, 1H), 4.57 (q, $J = 12.3$ Hz, 3H), 4.48 (d, $J = 9.7$ Hz, 1H), 3.75 (dd, $J = 10.9, 1.9$ Hz, 1H), 3.71 – 3.65 (m, 2H), 3.61 (t, $J = 9.3$ Hz, 1H), 3.51 – 3.43 (m, 2H), 2.94 – 2.79 (m, 2H), 2.58 (qd, $J = 7.3, 1.4$ Hz, 2H). ^{13}C NMR (126 MHz, CDCl_3) δ 138.7, 138.4, 138.2, 138.1, 136.1, 132.9, 130.4, 129.4, 128.8, 128.7, 128.6, 128.6, 128.6,

128.5, 128.2, 128.1, 128.0, 128.0, 127.9, 127.8, 127.5, 86.8, 85.5, 82.0, 79.3, 78.2, 76.0, 75.7, 75.3, 73.7, 69.4, 33.8, 30.8. HRMS m/z Calcd for C₄₄H₄₆ClO₅S [M+H]⁺ 721.2749, found 721.2784. $[\alpha]_D^{25} = -6.1$ (c = 0.47, DCM).

General procedure for glycosylation with blue LED irradiation:

A flame-dried 5 mL Pyrex reactor vial was charged with the glycosyl donor (1 equiv., 0.150 mmol), Umemoto's reagent (1.07 equiv., 0.160 mmol), the glycosyl acceptor (0.5 equiv., 0.0752 mmol), 150 mg of freshly activated 4 Å molecular sieves and 1 mL of dry dichloromethane under nitrogen atmosphere. The reactor vial was placed 1-2 cm away from the light source (4W blue LEDs, 2 strips, Sapphire Blue LED Flex Strips from Creative Lighting Solutions were wrapped around a 150 × 75 Pyrex crystallizing dish) and irradiated from the side for 24 hours. The reaction mixture was then filtered to remove molecular sieves and washed with 5 mL DCM. The crude products were concentrated and then purified by gradient silica gel chromatography to afford a mixture of anomeric products.

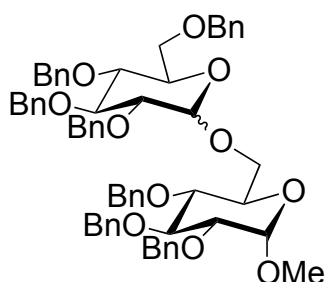
General procedure for glycosylation with violet LEDs:

A flame-dried 5 mL Pyrex reactor vial was charged with the glycosyl donor (1 equiv., 0.150 mmol), Umemoto's reagent (1.07 equiv., 0.160 mmol), the glycosyl acceptor (0.5 equiv., 0.0752 mmol), DTBMP (0.6 equiv., 0.090mmol), and 1 mL of dry dichloromethane under nitrogen atmosphere. The reactor vial was placed 1-2 cm away from the light source (4W violet LEDs, 2 strips, Purple/UV LED Flex Strips from Creative Lighting Solutions were wrapped around a 150 × 75 Pyrex crystallizing dish) and irradiated from the side for 2 hours. The crude products were concentrated and then purified by gradient silica gel chromatography to afford a mixture of anomeric products.

Determination of anomeric ratios:

The anomeric ratio ($\alpha:\beta$) was determined based on the integration of key resonances identified with the assistance of published ^1H NMR data. In the cases where spectral data was unavailable, the anomeric products were separated with silica gel chromatography or preparative TLC.

Synthesis of disaccharide **4.32**



Started with 0.108 g (0.15 mmol) of thioglycoside **4.27**, 0.064 g (0.16 mmol) Umemoto's reagent, 0.035 g (0.075 mmol) methyl 2,3,4-tri-O-benzyl- α -D-glucopyranoside **4.31**, 0.018 g (0.090 mmol) DTBMP), and 1 mL of dry dichloromethane. Silica gel chromatography (gradient run from 5% Et₂O in hexanes to 30% Et₂O in hexanes) afforded 0.061 g (83%; 1.2:1 $\alpha:\beta$) of a white solid, disaccharide **4.32**. Spectral data matched that previously reported in literature.²²

4.7 References

1. Lian, G.; Zhang, X.; Yu, B., *Carb. Res.* **2015**, 403, 13-22.
2. (a) Konradsson, P.; Udodong, U. E.; Fraser-Reid, B., *Tetrahedron Lett.* **1990**, 31, 4313-4316. (b) Konradsson, P.; Mootoo, D. R.; McDevitt, R. E.; Fraser-Reid, B., *J. Chem. Soc., Chem. Commun.* **1990**, 270-272.
3. Burkart, M. D.; Zhang, Z. Y.; Hung, S. C.; Wong, C. H., *J. Am. Chem. Soc.* **1997**, 119, 11743-11746.

4. (a) Ito, Y.; Ogawa, T., *Tetrahedron Lett.* **1988**, 29, 1061-1064. (b) Ito, Y.; Ogawa, T.; Numata, M.; Sugimoto, M., *Carbohydr. Res.* **1990**, 202, 165-175.
5. Crich, D.; Smith, M., *Org. Lett.* **2000**, 2, 4067-4069.
6. Lear, M. J.; Yoshimura, F.; Hiramama, M., *Angew. Chem. Int. Ed.* **2001**, 40, 946-949.
7. Ferrier, R. J.; Hay, R. W.; Vethaviasar, N., *Carbohydr. Res.* **1973**, 27, 55-61.
8. (a) Amatore, C.; Jutand, A.; Mallet, J-M.; Meyer, G.; Sinaÿ, P., *J. Chem. Soc., Chem. Commun.* **1990**, 718-719. (b) Balavoine, G.; Greg, A.; Fischer, J-C.; Lubineau, A., *Tetrahedron Lett.* **1990**, 31, 5761-5764.
9. Nakanishi, M.; Takahashi, D.; Toshima, K., *Org. Biomol. Chem.* **2013**, 52, 8441-8445.
10. Frasier-Reid, B.; Konradsson, P.; Mootoo, D. R.; Udodongs, U., *J. Chem. Soc., Chem. Commun.* **1988**, 823-825.
11. Yasu, Y.; Koike, T.; Akita, M., *Angew. Chem. Int. Ed.* **2012**, 51, 9567-9571.
12. Perlman, N.; Livneh, M.; Albeck, A., *Tetrahedron.* **2000**, 56, 1505-1516.
13. (a) Zeng, X.; Miao, C.; Wang, S.; Xia, C.; Sun, W., *Chem. Commun.* **2013**, 49, 2418-2420. (b) Lin, R.; Sun, H.; Yang, C.; Shen, W.; Xia, W., *Chem. Commun.* **2015**, 51, 399-401.
14. (a) Grzywacz, P.; Plum, L. A.; Clagett-Dame, M.; Deluca, H. F., *Bioorg. Chem.* **2013**, 47, 9-16. (b) Spell, M. L.; Deveaux, K.; Bresnahan, C. G.; Bernard, B. L.; Sheffield, W.; Kumar, R.; Ragains, J. R., *Angew. Chem. Int. Ed.* **2016**, 55, 6515-6519.
15. (a) Bonfand, E.; Motherwell, W. B.; Pennell, A. M. K.; Muhammed, K.; Ujjainwalla, F., *Heterocycles.* **1997**, 46, 523-534. (b) Ning, X-S.; Wang, M-M.; Yao, C-Z.; Chen, X-M.; Kang, Y-B., *Org. Lett.* **2016**, 18, 2700-2703.
16. (a) Bahde, R. J.; Rychnovsky, S. D., *Org. Lett.* **2008**, 10, 4017-4020. (b) Fisher, M. J.; Overman, L. E., *J. Org. Chem.* **1990**, 55, 1447-1459.
17. Mancini, R. S.; McClary, C. A.; Anthonipillai, S.; Taylor, M. S., *J. Org. Chem.* **2015**, 80, 8501-8510.
18. Jana, M.; Misra, A. K., *J. Org. Chem.* **2013**, 78, 2680-2686.
19. Mao, R-Z.; Xiong, D-C.; Guo, F.; Li, Q.; Duan, J.; Ye, X-S., *Org. Chem. Front.*

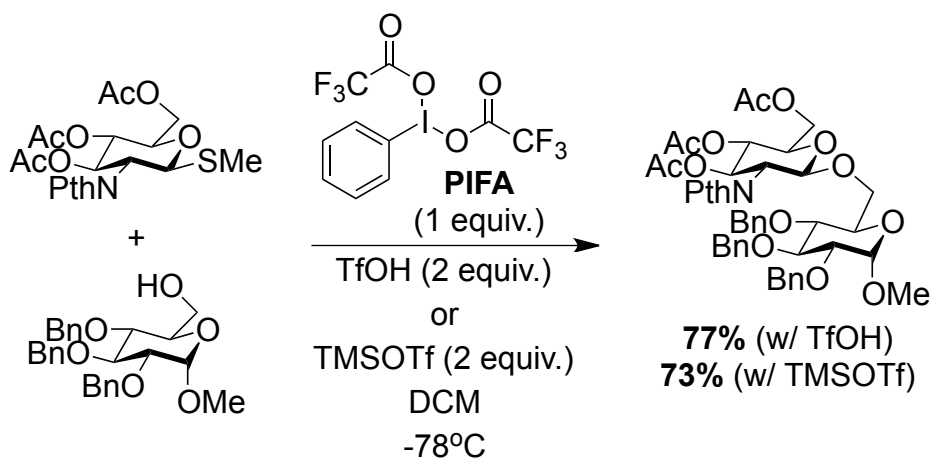
- 2016**, 3, 737-743. (b) Cumpstey, I.; Crich, D., *J. Carbohydr. Chem.* **2011**, 30, 469-485.
20. Lui, H.; Li, X., *J. Org. Chem.* **2014**, 79, 5834-5841.
21. Chao, C-S.; Yen, Y-F.; Hung, W-C.; Mong, K-K. T., *Adv. Synth. Catal.* **2011**, 353, 879-884.
22. Nokami, T.; Shibuya, A.; Tsuyama, H.; Suga, S.; Bowers, A. A.; Crich, D.; Yoshida, J., *J. Am. Chem. Soc.* **2007**, 129, 10922–10928.
23. Pangborn, A.B.; Giardello, M. A.; Grubbs, R. H.; Rosen, R. K.; Timmers, F. J., *Organometallics* **1996**, 15, 1518.
24. Cheng, Y.; Yuan, X.; Ma, J.; Yu, S., *Chem. Eur. J.* **2015**, 21, 8355-8359.

CHAPTER 5: DEVELOPMENT OF ACID-PROMOTED GLYCOSYLATION OF ALCOHOLS WITH THIOLYCOSIDES

5.1 Introduction

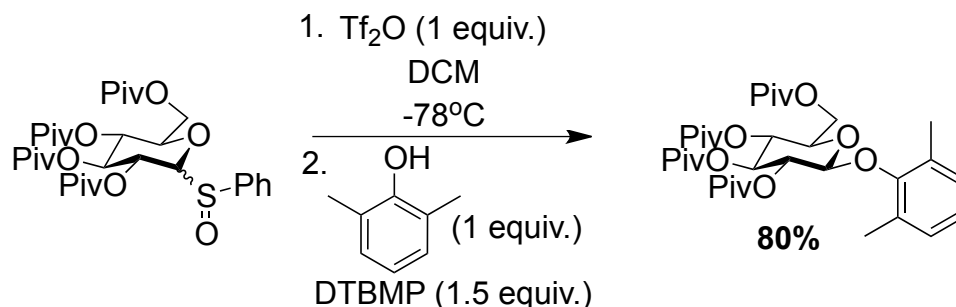
Halonium-based reagents such as *N*-bromosuccinimide (NBS) or *N*-iodosuccinimide (NIS) often accompany acid promotion when thioglycosides are used as *O*-glycosylation donors. For example, a popular combination, first reported by van Boom and co-workers, is trifluoromethanesulfonic acid (TfOH) and NIS¹. Alternatively, hypervalent iodine(III) reagents have provided mild access to electrophilic iodonium species for the activation of thioglycosides²⁻⁴. Recently, Kita and colleagues demonstrated that phenyliodine(III) bis(trifluoroacetate) (PIFA) in the presence of TfOH or trimethylsilyl trifluoromethanesulfonate (TMSOTf) was an effective promoter for thioglycoside activation (Scheme 5.1)⁴.

Another class of sulfur-containing glycosyl donors known as sulfinyl glycosides are commonly activated using triflic anhydride (Tf₂O) (Scheme 5.2)^{5a}. Activation of these sulfoxides is accompanied by bulky, non-nucleophilic bases, such as di-*tert*-butyl-4-methylpyridine (DTBMP), as acid scavengers. The reactivity of sulfinyl glycosides



Scheme 5.1 Hypervalent iodine(III) reagent (PIFA)-promoted glycosylation

obviates halonium-based reagents, however, they are less stable than thioglycosides and decomposition is often a limitation. A similar trend is seen with the frequently used trichloroacetimidate glycosyl donors^{5b,c} (Figure 5.1).



Scheme 5.2 Glycosylation with a Pivaloate-protected sulfinyl glycoside. (Piv = pivaloate)

In an effort to combine the best of both worlds (stability of thioglycosides and reactivity of trichloroacetimidate donors), we have developed an acid-catalyzed glycosylation with thioglycoside donors. Disaccharides were successfully obtained when 4-aryl-3-butenylthioglycosides reacted with selected glycosyl acceptors in the presence of acid. Optimization and development of this method is discussed herein.

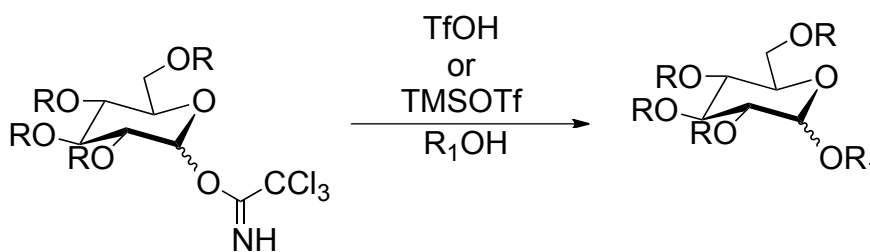
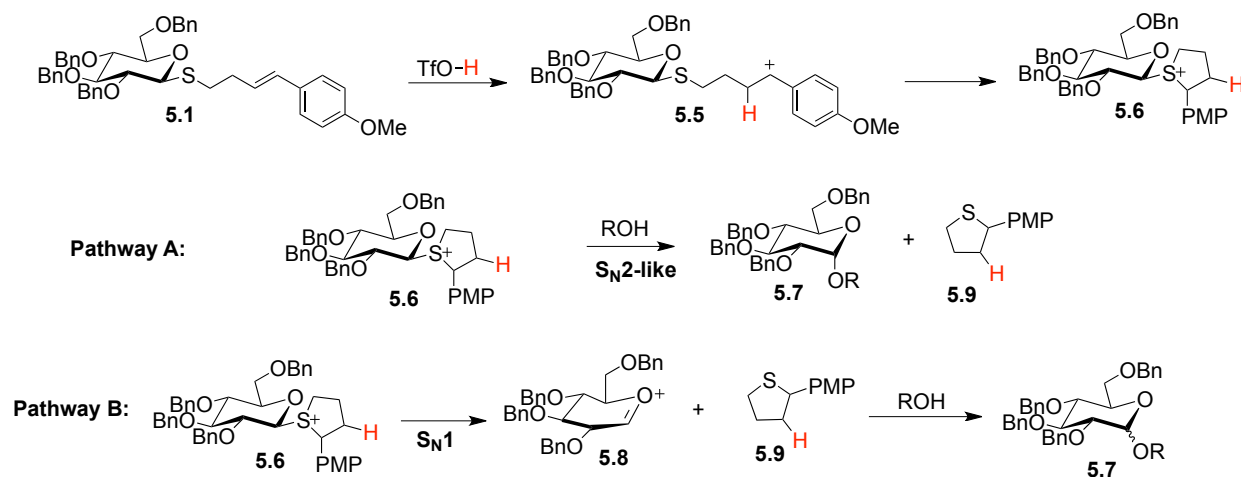


Figure 5.1 Trichloroacetimidate glycosyl donor

5.2 Mechanistic Proposal for Acid-Promoted Remote Glycosylation

We hypothesized that acid in the presence of the electron rich 4-aryl-3-butenylthioglycoside side chain could result in activation of the thioglycoside donor. We proposed a plausible mechanism for the transformation. The mechanistic proposal for

an acid-promoted glycosylation is shown in Scheme 5.3 and is similar to the visible-light glycosylation with Umemoto's reagent and **5.1**. Protonation of the styrenic moiety of 4-



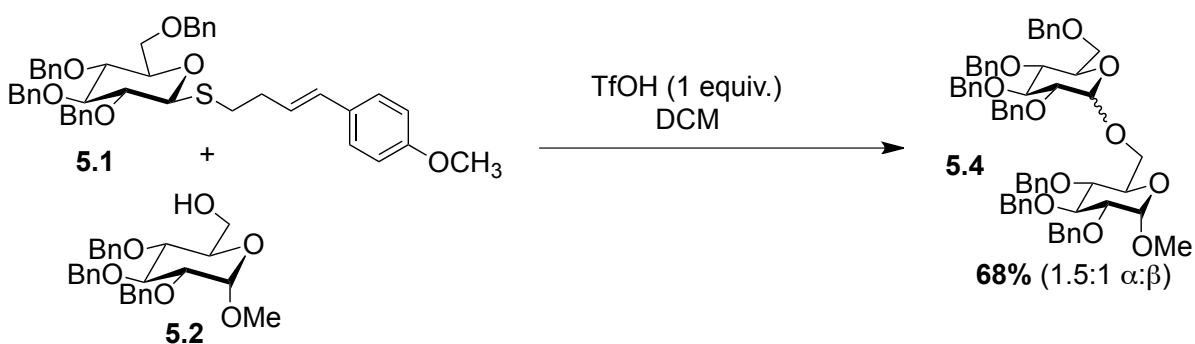
Scheme 5.3 Mechanistic proposal for acid-promoted glycosylation. PMP = *p*-methoxyphenyl

aryl-3-butenylthioglycoside **5.1** by triflic acid results in intermediate **5.5**. The stable benzylic carbocation can then be attacked by sulfur to generate sulfonium intermediate **5.6**. This activated donor is now suited to react with an acceptor (ROH) to form glycosidic linkages via an $\text{S}_{\text{N}1}$ or $\text{S}_{\text{N}2}$ -like pathway (B and A, respectively).

5.3 Pilot Experiment and Optimization of Glycosylation Method

Following the color change observation, I ran an experiment using 1 equivalent of triflic acid and omitted UV-light, DTBMP, and Umemoto's reagent in an effort to support the mechanistic proposal. To my surprise, the disaccharide was isolated in 68% yield (1.5:1 α : β) after one hour (Scheme 5.4). Tetrahydrothiophene **5.9** (Scheme 5.3) was isolated as a reaction by-product.

To begin optimization, we looked at the affect of the amount of acid on the thioglycoside donor (Figure 5.2). Lowering the equivalents of triflic acid to 10 mol % constituted an improvement (entry 2). After one hour, the desired disaccharide was



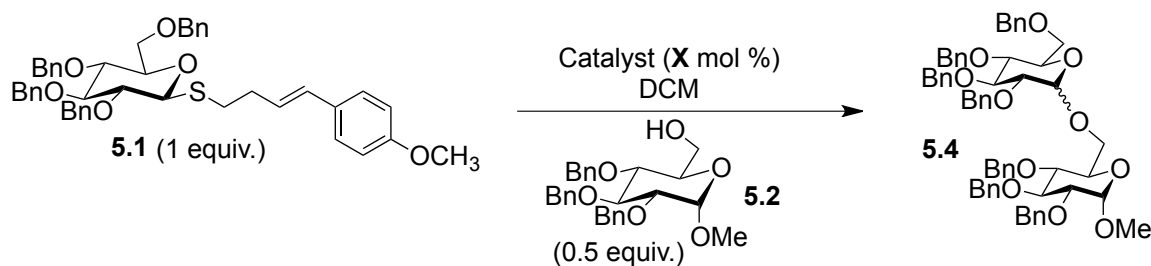
Scheme 5.4 Acid-promoted glycosylation using a 4-aryl-3-butenylthioglycoside

isolated in 87% yield (1.4:1 α : β). This result was very promising and thus represented an irradiation and metal-free/thiophile-free catalytic activation of a bench stable thioglycoside. Prior to attempting entry 5, glycosylation experiments were simply concentrated *in vacuo* upon complete consumption of the glycosyl acceptor. Quenching the reaction with sat. NaHCO_3 (aq), however, did not appear to have a beneficial effect on the reaction as the yield decreased to 61% with a negligible difference in the anomeric ratio (1.6:1 α : β). This result suggests that the presence of triflic acid in the workup doesn't cause epimerization at the anomeric carbon.

Interestingly, when trimethylsilyl trifluoromethylsulfonate (TMSOTf) was employed (instead of TfOH), 85% (1.4:1 α : β) of the disaccharide was isolated (entry 3) presumably as a result of triflic acid generated *in situ* via silylation of the alcohol by TMSOTf. Efforts to employ even milder acid sources were unsuccessful as attempts with 2-naphthol as a photoacid⁸ (irradiated with violet LEDs) showed no consumption of donor (entry 4). To probe the reactivity of the thioglycoside under these conditions at low temperatures, glycosylation was carried out at -20°C . After 5 hours of stirring at that temperature, there was no evidence of the desired product by TLC analysis (entry 7).

The same reaction was warmed to 0°C and yielded 70% of the disaccharide after 3 hours and slightly favored the *beta* anomer (1:1.1 α : β).

While entry 7 confirms that thioglycoside **5.1** performs better at warmer temperatures (0°C to r.t.) than at -20°C, this experiment also demonstrates the orthogonality of this thioglycoside donor to donors that react under acid catalysis at -20°C and lower. One can imagine activation of a trichloroacetimidate at a low

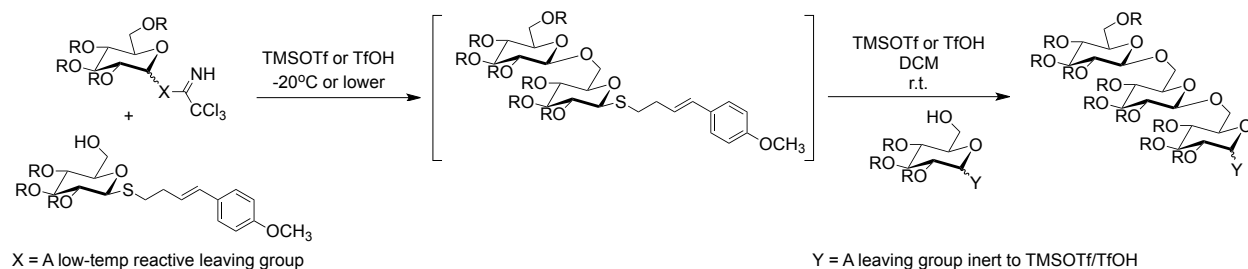


Entry	Catalyst	X	Additive	Time (h)	Yield (%)	α : β
1	TfOH	100	n.a	0.5	68	1.5:1
2	TfOH	10	n.a.	1	87	1.4:1
3	TMSOTf	10	n.a.	1	85	1.4:1
4 ^a	2-naphthol	30	n.a.	1	n.a.	n.a.
5 ^b	TfOH	10	n.a.	1	61	1.6:1
6 ^c	TfOH	10	4Å MS	1	n.a.	n.a.
7 ^d	TfOH	10	n.a.	8	70	1:1.1
8 ^e	n.a.	n.a.	AW-MS	1	n.a.	n.a.
9 ^e	TfOH	10	AW-MS	2	75	1.5:1

[a] Irradiated with violet LEDs for 5hrs. [b] Reaction quenched with 5 ml aq. NaHCO₃. [c] 150 mg 4Å molecular sieve. [d] Reaction stirred at -20 °C for 5 hrs. then warmed to 0 °C and stirred for 3 hrs. [e] Acid washed molecular sieves (AW-MS 150mg, crushed and heated to activate).

Figure 5.2 Glycosylation optimization

temperature with a 4-aryl-3-butenylthioglycoside-bearing acceptor (Scheme 5.5). Upon warming to room temperature, activation of the side chain with the acid-catalyzed



Scheme 5.5 4-aryl-3-butenylthioglycoside as an acceptor

conditions would result in a trisaccharide. Orthogonality is an important aspect of oligosaccharide synthesis and therefore the observation as a result of entry 7 is noteworthy.

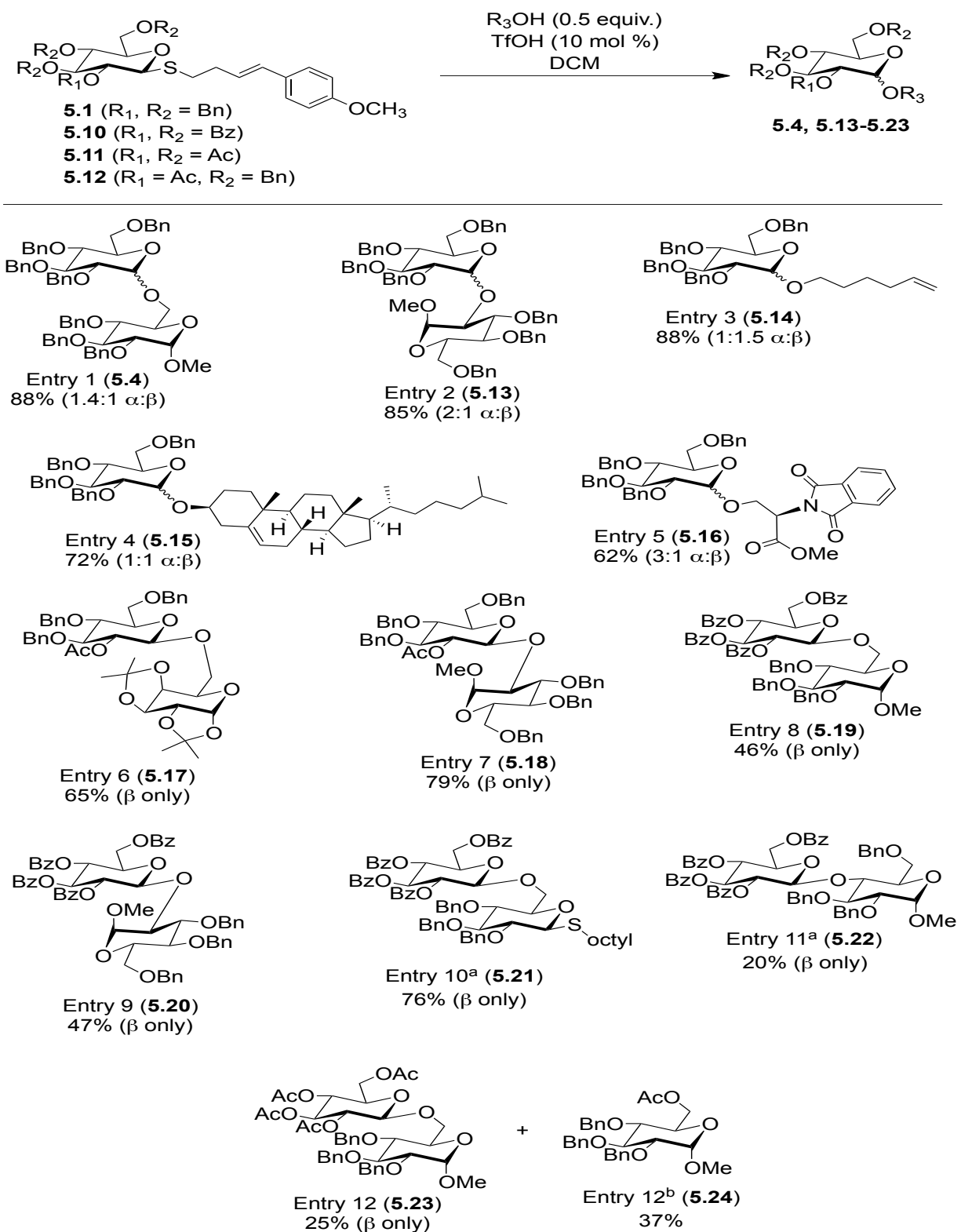
The effect of molecular sieves on the acid-promoted glycosylation was also tested. 150 mg of 4Å molecular sieves were added to the reaction, and after stirring for 1 hour, there was only a trace amount of the disaccharide (entry 6). This suggested that the molecular sieves effectively neutralized any triflic acid in previous visible-light glycosylation experiments. Further examination of crude ^1H NMR spectra from Ch. 4 photochemical glycosylations indicated that **5.9** was not present in these examples. Alternatively, to capitalize on the beneficial water absorbing quality of molecular sieves without neutralization of triflic acid, acid-washed molecular sieves (AW-MS) were used. While the reaction took longer to complete (2 hours), the disaccharide was obtained in 75% yield ($\alpha:\beta$) in the presence of 4Å AW-500 MS (entry 9). A report demonstrating glycosylation with alkyl- and arylthioglycosides in the presence of NIS and AW-MS⁷ prompted the experiment outlined in entry 8 in which only AW-MS were used as a potential acid catalyst. I discovered, however, that using only AW-MS was not an effective way to activate donor **5.1**.

5.4 Establishment Of Substrate Scope

Several additional donors and acceptors were screened using the optimal conditions for glycosylation (4-aryl-3-butenylthioglycoside **5.1** (0.150mmol) and a glycosyl acceptor (0.075 mmol), TfOH or TMSOTf (0.0150 mmol), and 1 mL dichloromethane) (Figure 5.2). These conditions were applied to several additional acceptors and donors. Donor **5.1** provided good to excellent yields of glycosides and disaccharides with relatively low stereoselectivity (entries 1-4, Figure 5.3).

Phtalimide-protected methyl-D-serine afforded 62% of the glycosidic product (entry 5) and favored the *alpha* anomer (3:1) while more challenging linkages using secondary acceptors were successful as disaccharide **5.13** (entry 2) was isolated in 85% yield with a 2:1 α : β ratio. Product **5.14** was formed in 88% yield when 5-hexen-1-ol was employed. It is important to note that this acceptor was not tolerated in the presence of the Umemoto's reagent, DTBMP, and UV-light (Chapter IV). Another alkene-containing acceptor, cholesterol (entry 4), resulted in a 72% of **5.15** (1:1 α : β). Given the reactivity that alkenes frequently exhibit to conditions that are also used to activate thioglycosides, this is a significant observation.^{7b}

With glycosyl donor **5.12** (acetate at the 2-position), neighboring group participation affords the *beta* anomer exclusively. C-2 acceptor (entry 7) showed a slight decrease in yield (79%) compared to donor **5.1** (85%, entry 2), however, only the *beta* anomer was isolated. Furthermore, entry 6 showed that acid sensitive protecting groups are also tolerated. Acetylated donor **5.11** (completely unreactive in the presence of Umemoto's reagent, 4Å molecular sieves, and blue LEDs) unexpectedly afforded 25% of disaccharide **5.23** (entry 12). Consumption of the acceptor, however, was sluggish as



Unless otherwise stated, 0.15 mmol donor, 0.075 mmol acceptor, and 10 mol% TfOH in 1 mL DCM were stirred until acceptor was consumed as determined via TLC. [a] 0.15 mmol donor, 0.15 mmol acceptor, 10 mol% TfOH in 1 mL DCM. [b] By-product isolated along with **5.11** from glycosylation with donor **5.11**.

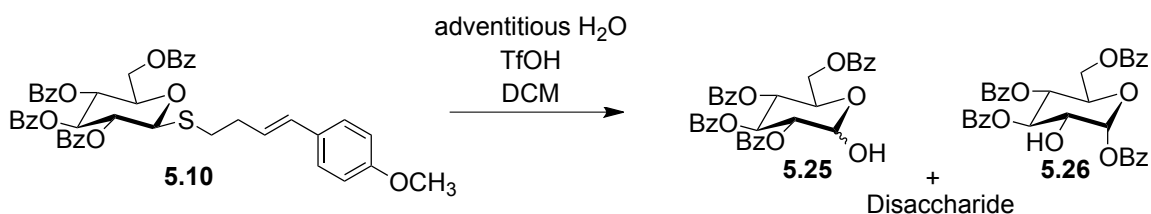
Figure 5.3 Glycosylation substrate scope

the reaction took 4 hours to complete. Under the reaction conditions, the nucleophilic C-6 acceptor was acetylated and glycoside **5.24** was isolated in 37% yield (entry 12^a).

Benzoylated thioglycoside donor **5.10** was synthesized and employed in an effort to suppress the acylation of the acceptor while still demonstrating activation of a disarmed donor (glycosyl donor with electron withdrawing protecting groups). Efforts with **5.10** were successful and afforded the *beta* anomers of C-6 and C-2 disaccharides (entries 8 and 9). Entry 10 further showed the orthogonality of alkyl thioglycosides to these conditions as the disaccharide using a 1-octylthioglycoside acceptor was isolated in 76% yield. Activation of donor **5.10** in the presence of 1-octylthioglycoside is especially noteworthy and could lead to the development of a one-pot method for oligosaccharide synthesis as many methods exist for glycosylation with alkylthioglycoside donors (Scheme 5.1, for example). Though entry 11 was low yielding, this result was very encouraging. C-4 acceptors are among the least reactive and most challenging linkages to form. Attempts to generate the corresponding disaccharide with donors **5.1** and **5.12** were successful in that crude ¹H NMR showed product formation. Purification, however, was extremely difficult. Disaccharide **5.22** was finally obtained in 21% yield from tetrabenzoyl donor **5.10** after silica gel chromatography and preparative TLC. Unsurprisingly, glycosylations with this disarmed donor and exceptionally unreactive acceptor took twice as long to go to completion but still performed much better than that tetraacetate thioglycoside **5.11**.

A slight drawback to using donor **5.10** was the hydrolysis by-products formed over the course of the reaction (Scheme 5.6). These impurities had retention factors on TLC that were very similar to the desired products and made purification very

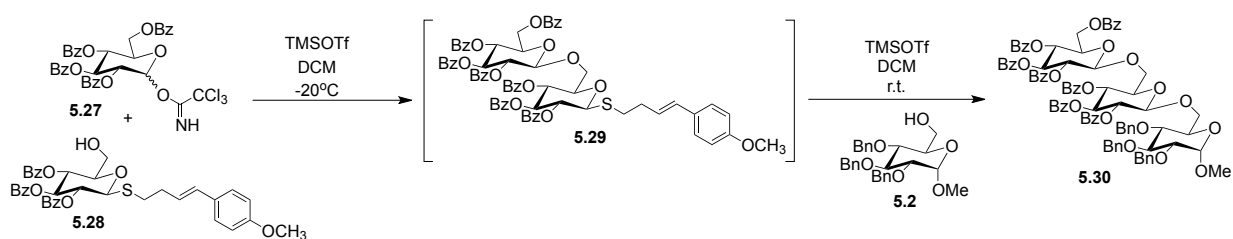
challenging. Isolation of the impurities and structural analysis of the NMR spectra confirmed that a mixture of the C-1 (**5.25**) and C-2 (**5.26**) hydroxyl products of hydrolysis were being formed. The desired disaccharides were obtained chromatographically through varying mixtures of DCM:EtOAc:Hexanes which still makes donor **5.10** an overall excellent choice for good yields and selectivity in spite of the by-products observed and difficult purification.



Scheme 5.6 By-products from glycosylation with tetrabenzoyl donor **5.10**

5.5 Future Work

Efforts are ongoing to demonstrate scalability of the developed glycosylation method through a 1 mmol scale reaction (optimized procedure: 0.1504 mmol). In addition to this, optimization of a one-pot synthesis of a trisaccharide is currently underway. As previously discussed, we intend to exploit the low reactivity of the 4-aryl-3-butenylthioglycoside at -20°C and capitalize on the reactivity of trichloroacetimidates at that temperature. Therefore, we envision synthesis of a trisaccharide (**5.30**, Scheme 5.7) using compound **5.28** with the styrenic moiety as the glycosyl acceptor at low



Scheme 5.7 Proposed synthesis of trisaccharide **5.30**

temperature to form disaccharide **5.29**. Subsequent warming to room temperature will enable the 4-aryl-3-butenylthioglycoside to form another glycosidic linkage with acceptor **5.2** using our method.

5.6 Conclusion

A method for remote activation of thioglycosides for O-glycosylation was developed using only a catalytic amount of triflic acid. The reaction conditions tolerated electroneutral alkene-containing acceptors as well as acid sensitive functional groups (acetonides) and very challenging linkages such as C-4 (**5.22**, Figure 5.3) were obtained albeit in low yields. In addition, benzoylated glycosyl donor **5.10** performed extremely well while also affording complete selectivity for the *beta* anomer along with donors **5.11** and **5.12**. Orthogonality was demonstrated when the 1-octylthioglycoside acceptor (Entry 10, Figure 5.3) was employed and, furthermore, the low reactivity of the styrenic side chain at low temperature provides an opportunity for a one-pot synthesis of trisaccharides. Overall, this user-friendly method will potentially be useful for the synthesis of oligosaccharides.

5.7 Experimental

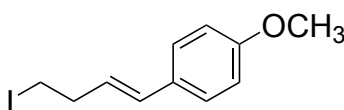
5.7.1 General Methods

Reagents were purchased from Sigma Aldrich and used as received. Flash column chromatography was performed using 60Å silica gel purchased from Sigma Aldrich. ¹H NMR and ¹³C NMR spectroscopy were performed on a Bruker AV-400 and AV- 500 spectrometer. Mass spectra were obtained using an Agilent 6210 electrospray time-of-flight mass spectrometer. Analytical and preparative TLC were conducted on aluminum sheets (Merck, silica gel 60, F254). Compounds were visualized by UV

absorption (254 nm) and staining with anisaldehyde. 5 mL Pyrex micro reaction vessels (Supelco) were used in the glycosylation reactions. Deuterated solvents were obtained from Cambridge Isotope Labs. All solvents were purified according to the method of Grubbs.²³

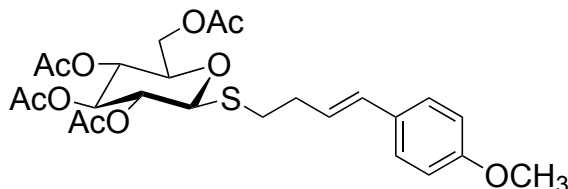
5.7.2 Procedures and Characterization

Synthesis of (*E*)-1-iodo-4-(4-methoxyphenyl)-3-butene



1.8 g (6.9 mmol) triphenylphosphine and 1.7 g (6.7 mmol) I₂ was dissolved in 26 mL CH₂Cl₂ and stirred for 10 minutes. 0.77 g (11 mmol) imidazole was added in one portion and the reaction stirred for another 10 minutes. A solution of 0.80 g (4.5 mmol) (*E*)-4-(4-methoxyphenyl)but-3-en-1-yl-*p*-toluenesulfonate⁹ in 5 mL CH₂Cl₂ was added to the reaction. 30 mL sat. Na₂S₂O₅ was added and the layers were separated. The aqueous layer was extracted with CH₂Cl₂ (2 x 30 mL) and the organic layers were dried over MgSO₄. Silica gel chromatography (5% EtOAc in hexanes) afforded 1.1 g (84%) of a yellow solid. Spectral data match that previously reported in literature.¹⁴

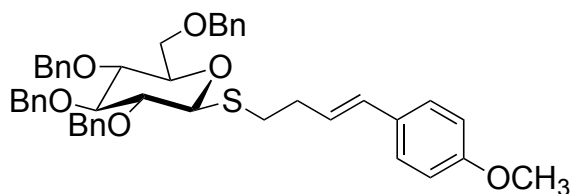
Synthesis of **5.11**



0.70 mL (4.7 mmol) of DBU was added to 1.7 g (4.7 mmol) of 2,3,4,6-tetra-*O*-acetyl-1-mercapto- β -D-glucopyranoside¹⁰ in 10 mL toluene at -10°C. After 10 minutes, 1.3 g (4.7 mmol) of (*E*)-1-iodo-4-(4-methoxyphenyl)-3-butene in 3.7 mL toluene was

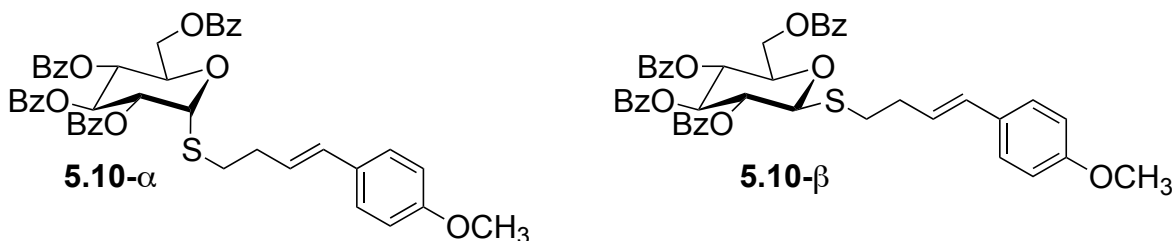
added dropwise. The reaction was stirred at -10°C until completed via TLC. 20 mL of H_2O was added to quench the reaction. The resulting solution was then extracted with CH_2Cl_2 (2 x 58 mL). The organic layer was further diluted with 58 mL CH_2Cl_2 , washed with 43 mL 1M H_2SO_4 , 43 mL sat. NaHCO_3 (aq), and 43 mL sat. NaCl (aq) then dried over Na_2SO_4 . Silica gel chromatography (gradient run from 15% EtOAc in hexanes to 25% EtOAc in hexanes) afforded 1.9 g (77%) of a white solid. Spectral data matched that previously reported in literature.¹⁴

Synthesis of **5.1**



To a solution of 1.9 g (3.6 mmol) **5.11** in 44.4 mL MeOH was 1.9 mL (1.9 mmol) of 1M NaOMe added. The reaction was stirred overnight at room temperature. Solvent was removed *in vacuo* and the resulting solid was redissolved in 36.0 mL DMF. To this solution was added 0.261 g (0.706 mmol) of TBAI followed by 1.1 g (26 mmol) of 60% oil dispersed NaH at 0°C . After 30 minutes at this temperature, 2.8 mL (24 mmol) of benzyl bromide was added dropwise. The reaction warmed slowly to room temperature and stirred overnight until complete via TLC. At 0°C the reaction was quenched with 45 mL sat. NH_4Cl (aq.) then extracted with Et_2O (2 x 45 mL), washed with 45 mL sat. NaCl (aq.), and dried over Na_2SO_4 . Silica gel chromatography (gradient run from 5% EtOAc in hexanes to 10% EtOAc in hexanes) afforded 0.960 g (37%) of a white solid. Spectral data matched that previously reported in literature.¹⁴

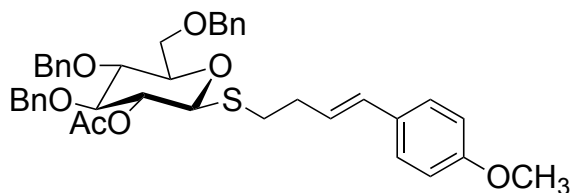
Synthesis of **5.10**



See synthesis of **5.11** for procedure. Started with 0.48 mL (3.2 mmol) DBU, 1.8 g (2.9 mmol) tetra-*O*-benzoyl-1-mercapto- β -D-glucopyranoside in 8 mL toluene, and 0.83 g (2.5 mmol) (*E*)-4-(4-methoxyphenyl)but-3-en-1-yl-*p*-toluenesulfonate⁹ in 4.8 mL toluene. Silica gel chromatography (gradient run from 35% DCM in hexanes to 80% DCM in hexanes then 20% EtOAc in hexanes) afforded 0.283 g (15%) α (off-white solid) and 1.07 g (55%) β (white solid) of **5.10**. α anomer: ¹H NMR (500 MHz, CDCl₃) δ 8.04 (d, *J* = 6.9 Hz, 2H), 7.96 (dd, *J* = 11.8, 7.0 Hz, 4H), 7.88 (d, *J* = 6.9 Hz, 2H), 7.54 – 7.45 (m, 3H), 7.42 (t, *J* = 7.5 Hz, 1H), 7.36 (ddd, *J* = 8.4, 6.9, 5.1 Hz, 6H), 7.28 (t, *J* = 7.8 Hz, 2H), 7.16 (d, *J* = 8.8 Hz, 2H), 6.79 (d, *J* = 8.7 Hz, 2H), 6.28 (d, *J* = 16.0 Hz, 1H), 6.09 (t, *J* = 9.8 Hz, 1H), 5.98 (d, *J* = 5.8 Hz, 1H), 5.93 (dt, *J* = 15.8, 7.0 Hz, 1H), 5.68 (t, *J* = 9.8 Hz, 1H), 5.52 (dd, *J* = 10.2, 5.7 Hz, 1H), 4.90 (ddd, *J* = 10.2, 5.7, 2.7 Hz, 1H), 4.61 (dd, *J* = 12.2, 2.8 Hz, 1H), 4.52 (dd, *J* = 12.2, 5.8 Hz, 1H), 3.77 (s, 3H), 2.77 (ddd, *J* = 12.8, 8.2, 6.5 Hz, 1H), 2.68 (dt, *J* = 12.8, 7.6 Hz, 1H), 2.51 – 2.42 (m, 2H). ¹³C NMR (126 MHz, CDCl₃) δ 166.31, 165.80, 165.61, 165.50, 159.08, 133.65, 133.37, 133.30, 131.26, 130.19, 130.18, 130.08, 129.89, 129.87, 129.78, 129.23, 129.02, 128.96, 128.65, 128.61, 128.58, 128.48, 127.40, 125.62, 114.04, 82.54, 71.89, 71.05, 69.74, 68.46, 63.29, 55.43, 33.12, 30.25. HRMS *m/z* Calcd for C₄₅H₄₀NaO₁₀S [M+Na]⁺ 795.2234, found 795.2250. $[\alpha]_D^{25} = +79.2$ (*c* = 1, DCM). β anomer: ¹H NMR (500 MHz, CDCl₃) δ 8.00 (d, *J* = 7.2 Hz, 2H), 7.93 (d, *J* = 7.2 Hz, 2H), 7.89 (d, *J* = 7.2 Hz, 2H), 7.80

(d, $J = 7.2$ Hz, 2H), 7.48 (q, $J = 7.3$ Hz, 3H), 7.40 (t, $J = 7.4$ Hz, 1H), 7.37 – 7.29 (m, 6H), 7.24 (d, $J = 7.5$ Hz, 2H), 7.15 (d, $J = 8.7$ Hz, 2H), 6.78 (d, $J = 8.7$ Hz, 2H), 6.27 (d, $J = 15.8$ Hz, 1H), 6.00 – 5.88 (m, 2H), 5.66 (t, $J = 9.8$ Hz, 1H), 5.56 (t, $J = 9.7$ Hz, 1H), 4.88 (d, $J = 10.0$ Hz, 1H), 4.64 (dd, $J = 12.2, 3.0$ Hz, 1H), 4.48 (dd, $J = 12.2, 5.5$ Hz, 1H), 4.21 – 4.13 (m, 1H), 3.78 (s, 3H), 2.93 – 2.85 (m, 1H), 2.85 – 2.76 (m, 1H), 2.55 – 2.43 (m, 2H). ^{13}C NMR (126 MHz, CDCl_3) δ 166.30, 166.00, 165.41, 159.08, 133.68, 133.52, 133.46, 133.34, 131.09, 130.31, 130.09, 130.05, 129.94, 129.93, 129.76, 129.33, 128.99, 128.95, 128.63, 128.61, 128.59, 128.51, 127.42, 125.88, 114.07, 84.24, 76.57, 74.29, 70.81, 69.81, 63.48, 55.48, 33.59, 30.28. HRMS m/z Calcd for $\text{C}_{45}\text{H}_{40}\text{NaO}_{10}\text{S}$ $[\text{M}+\text{Na}]^+$ 795.2234, found 795.2267. $[\alpha]_D^{25} = +4.4$ ($c = 1$, DCM).

Synthesis of **5.12**



See synthesis of **5.11** for procedure. Started with 0.10 mL (0.67 mmol) DBU, 0.320 g (0.629 mmol) 2-O-acetyl-3,4,6-tri-O-benzyl-1-deoxy-1-mercapto- β -D-glucopyranoside¹⁰ in 2 mL toluene, and 0.230 g (0.692 mmol) (*E*)-4-(4-methoxyphenyl)but-3-en-1-yl-*p*-toluenesulfonate⁹ in 1 mL toluene. Silica gel chromatography (gradient run from 15% DCM in hexanes to 20% DCM in hexanes, then 7.5% EtOAc in hexanes) afforded 0.299 g (71%) of a white solid. Spectral data matched that previously reported in literature.¹⁴

Representative procedure for optimized glycosylation conditions:

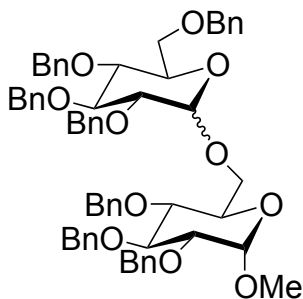
A 5 mL Pyrex reactor vial was charged with the glycosyl donor (1 equiv., 0.150

mmol), the glycosyl acceptor (0.5 equiv., 0.0752 mmol), and 1 mL of dry dichloromethane under nitrogen atmosphere. The reaction vessel was vacuum-purged and backfilled twice. Then, TfOH (0.1 equiv., 0.015 mmol) was added via gastight syringe. The reaction stirred at room temperature until consumption of acceptor was observed via TLC. Triethylamine (0.2 equiv., 0.030 mmol) was then added to the reaction mixture and the crude products were concentrated and then purified by gradient silica gel chromatography to afford the desired glycosides.

Determination of anomeric ratios:

The anomeric ratio (α : β) was determined based on the integration of key resonances identified with the assistance of published ^1H NMR data. In the cases where spectral data was unavailable, the anomeric products were separated with silica gel chromatography or preparative TLC.

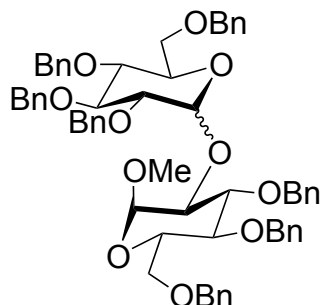
Synthesis of **5.4**



Started with 0.108 g (0.151 mmol) of glycosyl donor **5.1**, 0.035 g (0.075 mmol) of methyl-2,3,4-tri-*O*-benzyl- α -D-glucopyranoside, 1.3 μL (0.015 mmol) TfOH, in 1 mL of DCM. Silica gel chromatography (gradient run from 10% EtOAc in hexanes to 15% EtOAc in hexanes) afforded 0.065 g (88%, 1.4:1 α : β) of a white solid. Ratio determined via ^1H NMR analysis of the α : β mixture. Spectral data matched that previously reported

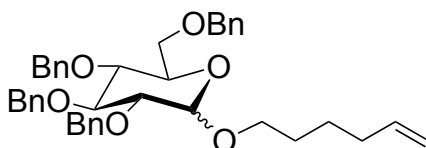
in literature.¹¹

Synthesis of **5.13**



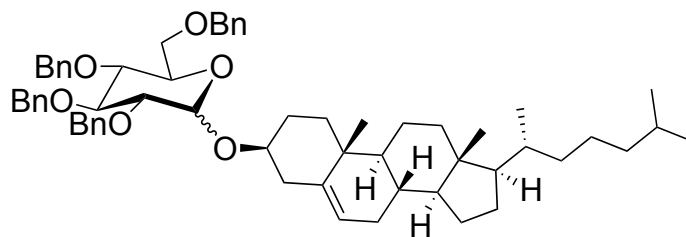
Started with 0.108 g (0.151 mmol) of glycosyl donor **5.1**, 0.035 g (0.075 mmol) of methyl-3,4,6-tri-*O*-benzyl- α -D-glucopyranoside, 1.3 μ L (0.015 mmol) TfOH, in 1 mL of DCM. Silica gel chromatography (gradient run from 1% Et₂O in DCM to 15% Et₂O in DCM) afforded 0.063 g (85%, 2:1 α : β) of a colorless oil. Anomers were separated and weighed to determine anomeric ratio. Spectral data matched that previously reported in literature.¹⁵

Synthesis of **5.14**



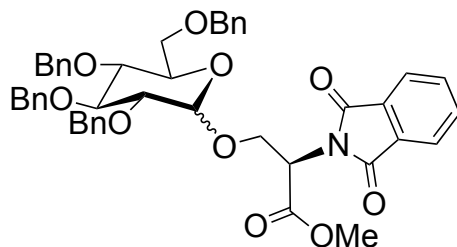
Started with 0.108 g (0.151 mmol) of glycosyl donor **5.1**, 9.0 μ L (0.07 mmol) of 5-hexen-1-ol, 1.3 μ L (0.015 mmol) TfOH, in 1 mL of DCM. Silica gel chromatography (gradient run from 5% EtOAc in hexanes to 25% EtOAc in hexanes) afforded 0.041 g (88%, 1:1.5 α : β) of a colorless oil. Ratio determined via ¹H NMR analysis of the α : β mixture. Spectral data matched that previously reported in literature.¹⁶

Synthesis of **5.15**



Started with 0.108 g (0.151 mmol) of glycosyl donor **5.1**, 0.029 g (0.075 mmol) of (3 β)-cholest-5-en-3-ol, 1.3 μ L (0.015 mmol) TfOH, in 1 mL of DCM. Silica gel chromatography (5% EtOAc in hexanes) afforded 0.049 g (72%, 1:1 α : β) of an off-white solid. Ratio determines via ^1H NMR analysis of the α : β mixture. Spectral data matched that previously reported in literature.¹⁷

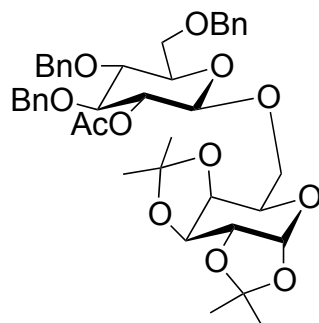
Synthesis of **5.16**



Started with 0.108 g (0.150 mmol) of glycosyl donor **5.1**, 0.019 g (0.076 mmol) of (R)-methyl 2-(1,3-dioxisoindolin-2-yl)-3-hydroxypropanoate, 1.3 μ L (0.015 mmol) TfOH, in 1 mL of DCM. Preparative TLC (1:4:6 DCM:EtOAc:hexanes) afforded 0.036 g (62%, 3:1 α : β) of an off-white solid. Ratio determined via ^1H NMR analysis of the α : β ratio, ^1H NMR (400 MHz, CDCl_3) δ 7.77 (dd, J = 5.5, 3.1 Hz, 2H), 7.72 (dd, J = 5.5, 3.1 Hz, 0.6H, β anomer), 7.65 – 7.59 (m, 3H), 7.38 – 7.20 (m, 23H), 7.19 – 7.15 (m, 1H), 7.14 – 7.09 (m, 1H), 7.09 – 7.00 (m, 3H), 6.91 (d, J = 6.8 Hz, 0.6H, β anomer), 5.29 (dd, J = 10.7, 4.4 Hz, 0.3H, β anomer), 5.24 (dd, J = 9.2, 5.4 Hz, 1H), 4.93 (d, J = 3.5 Hz, 1H), 4.82 (d, J = 10.9 Hz, 1H), 4.80 – 4.62 (m, 6H), 4.62 – 4.40 (m, 3H), 4.39 – 4.21 (m, 5H), 3.81 –

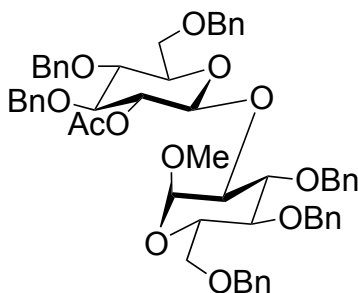
3.75 (m, 1H), 3.75 (m, 2H), 3.73 (s, 3H), 3.62 – 3.52 (m, 2H), 3.52 – 3.47 (m, 3H), 3.45 – 3.32 (m, 2H). ^{13}C NMR (100 MHz, CDCl_3) δ 167.98, 167.57, 138.97, 138.57, 138.50, 138.09, 134.31, 131.99, 128.56, 128.52, 128.50, 128.45, 128.41, 128.23, 128.11, 128.05, 127.95, 127.92, 127.87, 127.82, 127.69, 127.56, 123.75, 103.80, 96.61, 81.85, 79.87, 77.43, 75.74, 74.89, 73.71, 73.62, 73.03, 70.93, 68.25, 64.31, 53.04, 51.16. HRMS m/z Calcd for $\text{C}_{46}\text{H}_{45}\text{NaNO}_{10}$ $[\text{M}+\text{Na}]^+$ 794.2985, found 794.2966.

Synthesis of **5.17**



Started with 0.101 g (0.151 mmol) of glycosyl donor **5.12**, 0.020 g (0.077 mmol) of 1,2,3,4-di-*O*-isopropylidene-D-galactopyranose, 1.3 μL (0.015 mmol) TfOH, in 1 mL of DCM. Silica gel chromatography (gradient run from 7.5% EtOAc in hexanes to 10% EtOAc in hexanes) afforded 0.037 g (65%, β only) of a colorless oil. Spectral data matched that previously reported in literature.¹³

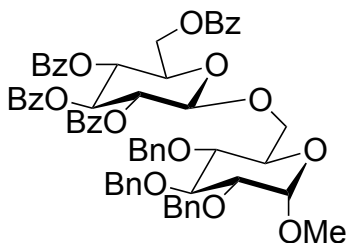
Synthesis of **5.18**



Started with 0.101 g (0.151 mmol) of glycosyl donor **5.12**, 0.035 g (0.075 mmol)

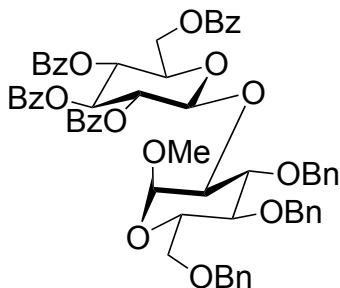
of methyl-3,4,6-tri-O-benzyl- α -D-glucopyranoside, 1.3 μ L (0.015 mmol) TfOH, in 1 mL of DCM. Silica gel chromatography (gradient run from 18% EtOAc in hexanes to 20% EtOAc in hexanes) afforded 0.056 g (79%, β only) of **5.18**. Spectral data matched that previously reported in literature.¹²

Synthesis of **5.19**



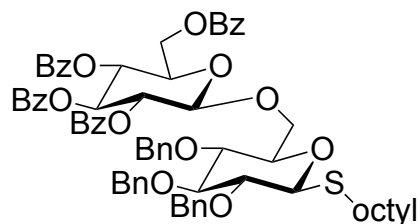
Started with 0.116 g (0.150 mmol) of glycosyl donor **5.10**, 0.070 g (0.151 mmol) of methyl-2,3,4-tri-O-benzyl- α -D-glucopyranoside, 1.3 μ L (0.015 mmol) TfOH, in 1 mL of DCM. Preparative TLC (6:1:3 DCM:EtOAc:hexanes) afforded 0.073 g (46%, β only) of a white solid. Spectral data matched that previously reported in literature.¹⁹

Synthesis of **5.20**



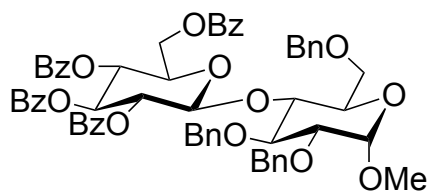
Started with 0.116 g (0.150 mmol) of glycosyl donor **5.10**, 0.070 g (0.151 mmol) of methyl-3,4,6-tri-O-benzyl- α -D-glucopyranoside, 1.3 μ L (0.015 mmol) TfOH, in 1 mL of DCM. Preparative TLC (5:1:4 DCM:EtOAc:hexanes) afforded 0.074 g (47%, 1.4:1 α : β) of a white solid. Spectral data matched that previously reported in literature.¹⁹

Synthesis of **5.21**



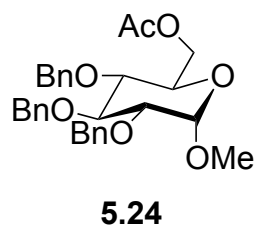
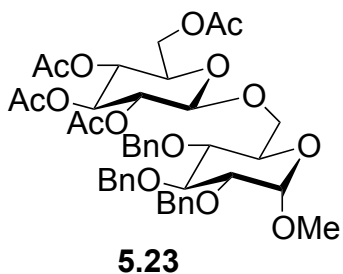
Started with 0.116 g (0.150 mmol) of glycosyl donor **5.10**, 0.044 g (0.076 mmol) of octyl β -D-1-thio-2,3,4-tri-O-benzylglucopyranoside, 1.3 μ L (0.015 mmol) TfOH, in 1 mL of DCM. Preparative TLC (30% EtOAc in hexanes) afforded 0.067 g (76%, β only) of a white solid. ^1H NMR (400 MHz, CDCl_3) δ 8.01 (d, $J = 7.2$ Hz, 2H), 7.91 (t, $J = 8.6$ Hz, 4H), 7.82 (d, $J = 7.3$ Hz, 2H), 7.55 – 7.38 (m, 5H), 7.38 – 7.21 (m, 20H), 7.14 (d, $J = 7.6$ Hz, 2H), 5.86 (t, $J = 9.6$ Hz, 1H), 5.68 (t, $J = 9.7$ Hz, 1H), 5.56 (t, $J = 7.9$ Hz, 1H), 4.91 (d, $J = 7.8$ Hz, 1H), 4.89 – 4.81 (m, 2H), 4.73 (d, $J = 11.0$ Hz, 1H), 4.65 (t, $J = 10.9$ Hz, 3H), 4.54 – 4.47 (m, 1H), 4.45 (d, $J = 11.0$ Hz, 1H), 4.33 (d, $J = 9.7$ Hz, 1H), 4.14 (d, $J = 10.7$ Hz, 1H), 4.07 (dt, $J = 8.4, 4.4$ Hz, 1H), 3.75 (dd, $J = 11.2, 5.1$ Hz, 1H), 3.57 (t, $J = 8.6$ Hz, 1H), 3.42 (m, 2H), 3.31 (t, $J = 9.3$ Hz, 1H), 2.64 (dt, $J = 13.7, 6.9$ Hz, 1H), 2.59 – 2.49 (m, 1H), 1.63 – 1.51 (m, 4H), 1.40 – 1.20 (m, 8H), 0.88 (t, $J = 6.7$ Hz, 3H). ^{13}C NMR (126 MHz, CDCl_3) δ 166.32, 166.02, 165.36, 165.18, 138.70, 138.22, 138.14, 133.60, 133.42, 133.37, 133.30, 130.04, 129.99, 129.97, 129.80, 129.48, 129.07, 129.04, 128.63, 128.60, 128.58, 128.57, 128.51, 128.03, 128.01, 127.90, 127.81, 101.47, 86.69, 85.10, 81.82, 78.83, 77.90, 75.79, 75.63, 75.05, 73.20, 72.40, 72.11, 69.92, 68.76, 63.36, 32.07, 30.77, 29.80, 29.47, 28.99, 22.90, 14.33. HRMS m/z Calcd for $\text{C}_{69}\text{H}_{72}\text{NaO}_{14}\text{S}$ $[\text{M}+\text{Na}]^+$ 1179.4535, found 1179.4559. $[\alpha]_D^{25} = +15.9$ ($c = 1$, DCM).

Synthesis of **5.22**



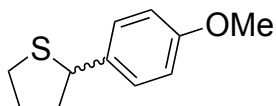
Started with 0.116 g (0.150 mmol) of glycosyl donor **5.10**, 0.035 g (0.075 mmol) of methyl-2,3,6-tri-*O*-benzyl- α -D-glucopyranoside, 1.3 μ L (0.015 mmol) TfOH, in 1 mL of DCM. Preparative TLC (5:1:4 DCM:EtOAc:hexanes) afforded 0.016 g (20%, β only) of a white solid. Spectral data matched that previously reported in literature.²⁰

Synthesis of **5.23** and **5.24**



Started with 0.079 g (0.151 mmol) of glycosyl donor **5.11**, 0.035 g (0.075 mmol) of methyl-2,3,4-tri-*O*-benzyl- α -D-glucopyranoside, 1.3 μ L (0.015 mmol) TfOH, in 1 mL of DCM. Silica gel chromatography (gradient run from 1% EtOAc in DCM to 5% EtOAc in DCM) afforded 0.015 g (25%, β only) of **5.23** (white solid) and 0.014 g (37%) of **5.24** (white solid). Spectral data matched that previously reported in literature.^{20, 21}

Synthesis of 2-(4-methoxyphenyl)tetrahydrothiophene



The compound was purified from early-eluting column chromatography fractions from an *O*-glycosylation procedure using preparative TLC with hexanes as eluent.

Spectral data matched that previously reported in literature²².

5.8 References

1. Veeneman, G. H.; van Leeuwen, S. H.; van Boom, J. H., *Tet. Lett.* **1990**, 31, 1331-1334.
2. Fukase, K.; Hasuoka, A.; Kinoshita, I.; Kusumoto, S., *Tet. Lett.* **1992**, 33, 7165-7168.
3. Fukase, K.; Kinoshita, I.; Kanoh, T.; Nakai, Y.; Hasuoka, A.; Kusumoto, S., *Tetrahedron* **1996**, 52, 3897-3904.
4. Kajimoto, T.; Morimoto, K.; Ogawa, R.; Dohi, T.; Kita, Y., *Chem. Pharm. Bull.* **2016**, 64, 838-844.
5. (a) Kahne, D.; Walker, S.; Cheng, Y.; Van Engen, D., *J. Am. Chem. Soc.* **1989**, 111, 6881-6882. (b) Schmidt, R. R.; Michel, J., *Angew. Chem. Int. Ed. Engl.* **1980**, 19, 731-732. (c) Schaubach, R.; Hemberger, J.; Kinzy, W., *Liebigs Ann. Chem.* **1991**, 607-614.
6. Das, R.; Mukhopadhyay, B., *ChemistryOpen*, **2016**, 5, 401-433.
7. (a) Yao, C-H.; Lee, J-C., *Tetrahedron* **2014**, 70, 6757-6762. (b) Goswami, M.; Ellern, A.; Pohl, N. L. B., *Angew. Chem.* **2013**, 125, 8599-8603.
8. Iwata, R.; Uda, K.; Takahashi, D.; Toshima, K., *Chem. Commun.* **2014**, 50, 10695-10698.
9. Stokes, B. J.; Opra, S. M.; Sigman, M. S., *J. Am. Chem. Soc.* **2012**, 134, 11408-11411.
10. Jana, M.; Misra, A. K. *J. Org. Chem.* **2013**, 78, 2680-2686.
11. Nokami, T.; Shibuya, A.; Tsuyama, H.; Suga, S.; Bowers, A. A.; Crich, D.; Yoshida, J. *J. Am. Chem. Soc.* **2007**, 129, 10922-10928.
12. He, H.; Zhu, X. *Org. Lett.* **2014**, 16, 3102-3105.
13. Halcomb, R.L.; Danishefsky, S.J. *J. Am. Chem. Soc.* **1989**, 111, 6661-6666.
14. Spell, M. L.; Deveaux, K.; Bresnahan, C. G.; Bernard, B. L.; Sheffield, W.; Kumar, R.; Ragains, J. R., *Angew. Chem. Int. Ed. Engl.* **2016**, 55, 6515-6519.
15. Petersen, J., *J. Org. Chem.* **2001**, 66, 6268-6275.
16. Rodebaugh, R.; Frasier-Reid, B., *Tetrahedron*, **1996**, 52, 7663-7678.

17. Xia, M-J.; Yao, W.; Meng, X-B.; Lou, Q-H.; Li, Z-J., *Tet. Lett.* **2017**, 58, 2389-2392.
18. Hast, S. J.; Bandara, M. D.; Rath, N. P. Demchenko, A. V., *J. Org. Chem.* **2017**, 82, 1904-1911.
19. Kaeothip, S.; Pornsuriyasak, P.; Demchenko, A. V., *Tet. Lett.* **2008**, 49, 1542-1545.
20. Lans, G.; Madsen, R., *Eur. J. Org. Chem.* **2016**, 2016, 3119-3125.
21. Crich, D.; Patel, M., *Carbohydr. Res.* **2006**, 341, 1467-1475.
22. Robertson, F. J.; Wu, J., *J. Am. Chem. Soc.* **2012**, 134, 2775-2780.
23. Pangborn, A.B.; Giardello, M. A.; Grubbs, R. H.; Rosen, R. K.; Timmers, F. J., *Organometallics* **1996**, 15, 1518.

APPENDIX A: COPYRIGHT RELEASES

JOHN WILEY AND SONS LICENSE TERMS AND CONDITIONS

Nov 13, 2017

This Agreement between Kristina Deveaux ("You") and John Wiley and Sons ("John Wiley and Sons") consists of your license details and the terms and conditions provided by John Wiley and Sons and Copyright Clearance Center.

License Number	4226140567258
License date	Nov 11, 2017
Licensed Content Publisher	John Wiley and Sons
Licensed Content Publication	Angewandte Chemie International Edition
Licensed Content Title	Remote Hydroxylation through Radical Translocation and Polar Crossover
Licensed Content Author	Kyle A. Hollister,Elizabeth S. Conner,Mark L. Spell,Kristina Deveaux,Léa Maneval,Michael W. Beal,Justin R. Ragains
Licensed Content Date	May 26, 2015
Licensed Content Pages	5
Type of use	Dissertation/Thesis
Requestor type	Author of this Wiley article
Format	Electronic
Portion	Full article
Will you be translating?	No
Title of your thesis / dissertation	Development of Remote Hydroxylation via Redox Catalysis and Mild Activation of Thioglycosides
Expected completion date	Nov 2017
Expected size (number of pages)	240
Requestor Location	Kristina Deveaux 10732 S Mall Drive Apt 1136 BATON ROUGE, LA 70809 United States Attn: Kristina Deveaux
Publisher Tax ID	EU826007151
Billing Type	Invoice
Billing Address	Kristina Deveaux 10732 S Mall Drive Apt 1136 BATON ROUGE, LA 70809 United States Attn: Kristina Deveaux
Total	0.00 USD
Terms and Conditions	

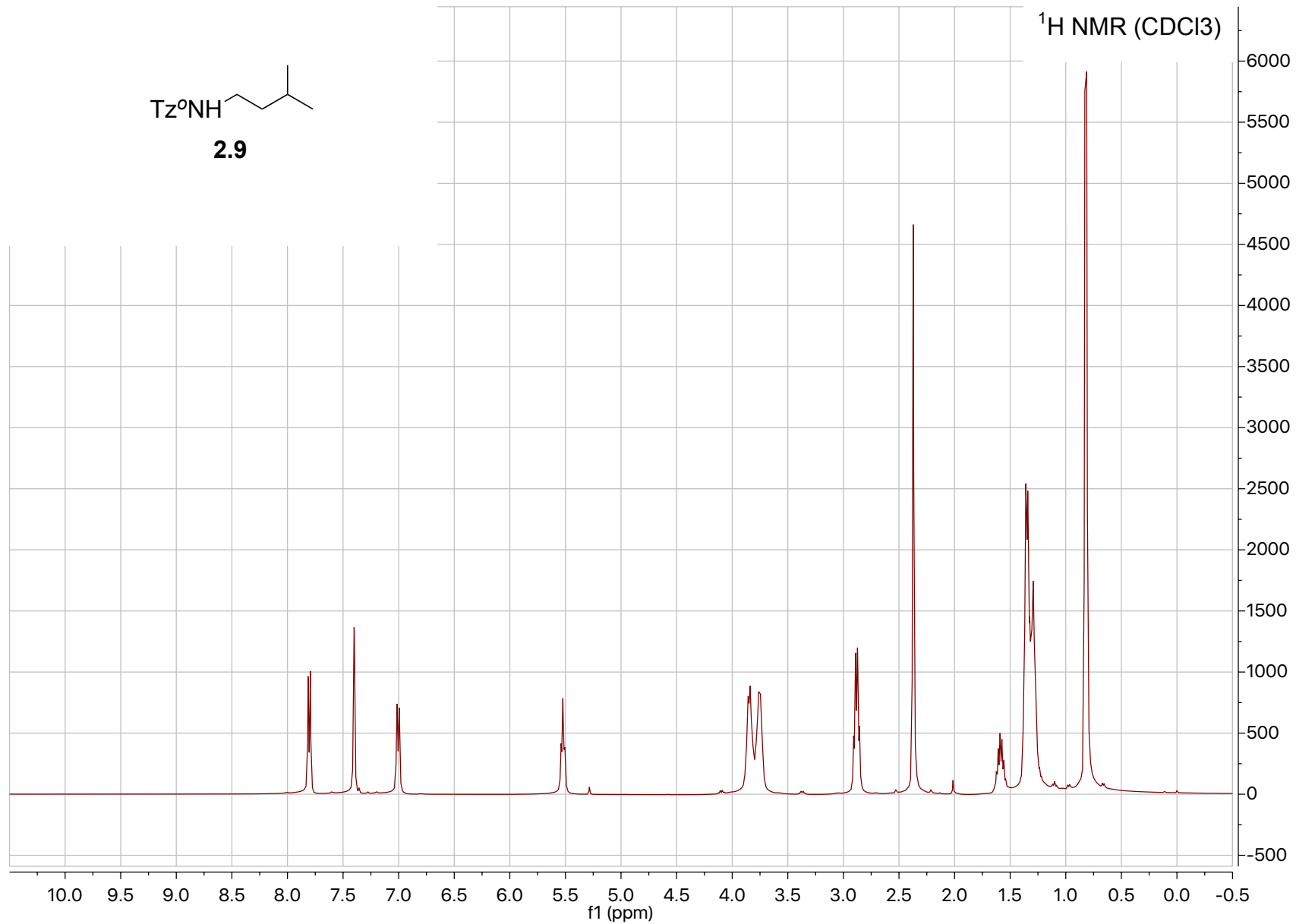
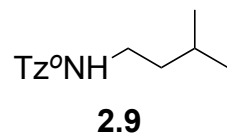
**JOHN WILEY AND SONS LICENSE
TERMS AND CONDITIONS**

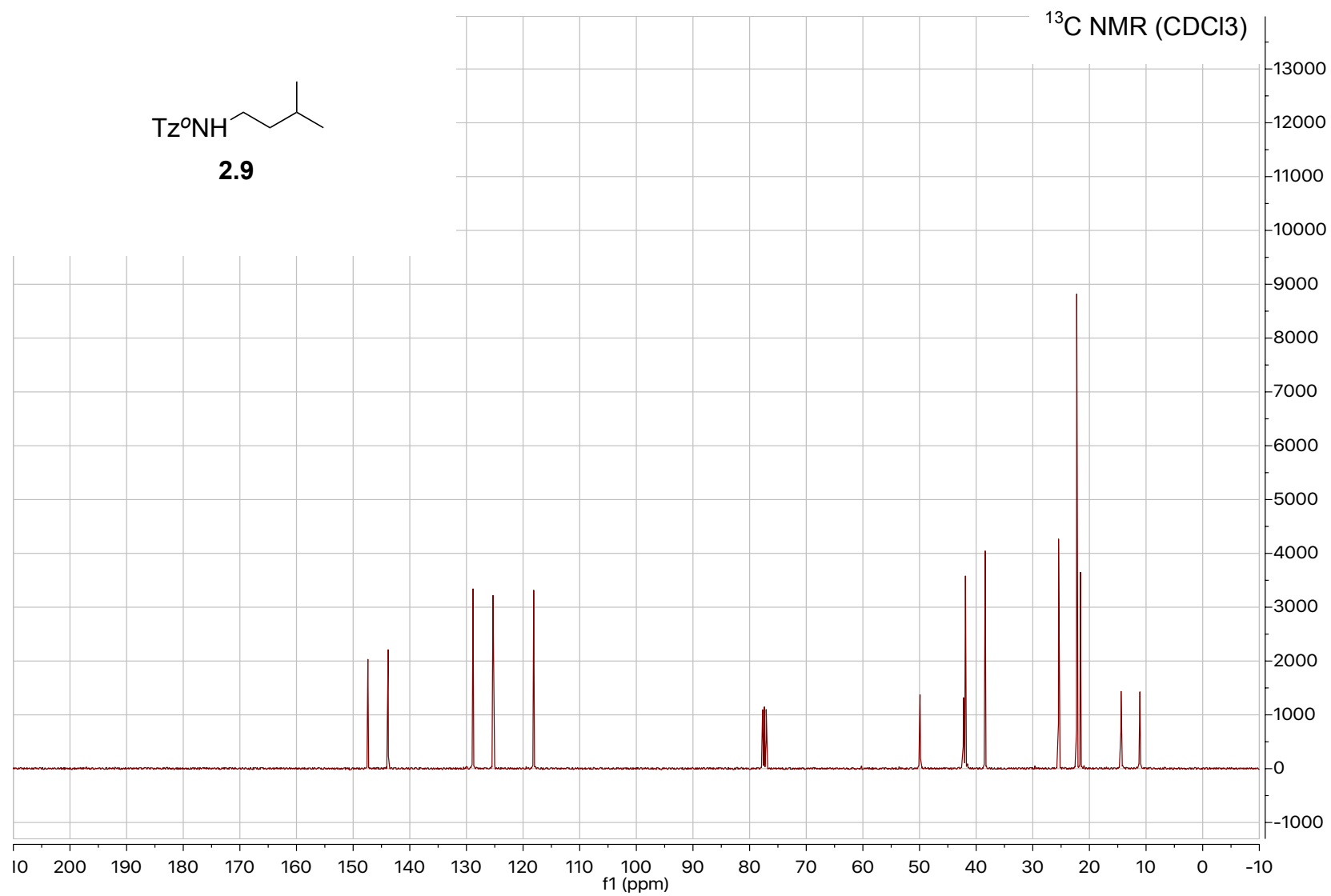
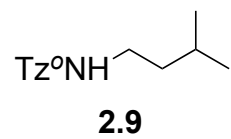
Nov 13, 2017

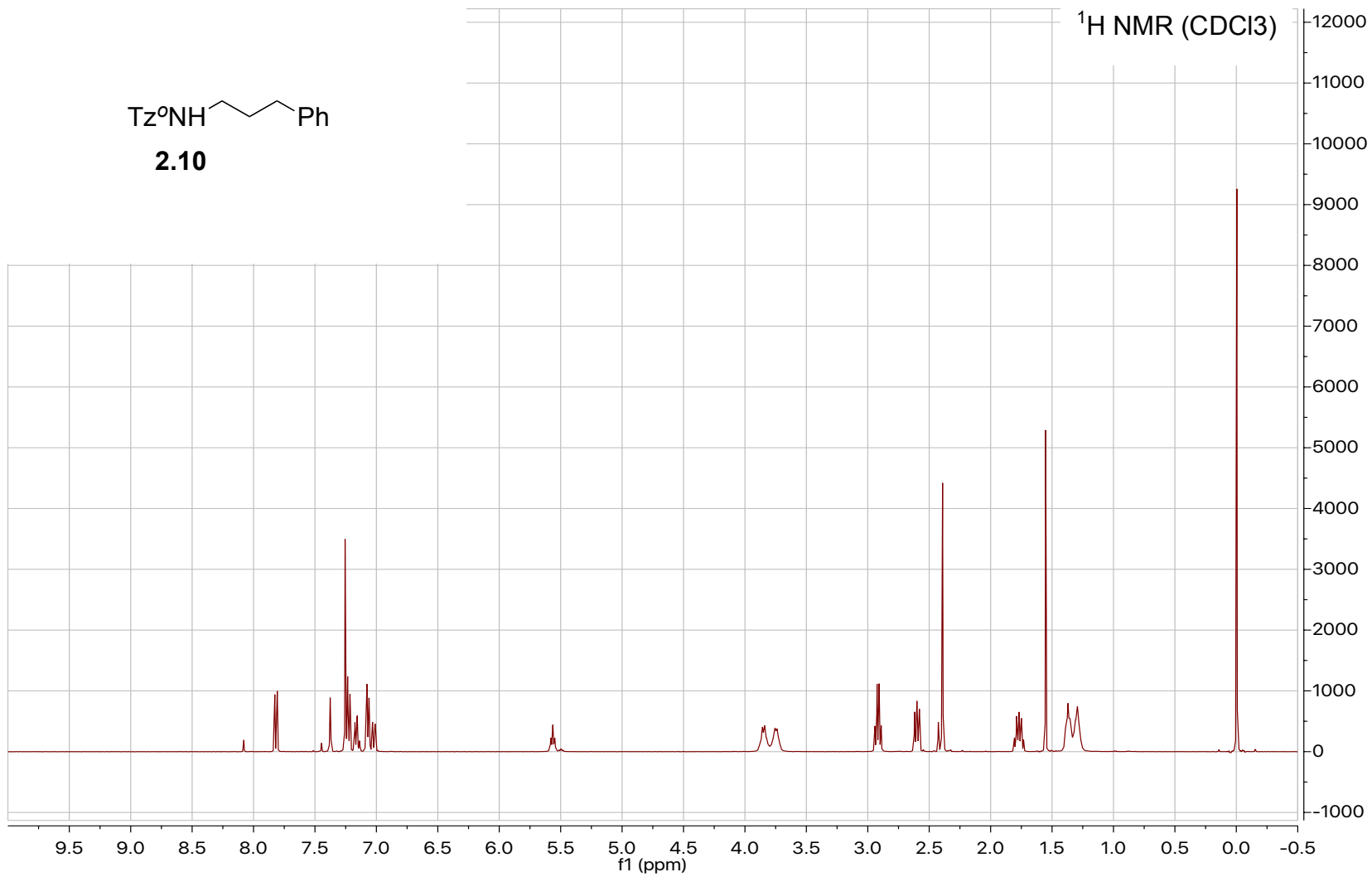
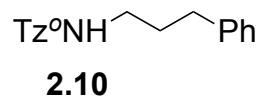
This Agreement between Kristina Deveaux ("You") and John Wiley and Sons ("John Wiley and Sons") consists of your license details and the terms and conditions provided by John Wiley and Sons and Copyright Clearance Center.

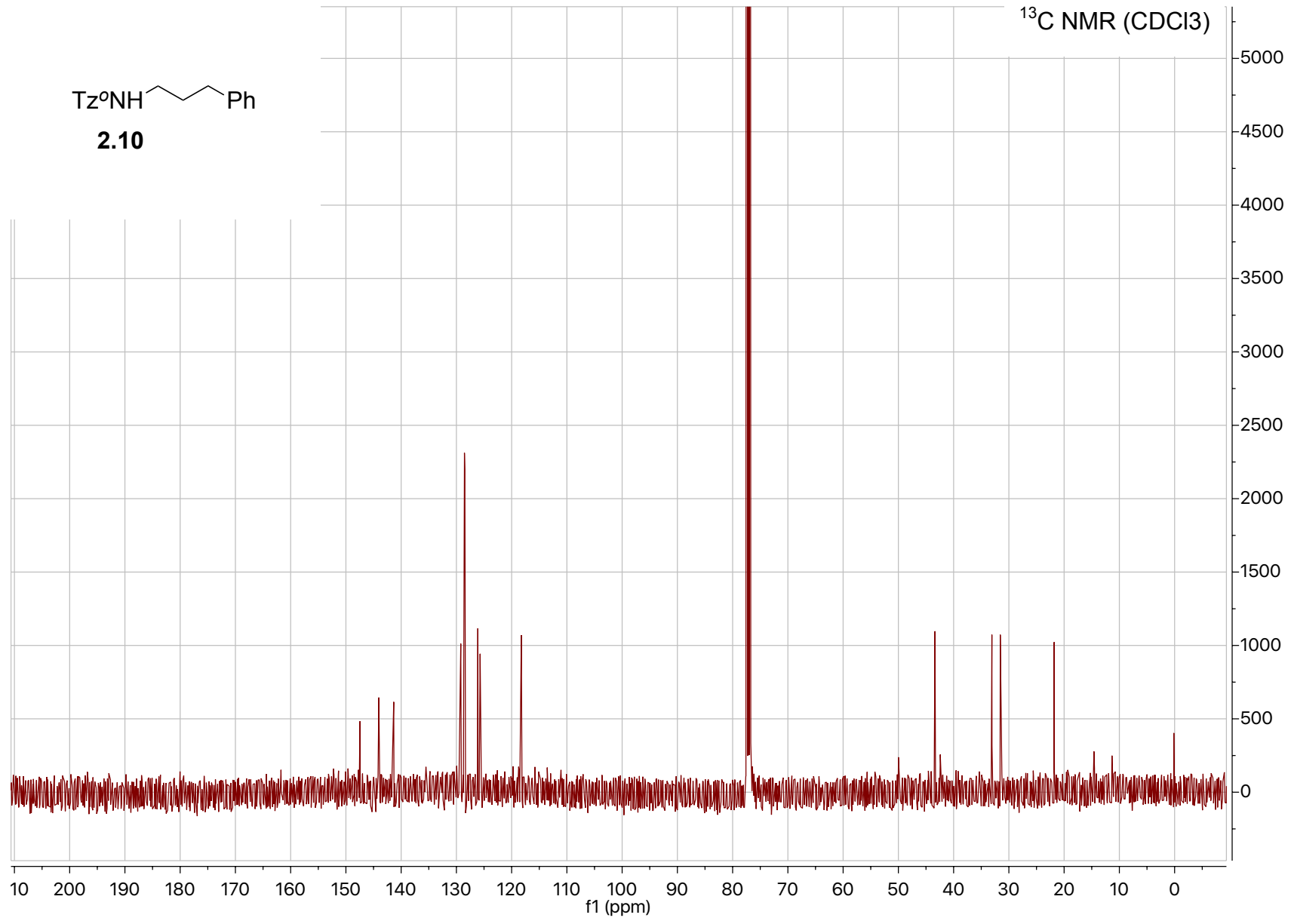
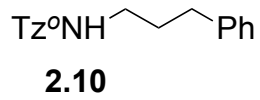
License Number	4226140789914
License date	Nov 11, 2017
Licensed Content Publisher	John Wiley and Sons
Licensed Content Publication	Angewandte Chemie International Edition
Licensed Content Title	A Visible-Light-Promoted O-Glycosylation with a Thioglycoside Donor
Licensed Content Author	Mark L. Spell,Kristina Deveaux,Caitlin G. Bresnahan,Bradley L. Bernard,William Sheffield,Revati Kumar,Justin R. Ragains
Licensed Content Date	Apr 18, 2016
Licensed Content Pages	5
Type of use	Dissertation/Thesis
Requestor type	Author of this Wiley article
Format	Electronic
Portion	Full article
Will you be translating?	No
Title of your thesis / dissertation	Development of Remote Hydroxylation via Redox Catalysis and Mild Activation of Thioglycosides
Expected completion date	Nov 2017
Expected size (number of pages)	240
Requestor Location	Kristina Deveaux 10732 S Mall Drive Apt 1136 BATON ROUGE, LA 70809 United States Attn: Kristina Deveaux
Publisher Tax ID	EU826007151
Billing Type	Invoice
Billing Address	Kristina Deveaux 10732 S Mall Drive Apt 1136 BATON ROUGE, LA 70809 United States Attn: Kristina Deveaux
Total	0.00 USD
Terms and Conditions	

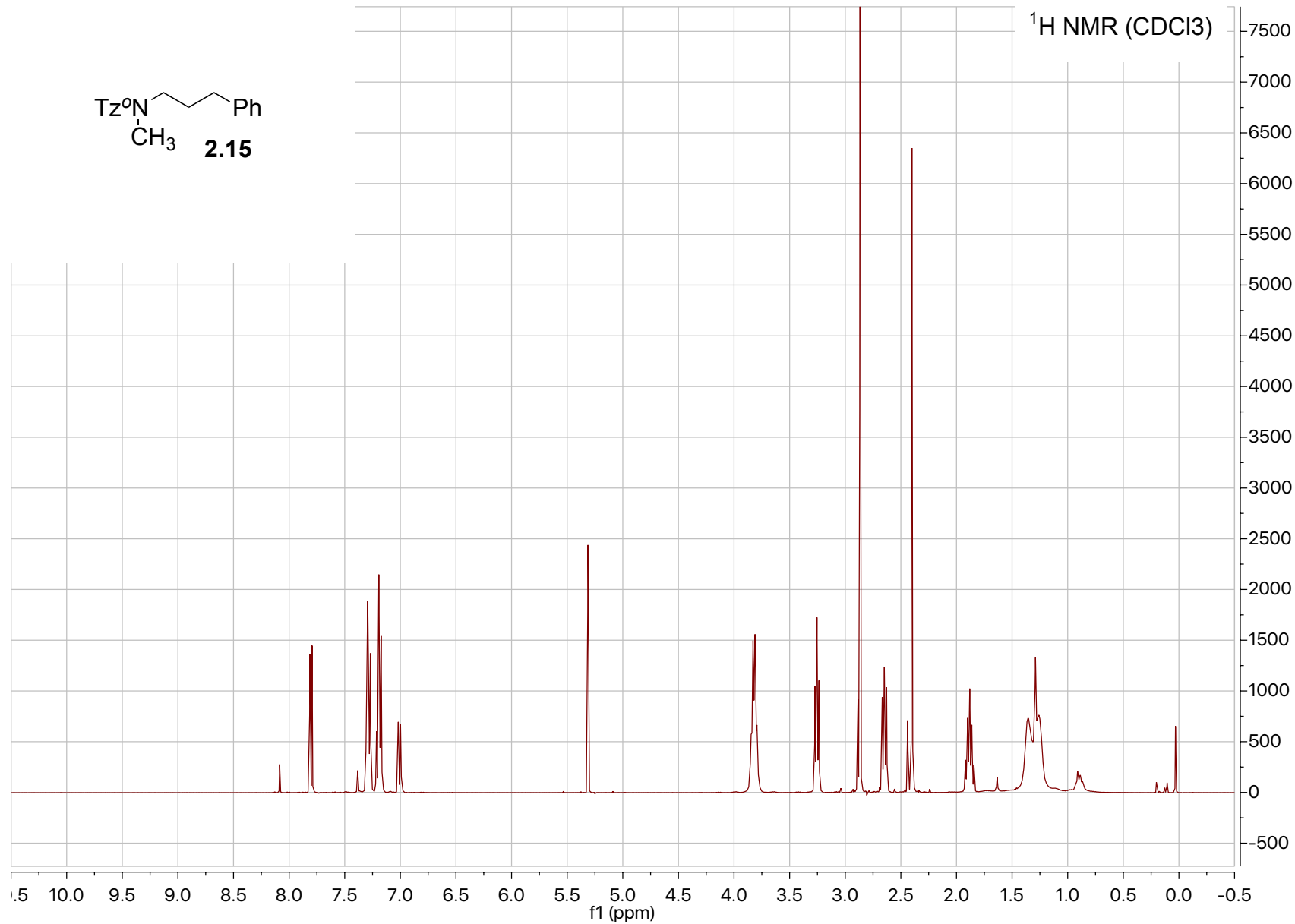
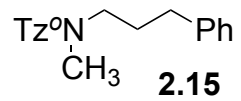
APPENDIX B: NMR SPECTRA OF COMPOUNDS FOUND IN CHAPTER 2

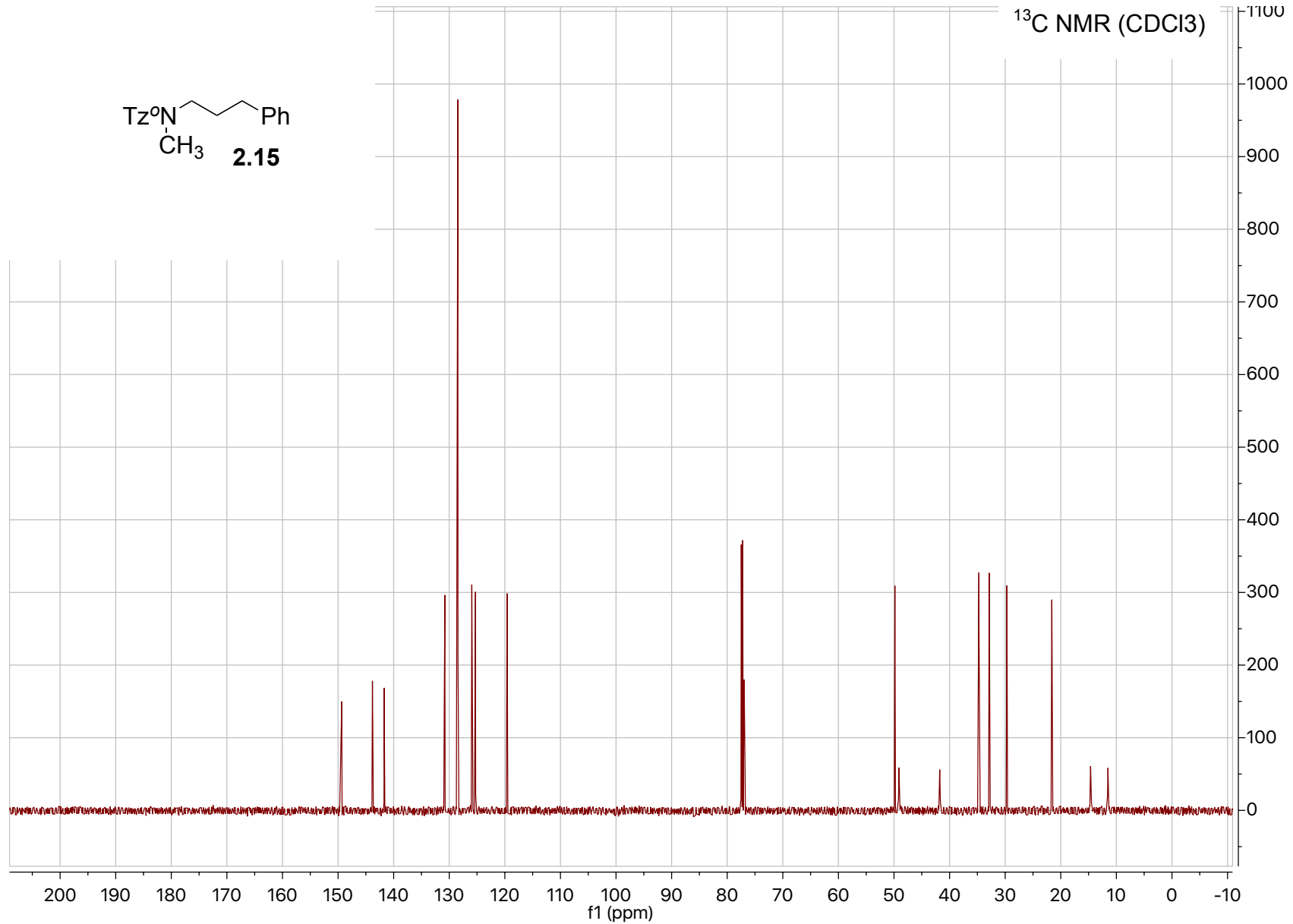
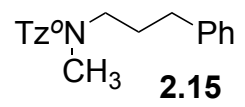


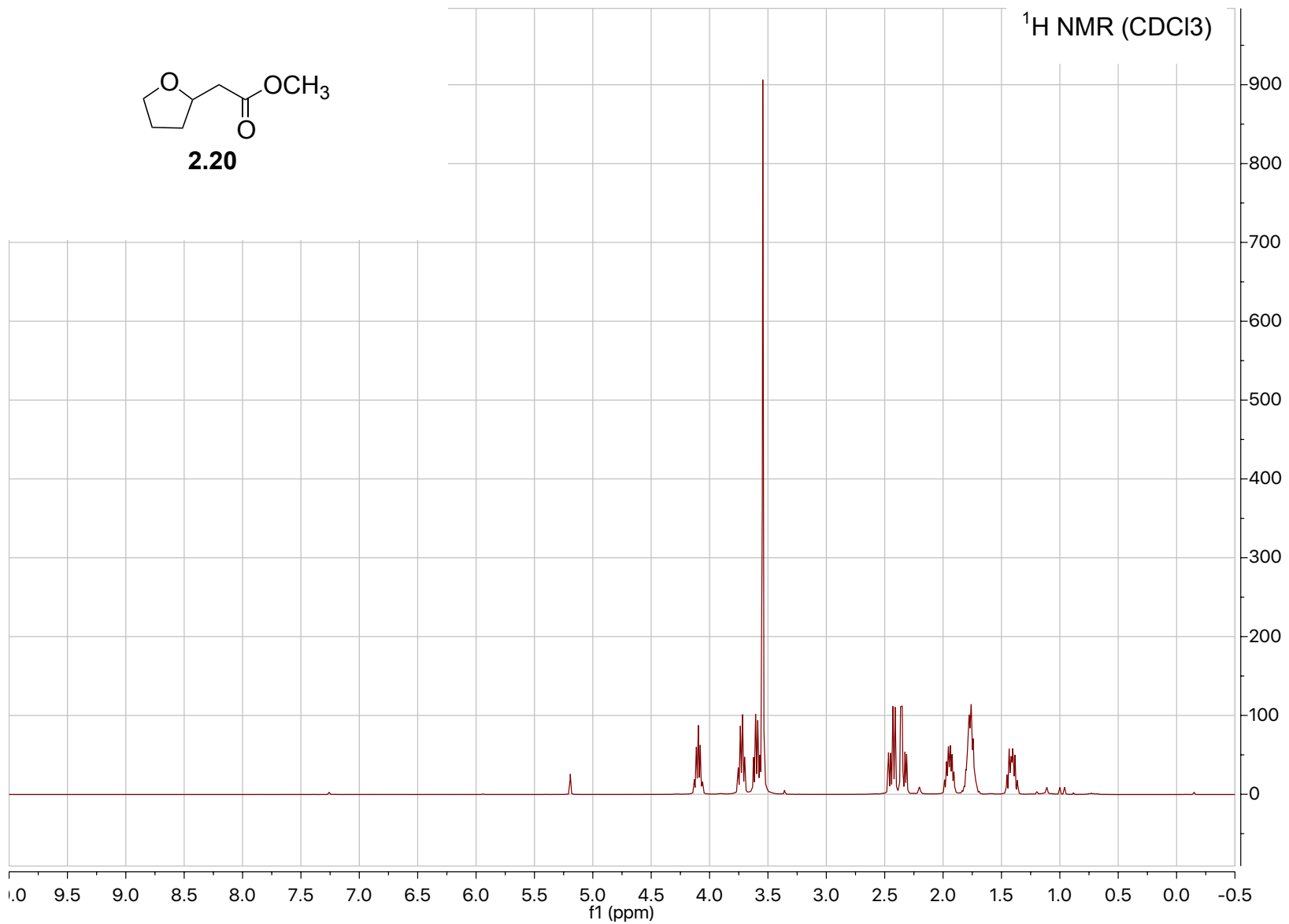
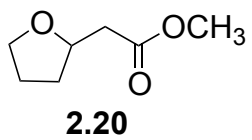


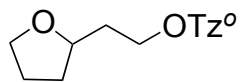




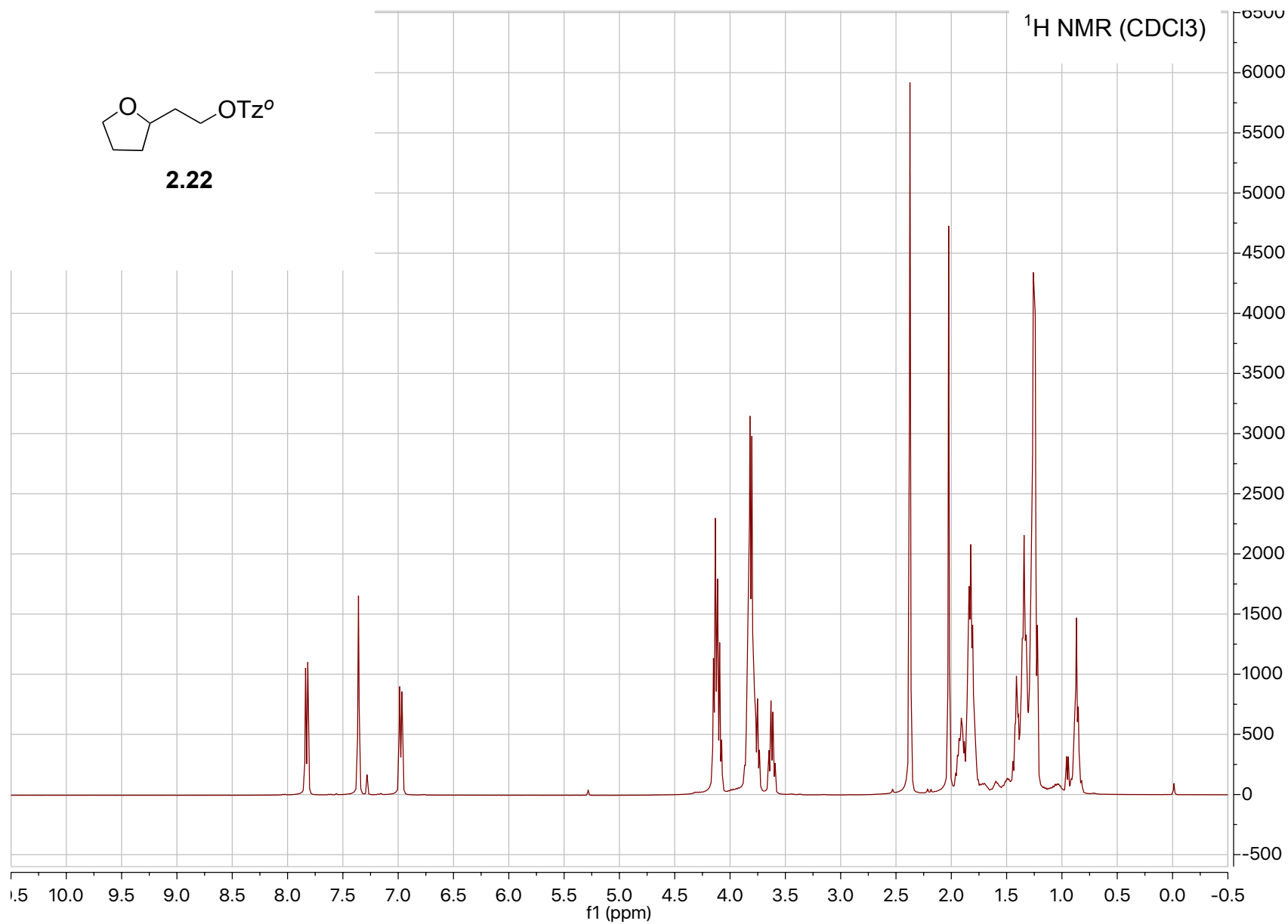


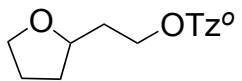




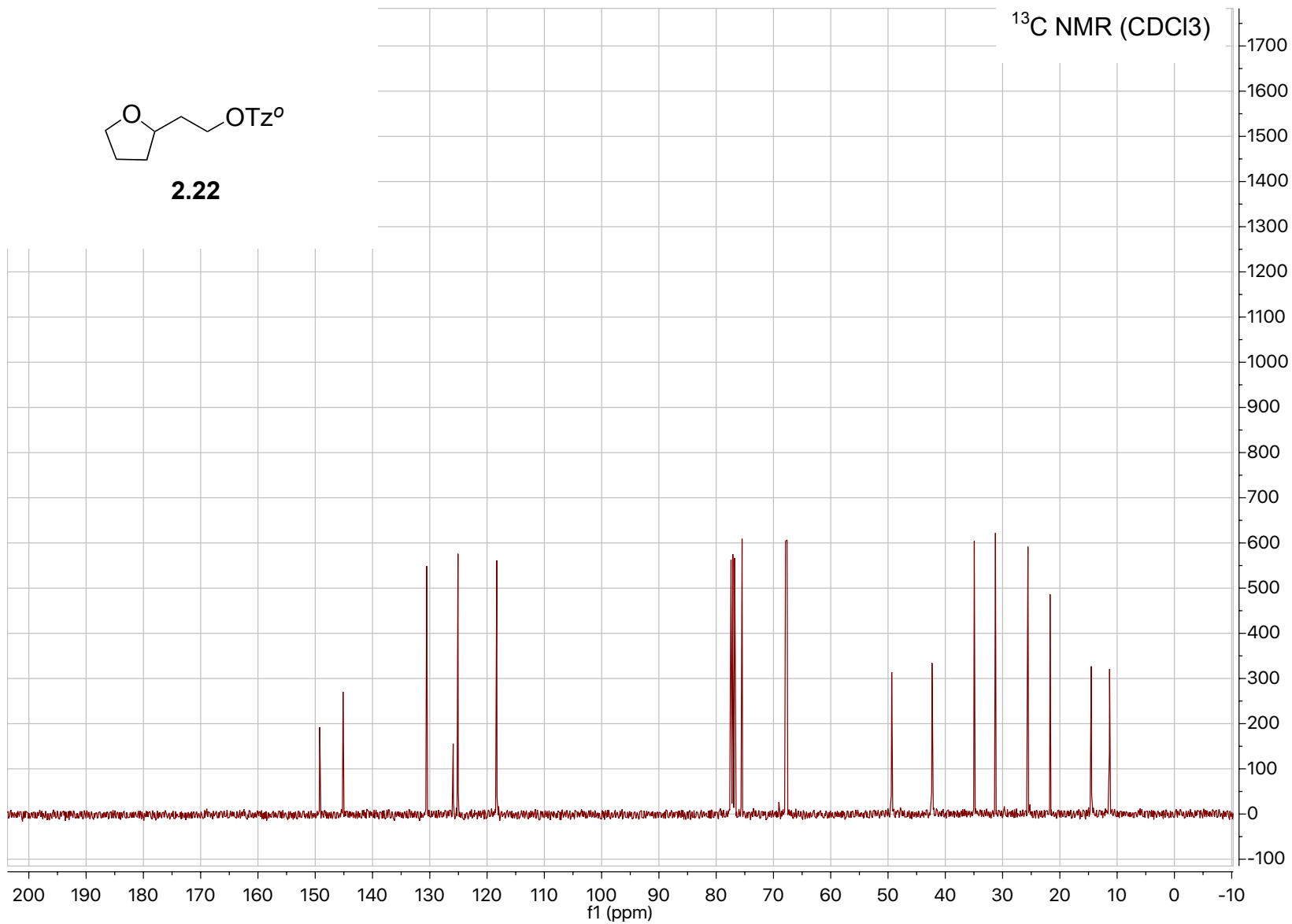


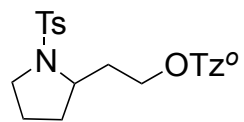
2.22





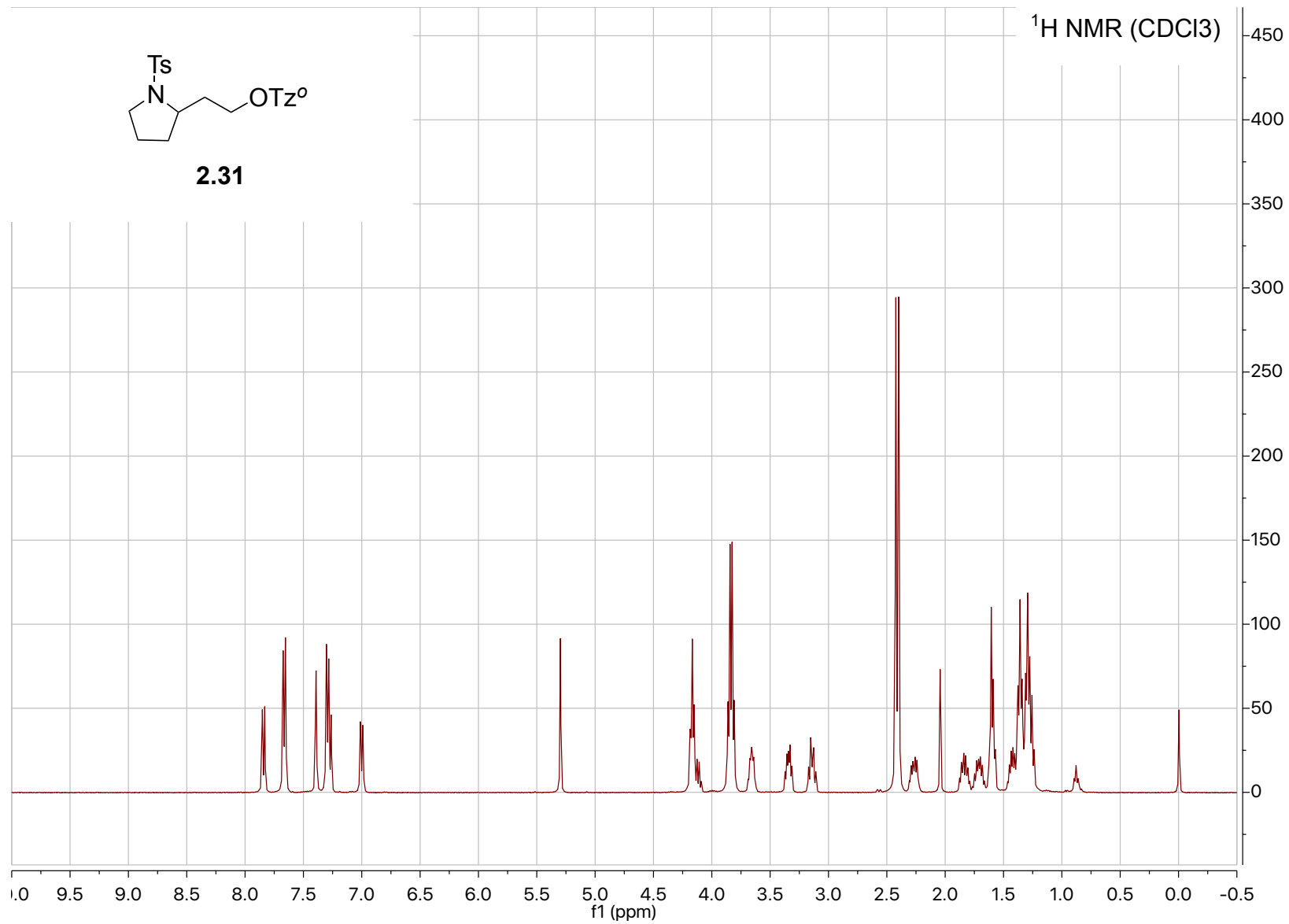
2.22

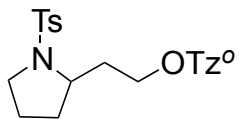




2.31

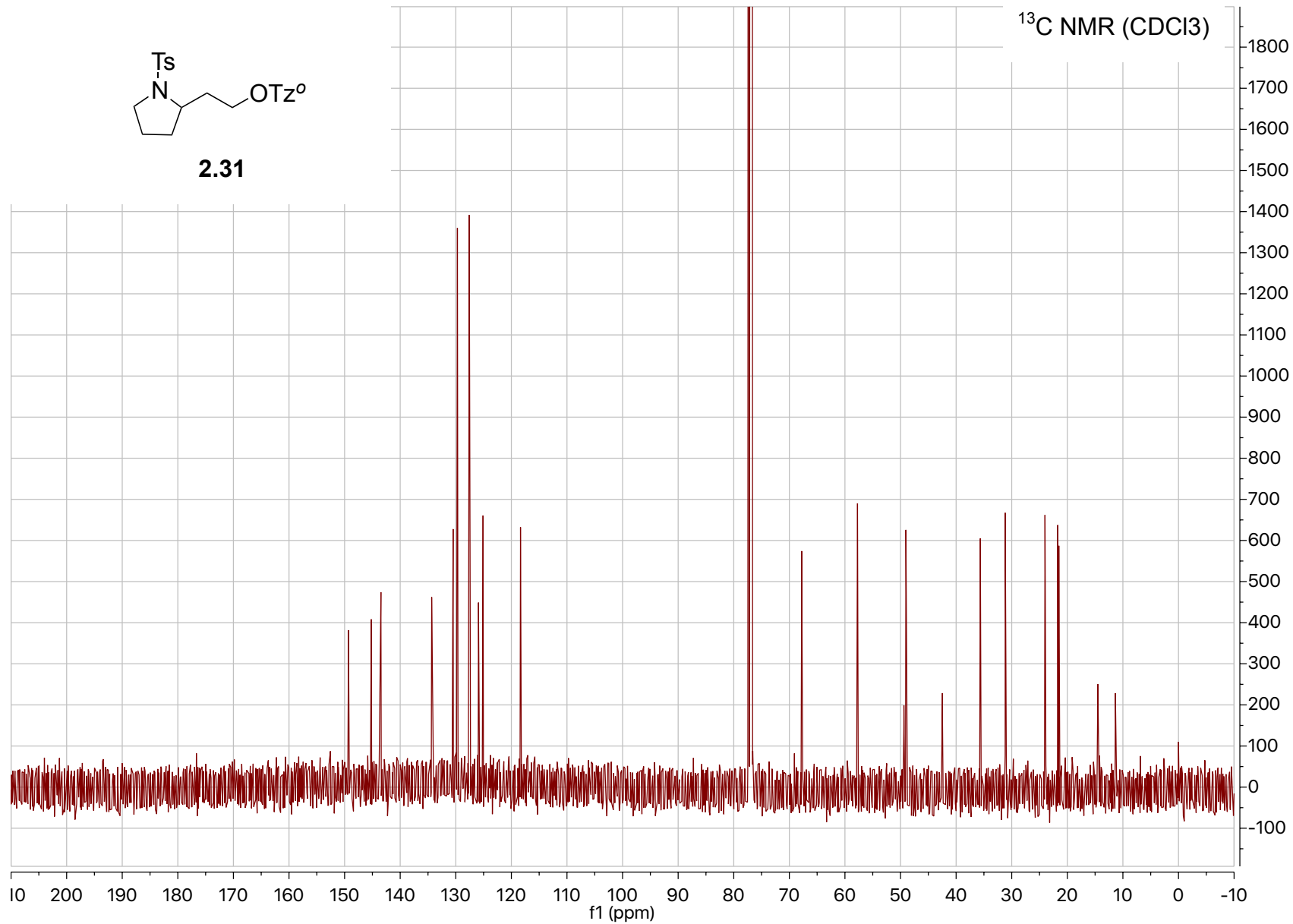
¹H NMR (CDCl₃)

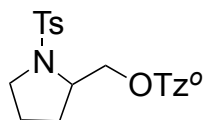




2.31

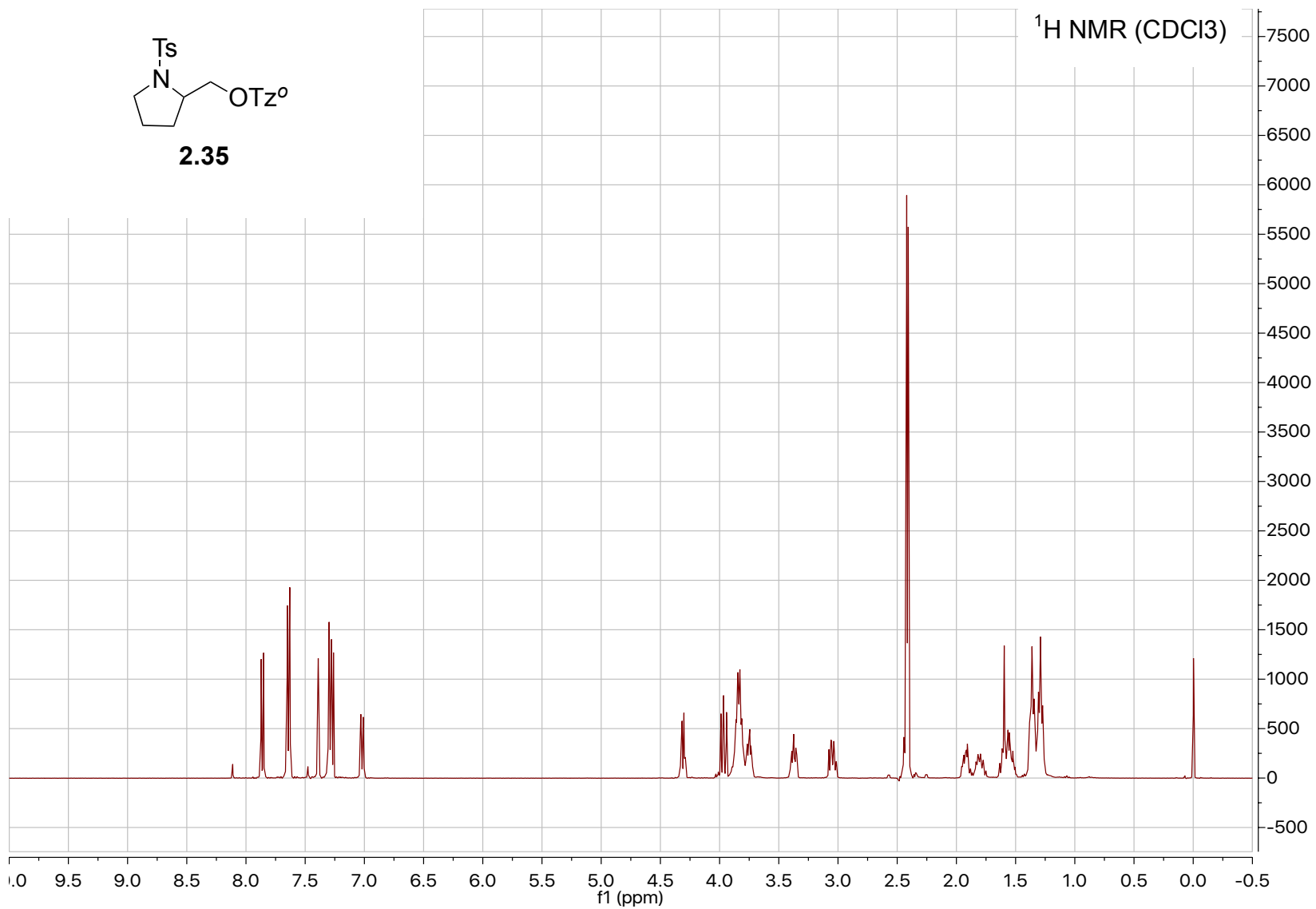
¹³C NMR (CDCl₃)

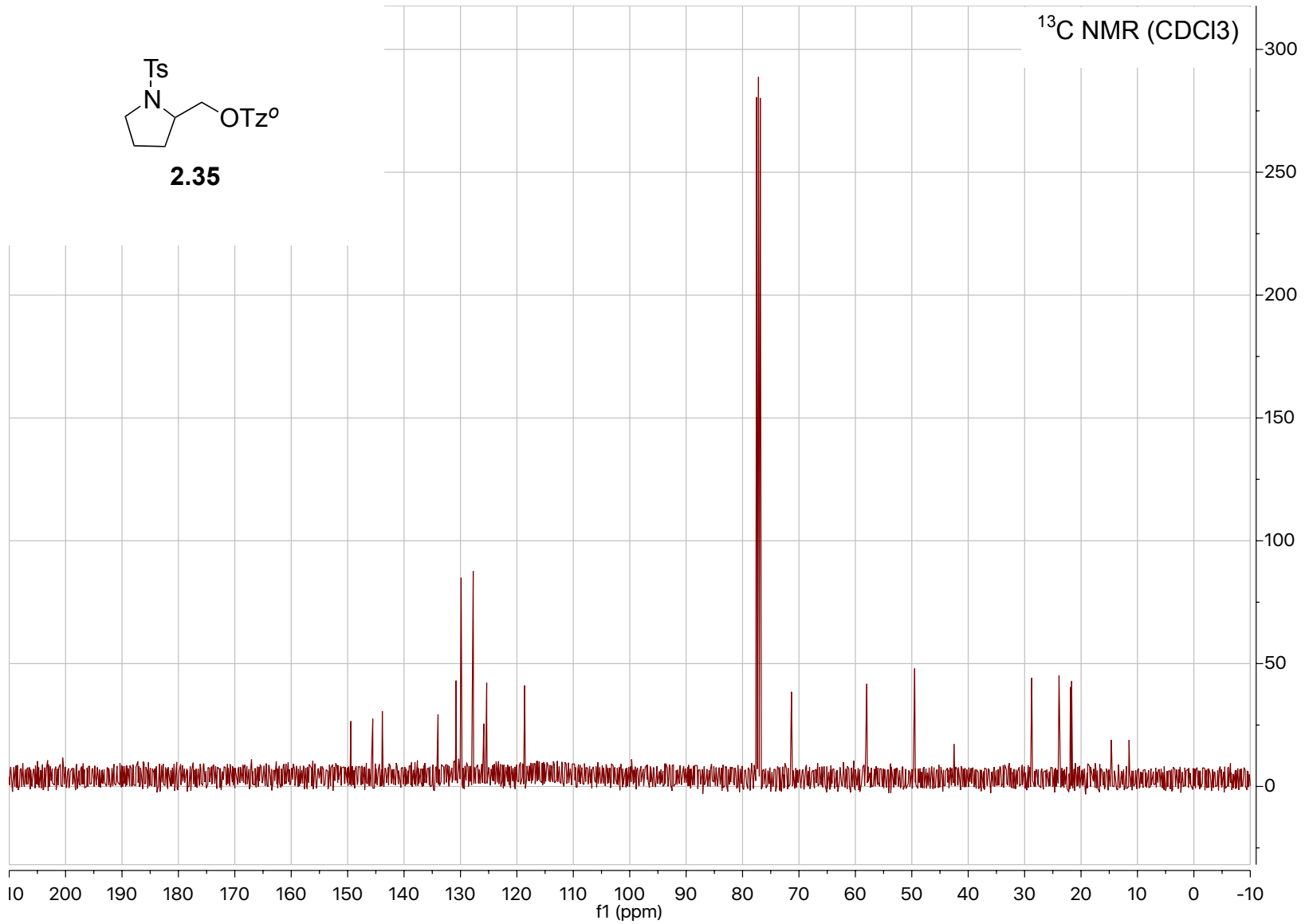


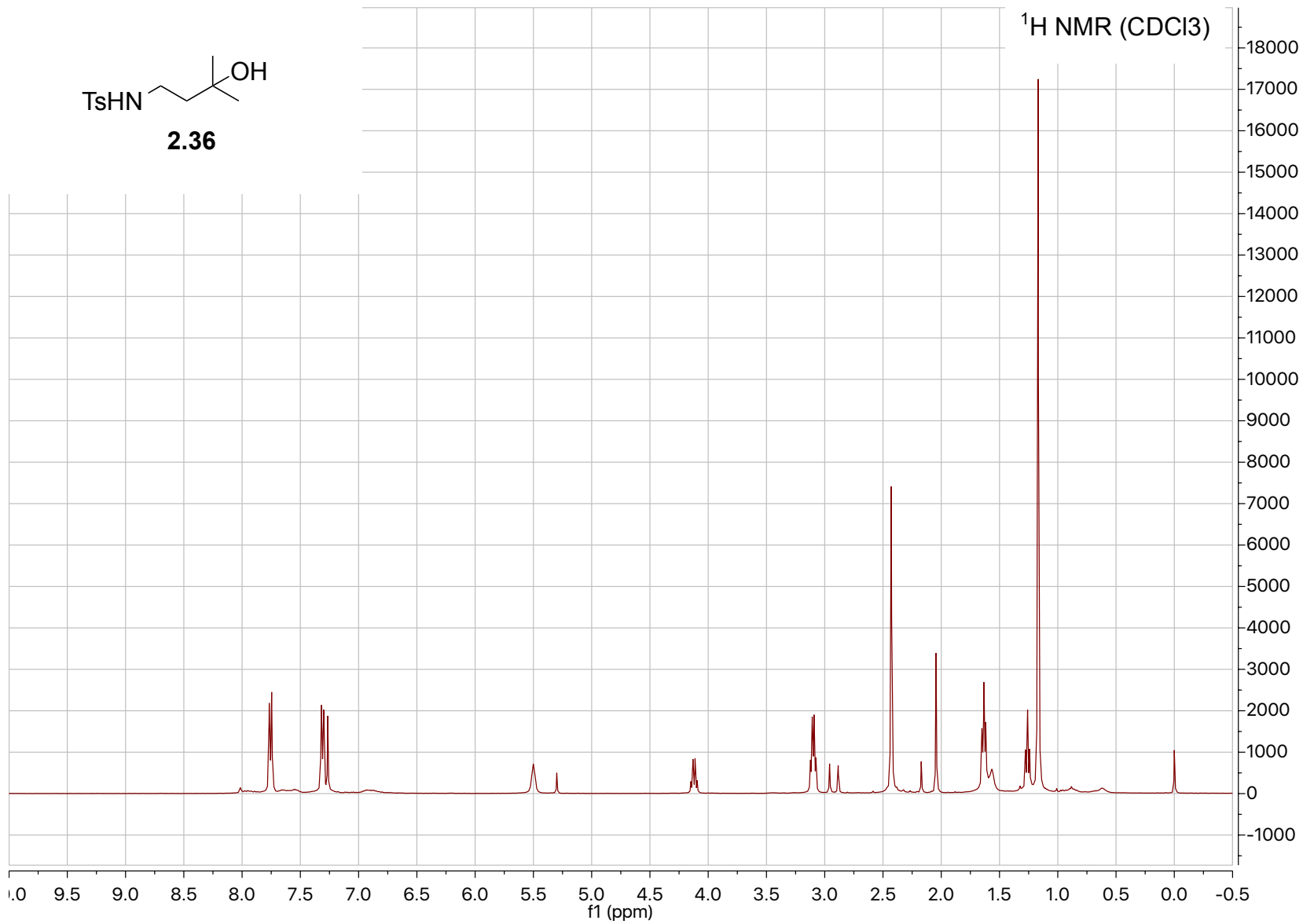
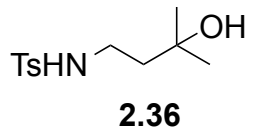


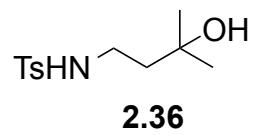
2.35

¹H NMR (CDCl₃)

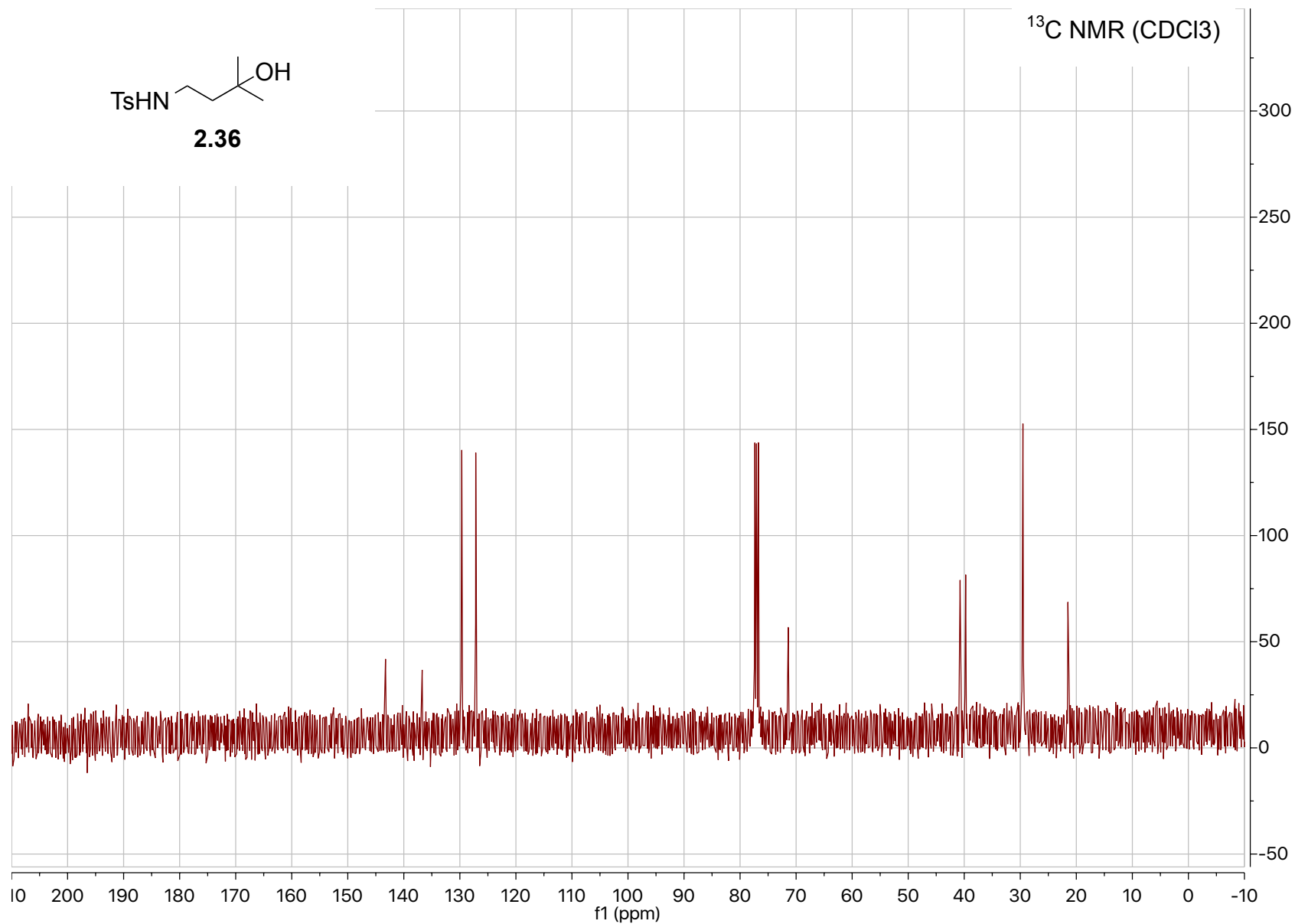


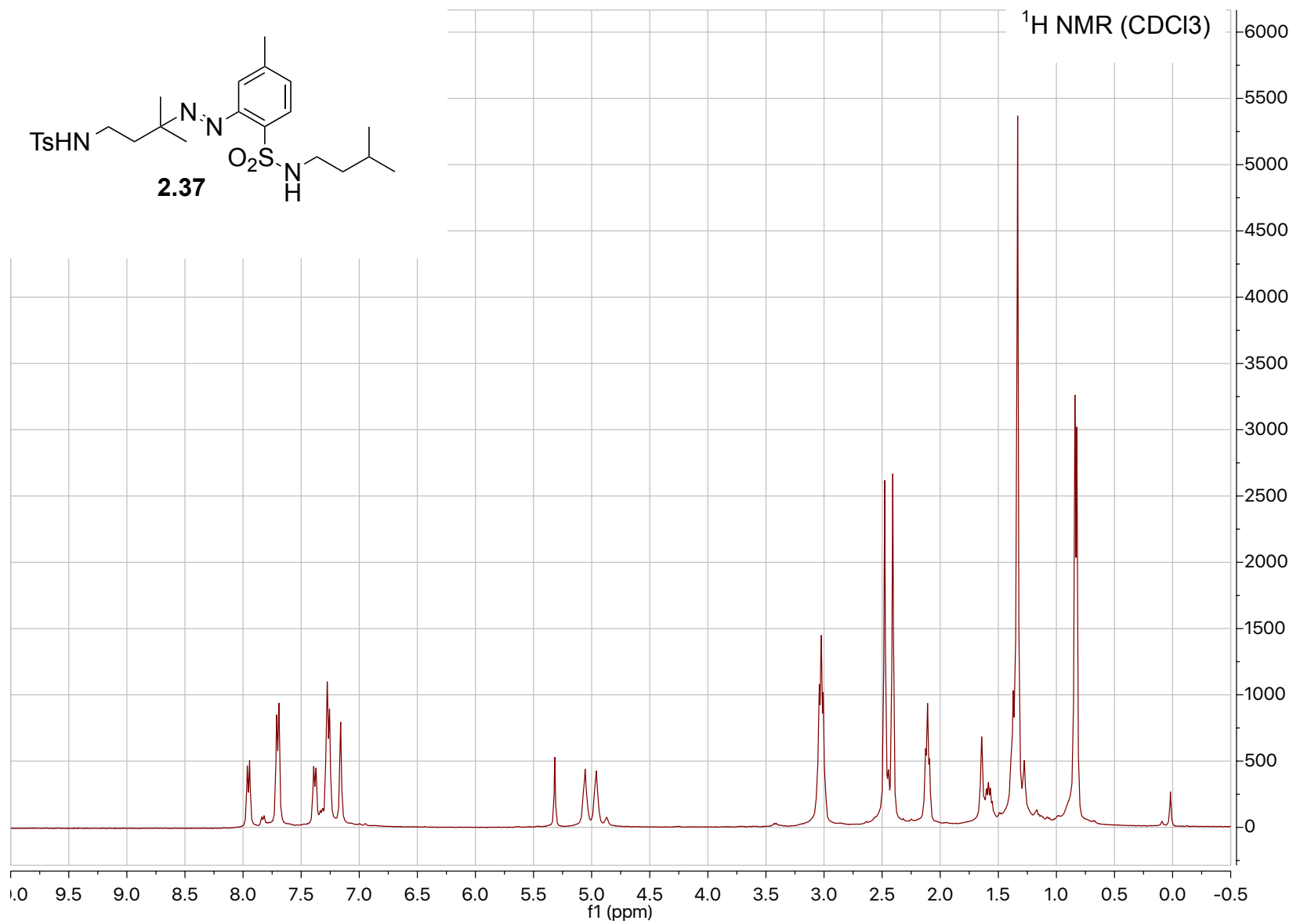
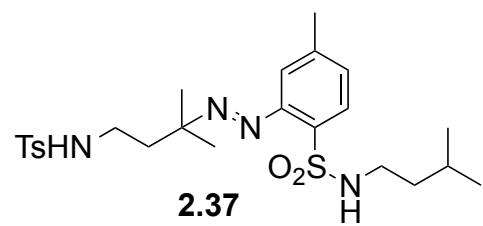


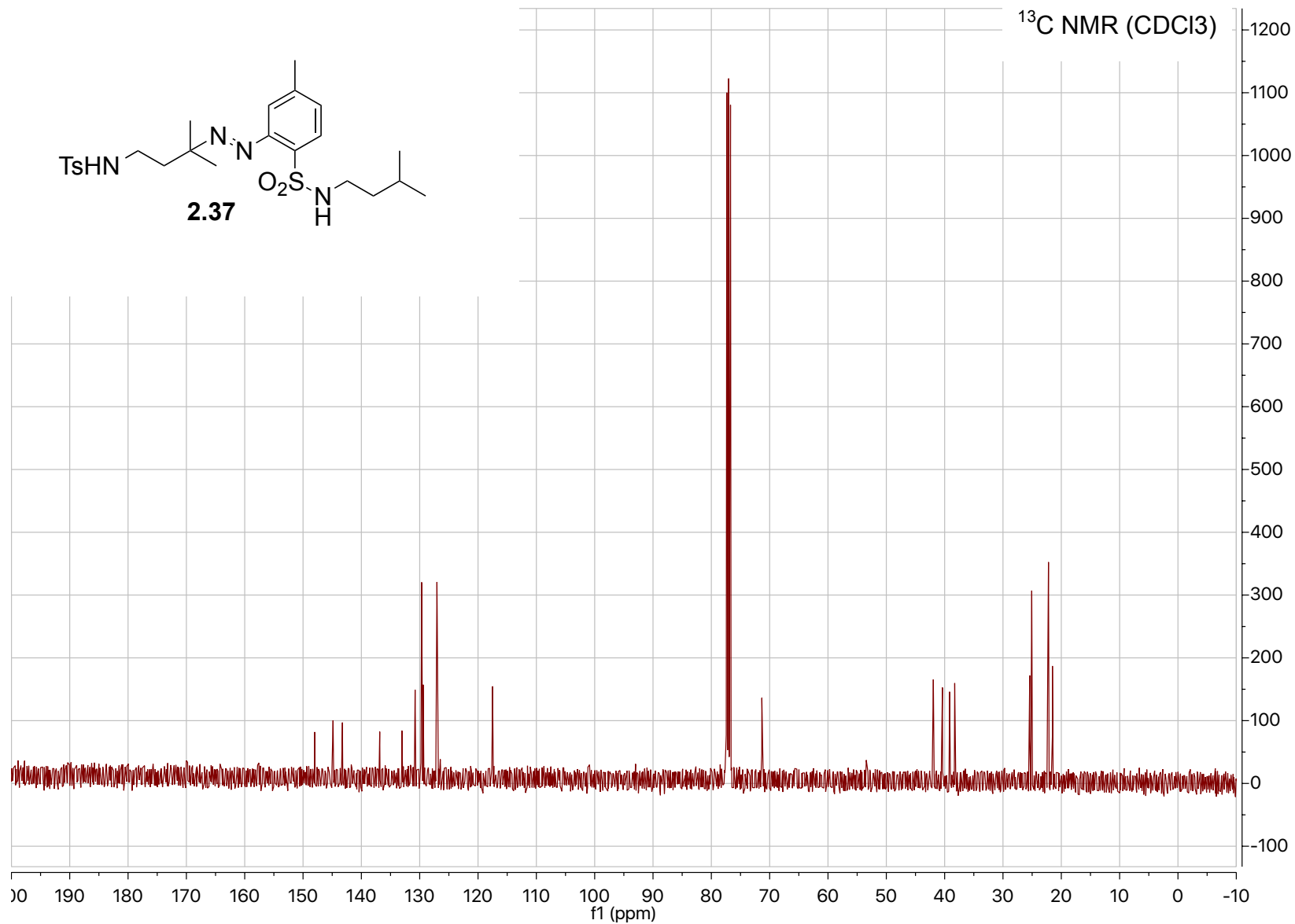
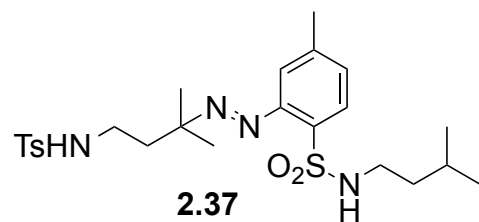


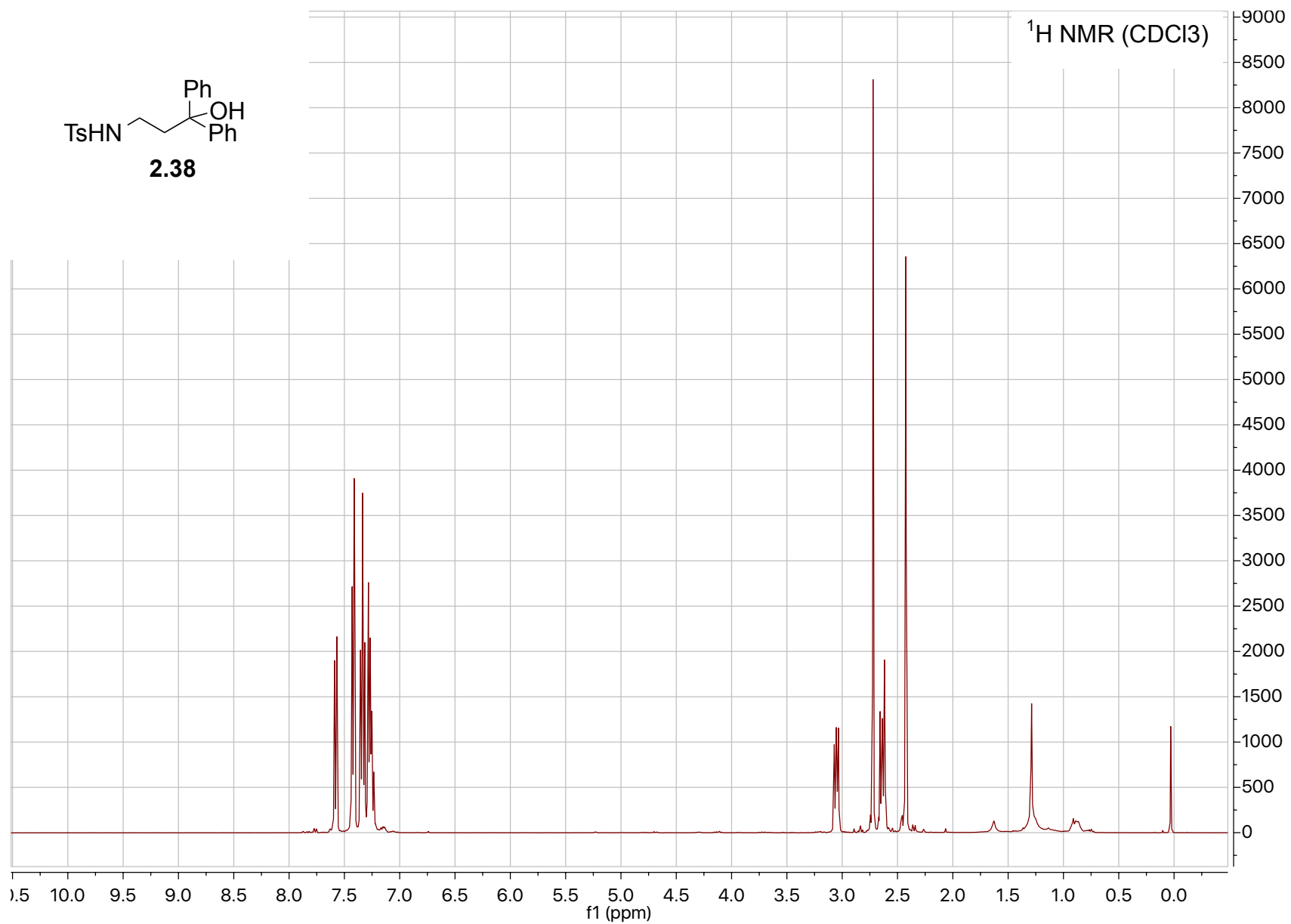
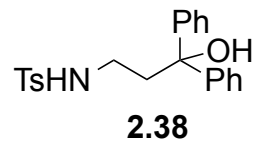


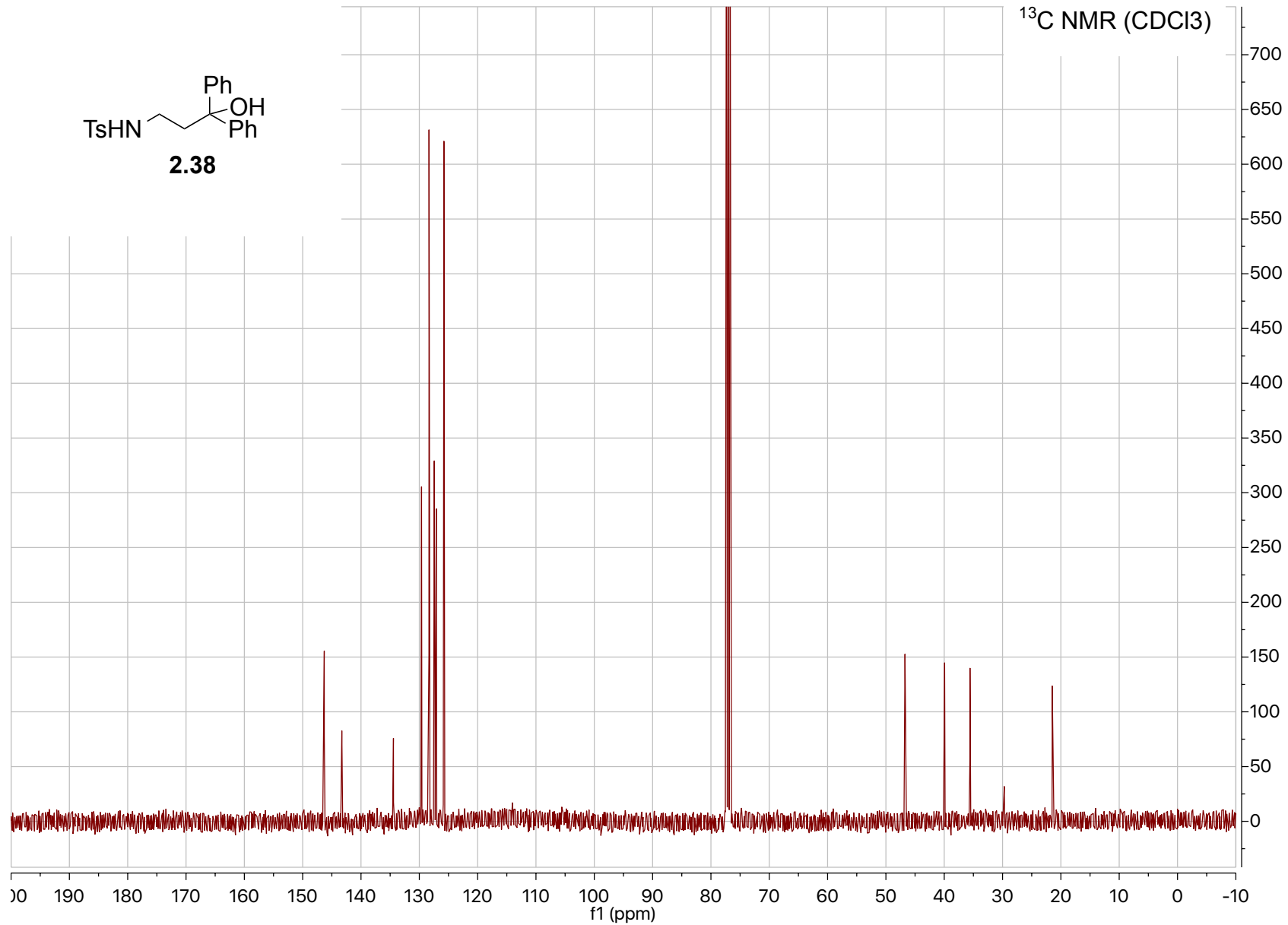
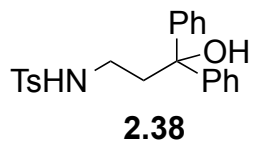
¹³C NMR (CDCl₃)

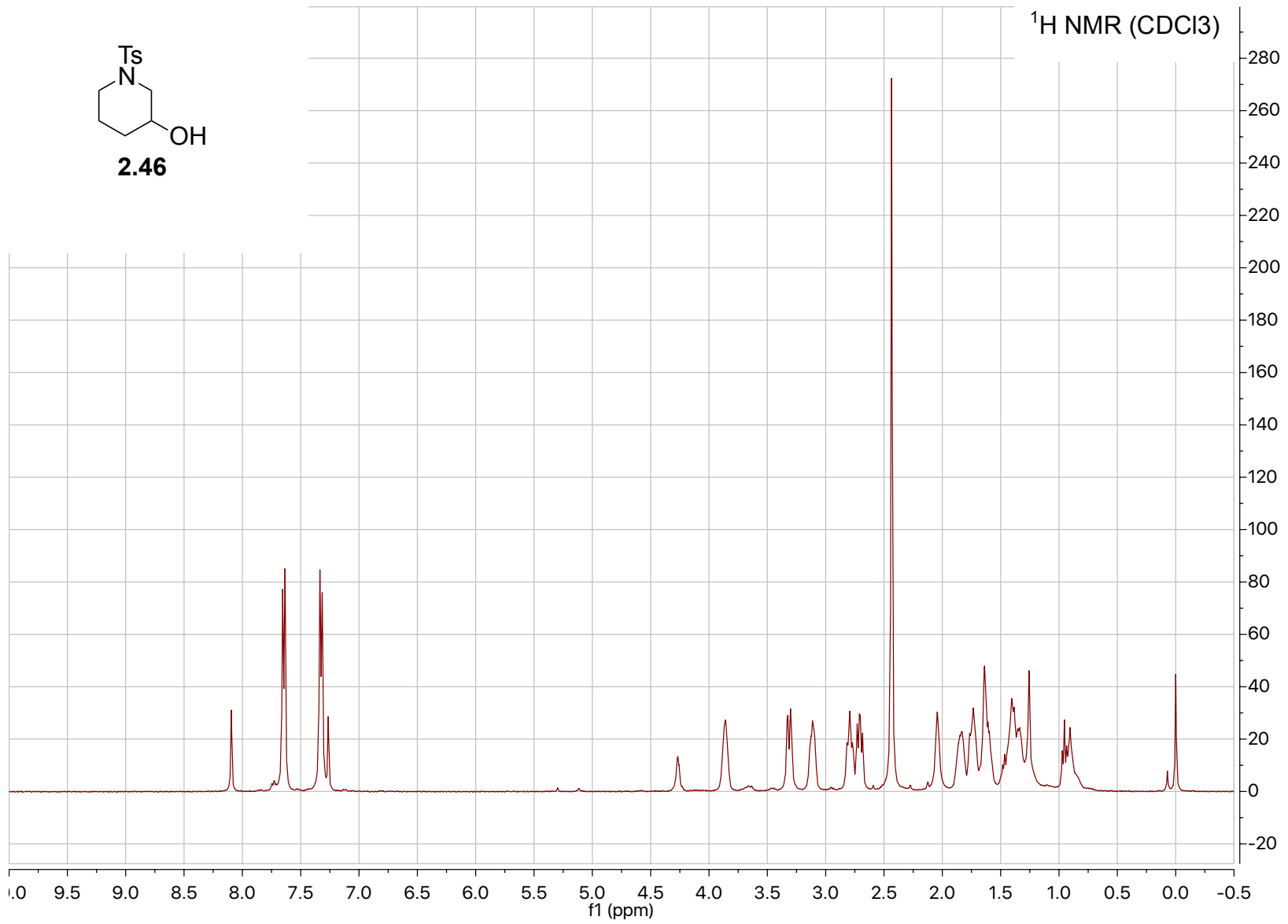
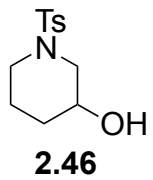


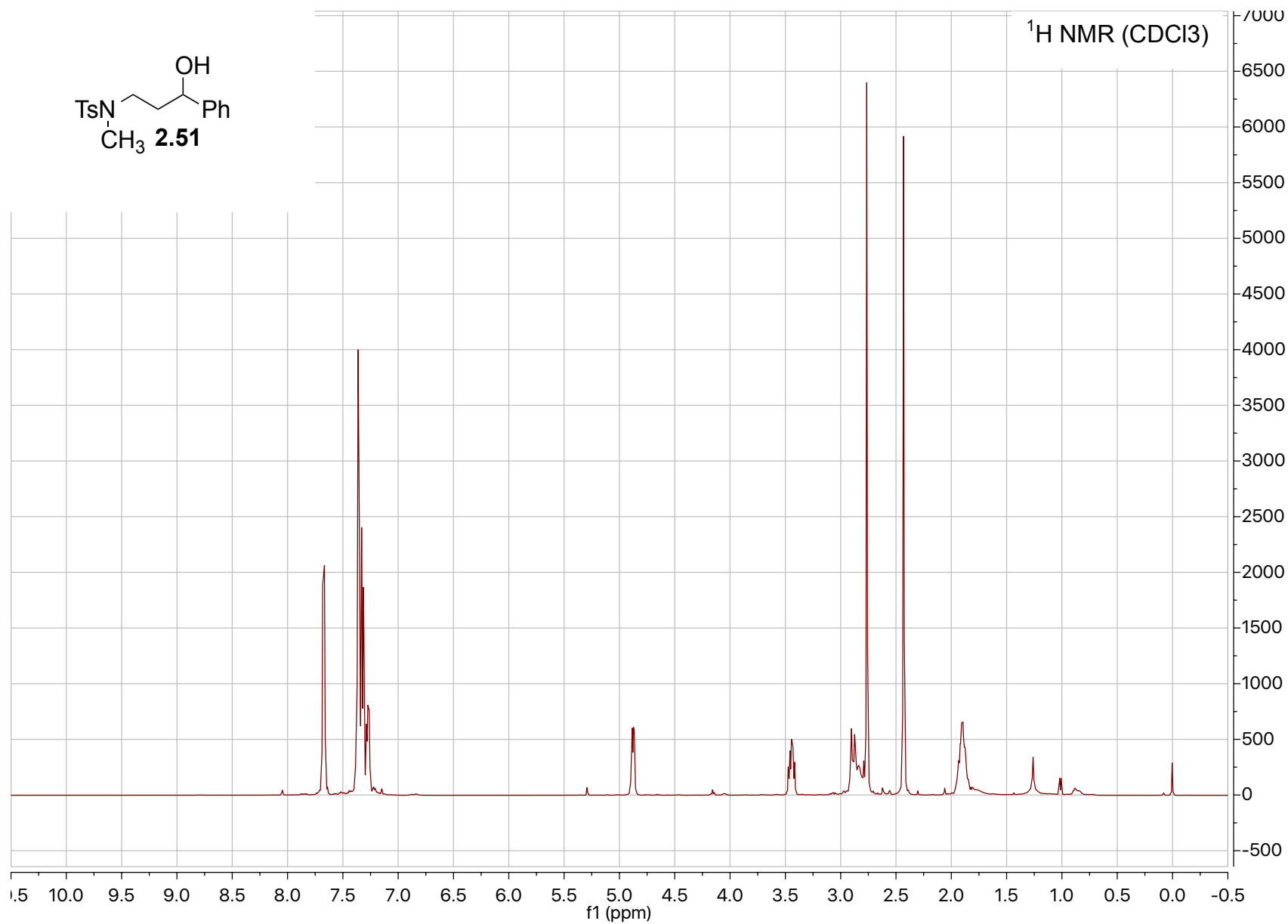
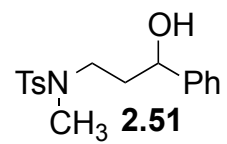


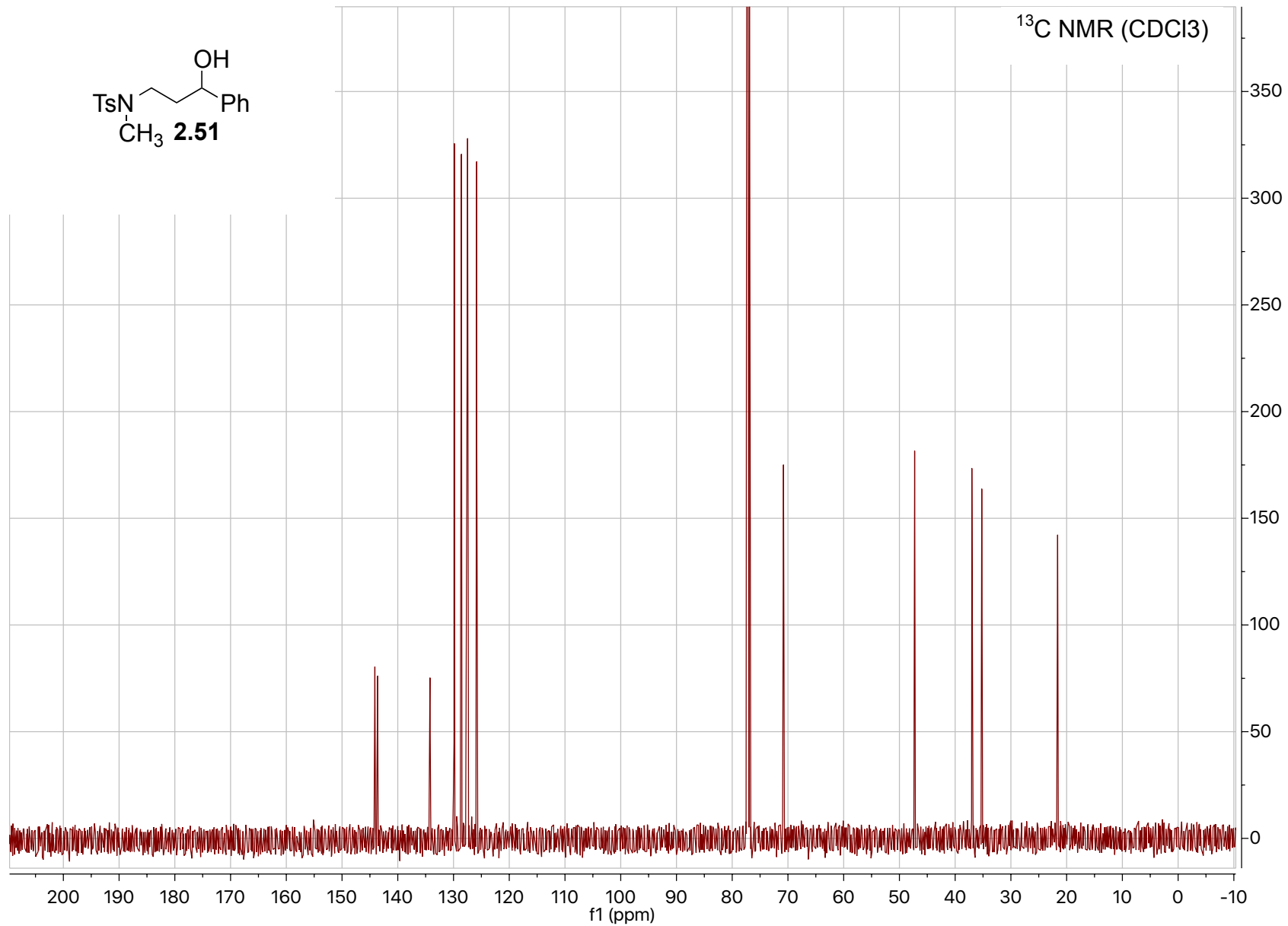
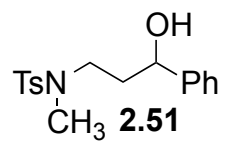


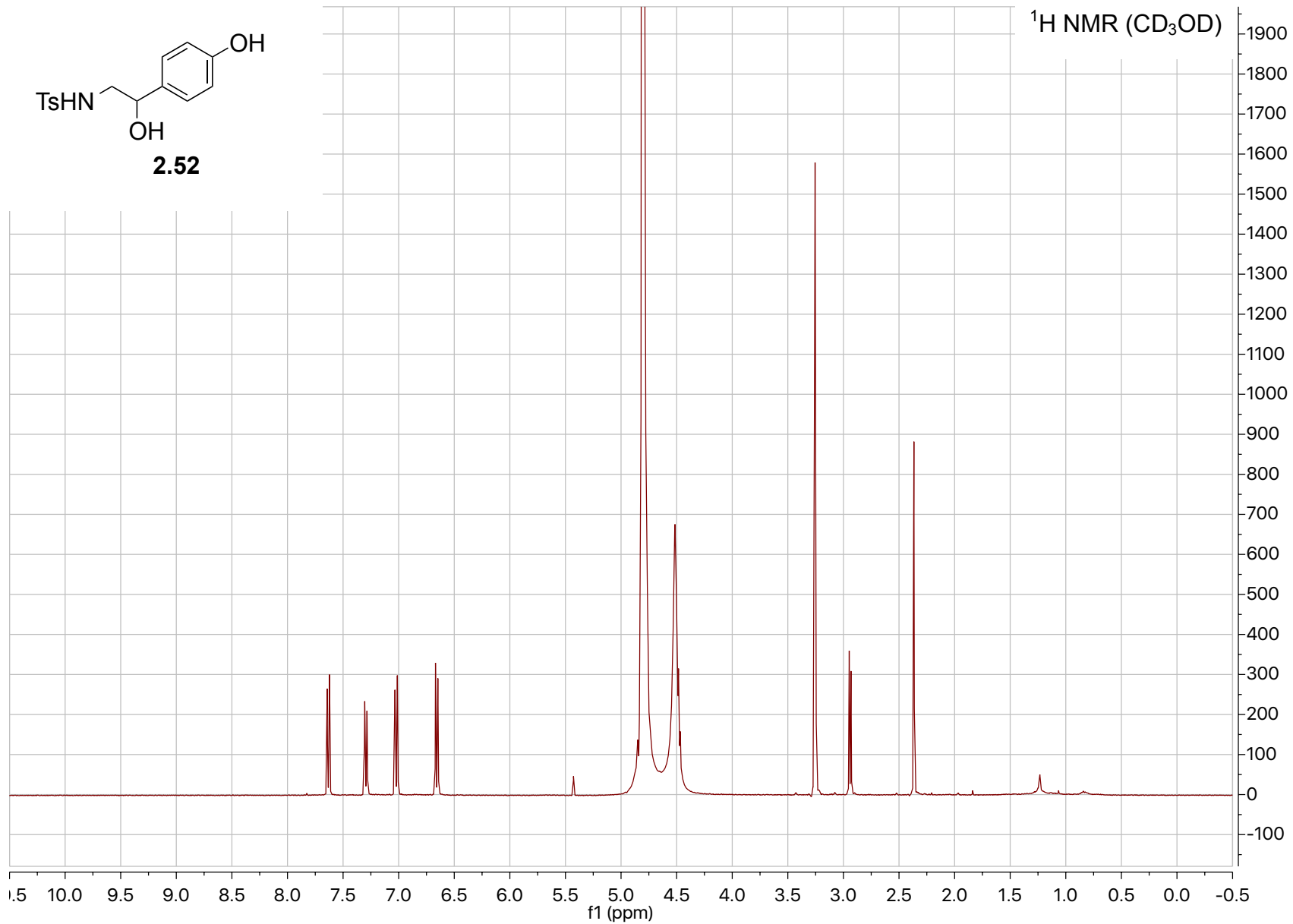
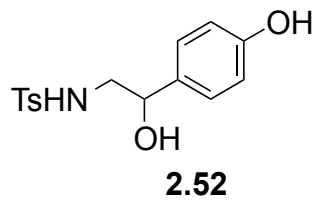


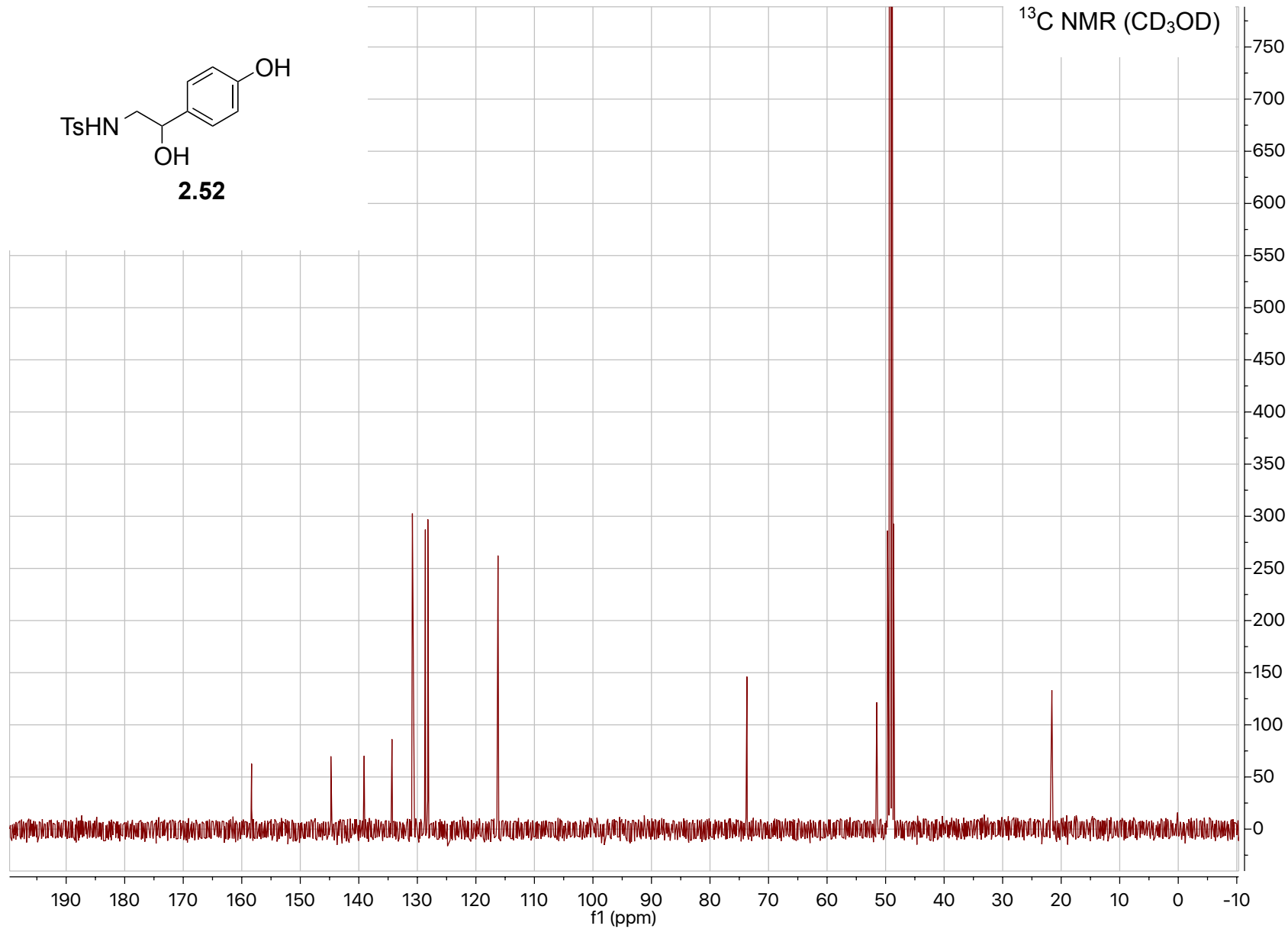
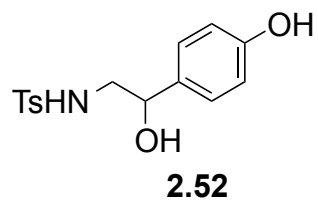


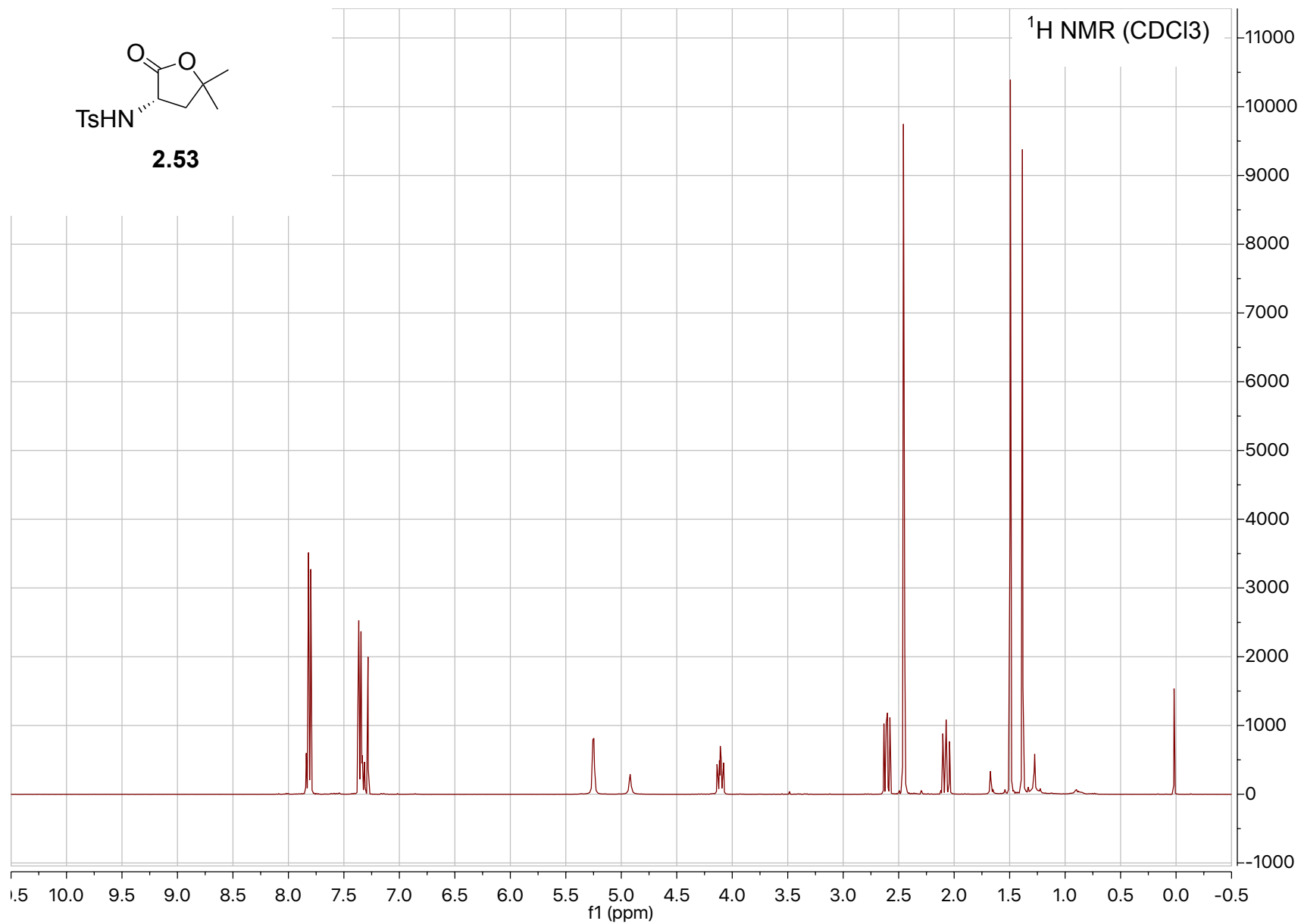
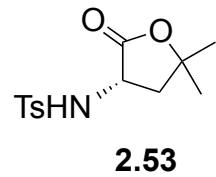


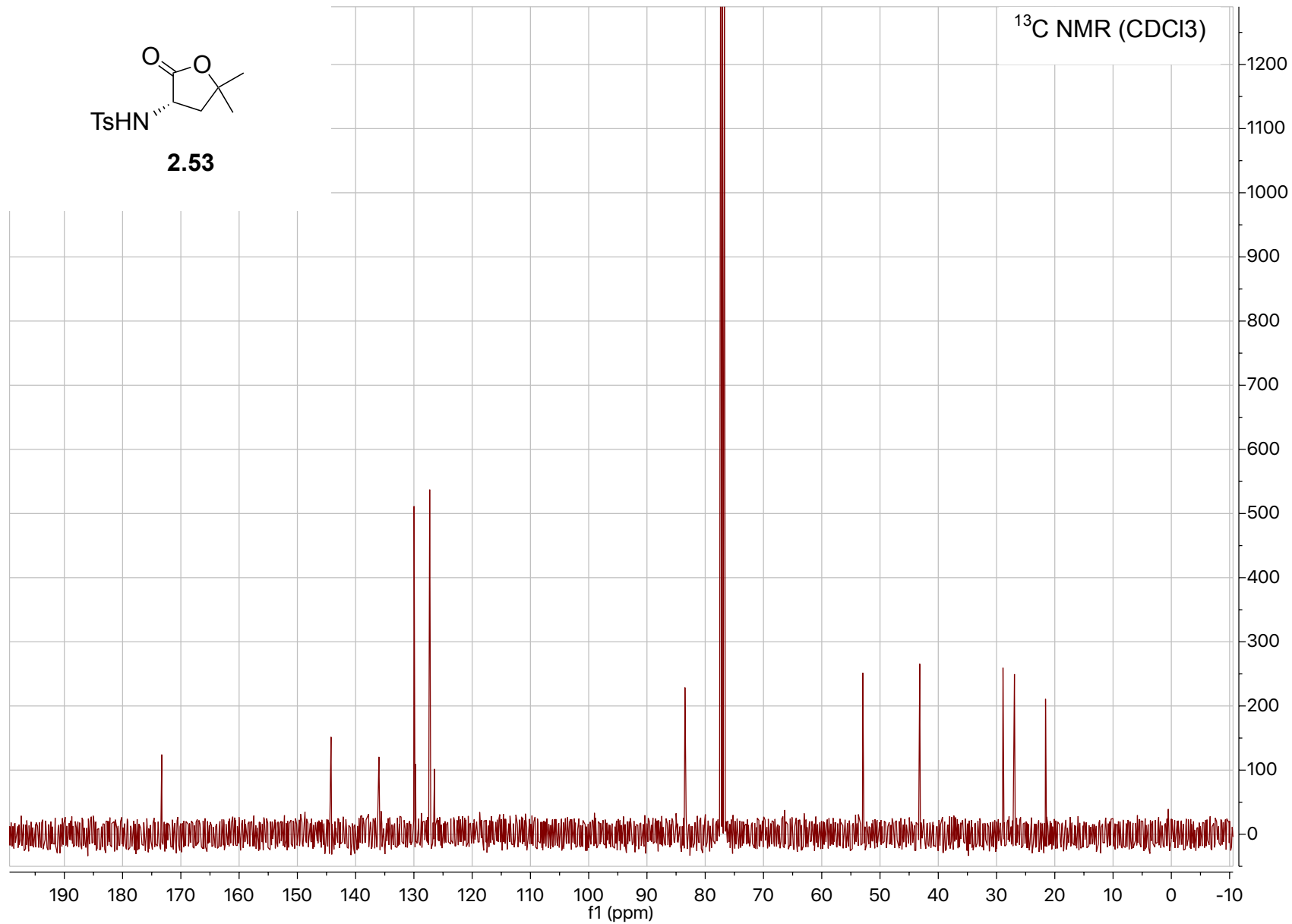
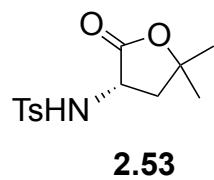


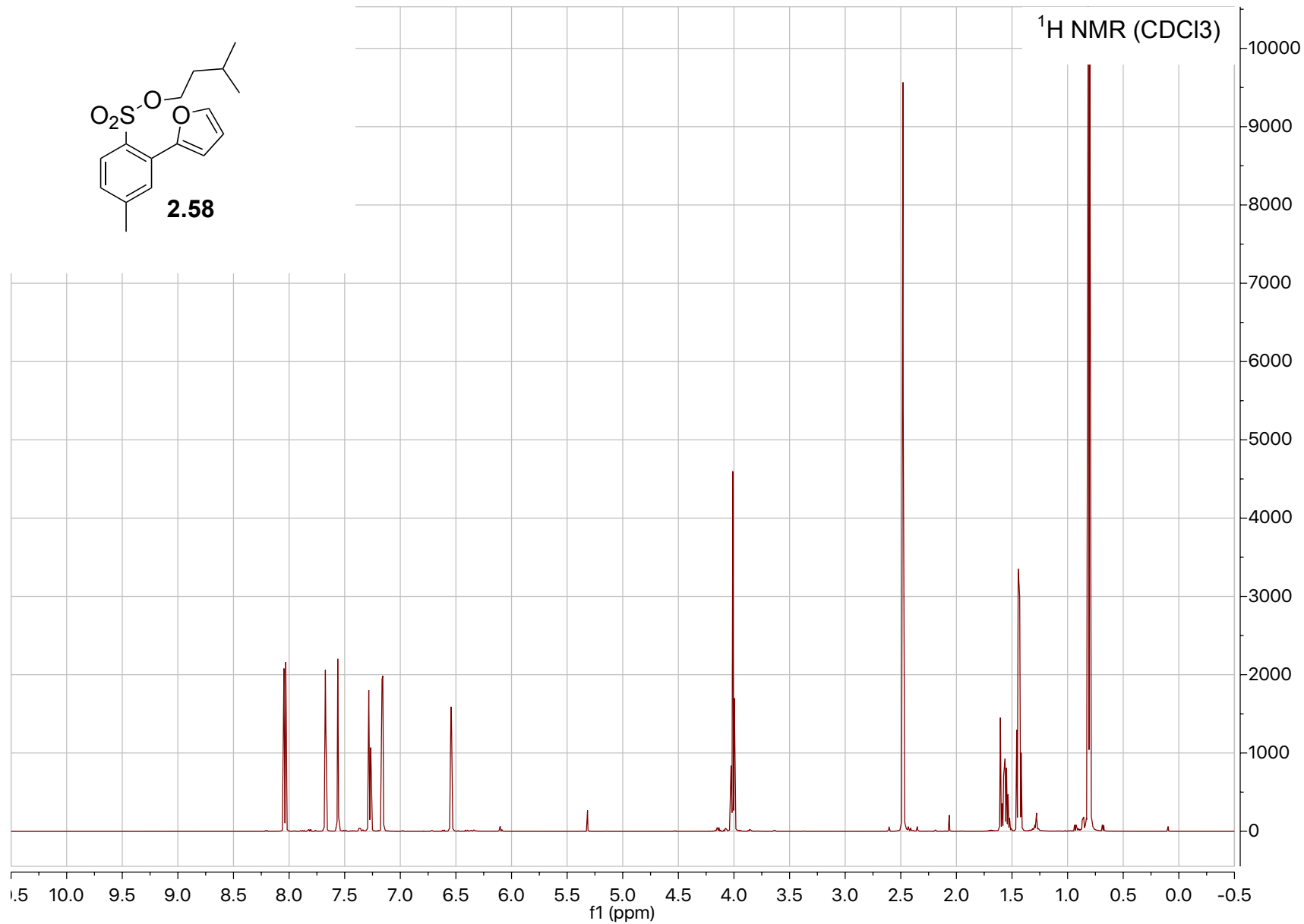
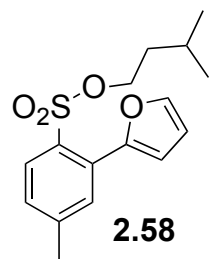


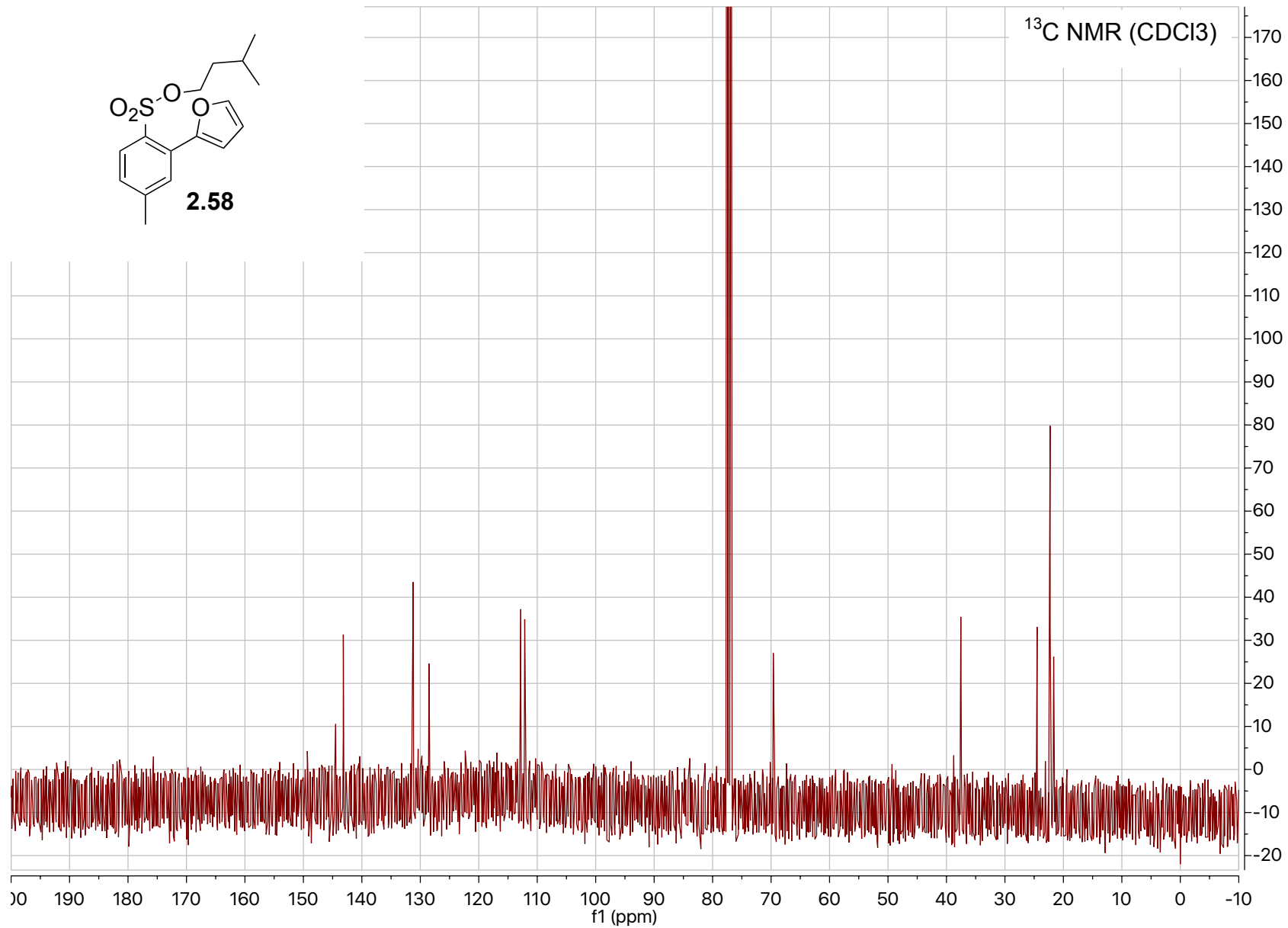
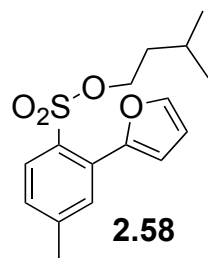




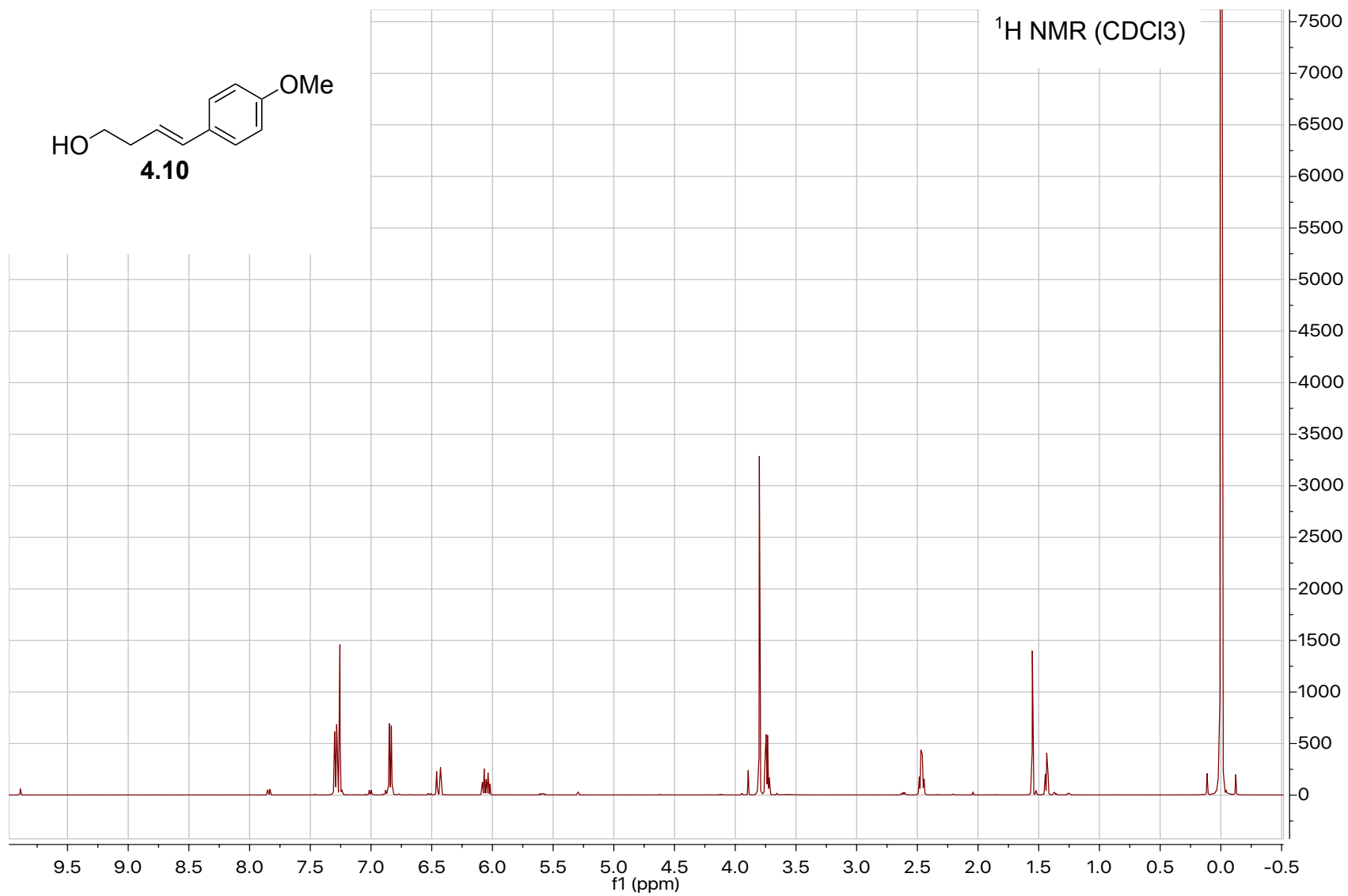
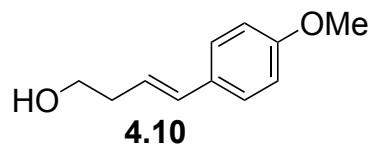


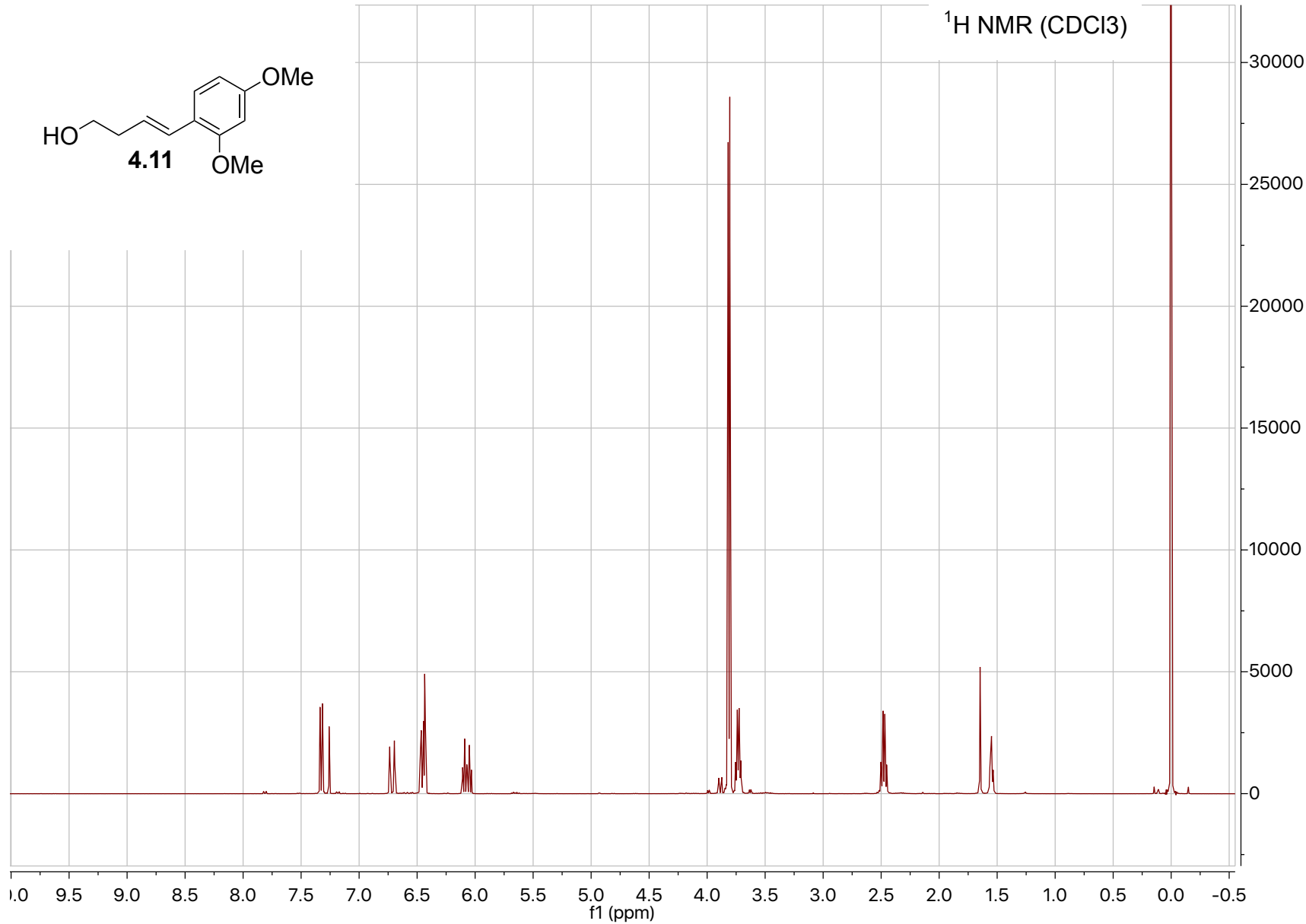
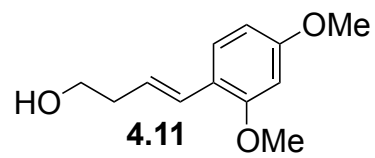


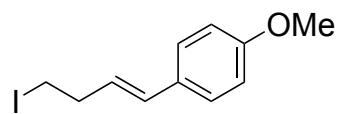




APPENDIX C: NMR SPECTRA OF COMPOUNDS FOUND IN CHAPTER 4

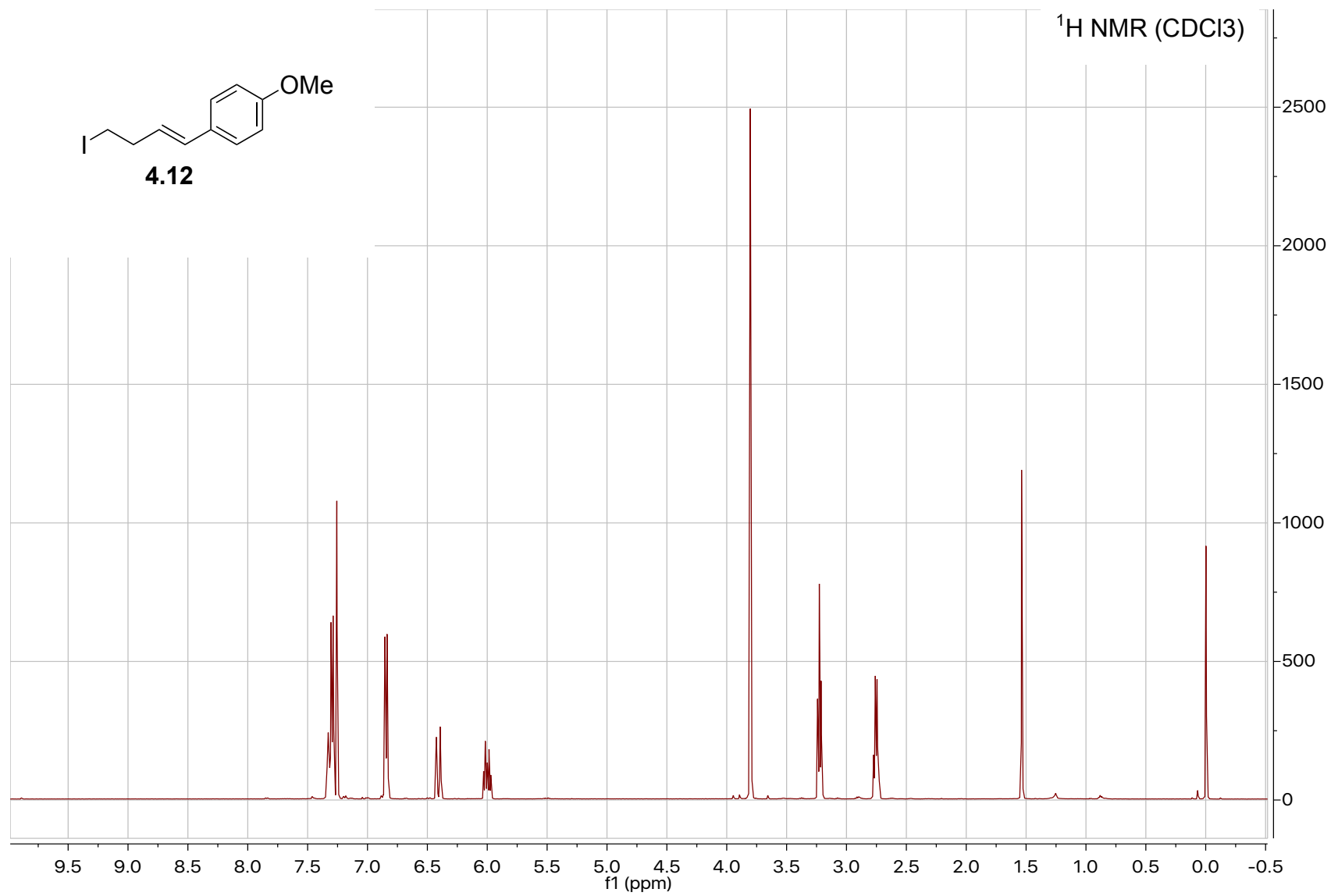


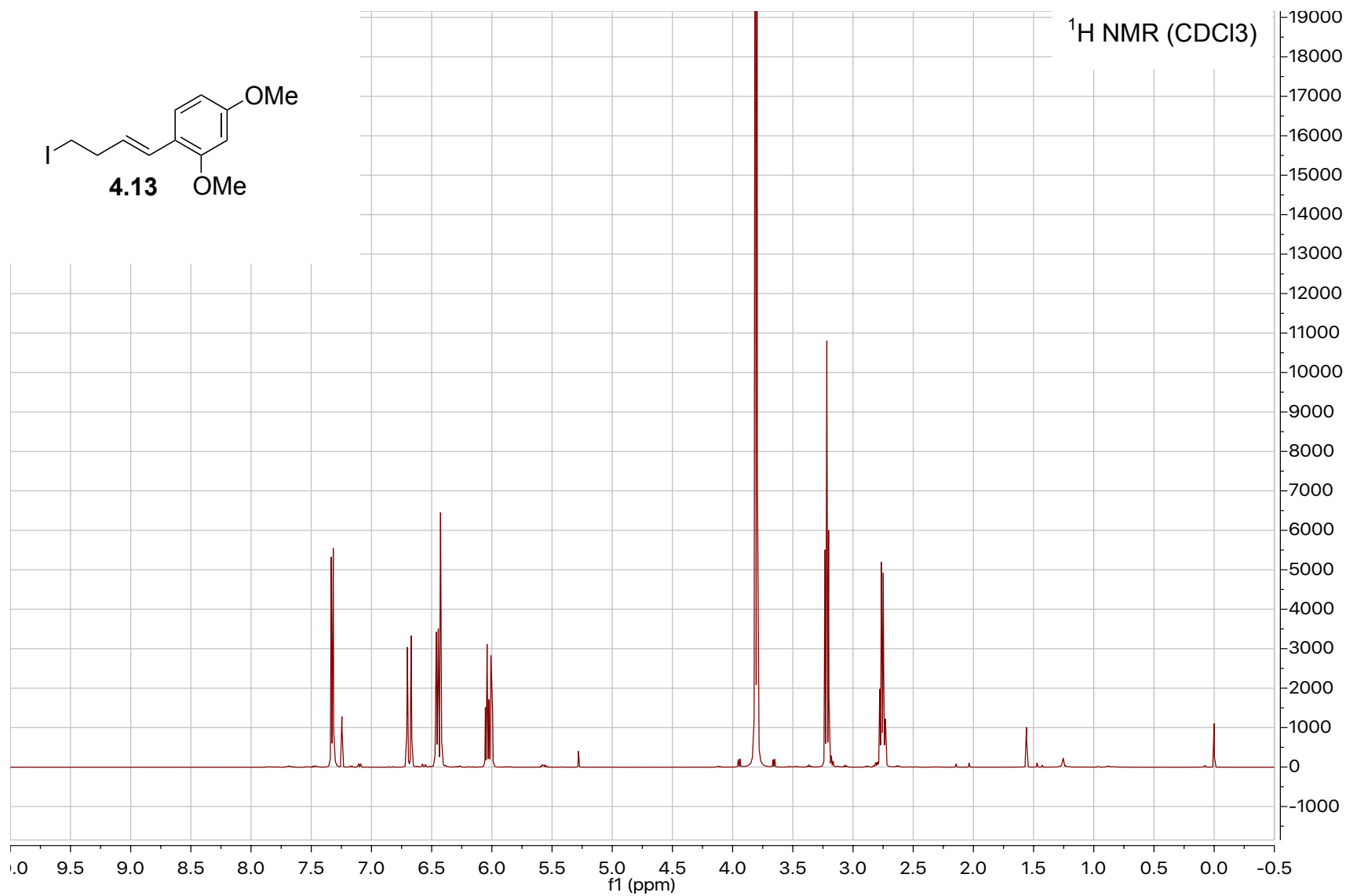
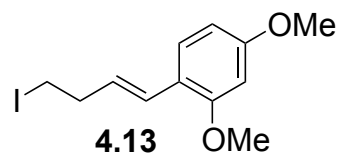


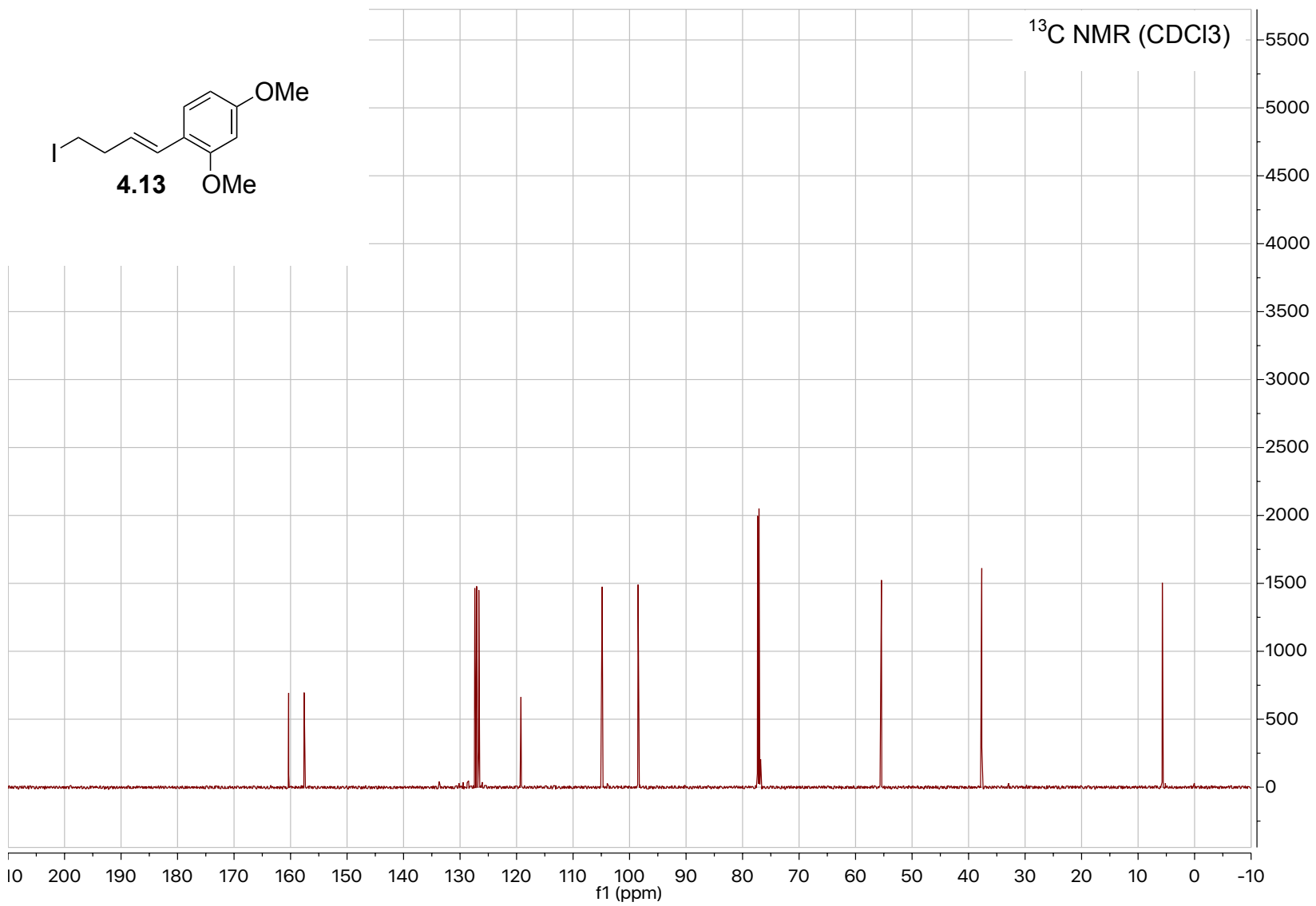
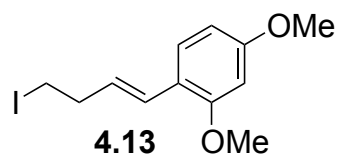


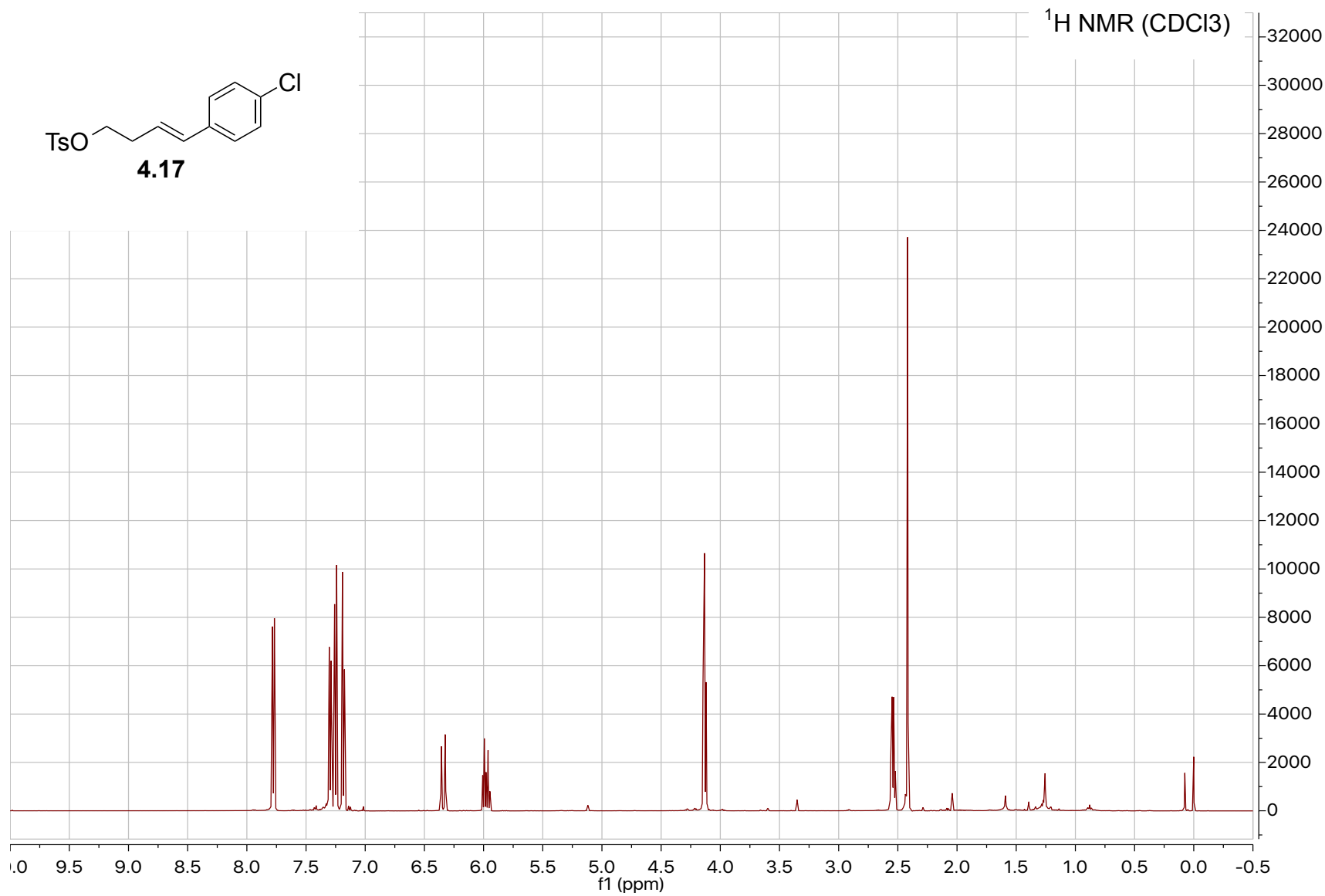
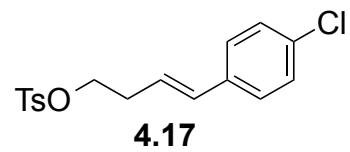
4.12

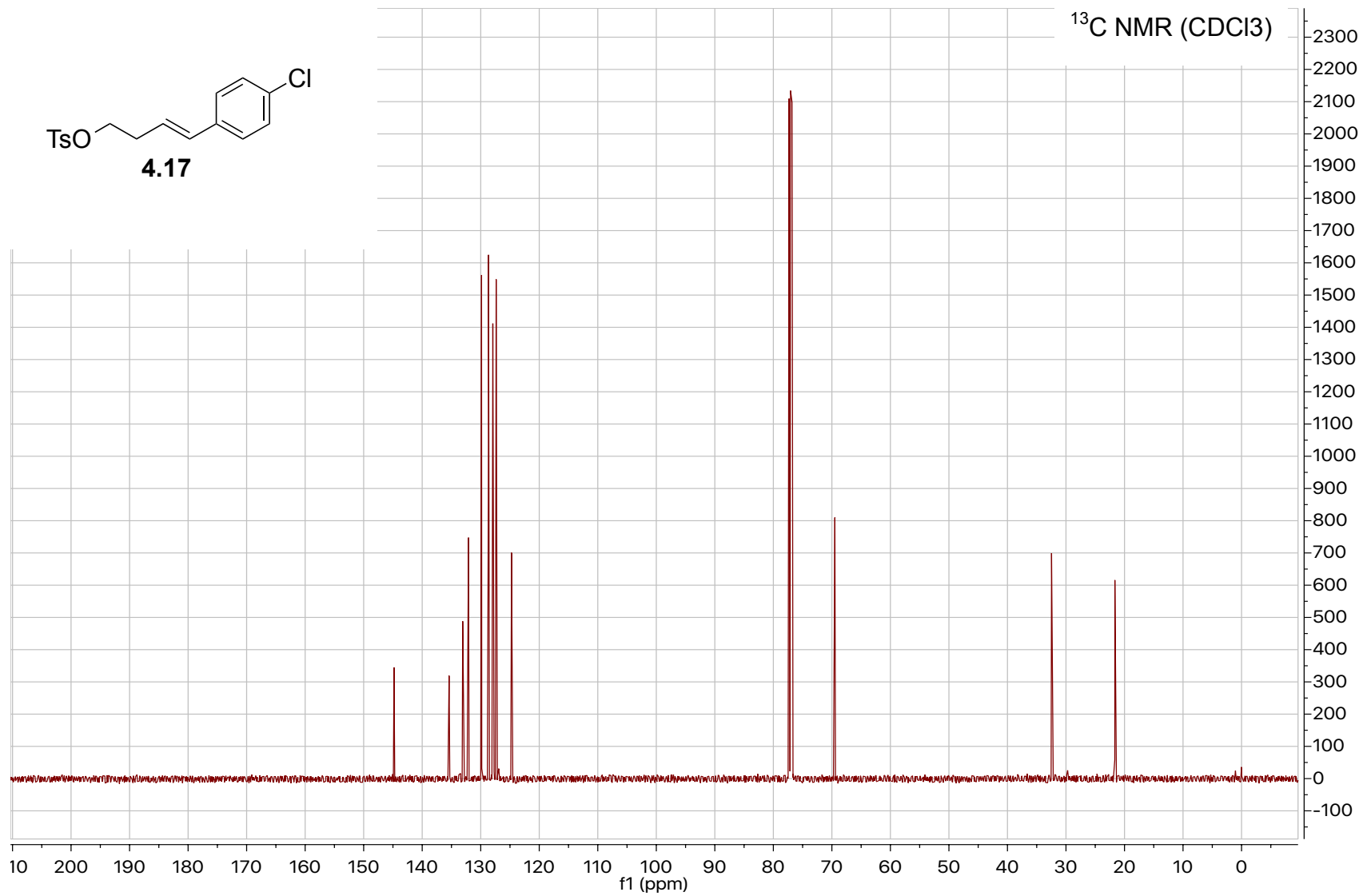
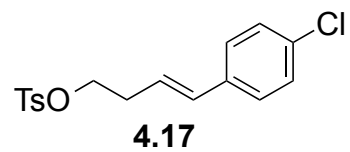
¹H NMR (CDCl₃)

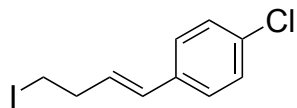






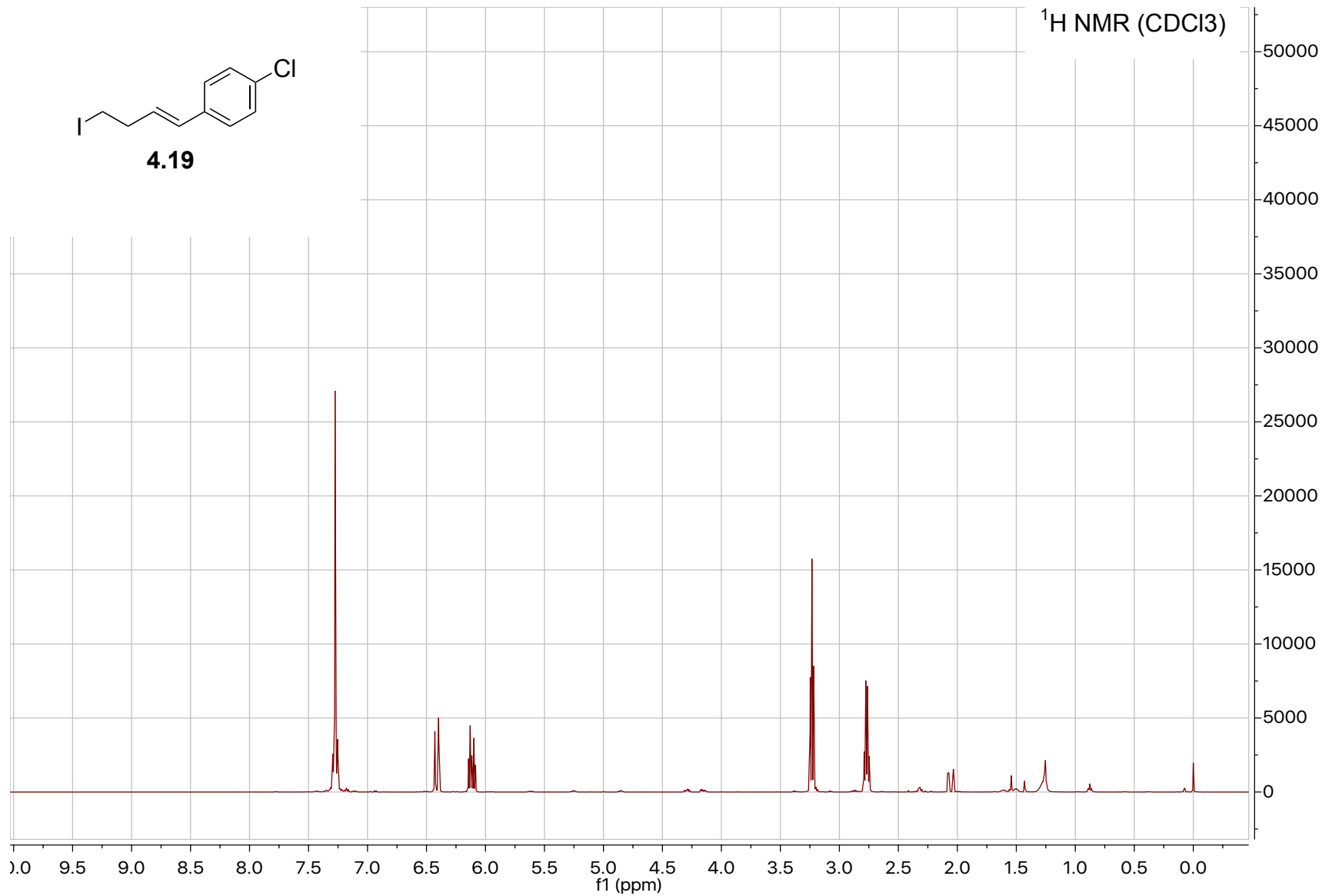


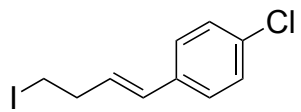




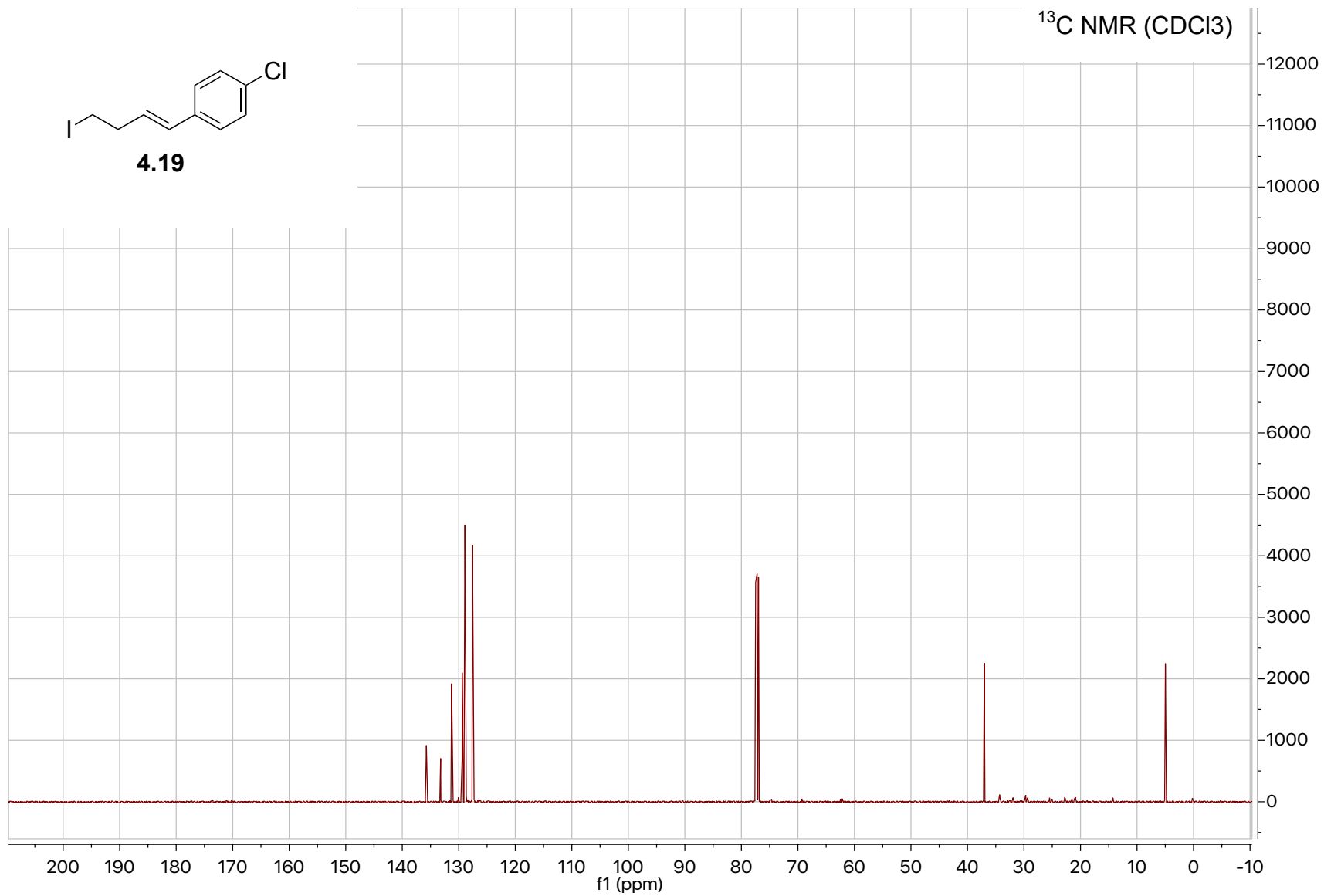
4.19

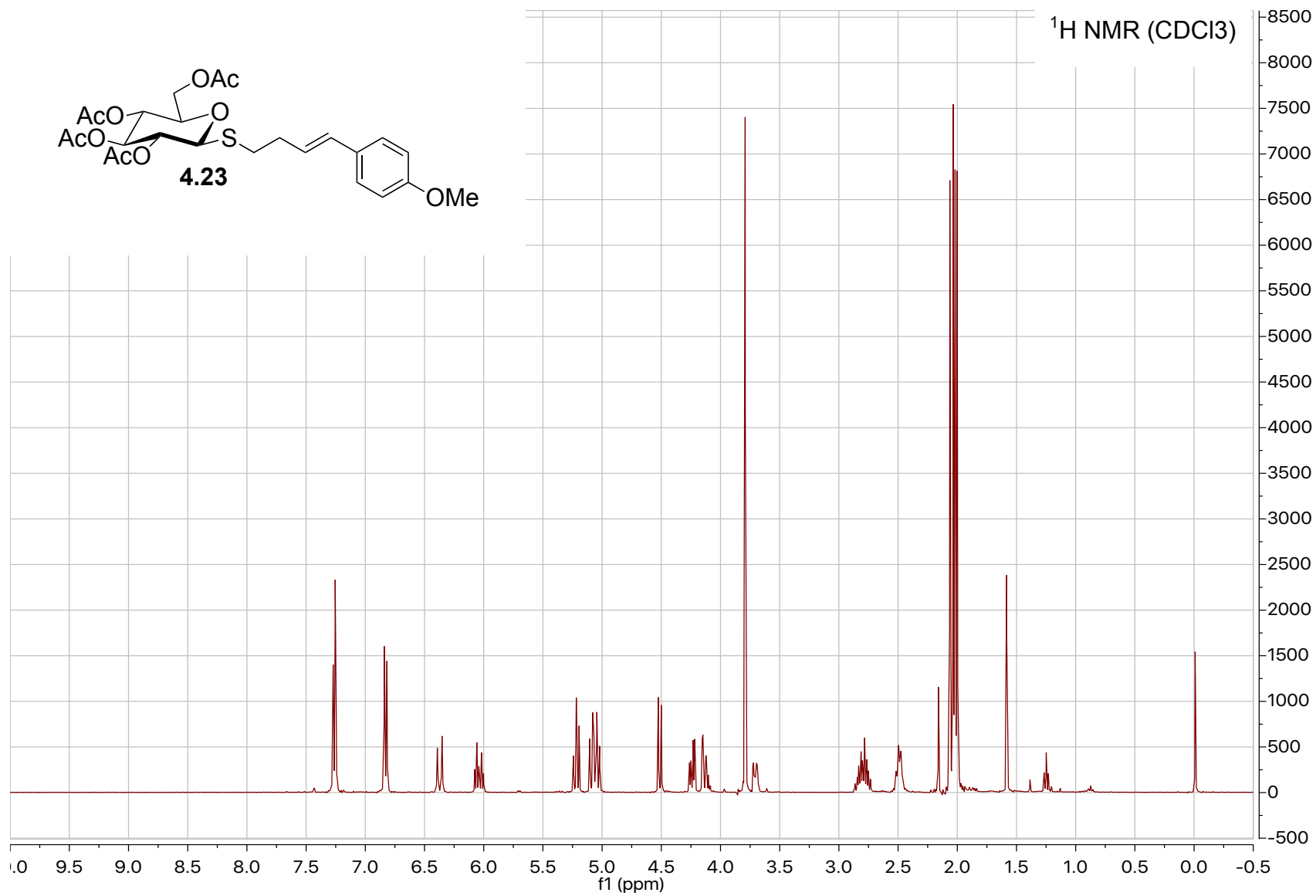
¹H NMR (CDCl₃)

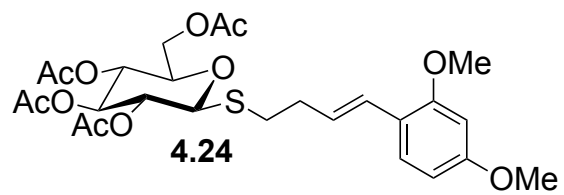




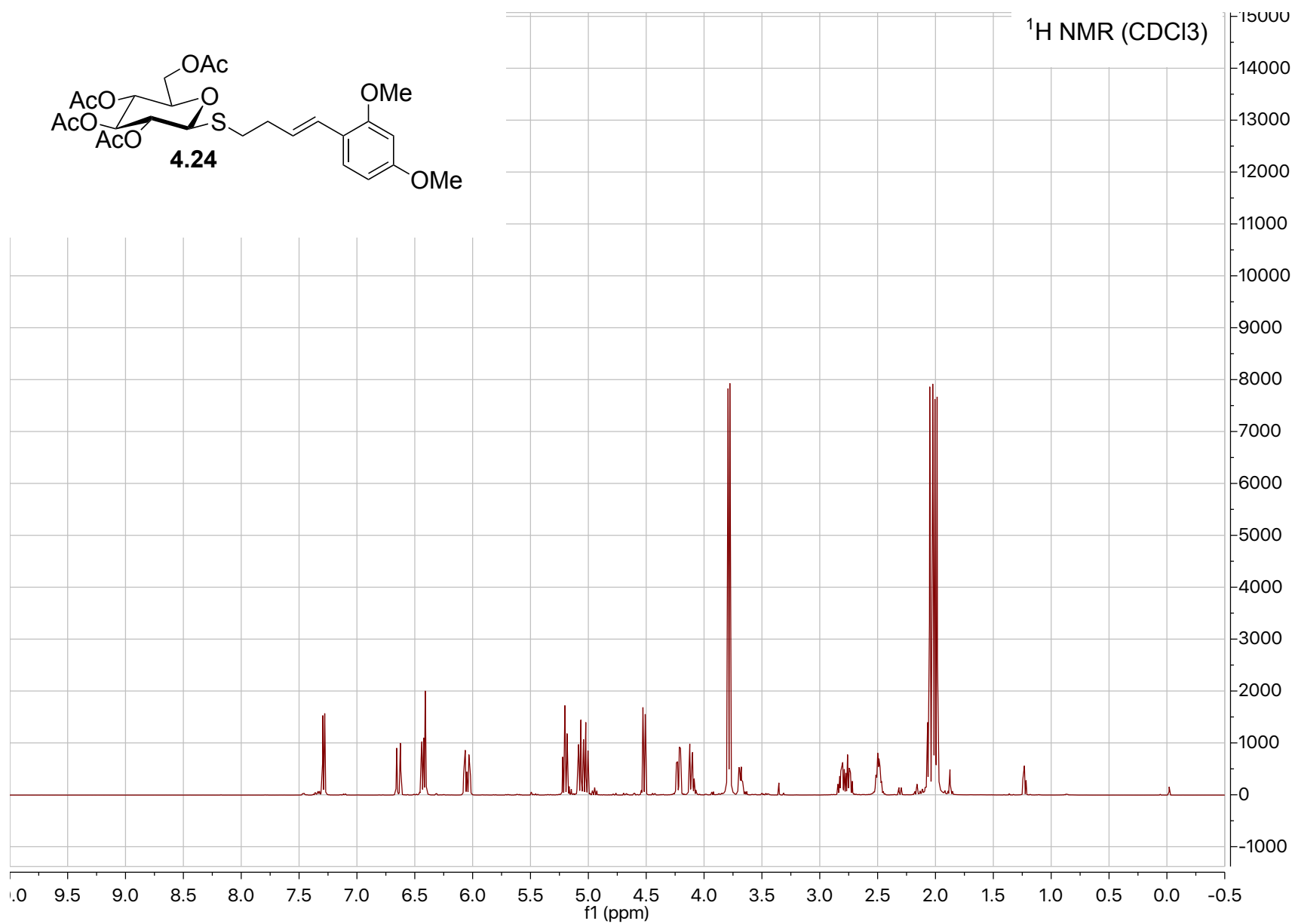
4.19

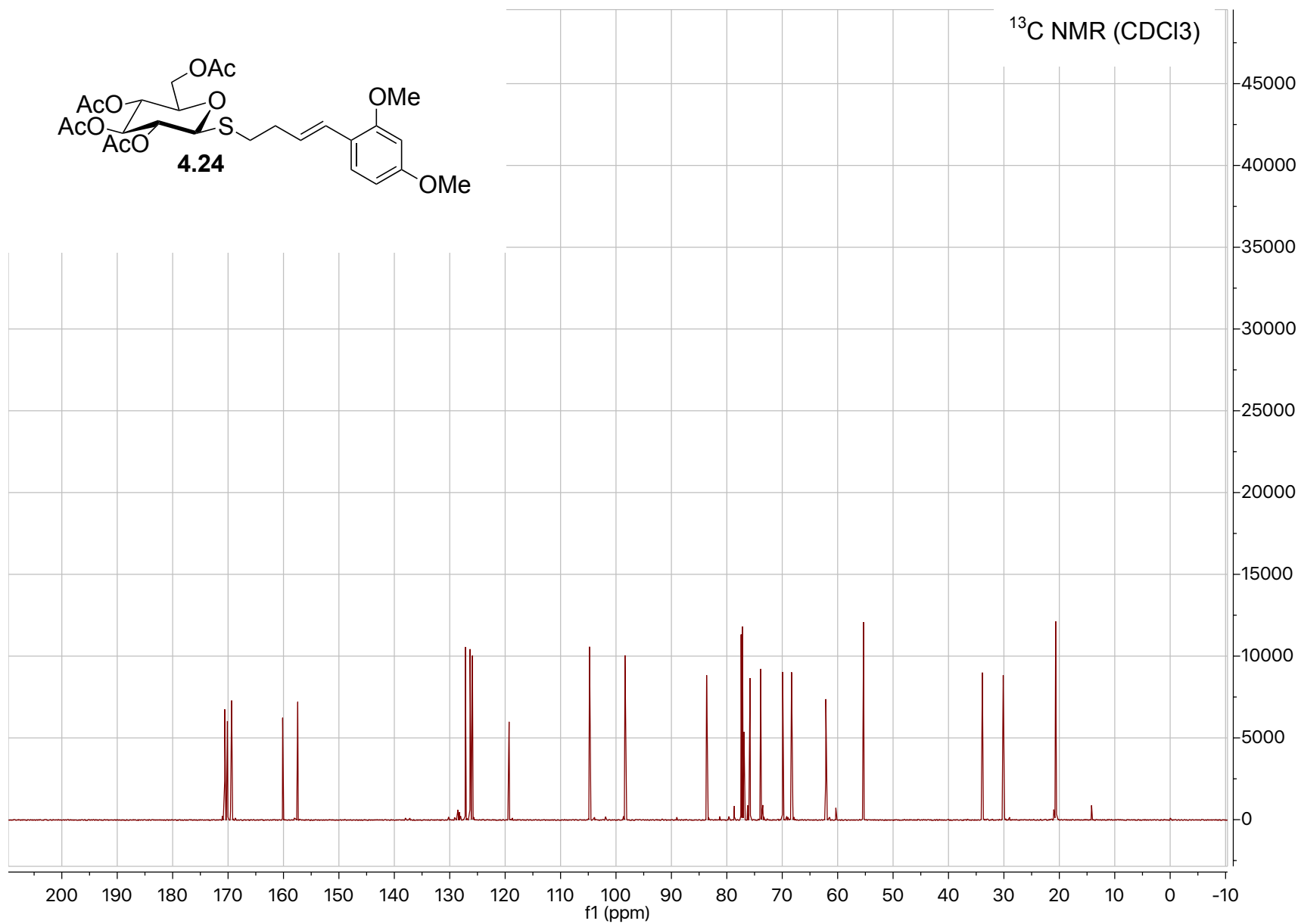
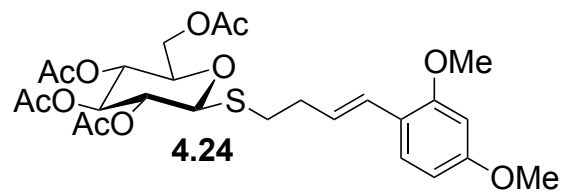


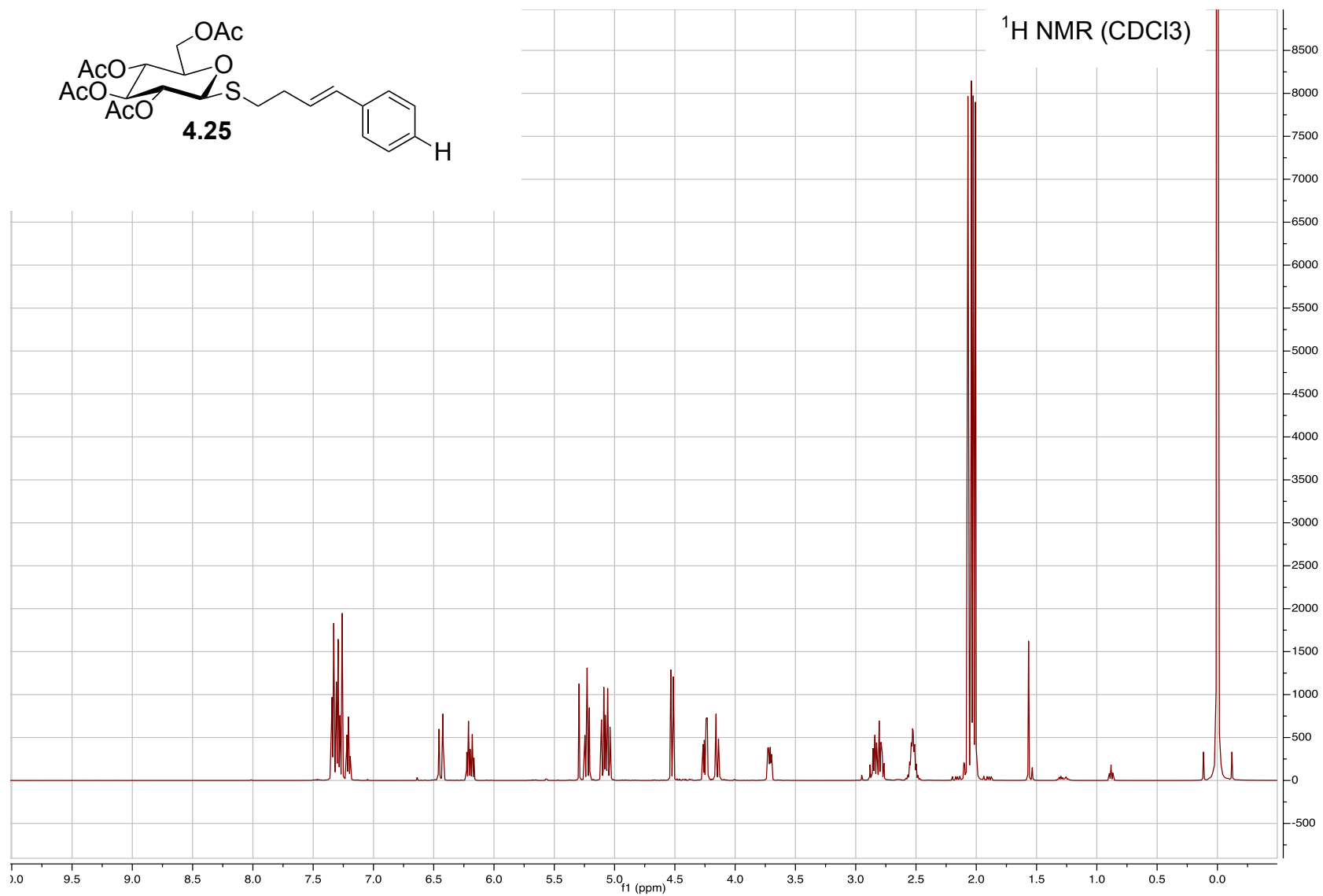
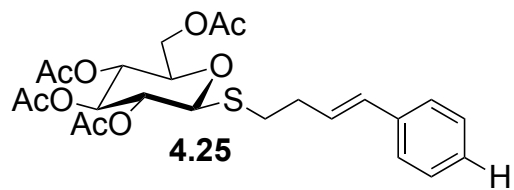


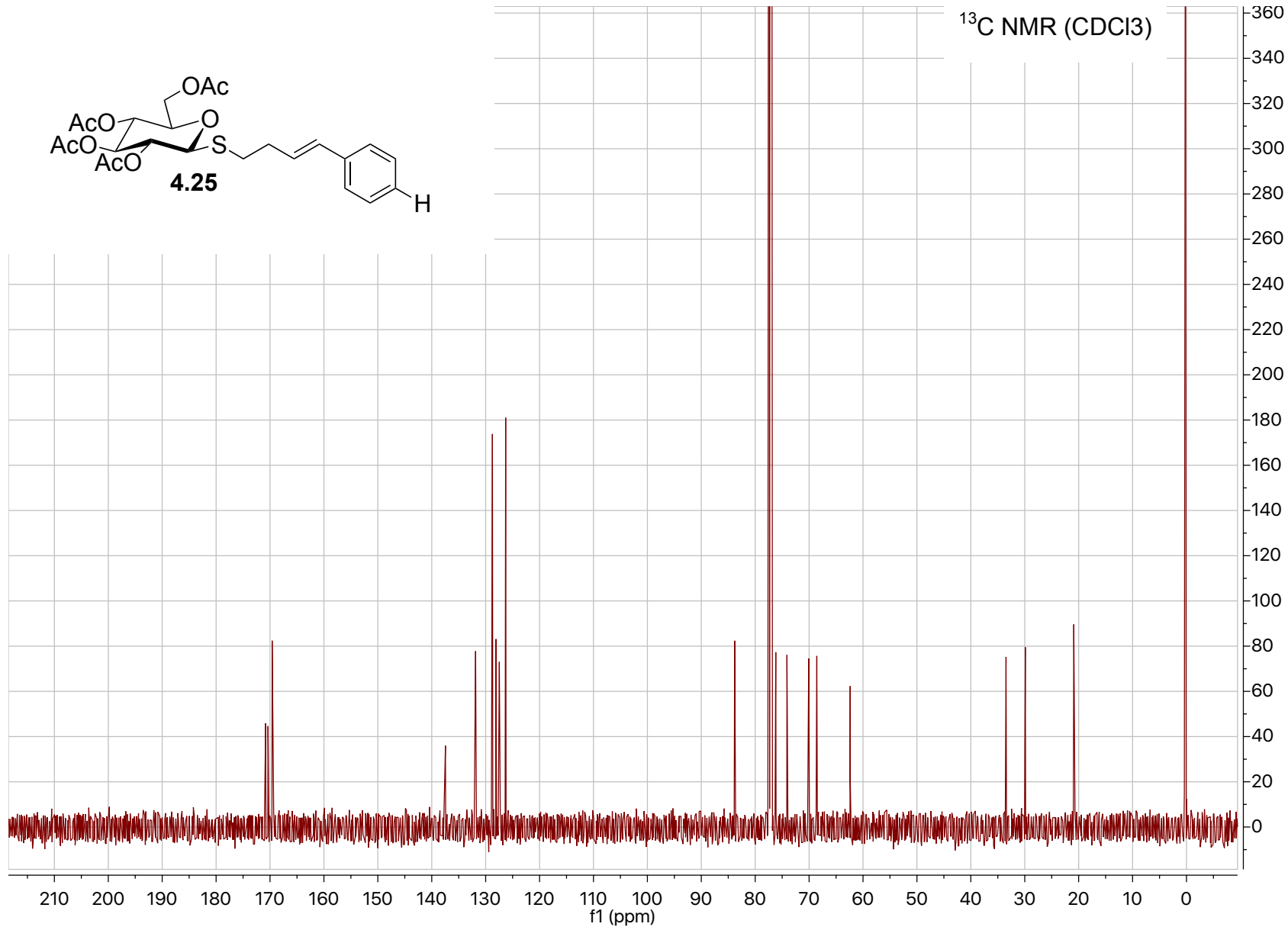
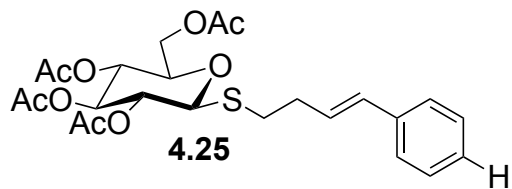


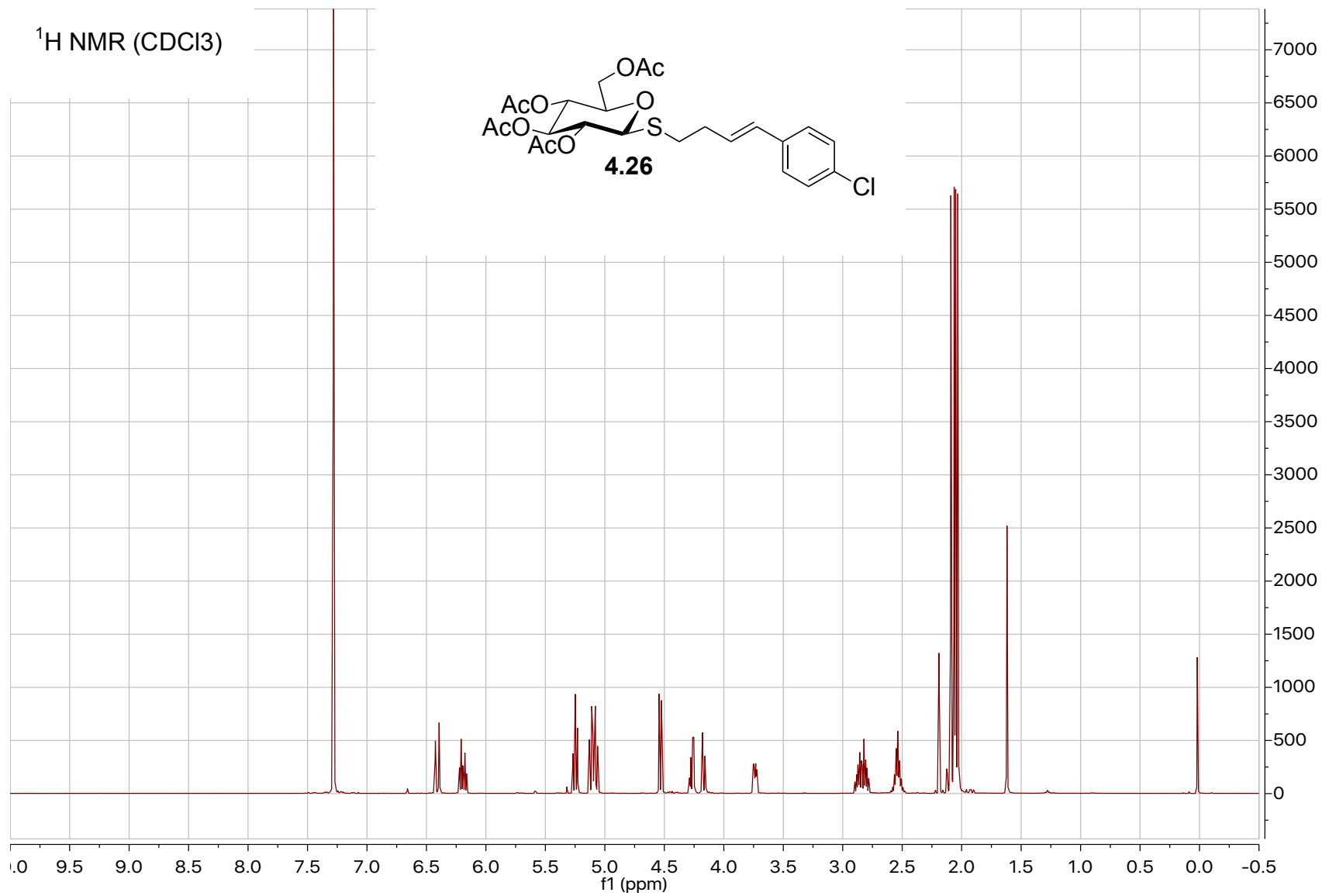
¹H NMR (CDCl₃)

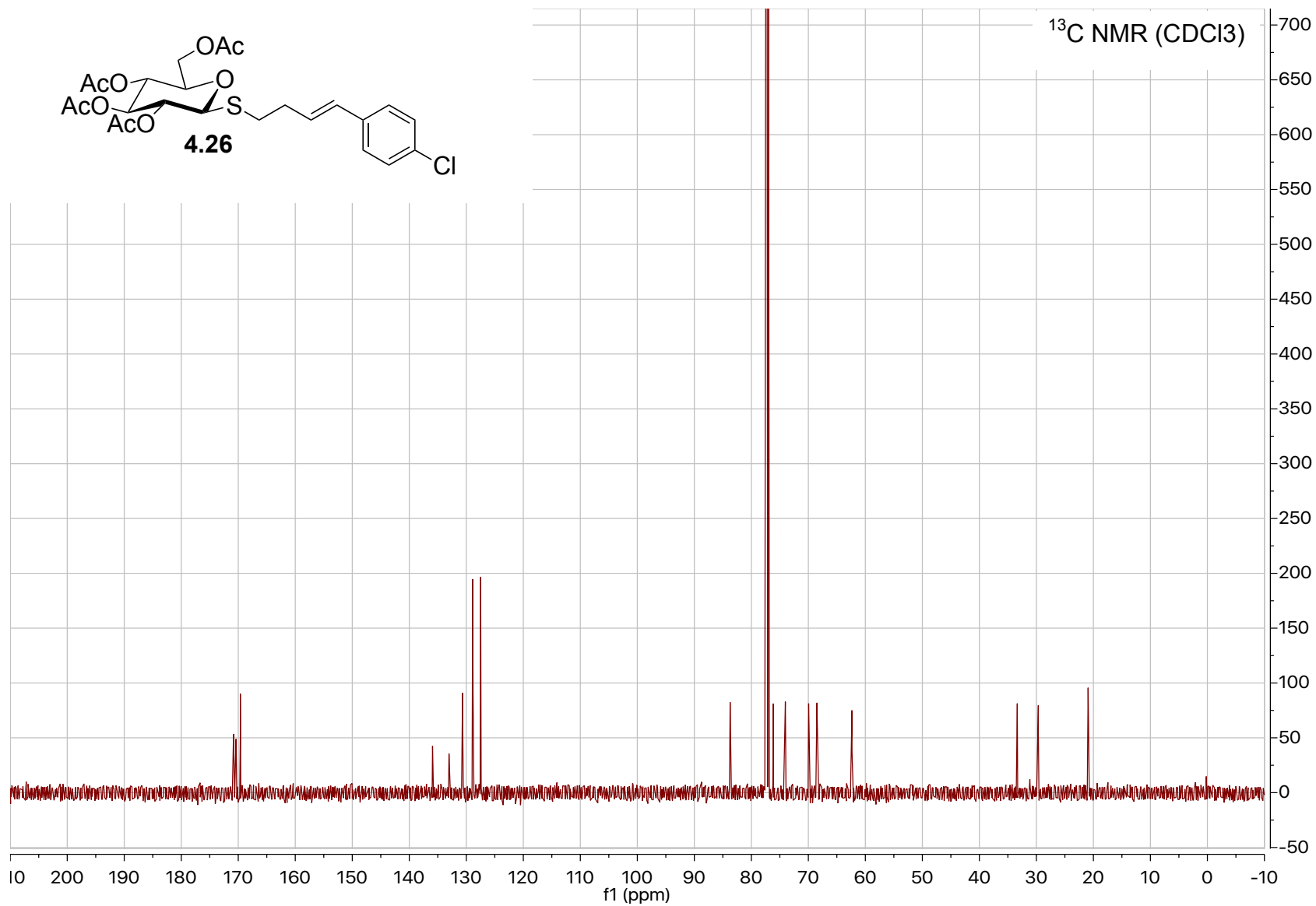
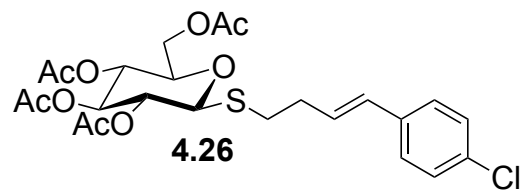


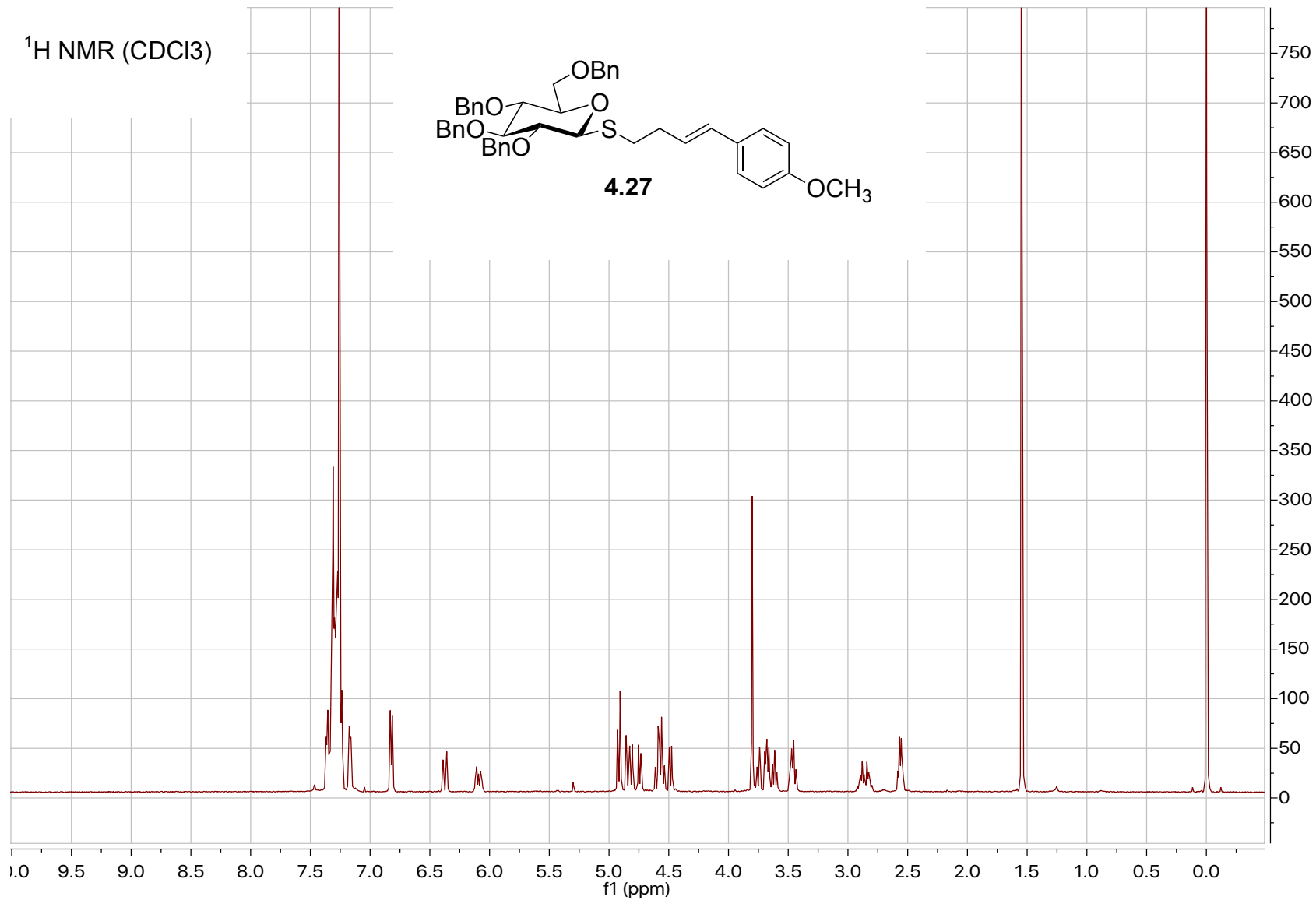


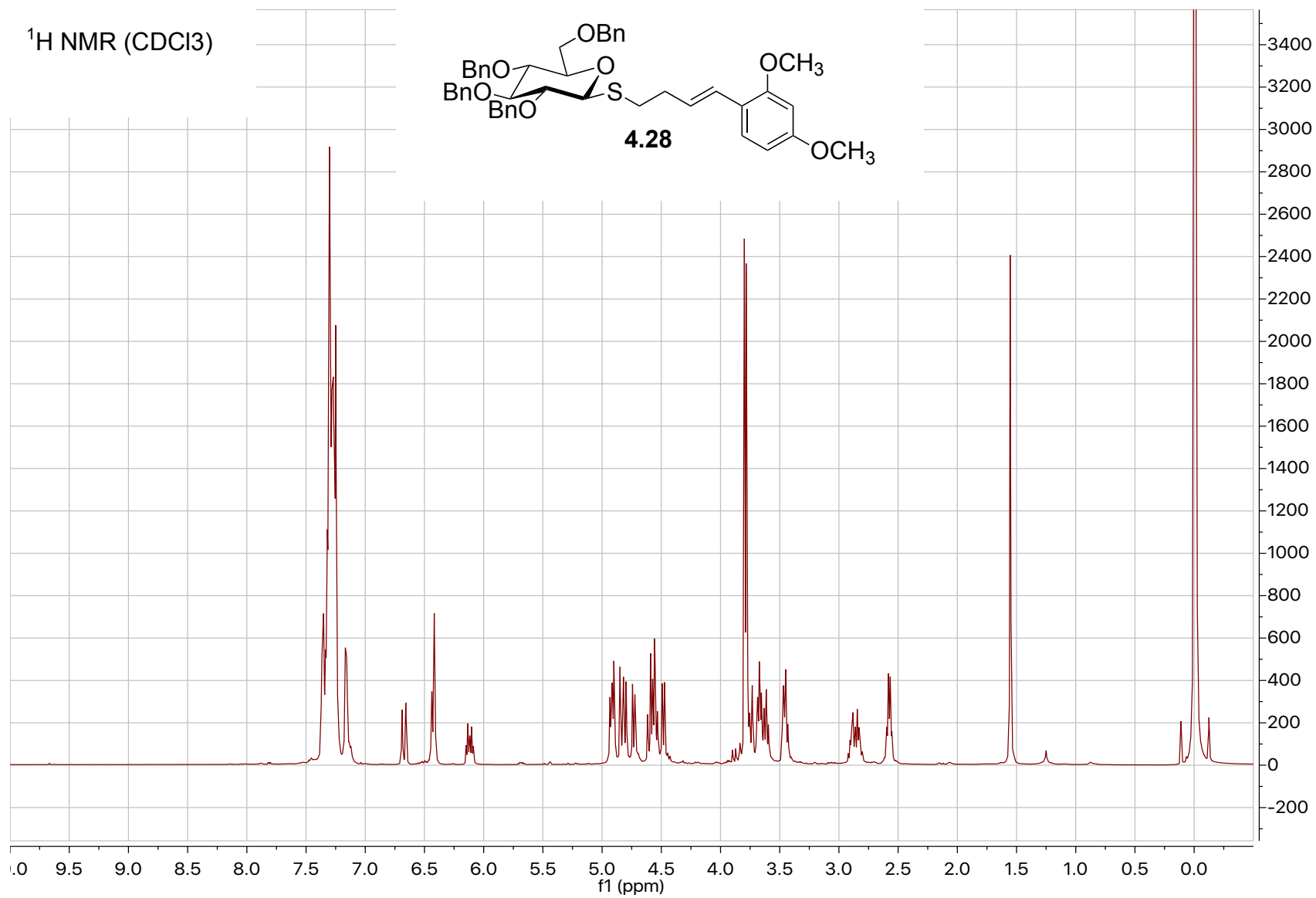


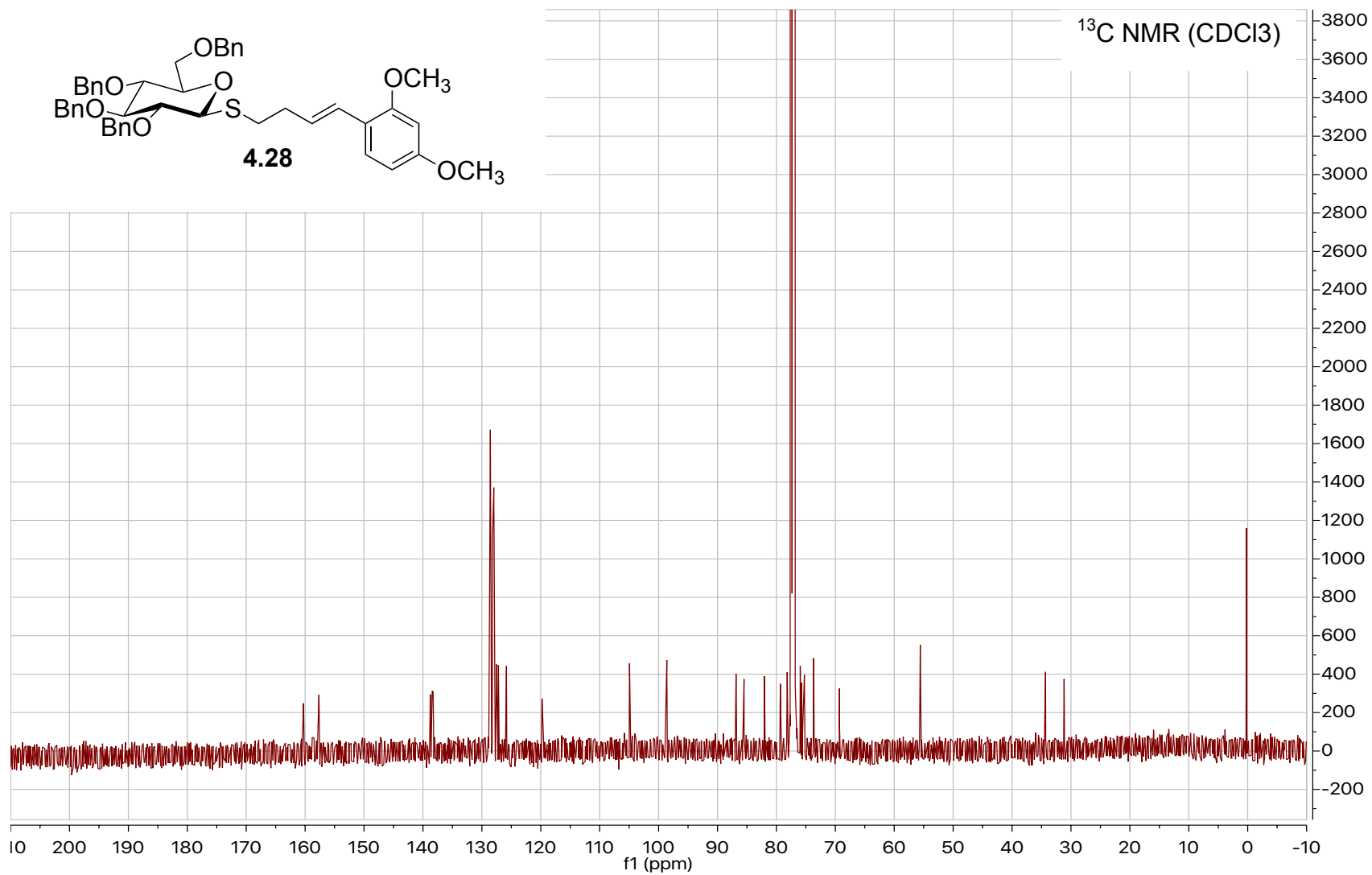
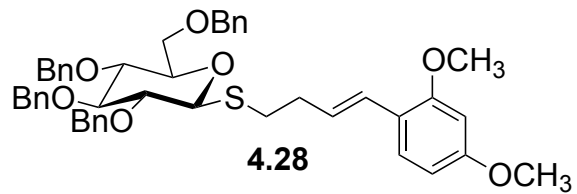


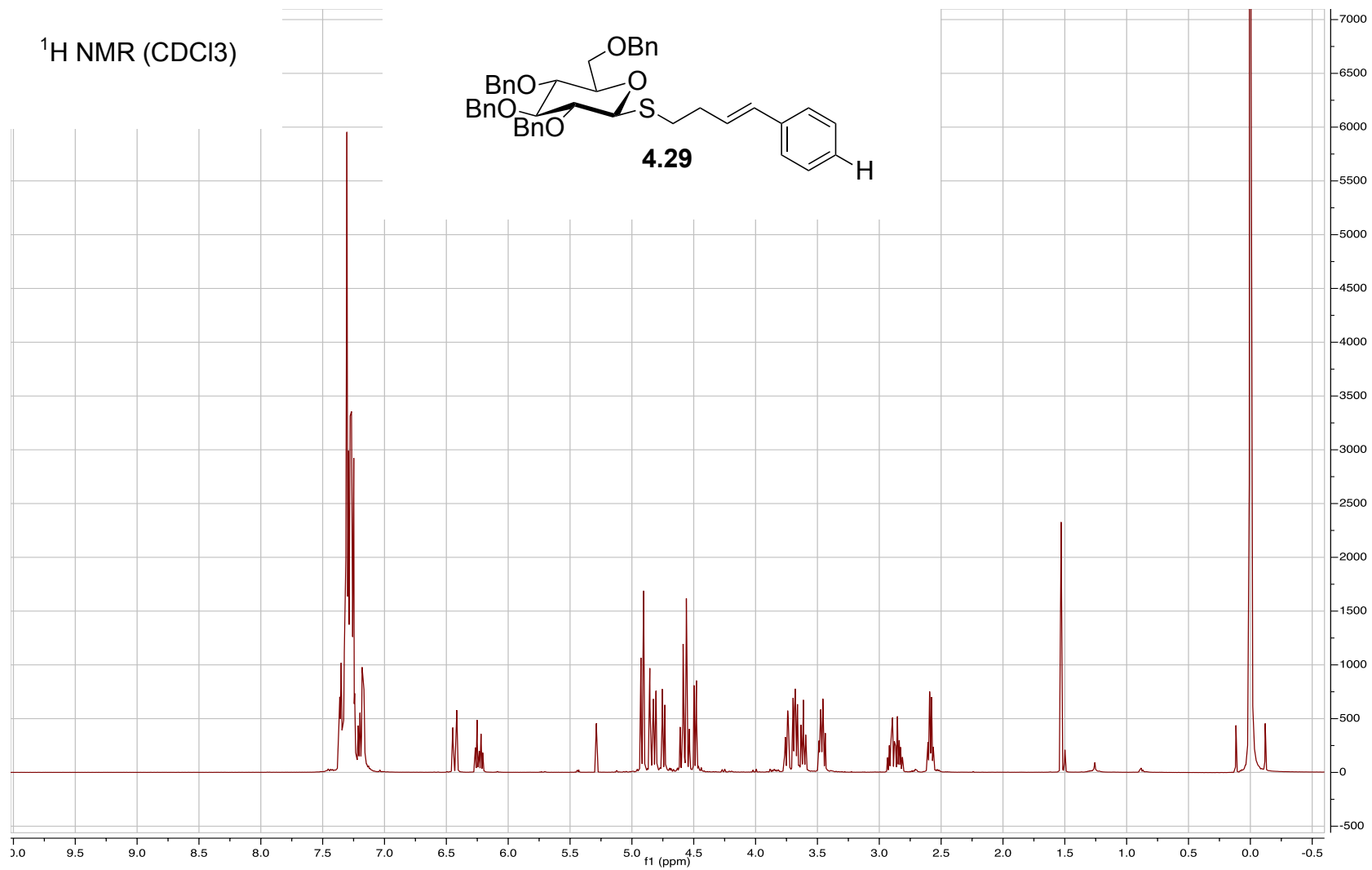


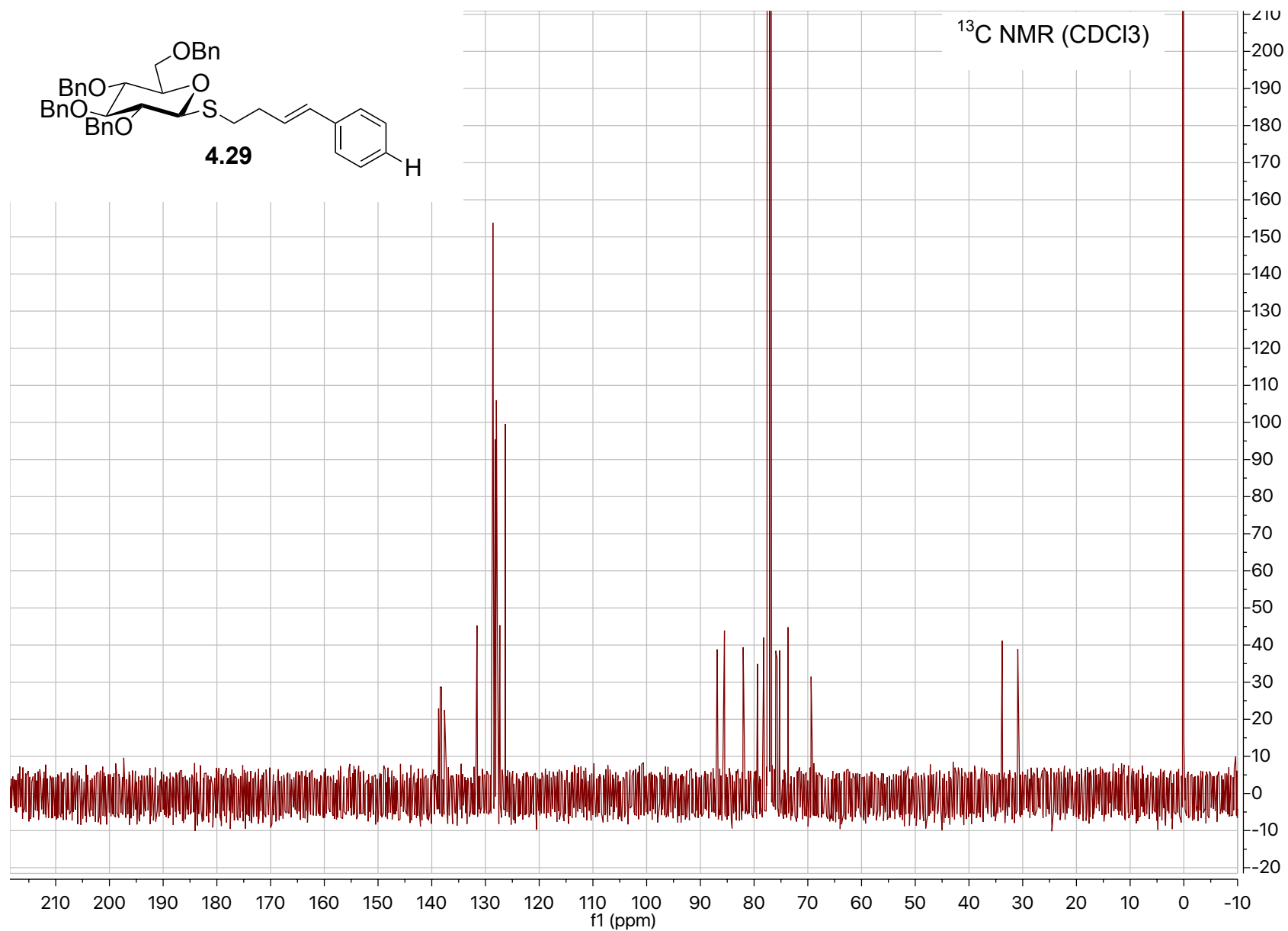
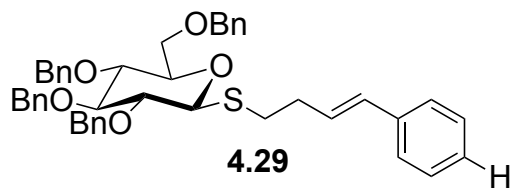




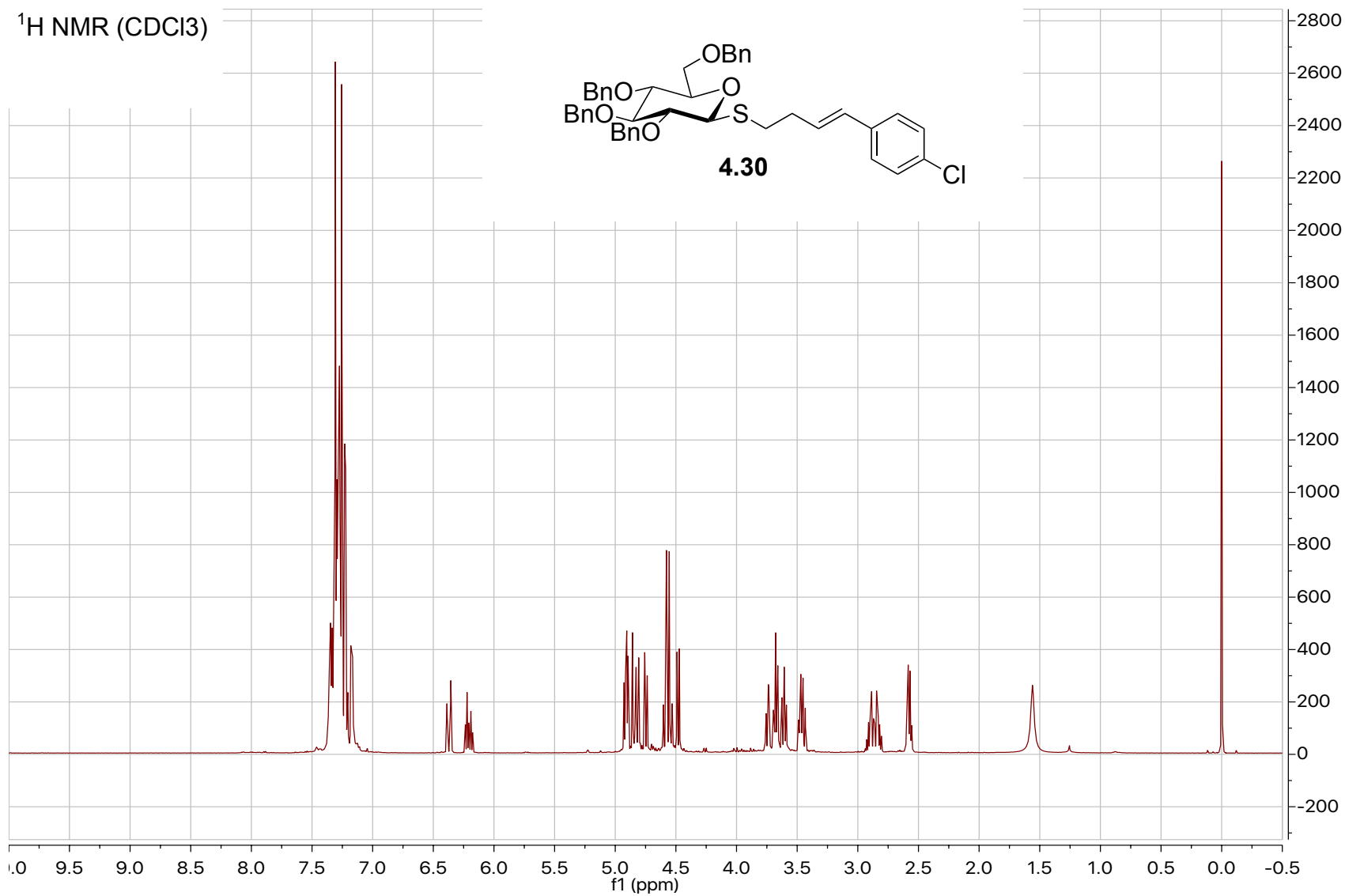


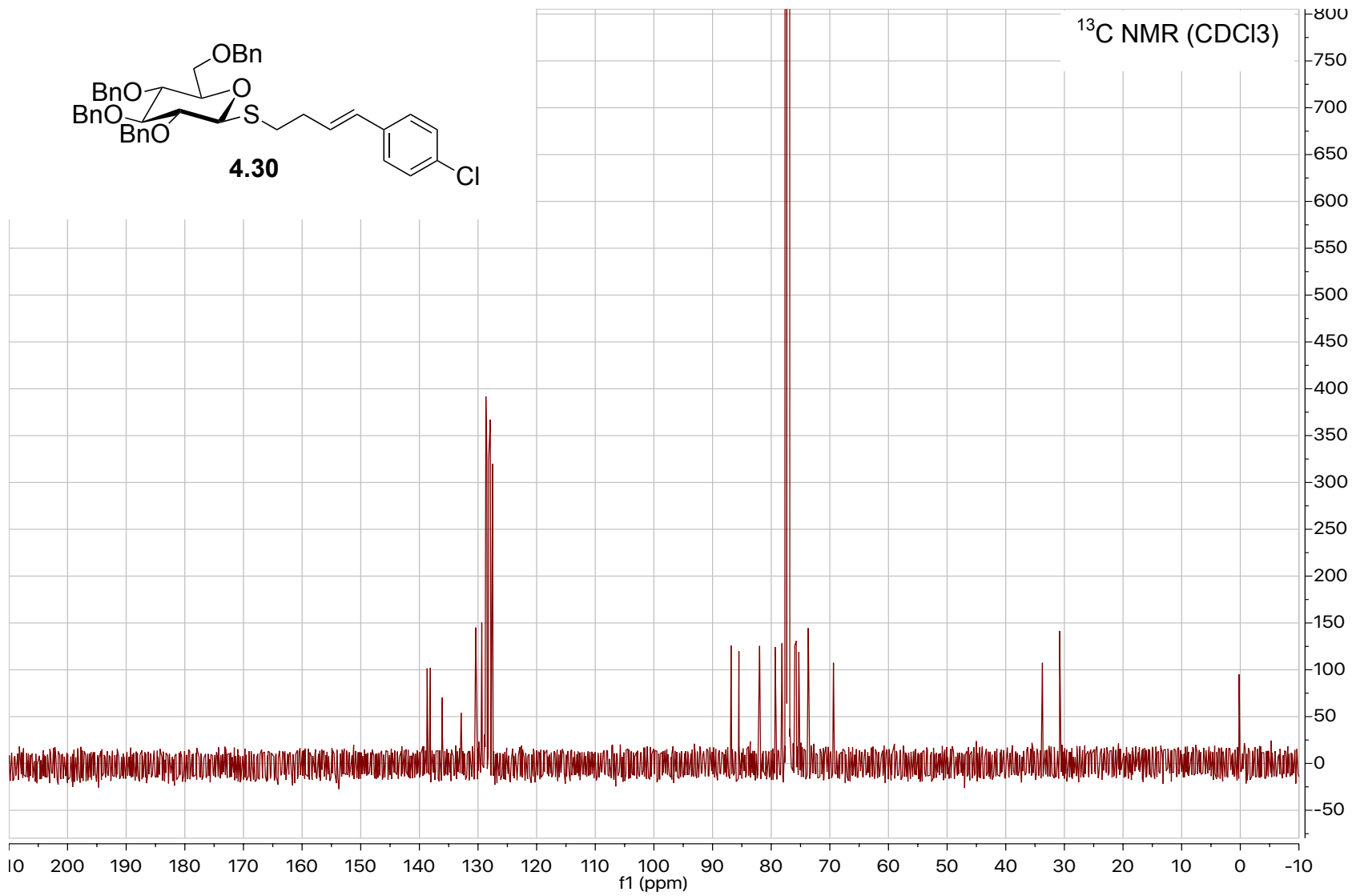
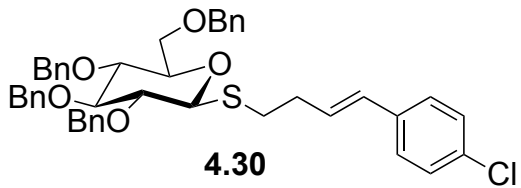


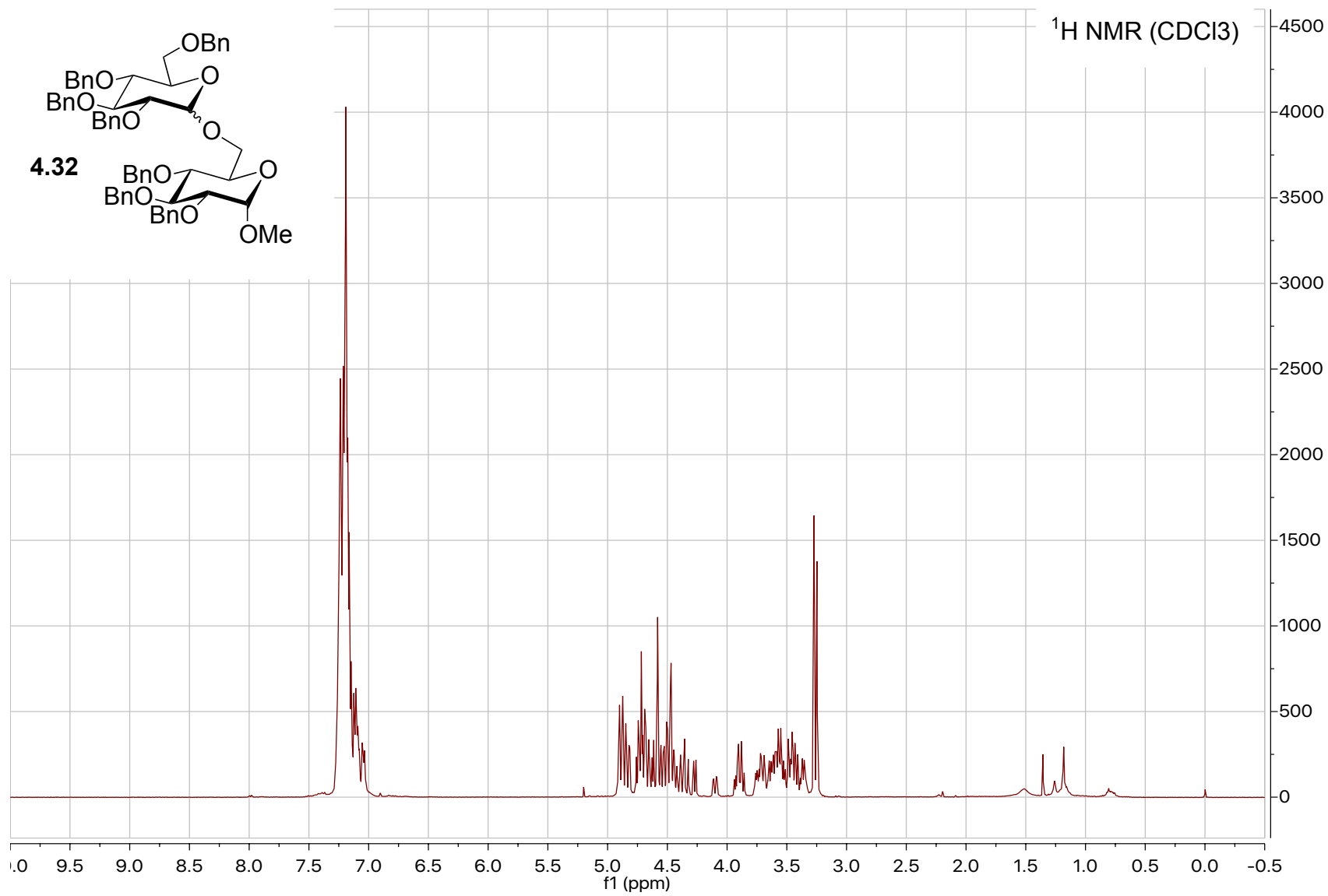




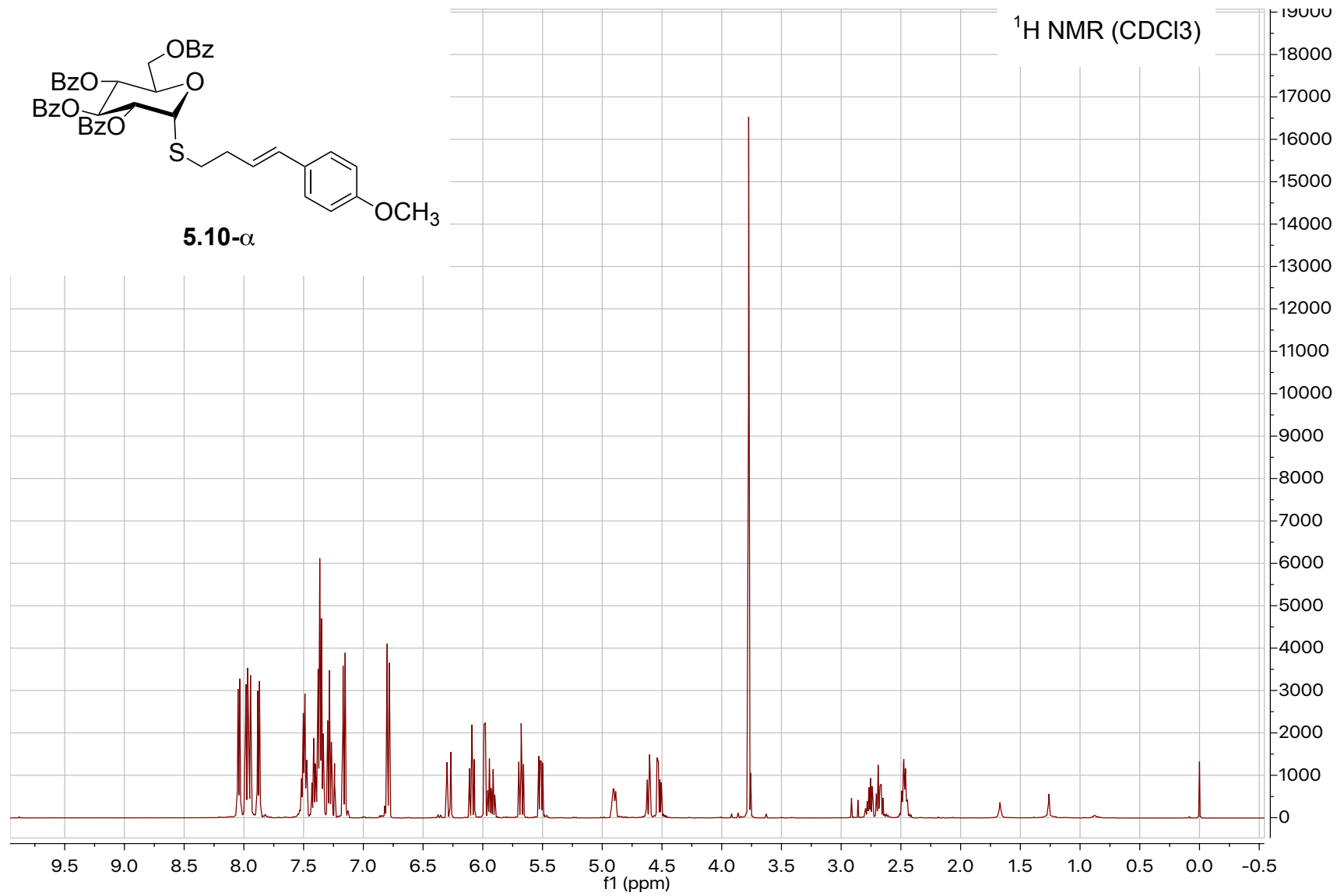
¹H NMR (CDCl₃)

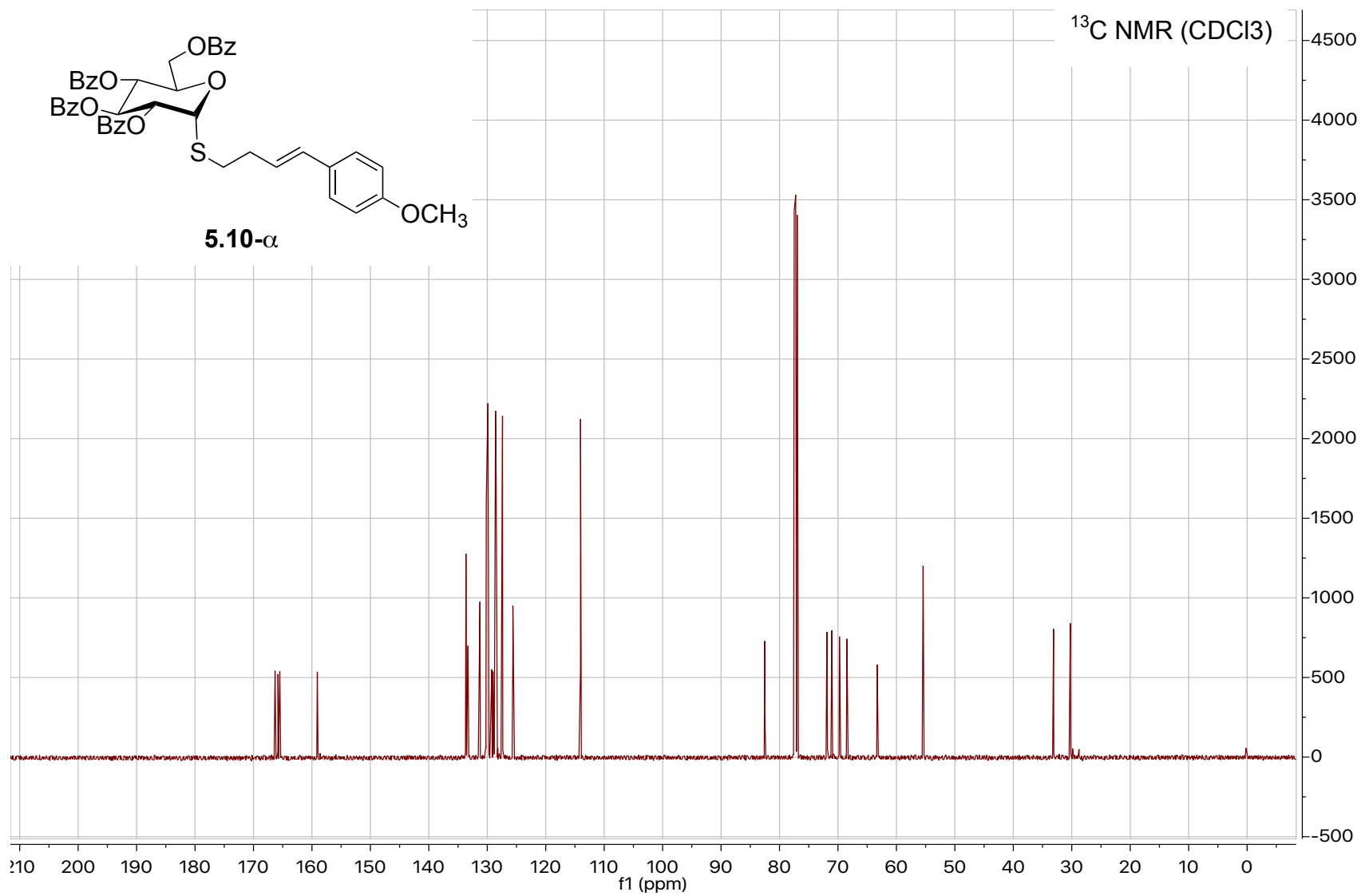


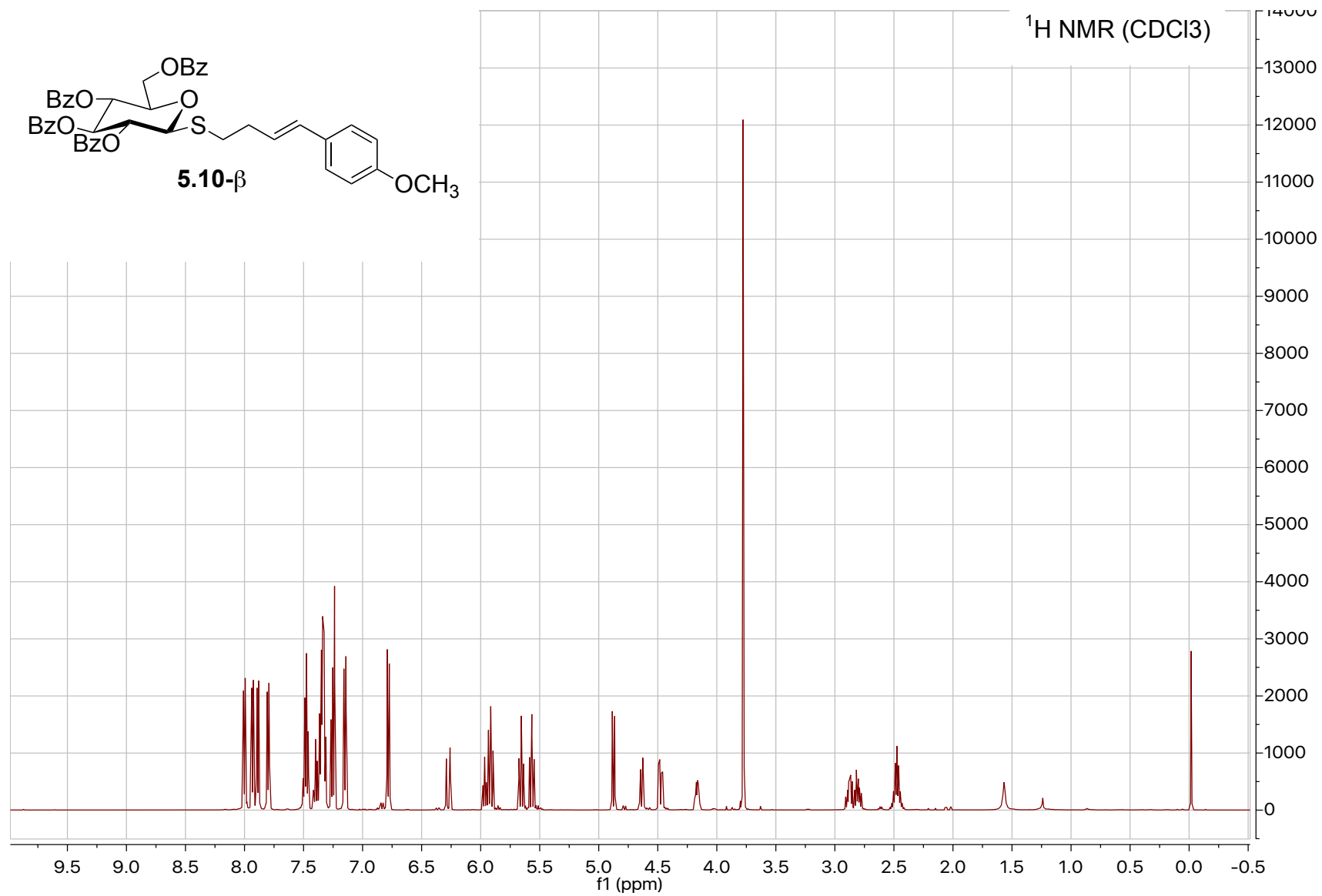


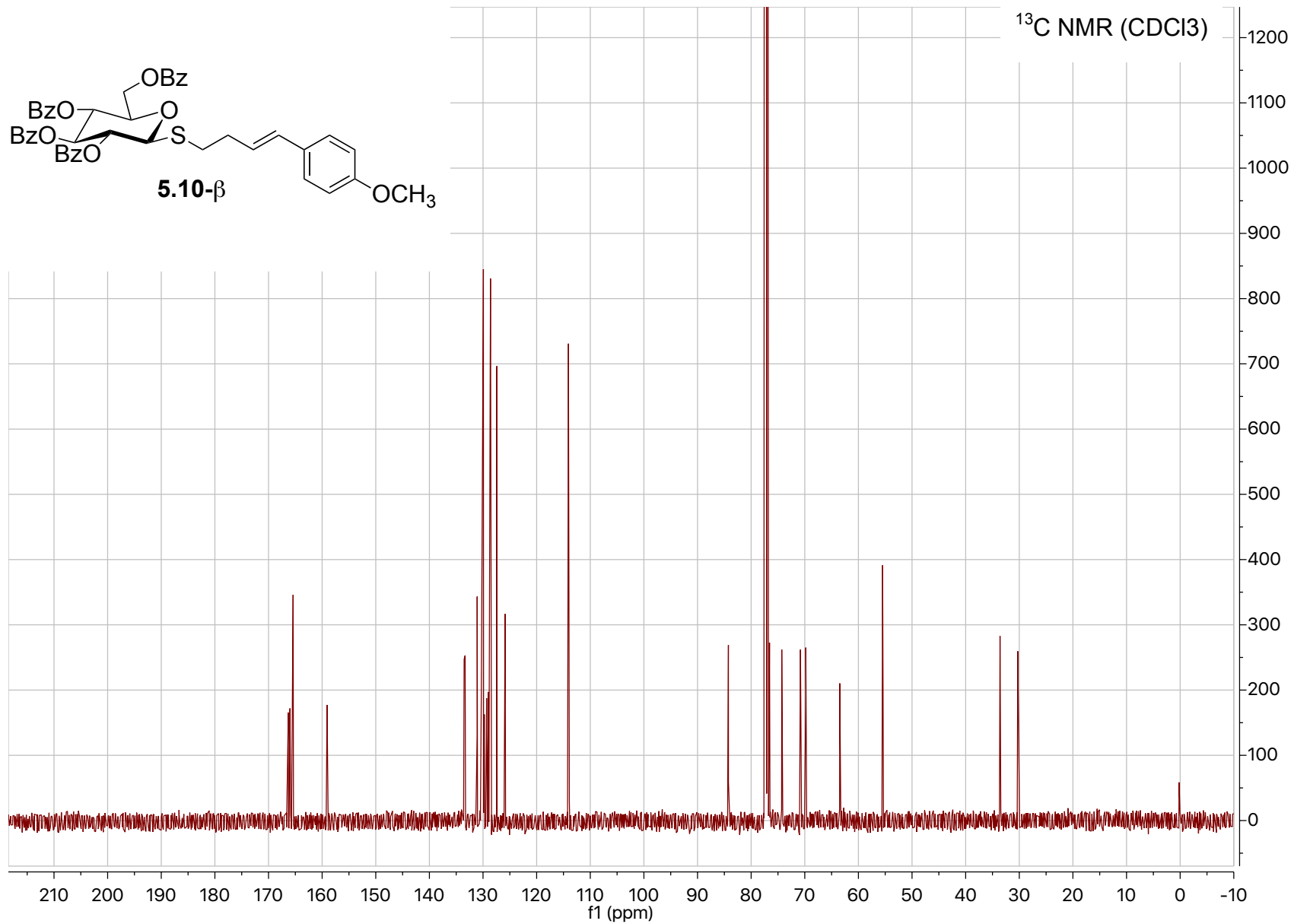


APPENDIX D: NMR SPECTRA OF COMPOUNDS FOUND IN CHAPTER 5

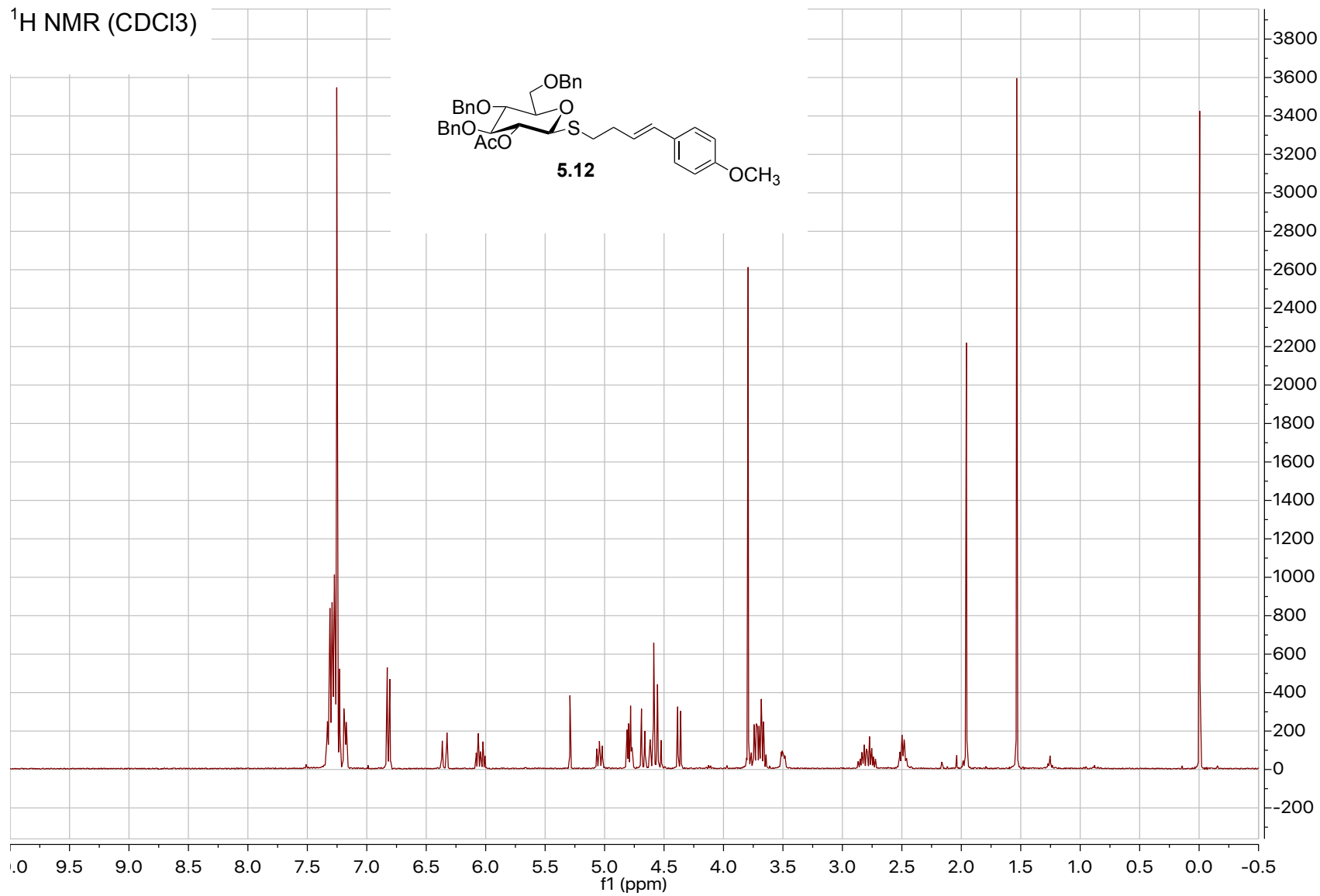


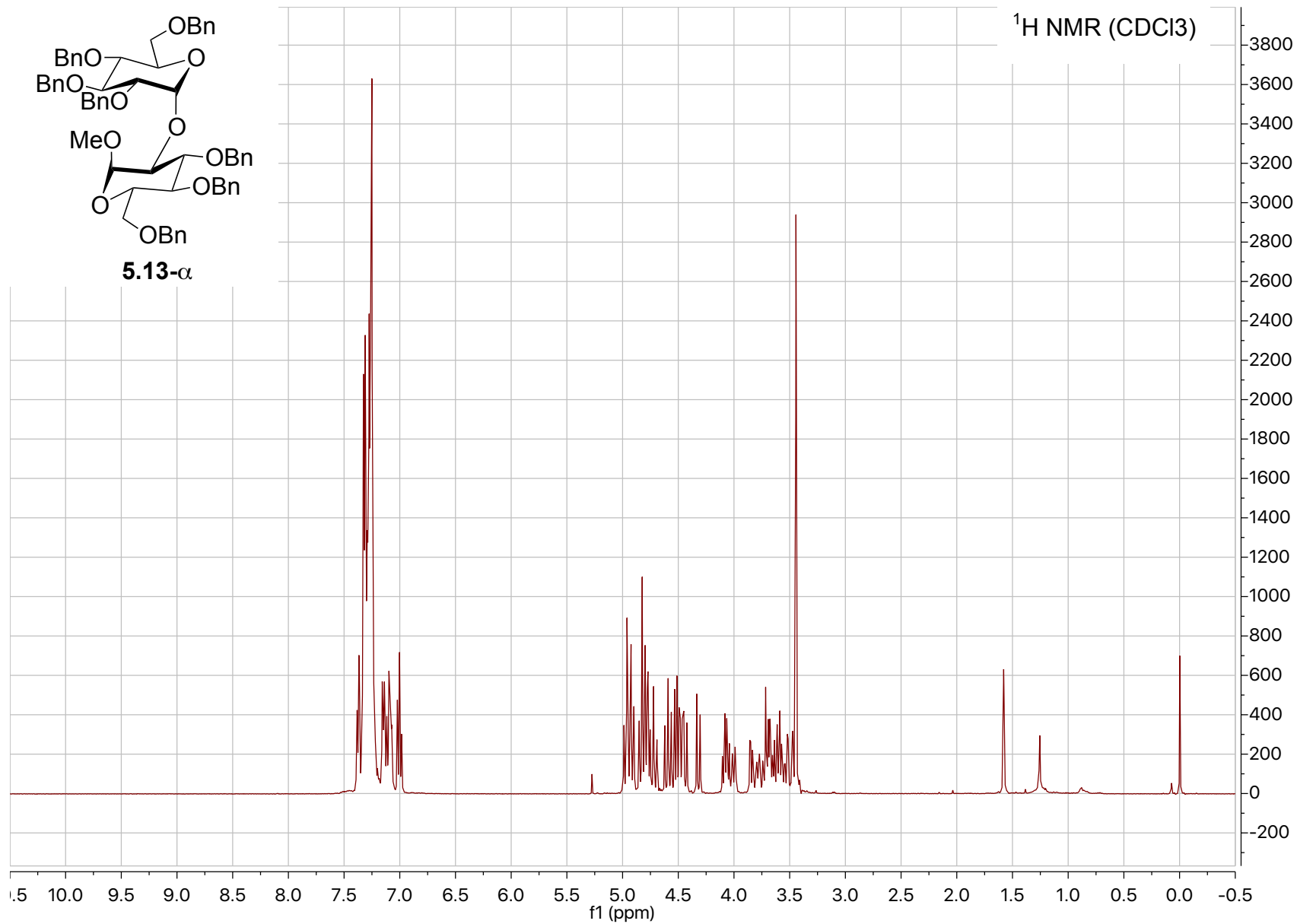


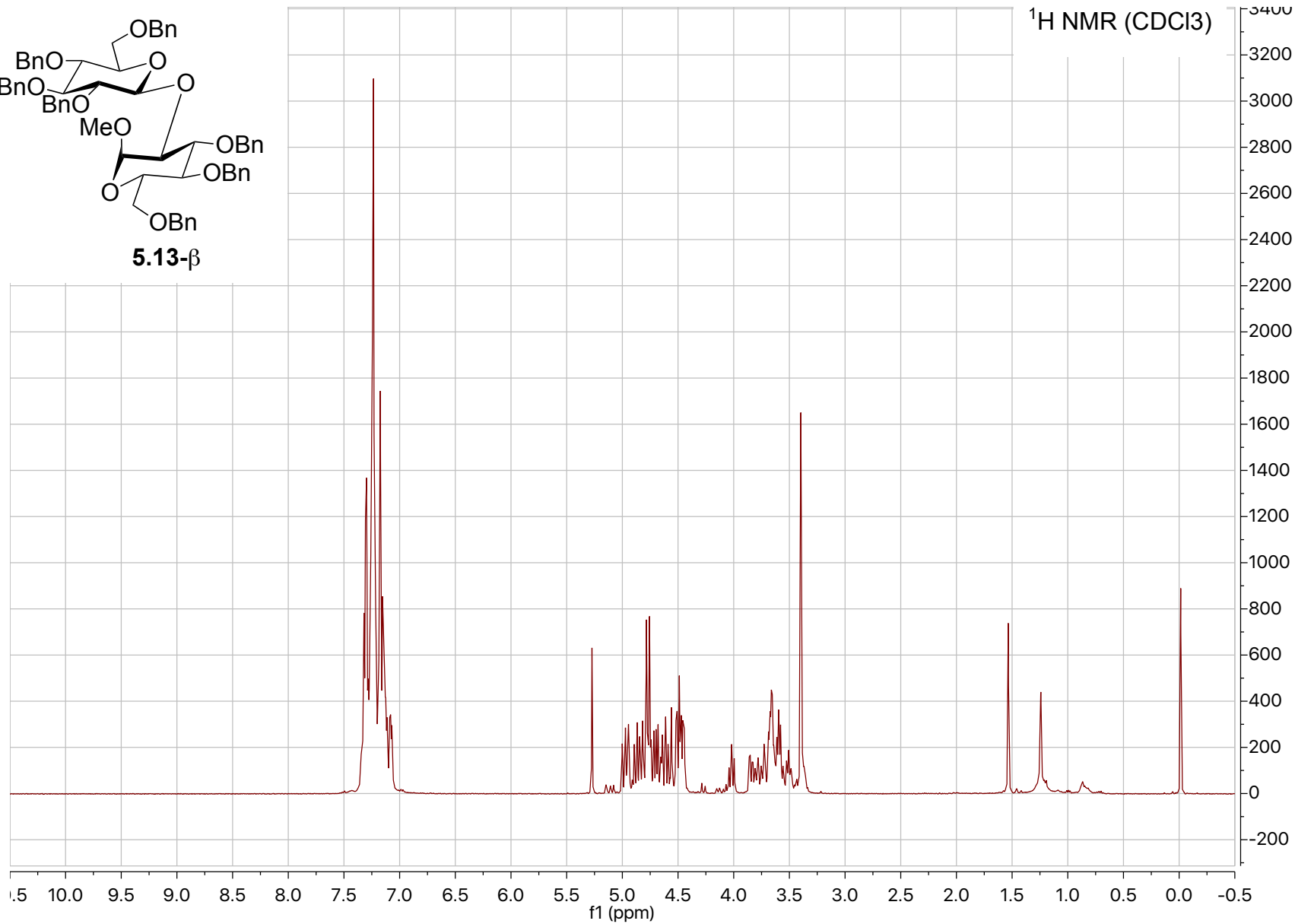
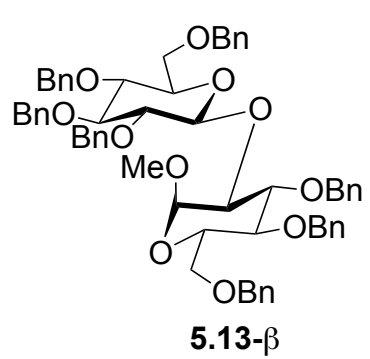




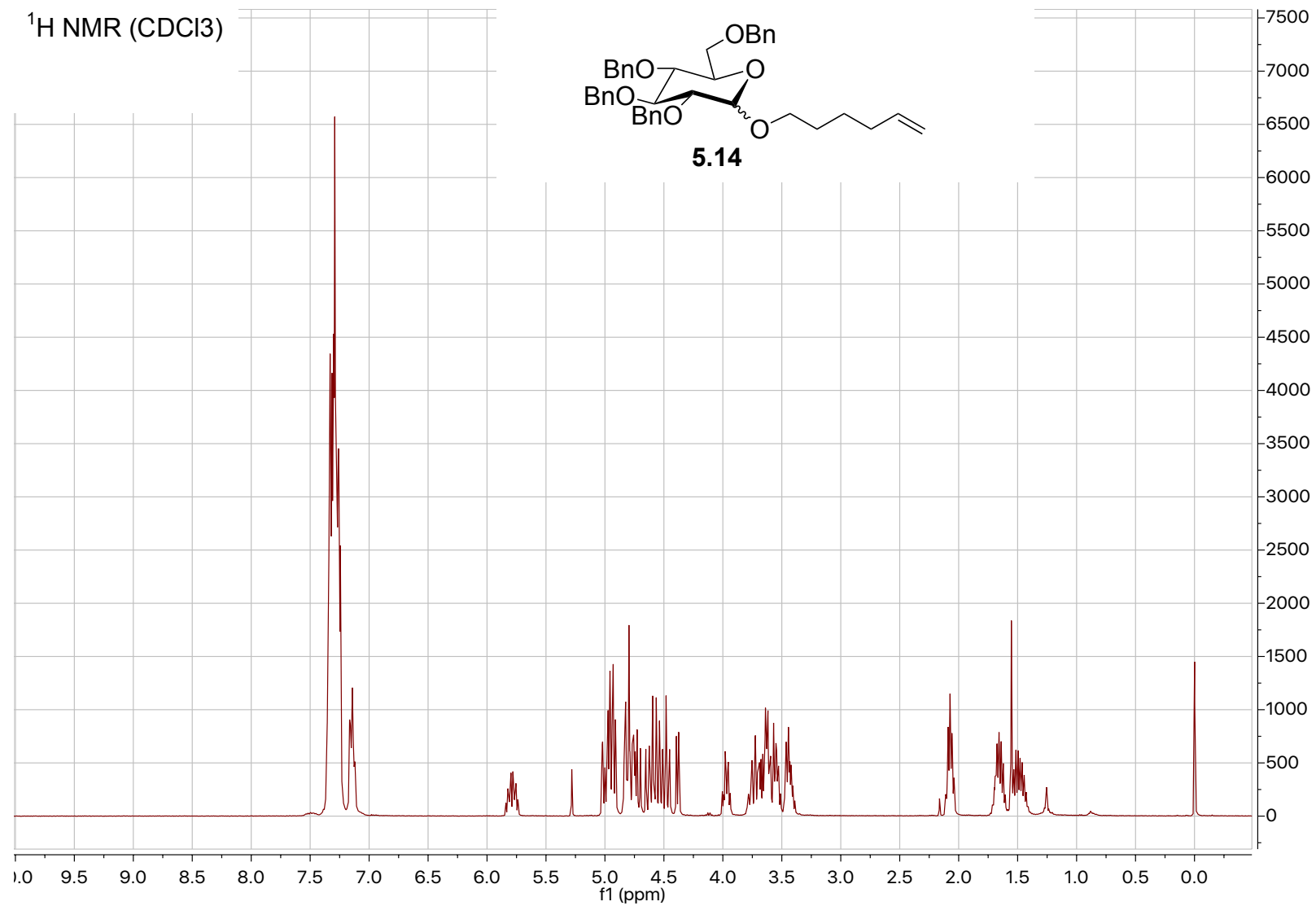
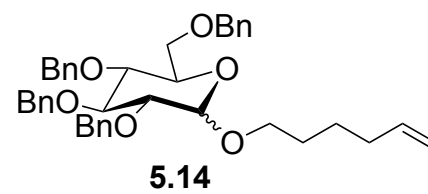
¹H NMR (CDCl₃)

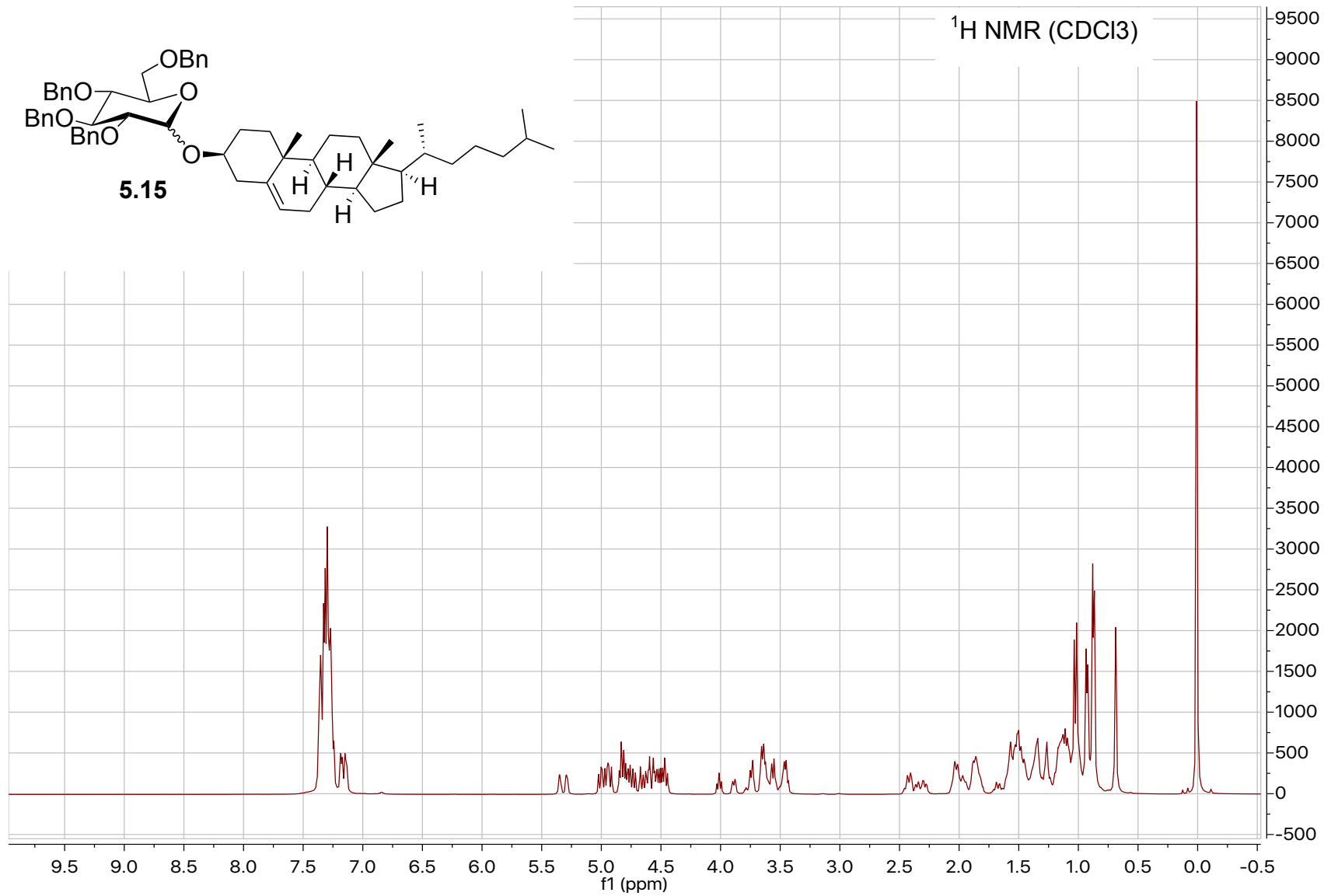


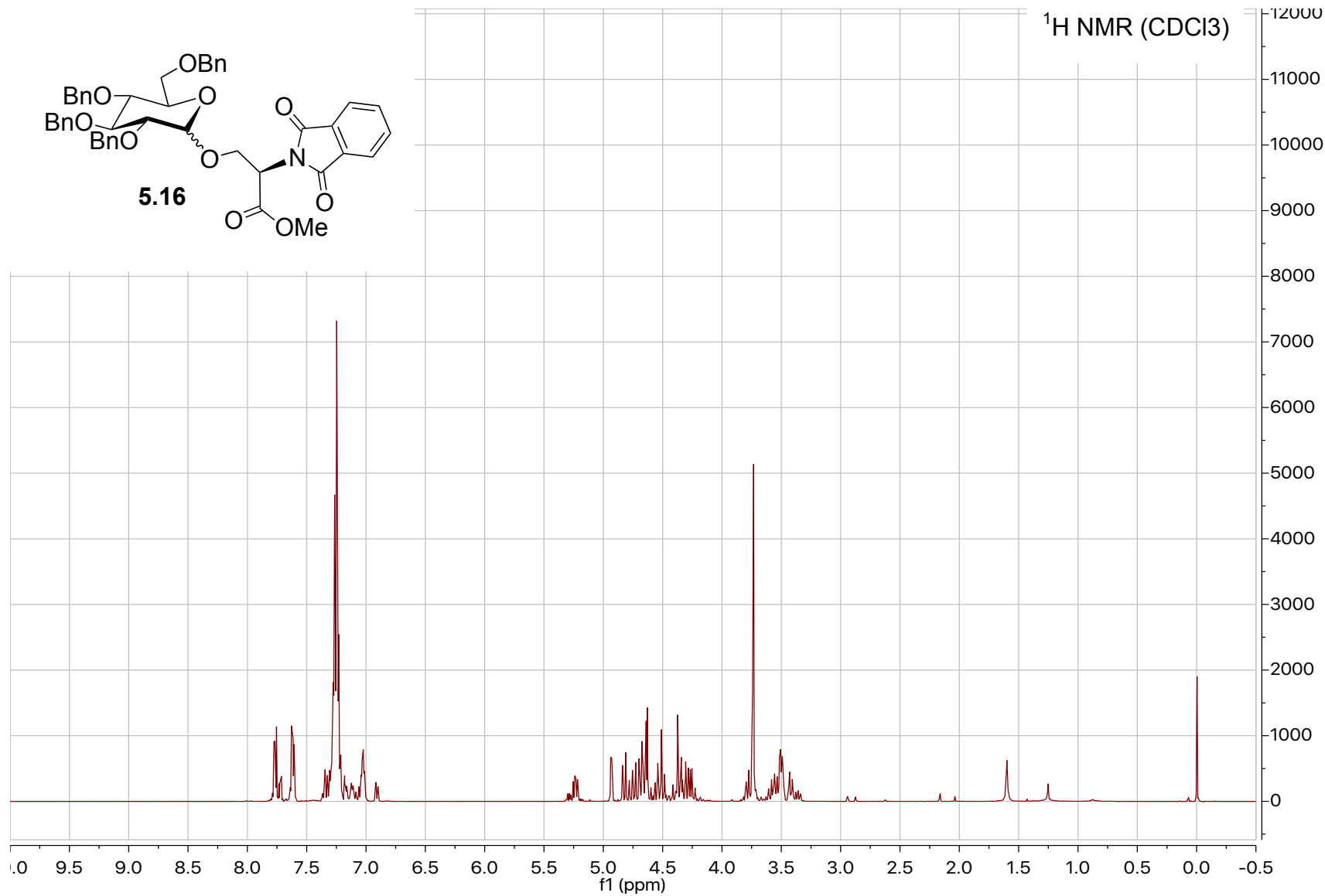
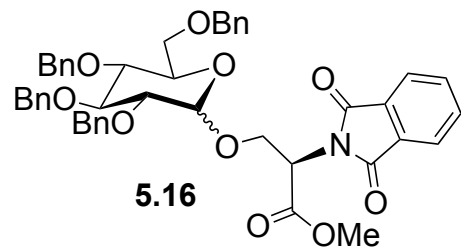


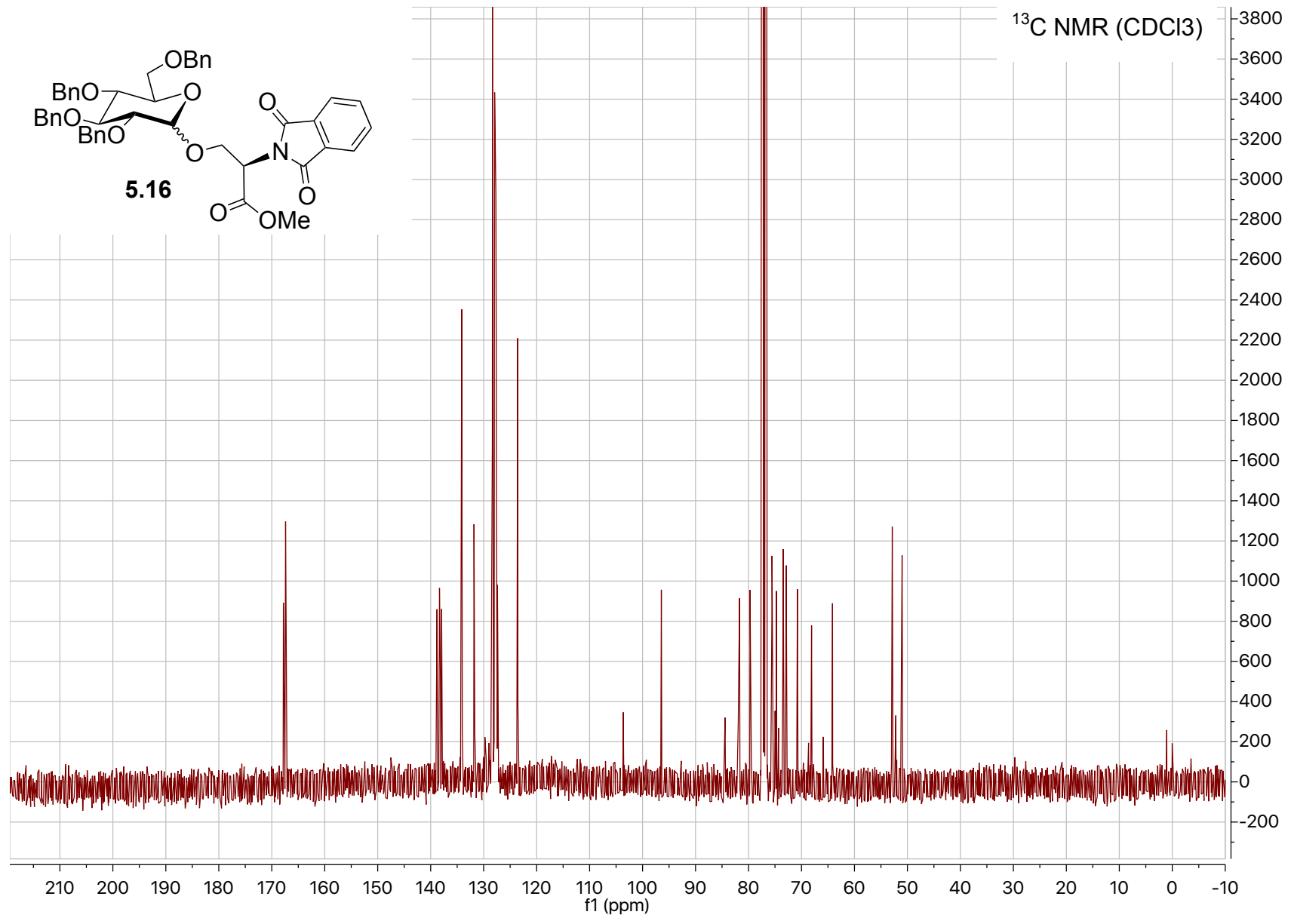


¹H NMR (CDCl₃)

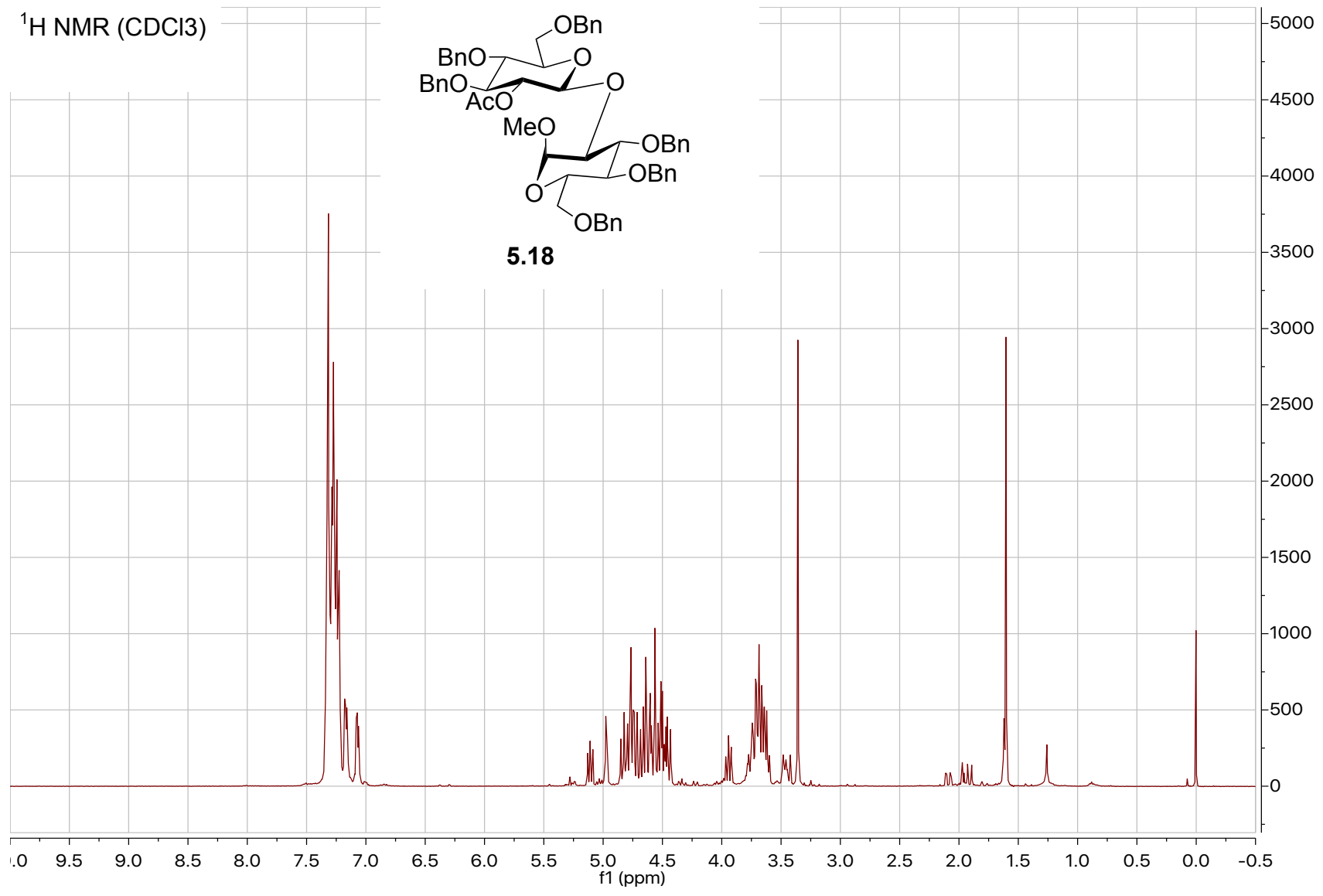
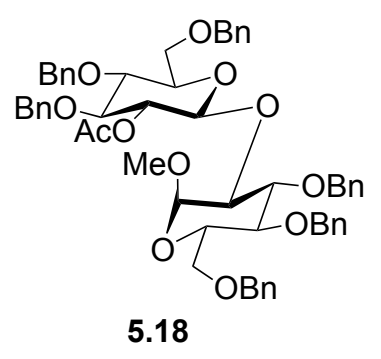


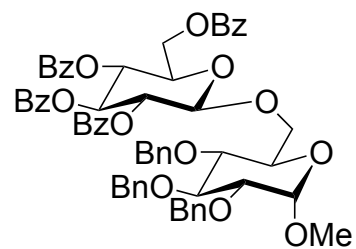




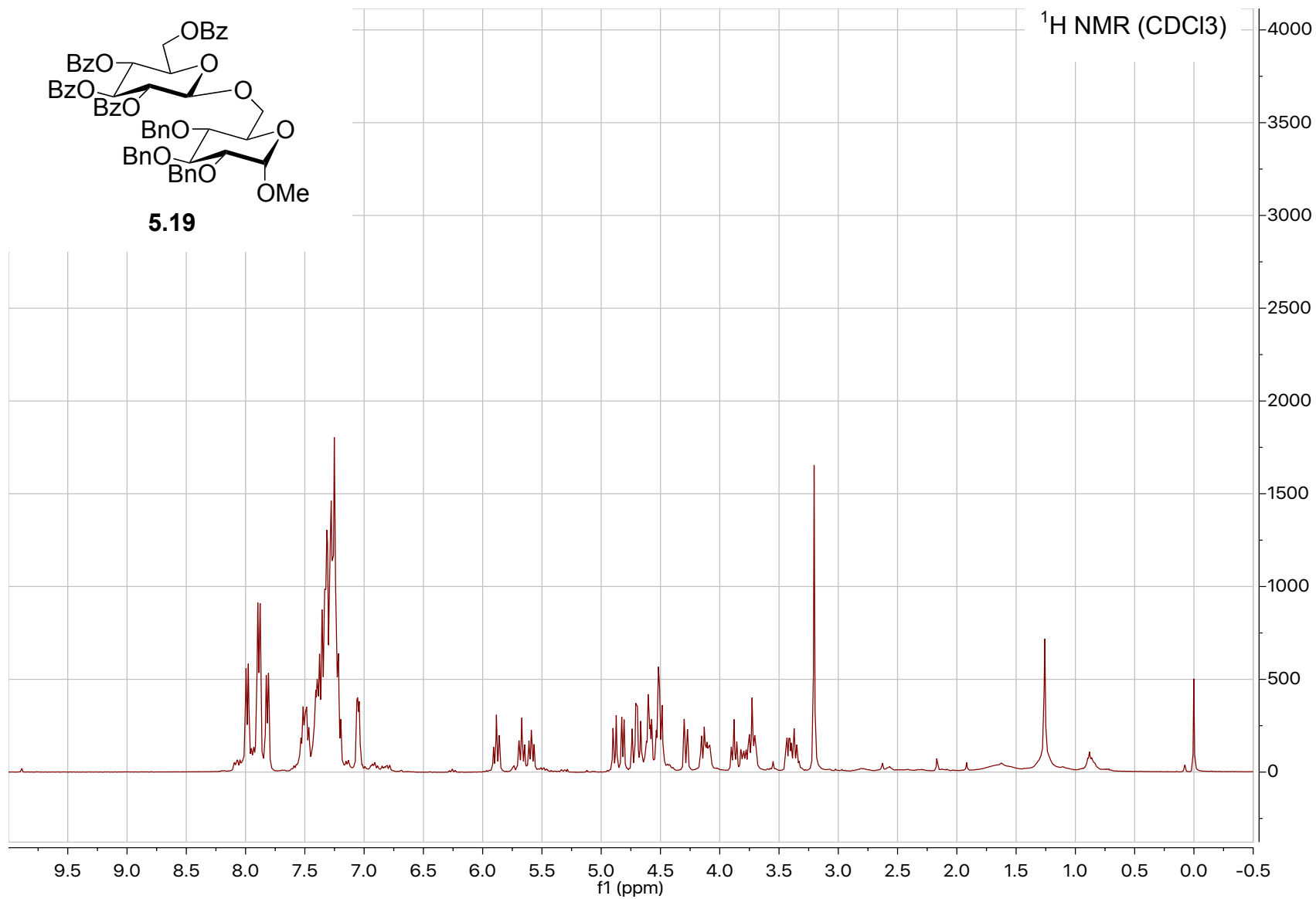


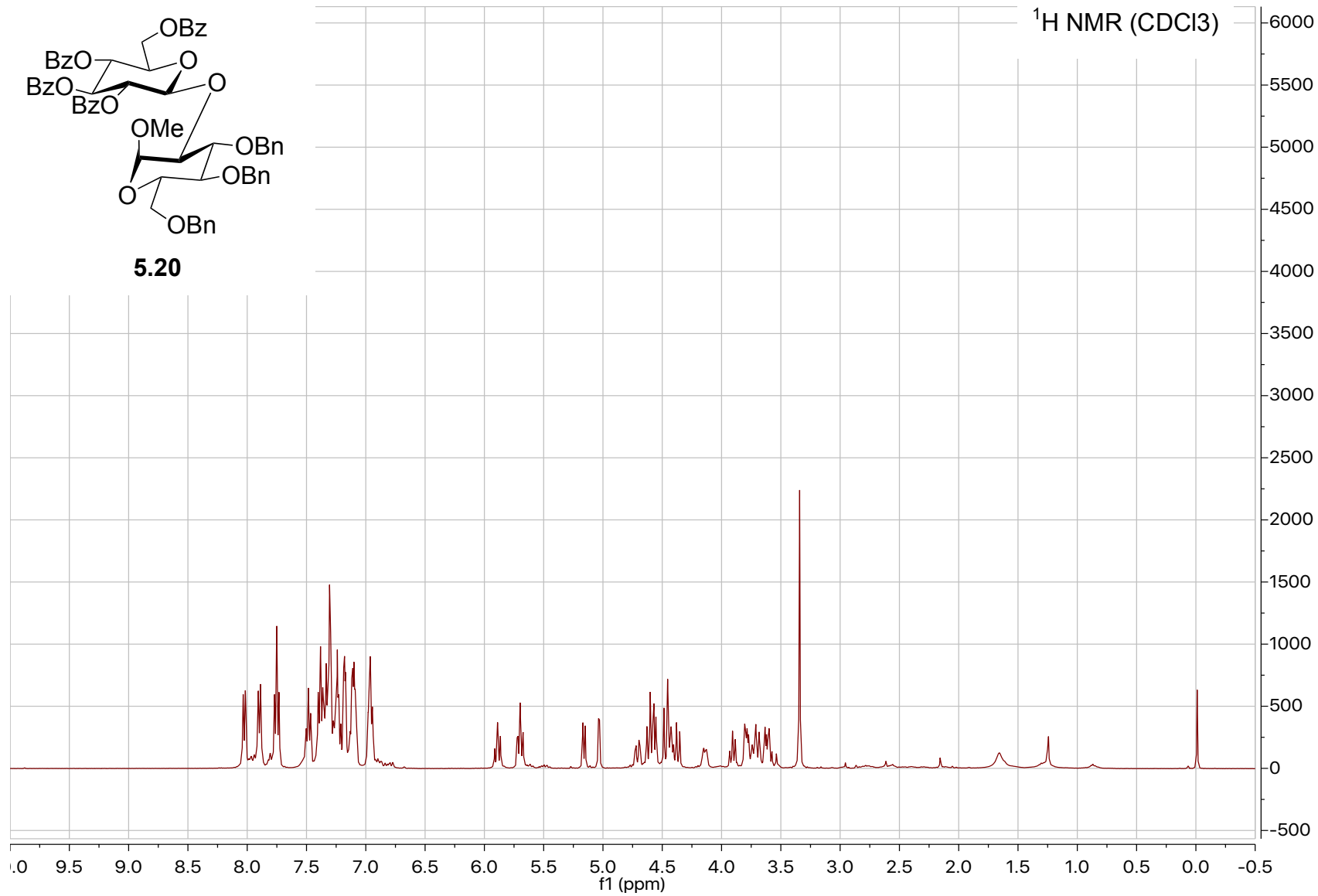
¹H NMR (CDCl₃)

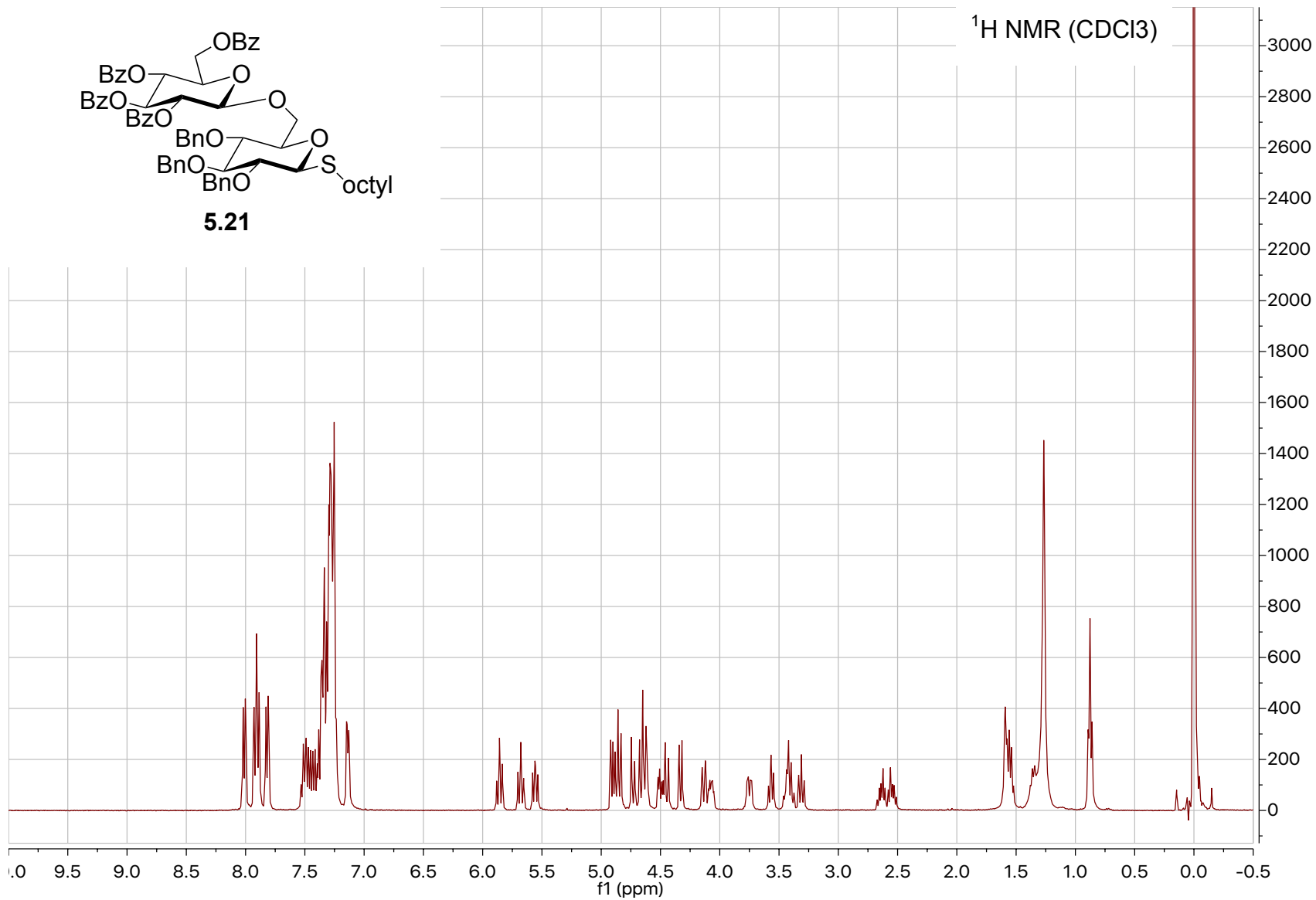
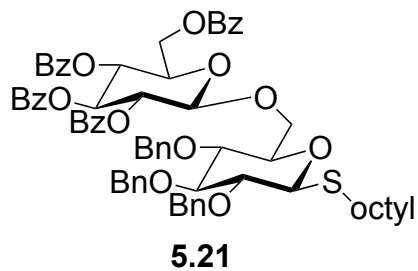


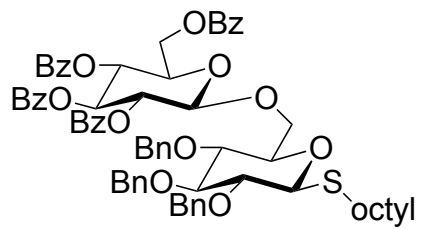


5.19

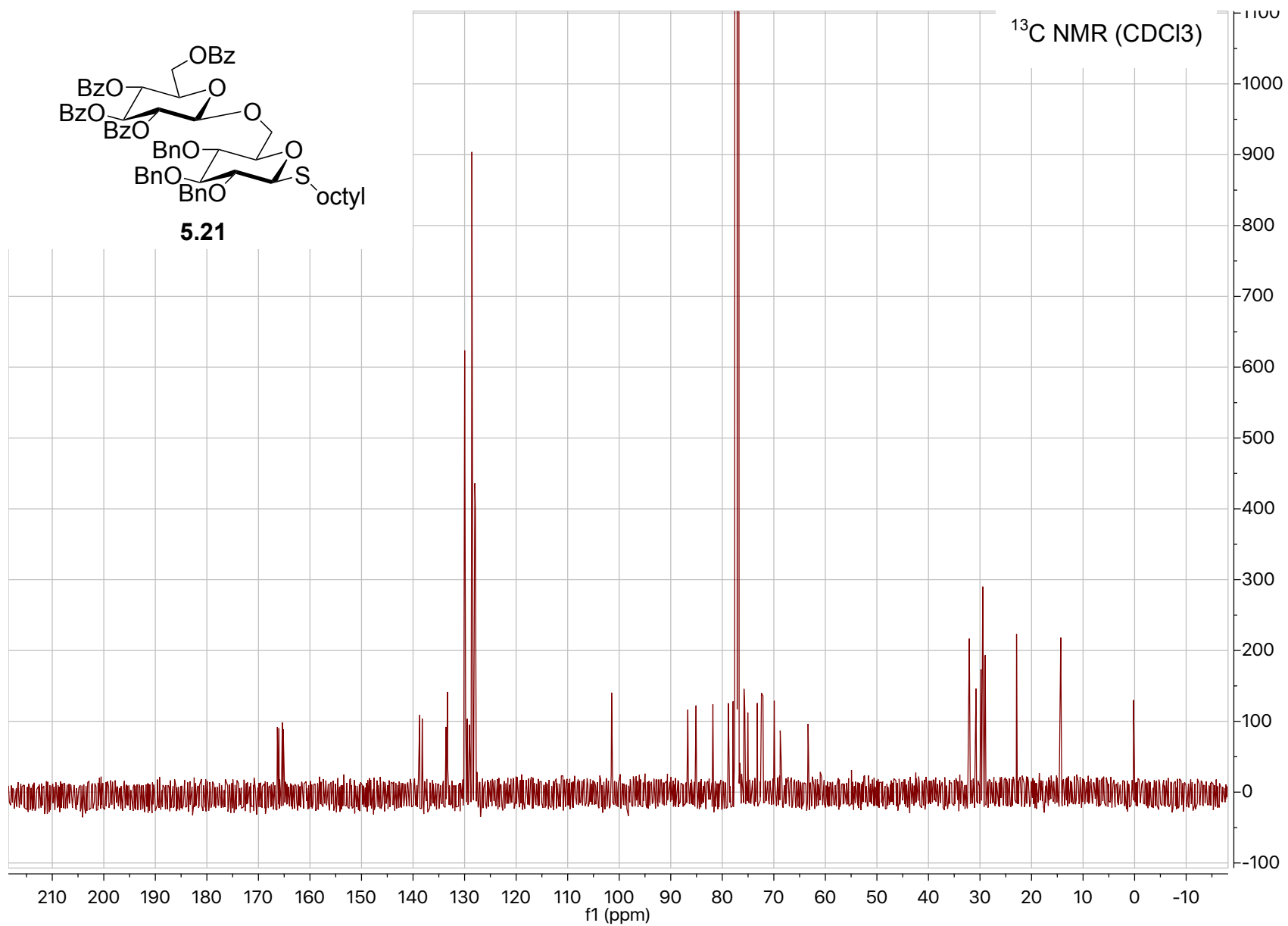




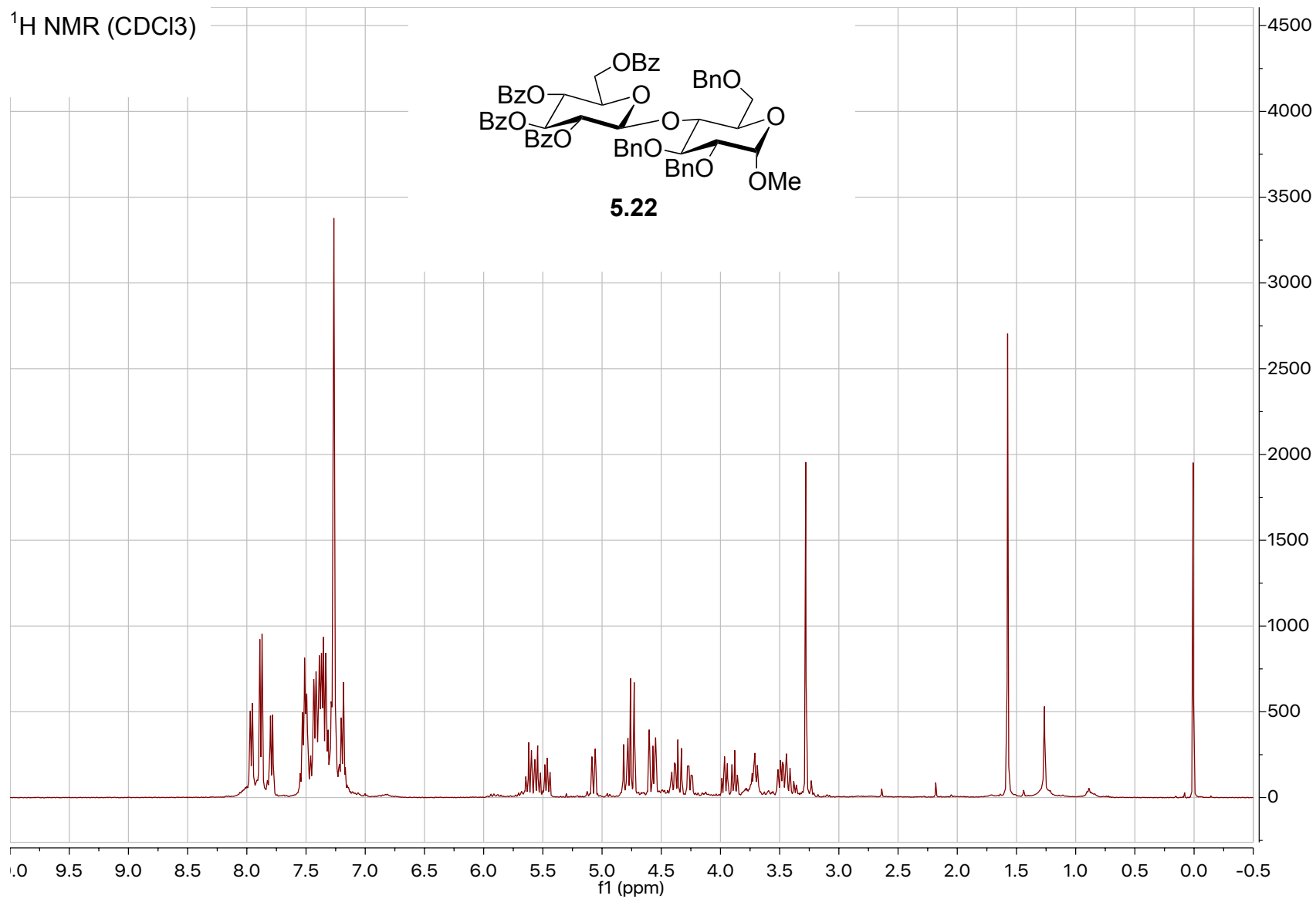
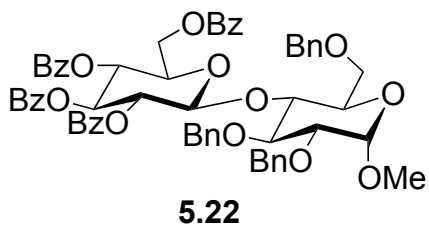


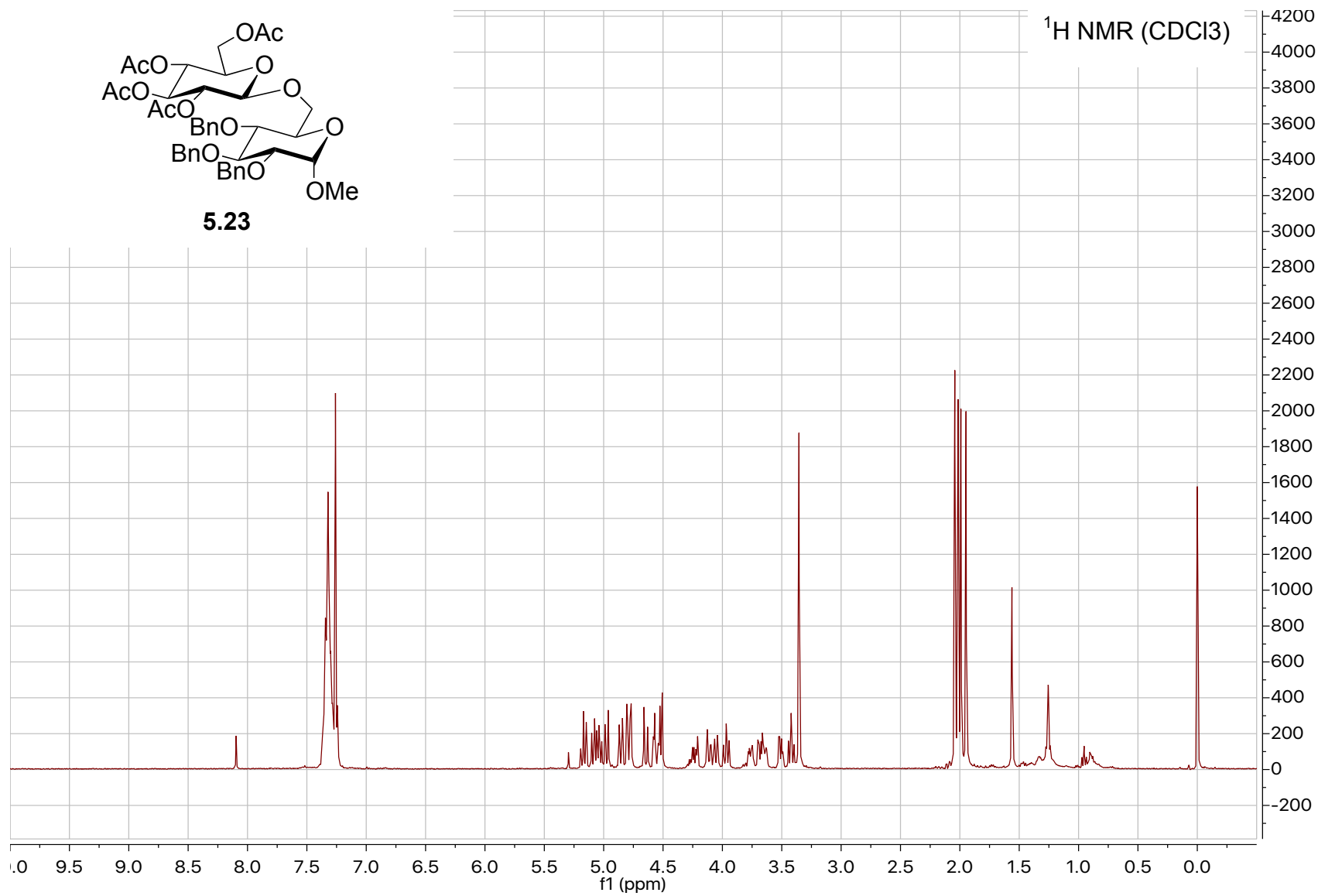
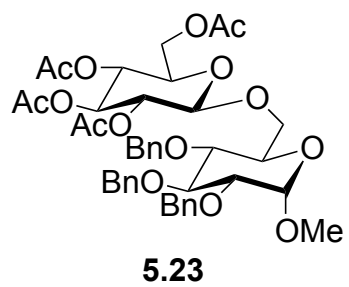


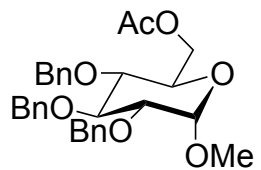
5.21



¹H NMR (CDCl₃)

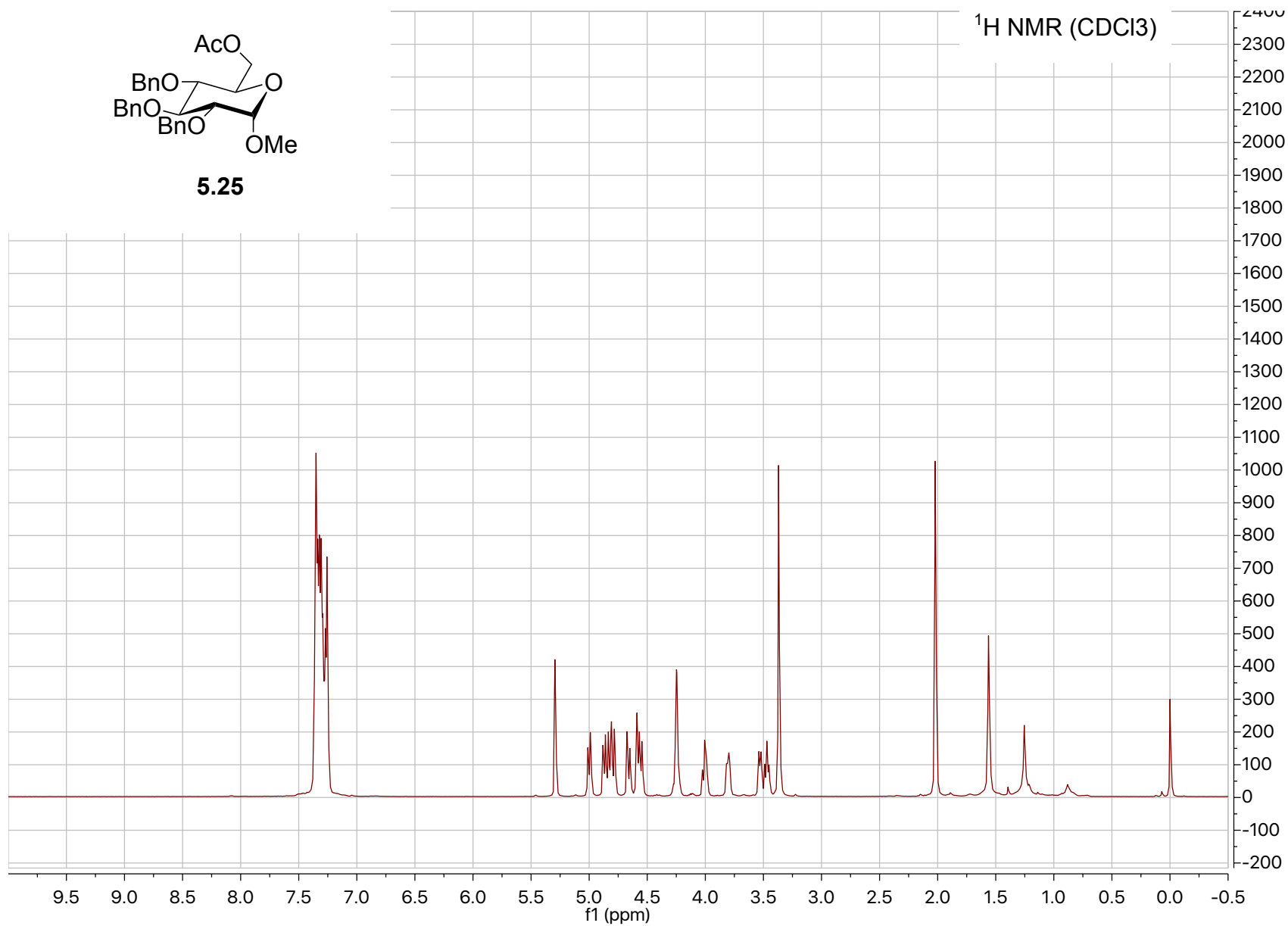


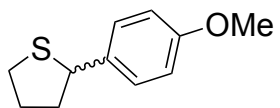




5.25

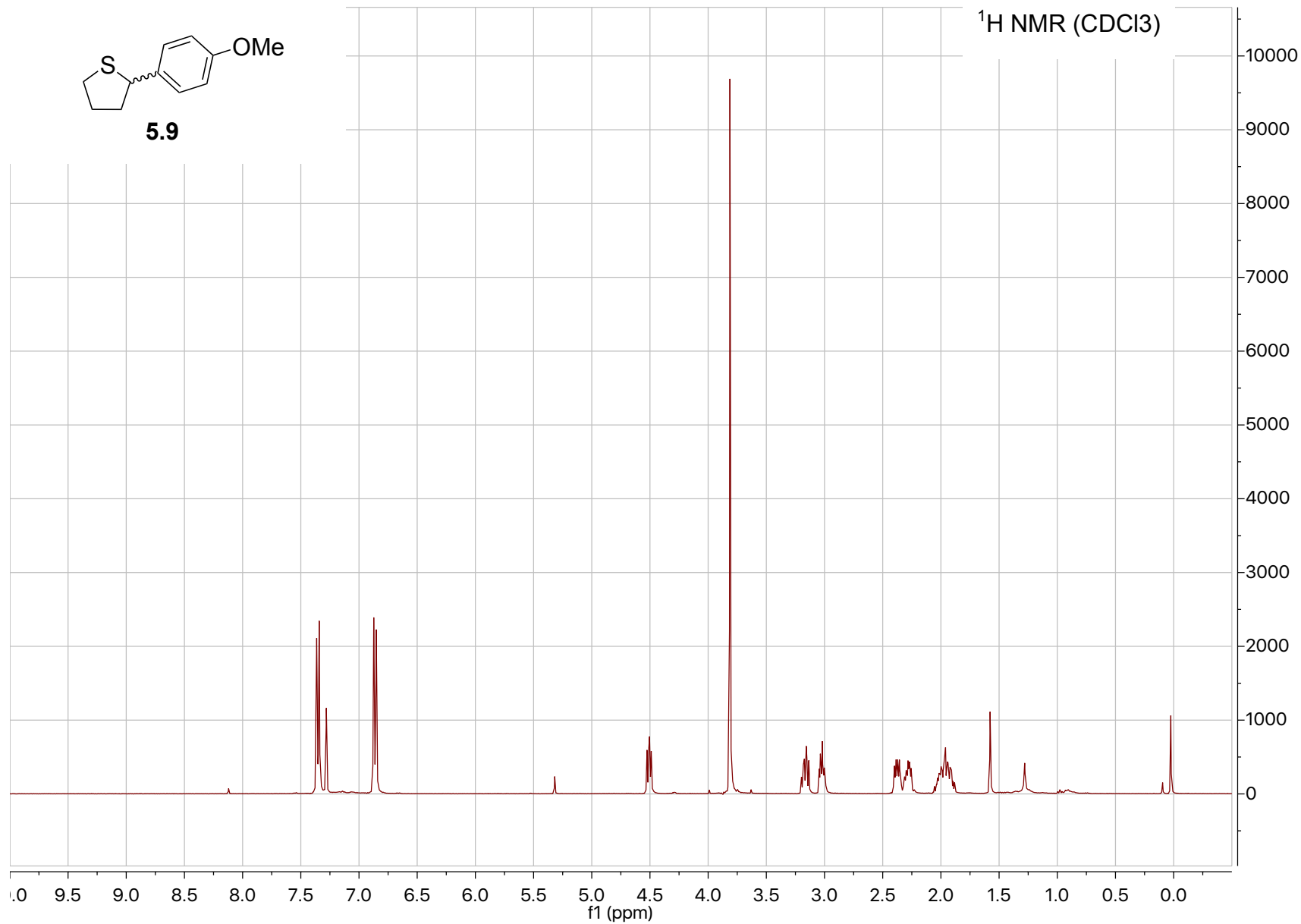
¹H NMR (CDCl₃)





5.9

¹H NMR (CDCl₃)



VITA

Kristina Danielle Deveaux-Lacey was born on the island of Grand Bahama in the beautiful country of The Bahamas to Wentworth C. Deveaux and Angela P. Deveaux. She is married to Brandon G. Lacey. After graduating high school, she began her studies at Georgia Southern University in Statesboro, Georgia. In 2012 she earned her Bachelor's degree in Chemistry and completed her honors thesis under the tutelage of Dr. Karelle Aiken. She then journeyed to Baton Rouge, Louisiana and joined the Department of Chemistry's doctoral program at Louisiana State University. Since January 2013 she has been a part of Dr. Justin R. Ragain's research group. Currently a PhD candidate, Kristina will be awarded with a doctoral degree in Chemistry at the December 2017 commencement ceremony.